

Macronutrient Availability Influences Antibiotic Susceptibility Through Changes in Microbiome Metabolic Function

Jenna I. Wurster

B.A. Smith College, 2014

A Dissertation Submitted in Partial Fulfillment of the Requirements for the Degree of Doctor of Philosophy in the Division of Biology and Medicine at Brown University

Providence, RI
February 2022

© Copyright 2022 by Jenna I. Wurster

SIGNATURE PAGE

This dissertation, presented by Jenna I. Wurster, is accepted in its present form by the Pathobiology Graduate Program and the Department of Molecular Microbiology & Immunology as satisfying the dissertation requirement for the degree of Doctor of Philosophy.

Date: _____

Peter Belenky, Ph.D. (Advisor)

Recommended to the Graduate Council

Date: _____

Shipra Vaishnava, Ph.D. (Reader & Chair)

Date: _____

Amanda M. Jamieson, Ph.D. (Reader)

Date: _____

Beth B. Fuchs, Ph.D. (Reader)

Date: _____

Suzanne Devkota, Ph.D. (Outside Reader)

Approved by the Graduate Council

Date: _____

Andrew Campbell, Ph.D.
Dean of the Graduate School

CURRICULUM VITAE

Jenna I. Wurster

EDUCATION

Brown University, Providence, RI 2021
Ph.D., Pathobiology

Smith College, Northampton, MA 2014
B.A., High Honors in Biological Sciences, *cum laude*

RESEARCH EXPERIENCE

Brown University 2016 – 2021
Providence, RI
Pre-Doctoral Research Fellow
Advisor: Peter Belenky, Ph.D.

Massachusetts Eye and Ear Infirmary 2014 – 2016
Boston, MA
Research Technician
Advisor: Michael S. Gilmore, Ph.D.

Smith College 2012 – 2014
Northampton, MA
Pre-Baccalaureate Research Fellow
Advisor: Michael J.F. Barresi, Ph.D.

New England BioLabs 2011
Ipswich, MA
Participant: Molecular Biology Summer Workshop

Smith College 2010 – 2014
Northampton, MA
Pre-Baccalaureate Research Fellow
Advisor: Steven A. Williams, Ph.D.

PUBLICATIONS

Wurster, J.I., Peterson, R.L., Brown, C.E., Penumutchu, S., Guzior, D.V., Neugebauer, K., Sano, W.H., Sebastian, M.M., Quinn, R.A., Belenky, P. (2021). Streptozotocin-Induced Hyperglycemia Alters the Cecal Metabolome and Exacerbates Antibiotic-Induced Dysbiosis. *Cell Reports*, 37, 110113. doi:10.1016/j.celrep.2021.110113

Heinzinger, L.R., Johnson, A., **Wurster, J.I.**, Nilson, R., Penumutchu, S., Belenky, P. (2020). Oxygen and Metabolism: Digesting Determinants of Antibiotic Susceptibility in the Gut. *iScience*, 23(12): 101875

Cabral, D.J.*, **Wurster, J.I.***, Korry, B.J., Penumutchu, S., Belenky, P. (2020). Consumption of a Western-style diet modulates the response of the murine microbiome to ciprofloxacin. *mSystems*, 5(4), e00317-20.

[* denotes equal contribution]

Cabral, D.J., Penumutchu, S., Reinhart, E.M., Zhang, C., Korry, B.J., **Wurster, J.I.**, Nilson, R., Guang, A., Sano, W.H., Rowan-Nash, A.D., Li, H., Belenky, P. (2019). Microbial Metabolism Modulates Antibiotic Susceptibility within the Murine Gut Microbiome. *Cell Metabolism*, 30, 800-823.

Wurster, J.I.*, Bispo, P.J.M.*, Van Tyne, D., Cadorette, J.J., Boody, R., Gilmore, M.S. (2018). *Staphylococcus aureus* from ocular and otolaryngology infections are frequently resistant to clinically important antibiotics and are associated with lineages of community and hospital origins. *PLoS ONE*, 13(12), e0208518.

[* denotes equal contribution]

Cabral, D.J.*, **Wurster, J.I.***, Belenky, P. (2018). Antibiotic persistence as a metabolic adaptation: stress, metabolism, the host, and new directions. *Pharmaceuticals*, 11(1), pp. 14-19

[* denotes equal contribution]

Zabat, M.A., Sano, W.H., Cabral, D.J., **Wurster, J.I.**, Belenky, P. (2018). The impact of vegan production of the kimchi microbiome. *Food Microbiology*, 74, 171-178.

Hilton, N.A., Sladewski, T.E., Perry, J.A., Pataki, Z., Sinclair-Davis, A.N., Muniz, R.S., Tran, H.L., **Wurster, J.I.**, Seo, J., de Graffenried, C.L. (2018). Identification of TOEFAZ1-interacting proteins reveals key regulators of *Trypanosoma brucei* cytokinesis. *Molecular Microbiology*, 109(3), 306-326.

Zabat, M.A., Sano, W.H., **Wurster, J.I.**, Cabral, D.J., Belenky, P. (2018). Microbial community analysis of sauerkraut fermentation reveals a stable and rapidly established community. *Foods*, 7(5), 77

Cabral, D.J., **Wurster, J.I.**, Flokas, M.E., Alevizakos, M., Zabat, M.A., Korry, B.J., Rowan, A.D., Sano, W.H., Andreatos, N., Ducharme, R.B., Chan, P.A., Mylonakis, E., Fuchs, B.B., Belenky, P. (2017). The salivary microbiome is consistent between subjects and resistant to impacts of short-term hospitalization. *Scientific Reports*, 7:11040, 1-13

Wurster, J.I., Saavedra, J.T., Gilmore, M.S. (2016). Impact of Antibiotic Use on the Evolution of *Enterococcus faecium*. *Journal of Infectious Diseases*, 213(12), pp. 1862-1865

Keroack, C.D., **Wurster, J.I.**, Decker, C.G., Williams, K.M., Slatko, B.E., Foster, J.M., Williams, S.A. (2016). Absence of the filarial endosymbiont *Wolbachia* in seal heartworm (*Acanthocheilonema spirocauda*) but evidence of ancient lateral gene transfer. *Journal of Parasitology*, 102(3), 312-318

MANUSCRIPTS IN PROGRESS

Pironti, A., Salamzade, R., Manson, A.L., Walker, B.J., Brennan-Krohn, T., Worby, C.J., Ma, P., He, L., Shea, T.P., Qu, J., Chapman, S.B., Howe, W., Young, S.K., **Wurster, J.I.**, Delaney, M.L., Kanjilal, S., Onderdonk, A.B., Bittencourt, C.E., Kim, D., Peterson, E.M., Ferraro, M.J., Hooper, D.C., Shenoy, E.S., Hung, D.T., Gilmore, M.S., Cosimi, L.A., Huang, S.S., Kirby, J.E., Pierce, V.M., Bhattacharyya, R.P., Earl, A.M. Tracing inter-species carbapenemase dynamics reveals horizontal gene transfer as driver of long-term persistence of carbapenem resistance. *Genome Medicine*. *Under Review*.

Banerjee, S., **Wurster, J.I.**, Jash, S., Belenky, P., Sharma, S. Proteinopathy and altered gut microbiome coupled with placental metabolic and immune dysregulation program pathologic changes in a human serum-based mouse model of gestational diabetes mellitus. *In Preparation*.

Ward, G., **Wurster, J.I.**, DeCost, G., Belenky, P., Monning, M.A. The Impact of Alcohol and Tobacco Consumption on Oral Microbiome Composition and its Relation to Alzheimer's Disease and Oral Cancers. *In Preparation*.

Wurster, J.I., Peterson, R.L., Guzior, D.V., Neugebauer, K., Quinn, R.A., Belenky, P. Streptozotocin-Induced Hyperglycemia is Associated with Disparate Microbiome Responses to Ciprofloxacin. *In Preparation*.

HONORS & AWARDS

National Science Foundation Graduate Research Fellowship Program	2018 – 2021
Brown University Charles “Chick” Kuhn Graduate Award in Disease Pathogenesis	2019
National Institute of Standard and Technology Summer Undergraduate Research Fellowship	2011 – 2014
Smith College Margaret Wemple Brigham Prize in Microbiology and Immunology	2014
Smith College Dean’s List	2011 – 2014

ABSTRACTS & PRESENTATIONS

Wurster, J.I. and Belenky, P. Host Hyperglycemia Exacerbates Antibiotic Toxicity within the Gut Microbiome. 26th Annual Boston Bacterial Meeting. Boston, MA. July 2020. **Flash Talk Presentation**

Wurster, J.I. and Belenky, P. Host Hyperglycemia Exacerbates Antibiotic Toxicity within the Gut Microbiome. Rhode Island Microbiome Symposium. South Kingstown, RI. January 2020. **Poster Presentation**

Wurster, J.I. and Belenky, P. Host Hyperglycemia Impacts Antibiotic Efficacy within the Gut Microbiome. Microbiome: Therapeutic Implications Keystone Symposia. Killarney, Kerry Co., Ireland. October 2019. **Poster Presentation**

Wurster, J.I., Cabral, D.J., Sano, W.H., Belenky, P. Host Hyperglycemia Impacts Antibiotic Efficacy within the Gut Microbiome. 27th Annual Pathobiology Graduate Program Retreat. East Providence, RI. September 2019. **Oral Presentation**

Wurster, J.I., Cabral, D.J., Sano, W.H., Belenky, P. Host Hyperglycemia Impacts Antibiotic Efficacy within the Gut Microbiome. 25th Annual Boston Bacterial Meeting. Boston, MA. June 2019. **Oral Presentation**

Wurster, J.I., Cabral, D.J., Sano, W.H., Belenky, P. Impacts of Acute Hyperglycemia on the Response of the Murine Microbiome to Antibiotic Exposure. 118th Annual Meeting of the American Society for Microbiology: ASM Microbe. Atlanta, GA. June 2018. **Poster Presentation**

Wurster, J.I., Cabral, D.J., Sano, W.H., Belenky, P. Impacts of Acute Hyperglycemia on the Response of the Murine Microbiome to Antibiotic Exposure. 24th Annual Boston Bacterial Meeting. Boston, MA. June 2018. **Poster Presentation**

Wurster, J.I., Van Tyne, D., Bispo, P.J.M., Haas, W., Cadorette, J.J., Boody, R.P., Gilmore, M.S. Application of Clinical and Molecular Epidemiological Surveillance to Monitor Antimicrobial-Resistant Lineages of *Staphylococcus aureus* in an Outpatient Hospital Setting. 21st Annual Boston Bacterial Meeting. Boston, MA. June 2015. **Poster Presentation**

Keroack, C.D., **Wurster, J.I.**, Decker, C.G., Williams, S.A. Absence of Wolbachia in Seal Heartworm (*Acanthocheilonema spirocauda*) with Evidence of Lateral Gene Transfer. 14th Annual Celebrating Collaborations Conference. Northampton, MA. May, 2015. **Poster Presentation**

Wurster, J.I. and Williams, S.A. Finding a Parasite Circadian Clock: Identification of clock gene functional conservation between *Caenorhabditis elegans* and *Brugia malayi*. Life Sciences Lunchbag Seminar Series at Smith College. Northampton, MA. April, 2014. **Oral Presentation**

Wurster, J.I., Keroack, C.D., Currens, R., Williams, S.A. Identification & Confirmation of pdf-1 functional conservation between *Caenorhabditis elegans* and *Brugia malayi*. 13th Annual Celebrating Collaborations Conference. Northampton, MA. May, 2014. **Poster Presentation**

Wurster, J.I., Keroack, C.D., Currens, R., Williams, S.A. Identification & Confirmation of pdf-1 functional conservation between *Caenorhabditis elegans* and *Brugia malayi*. 12th Annual Celebrating Collaborations Conference. Northampton, MA. May, 2013. **Poster Presentation**

TEACHING EXPERIENCE

Brown University, Providence, RI

Guest Lecturer: Host-Microbiome Interactions in Health and Disease 2020
Course Director: Shipra Vaishnava, Ph.D.

Teaching Assistant: Human Genetics and Genomics 2018
Course Director: Eric Morrow, M.D., Ph.D.

Teaching Certification: Reflective Teaching Practices 2016
Course Director: Harriet W. Sheridan Center for Teaching and Learning

Smith College, Northampton, MA

Teaching Assistant: Organic Chemistry I (Laboratory Section) 2013 – 2014
Course Director: Rebecca Thomas, Ph.D.

Tutor: Genetics I & Genetics II 2011 – 2014
Course Director(s): Robert B. Merritt, Ph.D. & Steven A. Williams, Ph.D.

Teaching Assistant: Genetics I (Laboratory Section) 2013
Course Director(s): Cait S. Kirby, Ph.D. & Lori Saunders, Ph.D.

Teaching Certification: International Tutor Training Program 2013
Course Director(s): Sherrerd Center for Teaching and Learning & College Reading and Learning Association

LEADERSHIP EXPERIENCE AND SERVICE

Boston Bacterial Meeting; Chair	2022
Boston Bacterial Meeting; Organizing Committee	2020, 2021
Massachusetts Science and Engineering Fair; Judge	2020, 2021
Pathobiology Graduate Program; Peer Mentoring Committee	2017 – 2021
Pathobiology Graduate Program; Admissions Committee	2018, 2019
Pathobiology Graduate Program; Retreat Student Coordinator	2019

PROFESSIONAL ASSOCIATIONS

Rients L.L.C.; Microbiology and Writing Consultant	2020 – present
American Society for Microbiology, Trainee Membership	2018 – present
Sigma Xi: The Scientific Research Honor Society, Associate Membership	2014 – present

PREFACE

The work presented in this thesis was performed in the laboratory of Dr. Peter Belenky at Brown University. Jenna I. Wurster performed all the experiments and analyses reported with the following exceptions:

Chapter 2 – Dr. Damien J. Cabral co-performed animal experiments, extracted nucleic acids from cecal samples, conducted the analysis of 16S rRNA amplicon data, and cowrote the original draft of the manuscript.

Chapter 3 – Rachel L. Peterson performed all intragastric *Salmonella enterica* infections and assisted with animal work related to Figures 7 and S5. Claire E. Brown performed cecal glucose quantification related to Figure 1, and assisted with animal work related to Figures 7, S1, and S5. Swathi Penumutthu assisted in several animal experiments. Douglas V. Guzior and Kerri Neugebauer performed LC-MS/MS, GNPS networking, and random-forest classification under the supervision of Dr. Robert Quinn. William A. Sano extracted nucleic acids and prepared 16S rRNA amplicon libraries related to Figures 1 and S1. Dr. Manu Sebastian performed GI pathology scoring related to Figures S1 and S5. Histology slides were prepared by David Silverberg at the Brown University Molecular Pathology Core as free-for-service. Q-TOF-MS metabolomics and ion annotation was performed by General Metabolics Inc. with fee-for-service.

Chapter 4 - Douglas V. Guzior and Kerri Neugebauer performed LC-MS/MS, GNPS networking, and random-forest classification under the supervision of Dr. Robert Quinn.

Appendix I - Dr. Damien J. Cabral and Jenna I. Wurster contributed equally to the writing of this review article

All electronic supplementary data for Chapters 2 and 3 have been deposited in the Brown Digital Repository and are publicly available at: <https://doi.org/10.26300/8qbm-pf70>

ACKNOWLEDGEMENTS

As I approach the apogee of my doctoral training and reflect on the cumulative experiences that have led to this moment, I can't help but feel a sense of quietude. My time in graduate school has been bittersweet. It has been the zenith of my professional development, has bolstered incredibly meaningful friendships, but has also been filled with moments of languish and deep isolation (not to mention the unique dynamics created by the SARS-COV-2 pandemic)... Perhaps the best analogy for graduate school is a marathon. It is rigorous, exhausting, requires a consistent and sustained effort, and can be incredibly rewarding. I can say with great certainty that I would not have made it to the end without the professional and personal support systems that have surrounded me these last few years. This acknowledgments section cannot accurately capture how grateful I am to every single person within those support systems.

*From the bottom of my heart
thank you*

I would first like to specifically thank my advisor, Peter Belenky. Thank you for taking a chance on me and providing the opportunity to train in your lab. Thank you for continually challenging me, helping me self-actualize as an independent researcher, and for all the little moments that keep me humble. Thank you for your patience with me on my worst days, and for celebrating with me on the best days. From day one, you've given me the freedom to explore personally and professionally fulfilling opportunities, even when they fell outside the lab, and you have never placed the expectation of a specific career trajectory onto me. Thank you for this freedom- I will always be appreciative of it. As a mentor, you continually strive to demonstrate compassion and remind us that we're all human and always learning. Thank you for all that you've taught me.

Next, I would like to thank the members of my dissertation committee: Drs. Shipra Vaishnava, Amanda Jamieson, and Beth Fuchs. Each of you has left a positive impact on my graduate experience, whether it be in the form of enthusiastic scientific discussion, general encouragement, advice in non-academic career development, helping navigate the unique challenges faced by women in STEM, or through fun chats over coffee, happy hours, and

department events. I am so grateful to have had each of you on my committee. Thank you to Dr. Suzanne Devkota for agreeing to be my external reader, and for accepting my invitation to speak at Brown's MMI seminar series earlier this fall. It was a pleasure to get to know you in advance of my dissertation defense, and I hope that we have an opportunity to cross paths again soon. Thank you to the MMI and Pathobiology administrative staff for their continued support over the years. Specifically, Michele Welindt and Jen Ducharme have always made the 6th floor of BioMed feel like a second home. They are two of the kindest people I've had the pleasure of meeting, and I am so incredibly grateful to have gotten to know them these last few years. And thank you to my colleagues in the Pathobiology program and on the Boston Bacterial Meeting Organizing Committee. You all are such supportive, energetic, and fun groups to be around, and my conversations with you all leave me fulfilled and excited about science. This has been a wonderful place to get my graduate degree and can't wait to be there to support each of you when it's your time to defend.

Within my professional network, I additionally owe thanks to the mentors that laid the groundwork for my interest in science. Thank you to Drs. Steven Williams, Michael Gilmore, Paulo Bispo, Daria Van Tyne, and Elizabeth Selleck. Steve- you were my undergraduate mentor, first PI, and continue to support me far beyond my tenure in your lab. Thank you for always cheering me on. Michael- thank you for taking me on as a research technician, for some tough-love styling mentoring, and for demonstrating the rigorous standards I hold myself to now. Paulo, Daria, Beth- your friendship and continued mentorship has meant the world to me. It has been such a joy to watch the directions your lives have taken since I started graduate school, and I cherish the rare moments when our professional paths cross. Thank you all for your mentorship over the years.

To my dearest friends and family- you are the unsung heroes of my success and are, without a doubt, the reason I'm still standing. As I write this, I find myself overwhelmed by how profoundly grateful I am to have you all in my life and to be able to share in your joys as you share in mine. I'm struggling to articulate my feelings, so I hope you can all bear with my clumsy words of affection.

To my mother Karen, you raised me all on your own and always tried your best to provide me with every opportunity and ounce of love that you never had, even when it came at great

personal sacrifice. Thank you. Those sacrifices laid the foundation for the woman I am and are why I can stand tall. I am so appreciative to have you as my parent. To Chris- you are like family, and I have always been so thankful of the support you've shown me and my mom. Thank you for being unapologetically you. To my in-laws, Frank, Ann, Lauren, and Bud, thank you for welcoming me as family from Day 1. You've all always given me some much needed outside perspective (and levity) during my graduate training, and I'm so thankful for all the laughs and major milestones we've experienced together. To my late dog Momo- although our time together was short, you were a beloved companion and made the loneliest days of graduate school a lot less isolating. Thank you for spending your year of freedom with me.

To my oldest and dearest friends, Jill, Caroline, Abbey, and Michelle. I love you to death. You are basically family and have stuck with me through the highest highs and the lowest lows of the last decade. I'm so thankful to have the type of friends where we can go from gut-busting laughter to heavy theoretical debate and back in a single chat thread. You all know how to keep me smiling even at the worst of times. You are just the best. Plain and Simple. To my newer but equally dear friends, Mae, Jackie, Angela, Swathi. One of the greatest parts of graduate school has been getting to know you and being able to call you friends. You each have made the dark days light, and the light days bright- thank you for all the small moments of joy throughout my time here. I so deeply admire each of you for your passions and can't wait to see where we all end up in the next few years. I'm also so thankful that I get to finish my graduate training within a week of my very first friend at grad school, Mae. I can't wait to cheer you on next week when it's your turn!

Finally, this section wouldn't be complete without acknowledging my husband, Jack Vorwald. Jack, you are my best friend. I am so thankful that building our life together has coincided with my time in graduate training. Growing alongside you has been an endless source of joy, support, and strength. You've kept me grounded, helped me when I've been truly struggling, and have relished in the successes with me. There's no one else I'd rather have by my side for when I truly "become a pro".

*I would like to dedicate this dissertation to my chosen family.
I love you all endlessly.*

TABLE OF CONTENTS

SIGNATURE PAGE	III
CURRICULUM VITAE	IV
PREFACE	IX
ACKNOWLEDGEMENTS	XI
TABLE OF CONTENTS	XIV

CHAPTER 1: INTRODUCTION	1
INTRODUCTION	2
FUNDAMENTALS OF THE MAMMALIAN MICROBIOME	3
<i>Defining the Microbiome</i>	3
<i>Compositional Characteristics of the Microbiome</i>	4
<i>Functional Roles of the Microbiome</i>	5
ANALYTICAL METHODS FOR STUDYING THE MICROBIOME	9
<i>Characterizing Microbiome Structure</i>	9
<i>Characterizing Microbiome Function</i>	10
IMPACTS OF DIETARY MACRONUTRIENT COMPOSITION ON MICROBIOME COMMUNITY DYNAMICS	12
IMPACTS OF HOST METABOLIC DISEASE ON MICROBIOME COMMUNITY DYNAMICS	13
THE RELATIONSHIP BETWEEN MICROBIAL METABOLISM AND ANTIBIOTIC SUSCEPTIBILITY	15
<i>Antibiotic-Induced Dysbiosis</i>	15
<i>Metabolism Determines Bactericidal Antibiotic Susceptibility</i>	17
THESIS OVERVIEW AND SUMMARY OF FINDINGS	19
REFERENCES	21

CHAPTER 2: CONSUMPTION OF A WESTERN-STYLE DIET MODULATES THE RESPONSE OF THE MURINE GUT MICROBIOME TO CIPROFLOXACIN	39
ABSTRACT	40
IMPORTANCE	41
KEYWORDS AND LIST OF ABBREVIATIONS	41
INTRODUCTION	42
RESULTS	46
<i>Consumption of a Western diet modifies the metabolic activity of the microbiome</i>	47
<i>Ciprofloxacin elicits unique shifts in gene expression on Western and control diets</i>	50
<i>Diet and ciprofloxacin alter gene expression within B. thetaiotaomicron and A. muciniphila</i> ...	53
DISCUSSION	57
ACKNOWLEDGEMENTS	61
AUTHOR CONTRIBUTIONS	61
DECLARATION OF INTERESTS	62
MATERIALS AND METHODS	63

MAIN FIGURES, TITLES, TABLES, AND LEGENDS	70
<i>Table 1. Diet formulation used in the study</i>	70
<i>Figure 1: Impact of diet and ciprofloxacin administration on murine gut microbiome composition</i>	71
<i>Figure 2: Consumption of a Western diet induces broad taxonomic and transcriptional changes at the community level</i>	72
<i>Figure 3: Ciprofloxacin elicits unique shifts in gene expression on Western and control diets at the community level</i>	74
<i>Figure 4: Diet and ciprofloxacin alter gene expression within <i>B. thetaiotaomicron</i> and <i>A. muciniphila</i></i>	76
SUPPLEMENTAL FIGURES, TITLES, AND LEGENDS	78
<i>Figure S1: Dietary composition and antibiotic treatment impact the diversity of the gut microbiome</i>	78
<i>Figure S2: Consumption of a Western diet induces broad taxonomic and transcriptional changes at the community and species level</i>	79
<i>Figure S3: Ciprofloxacin elicits unique shifts in gene expression on Western and control diets at the community and species level</i>	81
SUPPLEMENTAL FILES	83
REFERENCES	87

CHAPTER 3: STREPTOZOTOCIN-INDUCED HYPERGLYCEMIA ALTERS THE CECAL METABOLOME AND EXACERBATES ANTIBIOTIC-INDUCED DYSBIOSIS96

ABSTRACT	97
KEYWORDS AND LIST OF ABBREVIATIONS	98
GRAPHICAL ABSTRACT	98
INTRODUCTION	99
RESULTS	102
<i>Hyperglycemia Significantly Modifies the Cecal Metabolome and Metatranscriptome</i>	103
<i>Hyperglycemia Modifies the Composition of Bacteroidetes and Firmicutes after Amoxicillin Exposure</i>	107
<i>Hyperglycemia Exacerbates Antibiotic-Induced Dysbiosis and Shifts Microbial Metabolism ...</i>	108
<i>Streptozotocin and Amoxicillin Co-treatment Increases Susceptibility to <i>Salmonella enterica</i> Infection</i>	111
DISCUSSION	114
<i>Limitations of the Study</i>	119
ACKNOWLEDGEMENTS	121
AUTHOR CONTRIBUTIONS	121
DECLARATION OF INTERESTS	121
MATERIALS AND METHODS	123
MAIN FIGURES, TITLES, AND LEGENDS	141
<i>Figure 1: Streptozotocin modifies glucose levels and impacts microbiome composition after amoxicillin</i>	141
<i>Figure 2: Streptozotocin modifies the cecal metabolome and metatranscriptome</i>	142
<i>Figure 3: Streptozotocin and amoxicillin treatment modify the taxonomic composition of the cecal microbiome</i>	144
<i>Figure 4: Amoxicillin differentially alters the cecal metatranscriptome</i>	145

<i>Figure 5: Amoxicillin differentially alters the cecal metabolome</i>	146
<i>Figure 6: Streptozotocin treatment modifies transcriptomic and metabolomic responses of the microbiome to amoxicillin</i>	148
<i>Figure 7: Streptozotocin and amoxicillin increase susceptibility to Salmonella enterica infection</i>	149
SUPPLEMENTAL RESULTS	151
SUPPLEMENTAL DISCUSSION	154
SUPPLEMENTAL FIGURES, TITLES, AND LEGENDS	157
<i>Figure S1: The impact of streptozotocin treatment on host physiology and microbiome composition without antibiotic administration</i>	157
<i>Figure S2: Streptozotocin-induced hyperglycemia modifies both the cecal metabolome and metatranscriptome</i>	159
<i>Figure S3: Streptozotocin impacts taxonomic composition after amoxicillin treatment</i>	161
<i>Figure S4: Streptozotocin modifies the metatranscriptomic and metabolomic responses of the gut microbiome to amoxicillin</i>	162
<i>Figure S5: Streptozotocin and amoxicillin dual treatment worsens outcomes during Salmonella enterica infection</i>	164
SUPPLEMENTAL FILES	166
REFERENCES	170
CHAPTER 4: DISCUSSION AND FUTURE DIRECTIONS	185
LOCAL METABOLIC ENVIRONMENT AS A DETERMINANT OF <i>IN VIVO</i> ANTIBIOTIC SUSCEPTIBILITY	186
SPECIFICITY OF ANTIBIOTIC SELECTION TO MACRONUTRIENT AND METABOLISM-BASED SUSCEPTIBILITY: DIETARY COMPOSITION	187
SPECIFICITY OF ANTIBIOTIC SELECTION TO MACRONUTRIENT AND METABOLISM-BASED SUSCEPTIBILITY: HOST METABOLIC FUNCTION	189
STRUCTURAL AND COMPOSITIONAL VARIATION OF MACRONUTRIENTS IMPACTS MICROBIOME FUNCTION	195
DETANGLING THE COMPLEX PHENOTYPES OF METABOLIC DISEASES AND THEIR IMPACT ON MICROBIOME FUNCTION	201
CONCLUSIONS	204
MATERIALS AND METHODS	206
MAIN FIGURES, TITLES, AND LEGENDS	207
<i>Figure 1: Impact of streptozotocin and ciprofloxacin on microbiome function</i>	207
<i>Figure 2: Host hyperglycemia differentially impacts genus-level composition and metagenomic potential after ciprofloxacin</i>	208
<i>Figure 3: Hyperglycemia is associated with Q-TOF-MS metabolome divergence during ciprofloxacin treatment</i>	210
<i>Figure 4: Hyperglycemia is associated with LC-MS/MS metabolome divergence during ciprofloxacin treatment</i>	212
<i>Figure 5: Taxon-stratified community metabolic potential during STZ and ciprofloxacin treatment</i>	213
REFERENCES	214

APPENDIX I: ANTIBIOTIC PERSISTENCE AS A METABOLIC ADAPTATION: STRESS, METABOLISM, THE HOST, AND NEW DIRECTIONS	221
ABSTRACT	222
KEYWORDS & LIST OF ABBREVIATIONS	223
INTRODUCTION	224
PERSISTENCE AS AN EVOLUTIONARY ADAPTATION	225
BIOFILMS CAN PROMOTE ANTIBIOTIC PERSISTENCE IN CLINICAL SETTINGS	228
GROWTH, METABOLISM, AND ATP PRODUCTION	232
CARBON CATABOLITE REPRESSION SYSTEMS COORDINATE ANTIBIOTIC PERSISTENCE AND TOLERANCE	236
SUGAR METABOLISM AND THE ERADICATION OF PERSISTERS	238
CELLULAR PERMEABILITY, PROTON MOTIVE FORCE, AND PERSISTENCE	241
STRESS RESPONSES AND PERSISTENCE: THE STRINGENT RESPONSE	244
STRESS RESPONSES AND PERSISTENCE: THE SOS RESPONSE	247
FUTURE DIRECTIONS	249
ACKNOWLEDGEMENTS	251
AUTHOR CONTRIBUTIONS	251
DECLARATION OF INTERESTS	251
MAIN FIGURES, TITLES, AND LEGENDS	252
<i>Figure 1: Utilization of next-generation technologies for studying persister cells</i>	252
REFERENCES	254

Chapter 1: Introduction

Introduction

The discovery, commercialization, and widespread use of antibiotics is arguably one of the greatest medical innovations of the 20th century. Shortly following the discovery of penicillin in the 1920s and its widespread use during the second World War, the modern paradigm of empiric treatment with broad-spectrum antibiotics was established (Bigger, 1944; Fleming 1929; Ventola, 2015). While empiric therapy has facilitated increasingly invasive and complex medical procedures, by mitigating the risk of post-operative infection, this treatment strategy is not without drawbacks (Roberts and Morris, 2020; Salking and Rao, 2011). The first shortcoming of this approach is the rapid development of antibiotic resistance amongst nosocomial pathogens, which results in clinical failure, skyrocketing healthcare costs, and ever-increasing mortality rates (Centers for Disease Control & Prevention, 2013; Ventola, 2015). Second, systemic antibiotic use within the agricultural sector has generated environmental reservoirs of antibiotic resistance that can leak back into healthcare settings or promote the development of multidrug resistance in community-acquired pathogens (Lebreton et al., 2013; F. Ma et al., 2021; Manyi-Loh et al., 2018; Woolhouse et al., 2015). Finally, a critical shortcoming of the empiric antibiotic paradigm is a lack of drug specificity. Broad-spectrum antibiotics function on conserved biological processes within bacteria (Kohanski et al., 2010), thus both pathogenic and non-pathogenic species can exhibit sensitivity to these drugs. More specifically, it is widely understood that the symbiotic microbes comprising the mammalian microbiome are also susceptible to antibiotic-mediated killing (Blaser, 2011; Dethlefsen and Relman, 2011; Modi et al., 2013). Disruption of these beneficial microbial communities, termed dysbiosis, has a suite of acute and chronic negative consequences to the host (Ni et al., 2019; M. Y. Yoon and S. S. Yoon, 2018). Given these shortcomings, there is increased recognition for the need of a 21st century antibiotic paradigm. While there is still active debate

about what this new paradigm ultimately looks like, any novel therapeutic strategy should aim to mitigate off-target toxicity to the microbiome. To do so, it is imperative to gain a fundamental mechanistic understanding of why certain species within the microbiome have increased (or reduced) susceptibility relative to the community at large, and what are the biotic and abiotic factors that dictate said drug susceptibility.

Fundamentals of the Mammalian Microbiome

Defining the Microbiome

The term “microbiome” refers to the amalgam of microorganisms (bacteria, archaea, fungi, and viruses), genetic material, and small molecules contained in distinct ecological niches within the mammalian host (Berg et al., 2020; Gilbert et al., 2018; Ursell et al., 2012). After birth, compositionally and functionally distinct microbial communities assemble through primary ecological succession in tissue systems including the skin, nasopharyngeal tract, urogenital tract, and gastrointestinal tract (Dominguez-Bello et al., 2010; Gilbert and Lynch, 2019). In humans, these communities reach their steady state composition between ages 3 and 5, at which point they become stable and individualized (Eckburg et al., 2005; Faith et al., 2013; Jones et al., 2018; Schloissnig et al., 2013; Rodríguez et al., 2015; Yatsunenko et al., 2012). In fact, these microbial assemblages contain an approximate average of 10^{13} total bacterial cells, with significant spatial variation in density; the skin averages 10^4 - 10^6 total bacteria, while the lower gastrointestinal tract averages 10^{11} - 10^{12} total bacteria (Sender et al., 2016; The Human Microbiome Project Consortium, 2012; Costello et al., 2009; Grice et al., 2009; Lloyd-Price et al., 2017; Sender et al., 2016). This intense biogeographical variation speaks to inherent differences in the ecology of these body sites and the functional roles of resident microbes within a host. While the communities outside of the

gastrointestinal tract are significantly involved in host health and physiology, this introduction will specifically focus on microbes of lower gastrointestinal tract, due to their relevance to the findings presented in Chapters 2 and 3.

Compositional Characteristics of the Microbiome

The colonic microbiota is consistently dominated by the phyla Bacteroidetes and Firmicutes in both humans and mice, with Proteobacteria, Actinobacteria, Fusobacteria, and Verrucomicroba typically comprising the remaining bacterial portion (The Human Microbiome Project Consortium, 2012; Eckburg et al., 2005). This phylum-level compositional conservation initially fueled fervent efforts to identify a list of shared species that comprise a core “healthy” microbiome (The Human Microbiome Project Consortium, 2012; Costello et al., 2009). However, studies utilizing higher taxonomic resolution have consistently demonstrated that the gut microbiome exhibits significant inter-individual variation, even within closely related family members (Arumugam et al., 2011; Falony et al., 2016; Jones et al., 2018; Schloss et al., 2014). Currently no consistent species mixture has been found to be representative of a core microbiome across all healthy human populations. However, a core group of genes and enzymatic functions has been consistently and repeatedly identified (Arumugam et al., 2011; Tian et al., 2020; Yatsunenکو et al., 2012; Lloyd-Price et al., 2017), highlighting that the microbiome can be defined by its capability to fulfill niche-specific functional roles rather than by a list of specific taxa. Thus, the gut microbiome exhibits the ecological property of functional equivalence, where multiple species across varied taxonomic groups share overlapping functional roles within an ecosystem (B. H. Walker, 1992).

Ecological frameworks are regularly leveraged to describe compositional characteristics of the microbiome. For example, total biodiversity is used as a metric to assess ecosystem health, where high diversity is attributed to community resistance (capacity to withstand external stressors) and resilience (capacity with return to a pre-stressor steady state) (Gilbert and Lynch, 2019; Ives and Carpenter, 2007; Naeem and Li, 1997; Yachi and Loreau, 1999). In the absence of disease or external stressors, the microbiome exhibits high biodiversity, and reductions in total diversity are often initial biomarkers of community dysbiosis (Gilbert and Lynch, 2019; Kriss et al., 2018; Lozupone et al., 2012; Naeem et al., 1994). Dysbiosis itself represents a failure to exhibit resilience; the microbiome is incredibly resilient under normal circumstances and regularly undergoes taxonomic shifts in response to environmental stimuli while maintaining its mature composition throughout the lifetime of the host (Costello et al., 2009; Faith et al., 2013; Kriss et al., 2018; Wilkins et al., 2019). This has been partially attributed to functional redundancy within the microbiome, although the underlying mechanisms are not fully understood (Moya and Ferrer, 2016; Tian et al., 2020). Through the lens of community ecology, we currently envision that the gut microbiome is a taxonomically diverse system capable of significant resiliency, that is somewhat constricted to conserved functional roles within an individual host.

Functional Roles of the Microbiome

The microbiome is integral to the proper development of both systemic and mucosal immunity in mammals (Ahern and Maloy, 2020; Kuhn and Stappenbeck, 2013; Neish, 2014). The use of “germ-free” animals devoid of a native microbiome has enhanced our understanding of immune-microbiome interactions; germ-free rodents have a plethora of defects in both the adaptive and innate arms of the immune system, defects in the structure of lymphatic and splenic

morphology, and impaired development of secondary lymphoid structures within the intestinal epithelium like Peyer's and Crypt patches (Ahern and Maloy, 2020; Bauer et al., 1963; Kamada and Núñez, 2013; Smith et al., 2007). Germ-free animals are particularly hampered in their ability to maintain balance between pro and anti-inflammatory T cell populations, and this dysregulation has been attributed to the presence of microbes such as Segmented Filamentous Bacteria and microbially-derived compounds like polysaccharide A (Ahern and Maloy, 2020; Cox et al., 2014; Gaboriau-Routhiau et al., 2009; Ivanov et al., 2009; Kamada and Núñez, 2013; Mazmanian et al., 2005; Round and Mazmanian, 2009). Fecal transplantation of a donor microbiome, intragastric delivery of an engineered microbial consortium, or delivery of microbially-derived epitopes to germ-free animals can alleviate this T cell dysregulation (Ahern and Maloy, 2020; Kuczma et al., 2020; Lelie et al., 2021; Ostman et al., 2006). Analogously, disruption of the microbiota during the human neonatal period has lasting immunological consequences. Specifically, reducing microbial diversity through caesarian mode-of-delivery and pediatric antibiotic administration has been implicated in intestinal inflammatory phenotypes and the development of allergic disease (Ahmadizar et al., 2017; Cox et al., 2014; Dominguez-Bello et al., 2010; Lynch and Boushey, 2016; Riiser, 2015; Romano-Keeler et al., 2014), highlighting that both the presence and maintenance of the microbiome is critical to host immunological health.

Another primary function of the microbiome is to prevent pathogenic species from colonizing the gastrointestinal tract. The microbiota employs multiple strategies to provide colonization resistance which can be categorized into host-microbe interactions (promoting integrity of the intestinal epithelial barrier, immune activation and recruitment, and generation of antimicrobial compounds) and microbial interactions (synthesis of bacteriocins, bacteriophages, and nutrient-based competitive exclusion) (Ducarmon et al., 2019; Ghosh et al., 2021; Greathouse

et al., 2015; Kim et al., 2018). Specifically, the host physically partitions microbes away from the epithelium via a dense mucosal layer and secretion of antimicrobial peptides, while the microbiota bolsters the integrity of this barrier by providing metabolites that promote the expression of mucus synthesis and tight junction formation (Anderson et al., 2010; Cash et al., 2006; Ewaschuk et al., 2008; Ghosh et al., 2021; Hooper et al., 2003; Rajbir Singh et al., 2019; Woo et al., 2021). Accordingly, defects in the mucus barrier are a major determinant of enteric pathogen susceptibility. Antibiotic depletion of beneficial microbes or overgrowth of muciniphilic taxa like *Akkermansia muciniphila* can result in mucus breakdown and place the host in a pathogen-susceptible state (Alipour et al., 2016; Feng et al., 2019; Ganesh et al., 2013; Jakobsson et al., 2015; Theriot et al., 2016; Wlodarska et al., 2011). Thus, the composition of the microbiome is crucial to maintaining gut structural and spatial integrity (Ducarmon et al., 2019; Duncan et al., 2021; Zarepour et al., 2013). Antibiotic depletion of the microbiota also decreases colonization resistance because native species are known to generate pathogen-antagonistic metabolites; in fact, microbiota-derived bacteriocins and lethal pheromone plasmids have been identified to inhibit prominent infectious agents including, but not limited to, vancomycin-resistant *Enterococci*, *Clostridioides difficile*, enteropathogenic *Escherichia coli*, and *Salmonella enterica* (Corr et al., 2007; Gilmore et al., 2015; Hrala et al., 2021; Rea et al., 2010; Sharma et al., 2020).

Perhaps the most critical function of the microbiome is its role in nutrient metabolism and energy harvest. While the mammalian small intestine is highly efficient at nutrient absorption, certain molecules like complex polysaccharides and dietary fibers are undigestible by host enzymes (Chassard and Lacroix, 2013; Koepsell, 2020; Oliphant and Allen-Vercoe, 2019). Meanwhile, the colonic microbiome is highly adapted to the fermentation of these molecules, as it possesses an extensive carbohydrate-focused gene repertoire (Gill et al., 2006; Kaoutari et al.,

2013; Tasse et al., 2010). The metabolites generated by carbohydrate fermentation can be subsequently funneled back to the host; thus, the microbiota allows for energy salvage from otherwise inaccessible resources (Chassard and Lacroix, 2013; Hooper et al., 2001; Oliphant and Allen-Vercoe, 2019; J. L. Sonnenburg et al., 2005). For example, fiber fermentation generates short-chain fatty acids (SCFA) like acetate, butyrate, and propionate, which are a primary nutrient source for intestinal colonocytes (Chassard and Lacroix, 2013; Donohoe et al., 2011). Metabolically active colonocytes, in turn, lower the local pH and increase anaerobicity of the colon, thus effectively selecting for the presence of carbohydrate-fermenting obligate anaerobes (Furuta et al., 2001; Litvak et al., 2018). Although carbohydrates function as the primary nutrient source for intestinal microbes, the microbiome also participates in the digestion of proteins, lipids, vitamins, and xenobiotics (Jandhyala et al., 2015; Oliphant and Allen-Vercoe, 2019). The importance of the microbiome in nutritional harvest can be further gleaned from perturbation studies. For example, germ-free mice are notably leaner than their conventional counterparts, and experience rapid weight gain and fat storage after receiving microbiome transplantation without experiencing hyperphagia (Bäckhed et al., 2004). Computational analysis of the microbiome from obese mice indicates increased capacity for energy harvest compared to lean mice (Turnbaugh et al., 2006). Finally, antibiotic depletion of the microbiome changes colonic metabolism and reduces the overall capacity for dietary energy capture (Basolo et al., 2020; Zarrinpar et al., 2018). Together, it is undeniable that the intricate associations between mammals and their microbes are critical for proper health and development. It is likely that the functions of the microbiome have been critical to host survival, and this may explain why these communities are omnipresent and exhibit high functional redundancy.

Analytical Methods for Studying the Microbiome

Characterizing Microbiome Structure:

The development and commercialization of massively parallel sequencing technologies in the early 2000s was foundational to the study of the microbiome (Quail et al., 2012; Weinstock, 2012). Replicating the intestinal milieu via *in vitro* culture continues to be a major experimental roadblock for microbiome studies, thus the field has relied heavily on sequencing for sample capture (Hitch et al., 2021; Mori and Kamagata, 2014). Currently, taxonomic classification is conducted using either marker gene-based amplicon sequencing or shotgun metagenomics (Y.-X. Liu et al., 2021). The former relies on the small subunit of the 16S ribosomal RNA (rRNA) as a marker, since this gene has both near-ubiquitous conservation and mutable hypervariable regions (Pace, 1997; Clarridge, 2004; Gray et al., 1984; Patwardhan et al., 2014). While 16S rRNA sequencing is highly affordable, it suffers from hypervariable region-dependent amplification bias, fails to reach species and strain-level taxonomic resolution, and fails to provide functional information (Bukin et al., 2019; Poretsky et al., 2014). While computational approaches like PICRUSt have been developed to infer functionality from 16S data, shotgun metagenomics provides a more robust characterization of taxonomic composition and community functional potential (Douglas et al., 2020; Y.-X. Liu et al., 2021; Poretsky et al., 2014). Metagenomic sequencing can yield comprehensive annotations of bacteria, fungi, archaea, viruses, and eukaryotic parasites from a single sample due to lack of amplification bias during library generation (Y.-X. Liu et al., 2021; Qin et al., 2010; Vemuri et al., 2020). By providing coverage of entire genomes, metagenomics also allows for functional inference via gene content abundance (Qin et al., 2010). However, the sequencing depth required to obtain said coverage can make this method costly, and annotation of gene content is limited by the completeness of reference bases

used during sequence alignment (Raes et al., 2007; W.-L. Wang et al., 2015). Another drawback of metagenomics is that it is unable to provide transcriptional information, but parallel analyses are often employed alongside metagenomics to overcome this limitation.

Characterizing Microbiome Function:

Metatranscriptomics, the sequencing of total RNA from complex samples, provides a direct assessment of active transcription within the microbiome and, when paired with metagenomics, can yield gene expression data that is normalized for both taxonomic and gene abundances (Chung et al., 2020; Deng et al., 2018; Franzosa et al., 2018; Zhang et al., 2021). Just like metagenomics, metatranscriptomics requires incredibly high sequencing depth and can be cost prohibitive thus it is less frequently implemented in microbiome studies (Aguar-Pulido et al., 2016; Bashiardes et al., 2016; Monleon-Getino and Frias-Lopez, 2020). Sequencing reads can be mapped to multiple functional databases including the Kyoto Encyclopedia of Genes and Genomes, MetaCyc pathways, Carbohydrate-Active Enzymes, SEED Subsystems, antibiotic resistance genes, and others, facilitating a wide examination of functional activity within a single study (Cantarel et al., 2009; Kanehisa and Goto, 1999; Karp et al., 2000; B. Liu and Pop, 2009; Overbeek et al., 2014). Additionally, reads can be mapped to individual reference genomes allowing for single-species RNA sequencing from metatranscriptomics reads (Cabral et al., 2019; Deng et al., 2018). While this is robust, it is important to note that annotation and alignment are limited by the maintenance of the reference database of choice (Bashiardes et al., 2016). Another limitation of metatranscriptomics is that RNA preparations are typically contaminated with rRNAs and host-derived messenger RNAs, although library preparation protocols now routinely include rRNA and mRNA depletion steps, and *in silico* quality control methods can be implemented to remove

contaminating reads for which a reference genome or database is available (Aguiar-Pulido et al., 2016; Bashiardes et al., 2016; McIver et al., 2018).

An inherent limitation to metatranscriptomic data is that it fails to provide information regarding post-transcriptional enzymatic activity or biotransformation of environmental metabolites. Comprehensive study designs can use methods like metaproteomics and metabolomics alongside sequencing to provide these data (Abbondio et al., 2019; Aguiar-Pulido et al., 2016; Blakeley-Ruiz et al., 2019; Chuang et al., 2012; Kuang et al., 2020; Lei et al., 2011; Nusbaum et al., 2018; Obrenovich et al., 2017; Piccolo et al., 2018; Salvato and Hettich, 2021; Wikoff et al., 2009; Yasuda et al., 2020; Yu et al., 2018). Both metaproteomics and metabolomics employ chromatography, compound ionization, and mass spectrometry to provide spectral peaks affiliated with specific peptides or heterogeneous metabolites, respectively (Aguiar-Pulido et al., 2016; Isaac et al., 2019; Salvato and Hettich, 2021). These spectra are then aligned to relevant databases and thus are subject to the same database limitations as sequencing technologies (Isaac et al., 2019; Salvato and Hettich, 2021). Recently, some computational pipelines have begun to account for variations between anaerobic and aerobic compound metabolism and have generated anaerobically focused spectral databases (Han et al., 2021). Hopefully, the accuracy of these platforms will continue to improve alongside database annotation and curation as ion annotation is the major bottleneck of these technologies. Despite these limitations, an undeniable strength of metabolomics is the ability to perform quantitatively focused “targeted” or hypothesis agnostic “untargeted” analyses, and the capacity of the technology to detect compounds with significant variation in thermostability, volatility and polarity (Aguiar-Pulido et al., 2016; Chen et al., 2019; H. Luan et al., 2019). Ultimately, comprehensive analyses of microbial ecosystems should employ both structural and functional assessments in their study design.

Impacts of Dietary Macronutrient Composition on Microbiome Community Dynamics

Nutrient availability is one of the strongest selective pressures on the structure and function of the microbiome. Within the colon, nutrient abundance is shaped by the composition of the host diet, host macronutrient uptake efficiency, and host pancreaticobiliary sections, all of which subsequently impact microbial metabolic function (Reese and Carmody, 2019). Dietary composition has been postulated as a primary driver of mature microbiome assemblage in humans (Johnson et al., 2019; A. W. Walker et al., 2011; Xu and Knight, 2015). For example, the typical microbiota of industrialized nations significantly differs from those of hunter-gather tribes, in large part due to differences in the macronutrient content of their preferred diets (Smits et al., 2017; E. D. Sonnenburg and J. L. Sonnenburg, 2014). Industrialized (Western) diets are enriched for simple sugars, animal proteins, animal-derived fats, and are significantly lacking in dietary fiber compared to non-Western diets (Zinöcker and Lindseth, 2018). These macronutrient differences have significant impacts on carbohydrate and lipid metabolism within the microbiome and can induce multiple negative metabolic phenotypes for the host (Kanoski et al., 2014; Qi et al., 2009; Zinöcker and Lindseth, 2018). The low levels of fiber within a Western diet functionally starves obligate anaerobes that rely on carbohydrate fermentation, instead promoting mucolytic behavior in *Bacteroides* and bolstering the expansion of muciniphiles like *A. muciniphila* (Bisanz et al., 2019; Desai et al., 2016). The resultant cleavage of mucus oligosaccharides makes the underlying sugar structures available to other members of the community, further disrupting gut metabolic homeostasis (Desai et al., 2016; Turnbaugh et al., 2009; Chassard and Lacroix, 2013; Reese and Carmody, 2019; Smits et al., 2016). As previously stated, this disruption can prime the host for a slew of acute conditions including decreased colonization resistance, and these perturbed

phenotypes are transferable to germ-free animals during microbiome transplantation (Desai et al., 2016; Turnbaugh et al., 2008).

Consumption of Western diets also greatly perturbs lipid homeostasis, increasing the overall secretion of primary bile acids to increase fatty acid emulsification. While most bile acids are recycled in the upper GI a fraction does migrate to the colon (Reese and Carmody, 2019). Once there, primary bile acids can either exhibit bactericidal activity, promote the sporulation of intestinal pathogens like *C. difficile*, or be subjected to biotransformation by bile-resistant members of the microbiome (Greathouse et al., 2015; Reese and Carmody, 2019; Ridlon et al., 2014). Interestingly, Western diets can shift the preferential conjugation of primary bile acids from glycine to taurine, which is a more favorable conjugation for pathobiont expansion (David et al., 2014; Devkota et al., 2012). Changes in microbiome metabolism in response to Western diet consumption can occur within 12 hours, and can additionally involve modifications to protein, polyphenol, and vitamin metabolism (Reese and Carmody, 2019; Schoeler and Caesar, 2019; X. Zheng et al., 2017). Thus, the degree to which dietary composition influences the microbiome is profound and represent a near-constant selective pressure on this ecosystem.

Impacts of Host Metabolic Disease on Microbiome Community Dynamics

Given its significant role in macronutrient metabolism, the microbiome and host metabolic function are dynamically linked. This is especially apparent when examining patient populations with metabolic diseases like dysglycemia, type-I and type-II diabetes mellitus, and obesity. These diseases have complex pathologies involving multiple organ systems, but all feature notable shifts in microbiome composition and function (Aw and Fukuda, 2018; Fabbiano et al., 2017; Hartstra et al., 2015; Herrema and Niess, 2020; Sabatino et al., 2017; Scheithauer et al., 2020; P. Zheng et

al., 2018). Metabolic dysregulation has been characterized by the loss of multiple SCFA-producing and carbohydrate-fermenting taxa that is concurrent with the expansion of pro-inflammatory pathobionts in multiple clinical cohorts with varying age and geographic locals (Kostic et al., 2015; Y. Liu et al., 2020; Q. Ma et al., 2020; Qin et al., 2012; Rotimi, 2020; Thingholm et al., 2019). This taxonomic restructuring regularly occurs before diagnosis and can be used to predict if certain therapies will ameliorate glucose dysregulation (Boursi et al., 2015; Kostic et al., 2015; Y. Liu et al., 2020). Functionally, the microbiota of metabolically perturbed hosts has reduced capacity for carbohydrate fermentation and modified expression of genes involved in the metabolism of branched chain and aromatic amino acids, long-chain fatty acids, polyunsaturated fatty acids, and oxidative stress responses, as well as an overall shift away from nutrient biosynthesis in favor of passive nutrient transport (Kostic et al., 2015; Org et al., 2017; Qin et al., 2012; Wu et al., 2020; Zhou et al., 2019). In some cases, dysglycemic patients experience microbial infiltration of the epithelial mucosa, demonstrating a conversion towards mucolytic behavior by the microbiota (Chassaing et al., 2017).

Drastic shifts in microbiome taxonomy and function also occur in animal models of metabolic disease. There are many strategies to perturb metabolic homeostasis in rodents, although no model perfectly recapitulates the complex pathology of human disease. Models can elicit desired phenotypes via genetic manipulation (*ob/ob*, NOD, Akita), dietary supplementation (diet-induced obesity), or chemotherapeutic administration (streptozotocin, alloxan), and the selection of model is dependent on research questions and which variables are most desired to control for (Al-awar et al., 2016; Deeds et al., 2011; Skovsø, 2014; C.-Y. Wang and Liao, 2011). Early work in *ob/ob* mice demonstrated that, like in humans, microbial gene content can be correlated with obesity, dyslipidemia, and fatty liver disease (Devaraj et al., 2013; Ley et al., 2005). The reduction

of carbohydrate fermenting taxa upon type-II diabetic onset occurs in multiple rodent models, and is concurrent with increased mucolytic activity and oxidative stress within the microbiome, suggesting that diabetic host signaling can directly impact microbiology ecology in the gut (S. Liu et al., 2019; Q. Ma et al., 2020; Piccolo et al., 2018; Sabatino et al., 2017; Thaïss et al., 2018). Interestingly, recent work has demonstrated that antibiotic-mediated disruption of Firmicutes within the gut can perturb carbohydrate and lipid metabolism, and that early-life antibiotic administration accelerates the onset of metabolic disease phenotypes in susceptible mouse strains (Livanos et al., 2016; Patterson et al., 2015; Rajpal et al., 2015). Together, clinical and animal data highlight how tightly connected microbial and host health are in relation to metabolic homeostasis. Additionally, these data reveal how disruption of either the host or the microbiome has profound impacts on the other. Microbial metabolism in the gut ecosystem is inextricably linked to host-provided metabolites that are, in part, dictated by host metabolic well-being.

The Relationship Between Microbial Metabolism and Antibiotic Susceptibility

Antibiotic-Induced Dysbiosis

Microbiome dysbiosis related to antibiotic administration significantly perturbs the gut ecosystem and has both chronic and acute consequences for the host, including impairments in metabolic function, colonization resistance, and immune regulation, as mentioned previously (Buffie et al., 2012; Cox et al., 2014; Kim et al., 2018; Ni et al., 2019; M. Y. Yoon and S. S. Yoon, 2018). Antibiotics deplete taxonomic diversity within hours of administration, reducing the abundance of carbohydrate-fermenting obligate anaerobes and promoting the outgrowth of facultative anaerobes like Proteobacteria (Cabral et al., 2019; Dethlefsen and Relman, 2011; Litvak et al., 2017). The exact taxonomic shifts that occur in response to antibiotics are dictated by a

combination of antibiotic spectrum of activity, length of treatment, route of administration, and individual differences in host diet, and physiology (Cabral et al., 2019; Dethlefsen and Relman, 2011; Ferrer et al., 2017; Gao et al., 2019; Iizumi et al., 2017; Ng et al., 2019). Changes in taxonomic composition can also be influenced by intrinsic and acquired antibiotic resistances amongst gut microbes (Hollenbeck and Rice, 2012; Penders et al., 2013). Perhaps unsurprisingly, antibiotic treatment elicits significant changes to the functional capacity of the microbiome as measured via multi-omic methodologies (Antunes et al., 2011; Cabral et al., 2019; Ferrer et al., 2017; Hernandez et al., 2013; Korry et al., 2020). Drug challenge profoundly perturbs metabolic homeostasis of carbohydrates, bile acids, and steroid hormone conjugations, impacting almost 90 percent of the intestinal metabolome in some studies (Antunes et al., 2011; Cabral et al., 2019; Hernandez et al., 2013). Antibiotic treatment can also elicit transcriptional changes in the resistome (gene content specifically involved in antibiotic resistance) by creating intense selective pressure for resistance acquisition (Korry et al., 2020; Penders et al., 2013). Because the microbiome is natively resilient, much of its compositional diversity returns after antibiotic cessation, however this can be delayed by months or years, and many individual strains are permanently lost (Koo et al., 2019; Lozupone et al., 2012; Ng et al., 2019; L. P. Shaw et al., 2019). This is particularly true of antibiotic administration during the neonatal period, which has lasting impacts on microbiome function throughout life (Ainonen et al., 2021; Cox et al., 2014; S. Y. Shaw et al., 2010; Stewart et al., 2018). However, functional redundancy within the microbiome ensures that most of the primary functions of the microbiome are still fulfilled to a degree. A pressing question within the field has been what factors dictate the functional responses of the microbiota to drug challenge.

Metabolism Determines Bactericidal Antibiotic Susceptibility

Until recently, the prevailing school of thought has been that bactericidal antibiotics were able to actively kill bacterial cells through the inhibition of their primary biological target. For example, β -lactam antibiotics inhibit cell wall synthesis by interrupting the cross-linking of peptidoglycan while fluoroquinolones inhibit the replication machinery by blocking DNA gyrase and topoisomerase IV (Cho et al., 2014; de Lastours and Fantin, 2015; Falla and Chopra, 1998). Interruption of these processes leads to cell lysis and lethal double-stranded DNA breaks, respectively.

In the early 2000s it was proposed that futile cycling also induces bactericidal activity via the generation and accumulation of reactive oxygen species (ROS) (Kohanski et al., 2007). Once an antibiotic has locked into its target substrate, the bacterial cell is subsequently sent into a toxic futile cycle where it continues to synthesize cellular components that are doomed for immediate breakdown (Adolfson and Brynildsen, 2015). Ultimately, the continual synthesis and degradation of cellular components incurs a high metabolic demand and induces cell death via depletion of intracellular ATP stores and concurrent ROS toxicity (Adolfson and Brynildsen, 2015; Stokes et al., 2019). Multiple research groups have provided supporting evidence for this model, suggesting that bactericidal activity is a multidimensional process that involves a metabolic component (Belenky et al., 2015; Cho et al., 2014; Dwyer et al., 2014; Ferrándiz et al., 2016; Hong et al., 2019; Lam et al., 2020; G. Luan et al., 2018; Stokes et al., 2019; Van Acker and Coenye, 2017; Zhao et al., 2015). Bacterial metabolic state has been demonstrated to mediate antibiotic susceptibility, where permissive metabolic processes that generate ATP (like the tricarboxylic acid cycle (TCA)) contribute to antibiotic lethality via ROS toxicity (Adolfson and Brynildsen, 2015; Belenky et al., 2015; Lobritz et al., 2015; Meylan et al., 2017; Mok et al., 2015; Ranji Singh et al.,

2009; Stokes et al., 2019; Thomas et al., 2013). Furthermore, metabolic starvation and mutations that divert metabolism away from the TCA cycle or reduce electron transport are known antibiotic tolerance mechanisms in select pathogens (Ahn et al., 2016; Cabral et al., 2018; Lee et al., 2018; Nguyen et al., 2011; Ranji Singh et al., 2009; Thomas et al., 2013). Thus, changes in metabolism that decrease metabolic rate, like a switch to fermentation or use of anaerobic electron acceptors, reduce bactericidal drug activity (Baek et al., 2011; Conlon et al., 2016; Greulich et al., 2015; Gusarov et al., 2009; Lobritz et al., 2015). In fact, bacterial metabolic rate was recently demonstrated to be one of the best predictors of susceptibility *in vitro* (Lopatkin et al., 2019). While these works have revolutionized our mechanistic understanding of antibiotic susceptibility, the bulk of this work has been conducted *in vitro* with species that are highly genetically tractable. The question then becomes if this holds true within dynamic polymicrobial ecosystems like the microbiome.

Cabral et al. recently demonstrated that microbial metabolism is tightly linked with bactericidal antibiotic activity within the context of the gut microbiome (Cabral et al., 2019). 12-hour administration of amoxicillin reduces the overall metabolic capacity of the microbiome, suggesting that the taxa who survive drug treatment can induce a metabolic-based tolerance phenotype. In this work, the gut symbiont *Bacteroides thetaiotaomicron* was able to dominate the post-antibiotic treated microbiome by efficiently prioritizing the fermentation of dietary-derived complex polysaccharides. Cabral et al. found that supplementation with glucose modulated amoxicillin susceptibility in this species both *in vivo* and *in vitro*, proposing that carbohydrate substrate availability can impact bactericidal activity *in vivo* via modifications of microbial metabolism (Cabral et al., 2019).

Thesis Overview and Summary of Findings

The goal of this dissertation is to expand upon the hypothesis that carbon source availability and microbial metabolism dictate the severity of antibiotic-induced dysbiosis within the microbiome. Specifically, this work aims to take an ecology and systems-sensitive examination of host-related factors that can shape the local nutrient pool within the cecum, including dietary composition and host metabolic health. This work utilizes and integrates multiple high throughput ‘omics methods including metagenomics, metatranscriptomics, and metabolomics, to gain a holistic examination of diet and host metabolism on gut microbiome function during antibiotic treatment. Chapter 2 characterizes the impact that short-term consumption of a Western diet has on ciprofloxacin toxicity within the gut. We found that the microbiota of mice consuming the Western diet was enriched for mucolytic behavior and simple sugar sequestration which subsequently increased transcription of glycolysis and reduced polysaccharide fermentation. By placing the community in a more metabolically permissive state, the Western diet enhanced the microbiome’s susceptibility to ciprofloxacin, demonstrating that dietary-induced changes in the gut nutrient pool can potentiate bactericidal antibiotics.

Chapter 3 examines the degree to which host metabolic dysfunction contributes to antibiotic-induced dysbiosis. In this work we used the chemotherapeutic streptozotocin (STZ) to induce rapid hyperglycemia in mice without dietary modification, then performed multi-omic profiling of the cecum before and after amoxicillin administration. We found that STZ-induced hyperglycemia caused an expansion of *A. muciniphila* and significantly restructured both the transcriptional and metabolite landscape of the cecum before antibiotic treatment. Specifically, STZ promoted a shift away from polysaccharide fermentation and increased primary respiration by the microbiota. This resulted in significantly higher antibiotic susceptibility within the gut. STZ

pre-treatment exaggerated the loss of Firmicutes and expansion of *B. thetaiotaomicron*, and completely restructured how the larger community and *B. thetaiotaomicron* transcriptionally responded to amoxicillin exposure. Lastly, we challenged STZ and amoxicillin co-treated mice (as well as normoglycemic controls) with an intragastric infection of *S. enterica* Typhimurium to assess how STZ and amoxicillin co-treatment impacted colonization resistance. We found that hyperglycemic animals were more susceptible to colonization, suffered further microbiome dysbiosis, and had reduced survival compared to normoglycemic and vehicle-treated control animals.

Together the data presented in Chapters 2 and 3 demonstrate that alterations to the cecal nutrient pool, either through diet or through disruption of host metabolic homeostasis, are sufficient to worsen bactericidal antibiotic-induced dysbiosis. Additionally, these data show that these antibiotics are potentiated in Western diet-fed and hyperglycemic animals due to changes in the metabolic behavior of the gut microbiome. Overall, these data highlight the need to contextualize host-related activities in any examination of microbiome-related antibiotic damage, and that host behavior should be considered during the development of therapeutic strategies designed to mitigate dysbiosis.

References

- Abbondio, M., Palomba, A., Tanca, A., Fraumene, C., Pagnozzi, D., Serra, M., Marongiu, F., Laconi, E., Uzzau, S., 2019. Fecal Metaproteomic Analysis Reveals Unique Changes of the Gut Microbiome Functions After Consumption of Sourdough Carasau Bread. *Front. Microbiol.* 10, 1–13. doi:10.3389/fmicb.2019.01733
- Adolfson, K.J., Brynildsen, M.P., 2015. Futile cycling increases sensitivity toward oxidative stress in *Escherichia coli*. *Metab. Eng.* 29, 26–35. doi:10.1016/j.ymben.2015.02.006
- Aguiar-Pulido, V., Huang, W., Suarez-Ulloa, V., Cickovski, T., Mathee, K., Narasimhan, G., 2016. Metagenomics, Metatranscriptomics, and Metabolomics Approaches for Microbiome Analysis: Supplementary Issue: Bioinformatics Methods and Applications for Big Metagenomics Data. *Evol. Bioinform.* 12, 1–12. doi:10.4137/EBO.S36436
- Ahern, P.P., Maloy, K.J., 2020. Understanding immune–microbiota interactions in the intestine. *Immunology* 159, 4–14. doi:10.1111/imm.13150
- Ahmadizar, F., Vijverberg, S., Arets, H., de Boer, A., Lang, J.E., Garssen, J., Kraneveld, A., Maitland-van der Zee, A.H., 2017. Early-life antibiotic exposure increases the risk of developing allergic symptoms later in life: A meta-analysis. *Allergy* 73, 971–986. doi:10.1111/all.13332
- Ahn, S., Jung, J., Jang, I.-A., Madsen, E.L., Park, W., 2016. Role of Glyoxylate Shunt in Oxidative Stress Response. *J. Biol. Chem.* 291, 11928–11938. doi:10.1074/jbc.M115.708149
- Ainonen, S., Tejesvi, M.V., Mahmud, M.R., Paalanne, N., Pokka, T., Li, W., Nelson, K.E., Salo, J., Renko, M., Vänni, P., Pirttilä, A.M., Tapiainen, T., 2021. Antibiotics at birth and later antibiotic courses: effects on gut microbiota. *Pediatr. Res.* 1–9. doi:10.1038/s41390-021-01494-7
- Al-awar, A., Kupai, K., Veszelka, M., Szücs, G., Attieh, Z., Murlasits, Z., Török, S., Pósa, A., Varga, C., 2016. Review Article Experimental Diabetes Mellitus in Different Animal Models. *J. Diabetes Res.* 2016, 1–12. doi:10.1155/2016/9051426
- Alipour, M., Zaidi, D., Valcheva, R., Jovel, J., Martínez, I., Sergi, C., Walter, J., Mason, A.L., Wong, G.K.-S., Dieleman, L.A., Carroll, M.W., Huynh, H.Q., Wine, E., 2016. Mucosal Barrier Depletion and Loss of Bacterial Diversity are Primary Abnormalities in Paediatric Ulcerative Colitis. *J. Crohns Colitis* 10, 462–471. doi:10.1093/ecco-jcc/jjv223
- Anderson, R.C., Cookson, A.L., McNabb, W.C., Park, Z., McCann, M.J., Kelly, W.J., Roy, N.C., 2010. *Lactobacillus plantarum* MB452 enhances the function of the intestinal barrier by increasing the expression levels of genes involved in tight junction formation. *BMC Microbiol.* 10, 1–11. doi:10.1186/1471-2180-10-316
- Antunes, L.C.M., Han, J., Ferreira, R.B.R., c, P.L., Borchers, C.H., Finlay, B.B., 2011. Effect of antibiotic treatment on the intestinal metabolome. *Antimicrob. Agents Chemother.* 55, 1494–1503. doi:10.1128/AAC.01664-10
- Arumugam, M., Raes, J., Pelletier, E., Le Paslier, D., Yamada, T., Mende, D.R., Fernandes, G.R., Tap, J., Bruls, T., Batto, J.-M., Bertalan, M., Borruel, N., Casellas, F., Fernandez, L., Gautier, L., Hansen, T., Hattori, M., Hayashi, T., Kleerebezem, M., Kurokawa, K., Leclerc, M., Levenez, F., Manichanh, C., Nielsen, H.B., Nielsen, T., Pons, N., Poulain, J., Qin, J., Sicheritz-Ponten, T., Tims, S., Torrents, D., Ugarte, E., Zoetendal, E.G., Wang, J., Guarner, F., Pedersen, O., De Vos, W.M., Brunak, S., Doré, J., Weissenbach, J., Ehrlich, S.D., Bork, P., 2011. Enterotypes of the human gut microbiome. *Nature* 473, 174–180. doi:10.1038/nature09944

- Aw, W., Fukuda, S., 2018. Understanding the role of the gut ecosystem in diabetes mellitus. *J. Diabetes Investig.* 9, 5–12. doi:10.1111/jdi.12673
- Baek, S.-H., Li, A.H., Sassetti, C.M., 2011. Metabolic Regulation of Mycobacterial Growth and Antibiotic Sensitivity. *PLoS Biol.* 9, e1001065. doi:10.1371/journal.pbio.1001065
- Bashiardes, S., Zilberman-Schapira, G., Elinav, E., 2016. Use of Metatranscriptomics in Microbiome Research. *Bioinform. Biol. Insights* 10, 1–7. doi:10.4137/BBI.S34610
- Basolo, A., Hohenadel, M., Ang, Q.Y., Piaggi, P., Heinitz, S., Walter, M., Walter, P., Parrington, S., Trinidad, D.D., Schwartzenberg, R.J., Turnbaugh, P.J., Krakoff, J., 2020. Effects of underfeeding and oral vancomycin on gut microbiome and nutrient absorption in humans. *Nat. Med.* 26, 589–598. doi:10.1038/s41591-020-0801-z
- Bauer, H., Horowitz, R.E., Levenson, S.M., Popper, H., 1963. The Response of the Lymphatic Tissue to the Microbial Flora. Studies on Germfree Mice. *Am. J. Pathol.* 42, 471–483.
- Bäckhed, F., Ding, H., Wang, T., Hooper, L.V., Koh, G.Y., Nagy, A., Semenkovich, C.F., Gordon, J.I., 2004. The gut microbiota as an environmental factor that regulates fat storage. *Proc. Natl. Acad. Sci. USA.* 101, 15718–15723. doi:10.1073/pnas.0407076101
- Belenky, P., Ye, J.D., Porter, C.B.M., Cohen, N.R., Lobritz, M.A., Ferrante, T., Jain, S., Korry, B.J., Schwarz, E.G., Walker, G.C., Collins, J.J., 2015. Bactericidal Antibiotics Induce Toxic Metabolic Perturbations that Lead to Cellular Damage. *Cell Rep.* 13, 968–980. doi:10.1016/j.celrep.2015.09.059
- Berg, G., Rybakova, D., Fischer, D., Cernava, T., Vergès, M.-C.C., Charles, T., Chen, X., Cocolin, L., Eversole, K., Corral, G.H., Kazou, M., Kinkel, L., Lange, L., Lima, N., Loy, A., Macklin, J.A., Maguin, E., Mauchline, T., McClure, R., Mitter, B., Ryan, M., Sarand, I., Smidt, H., Schelkle, B., Roume, H., Kiran, G.S., Selvin, J., de Souza, R.S.C., Overbeek, L., Singh, B.K., Wagner, M., Walsh, A., Sessitsch, A., Schloter, M., 2020. Microbiome definition re-visited: old concepts and new challenges. *Microbiome* 8, 1–22. doi:10.1186/s40168-020-00875-0
- Bigger, J.W., 1944. Treatment of Staphylococcal Infections with Penicillin by Intermittent Sterilisation. *The Lancet* 244, 497–500. doi:10.1016/S0140-6736(00)74210-3
- Bisanz, J.E., Upadhyay, V., Turnbaugh, J.A., Ly, K., Turnbaugh, P.J., 2019. Meta-Analysis Reveals Reproducible Gut Microbiome Alterations in Response to a High-Fat Diet. *Cell Host Microbe* 26, 265–272. doi:10.1016/j.chom.2019.06.013
- Blakeley-Ruiz, J.A., Erickson, A.R., Cantarel, B.L., Xiong, W., Adams, R., Jansson, J.K., Fraser, C.M., Hettich, R.L., 2019. Metaproteomics reveals persistent and phylum-redundant metabolic functional stability in adult human gut microbiomes of Crohn’s remission patients despite temporal variations in microbial taxa, genomes, and proteomes. *Microbiome* 7, 1–15. doi:10.1186/s40168-019-0631-8
- Blaser, M., 2011. Antibiotic overuse: Stop the killing of beneficial bacteria. *Nature* 476, 393–394. doi:10.1038/476393a
- Boursi, B., Mantani, R., Haynes, K., Yang, Y.-X., 2015. The effect of past antibiotic exposure on diabetes risk. *Eur. J. Endocrinol.* 172, 639–648. doi:10.1530/EJE-14-1163
- Buffie, C.G., Jarchum, I., Equinda, M., Lipuma, L., Gouberne, A., Viale, A., Ubeda, C., Xavier, J., Pamer, E.G., 2012. Profound alterations of intestinal microbiota following a single dose of clindamycin results in sustained susceptibility to *Clostridium difficile*-induced colitis. *Infect. Immun.* 80, 62–73. doi:10.1128/IAI.05496-11
- Bukin, Y.S., Galachyants, Y.P., Morozov, I.V., Bukin, S.V., Zakharenko, A.S., Zemskaya, T.I., 2019. The effect of 16S rRNA region choice on bacterial community metabarcoding results. *Sci. Data* 6, 190007. doi:10.1038/sdata.2019.7

- Cabral, D.J., Penumutchu, S., Reinhart, E.M., Zhang, C., Korry, B.J., Wurster, J.I., Nilson, R., Guang, A., Sano, W.H., Rowan-Nash, A.D., Li, H., Belenky, P., 2019. Microbial Metabolism Modulates Antibiotic Susceptibility within the Murine Gut Microbiome. *Cell Metab.* 30, 800–823. doi:10.1016/j.cmet.2019.08.020
- Cabral, D.J., Wurster, J.I., Belenky, P., 2018. Antibiotic Persistence as a Metabolic Adaptation: Stress, Metabolism, the Host, and New Directions. *Pharmaceuticals* 11, 1–19. doi:10.3390/ph11010014
- Cantarel, B.L., Coutinho, P.M., Rancurel, C., Bernard, T., Lombard, V., Henrissat, B., 2009. The Carbohydrate-Active EnZymes database (CAZy): an expert resource for Glycogenomics. *Nucleic Acids Res.* 37, D233–D238. doi:10.1093/nar/gkn663
- Cash, H.L., Whitham, C.V., Behrendt, C.L., Hooper, L.V., 2006. Symbiotic Bacteria Direct Expression of an Intestinal Bactericidal Lectin. *Science* 313, 1126–1130. doi:10.1126/science.1127119
- Centers for Disease Control and Prevention, 2013. Antibiotic resistance threats in the United States. CDC Website. September 16th, 2013
- Chassaing, B., Raja, S.M., Lewis, J.D., Srinivasan, S., Gewirtz, A.T., 2017. Colonic Microbiota Encroachment Correlates with Dysglycemia in Humans. *Cell. Mol. Gastroenterol. Hepatol.* 4, 205–221. doi:10.1016/j.jcmgh.2017.04.001
- Chassard, C., Lacroix, C., 2013. Carbohydrates and the human gut microbiota. *Curr. Opin. Clin. Nutr. Metab. Care* 16, 453–460. doi:10.1097/MCO.0b013e3283619e63
- Chen, M.X., Wang, S.-Y., Kuo, C.-H., Tsai, I.-L., 2019. Metabolome analysis for investigating host-gut microbiota interactions. *J. Formos. Med. Assoc.* 118, S10–S22. doi:10.1016/j.jfma.2018.09.007
- Cho, H., Uehara, T., Bernhardt, T.G., 2014. Beta-lactam antibiotics induce a lethal Malfunctioning of the bacterial cell wall synthesis machinery. *Cell* 159, 1300–1311. doi:10.1016/j.cell.2014.11.017
- Chuang, H.-L., Huang, Y.-T., Chiu, C.-C., Liao, C.-D., Hsu, F.-L., Huang, C.-C., Hou, C.-C., 2012. Metabolomics characterization of energy metabolism reveals glycogen accumulation in gut-microbiota-lacking mice. *J. of Nutr. Biochem.* 23, 752–758. doi:10.1016/j.jnutbio.2011.03.019
- Chung, Y.W., Gwak, H.-J., Moon, S., Rho, M., Ryu, J.-H., 2020. Functional dynamics of bacterial species in the mouse gut microbiome revealed by metagenomic and metatranscriptomic analyses. *PLoS ONE* 15, e0227886–19. doi:10.1371/journal.pone.0227886
- Clarridge, J.E., III, 2004. Impact of 16S rRNA gene sequence analysis for identification of bacteria on clinical microbiology and infectious diseases. *Clin. Microbiol. Rev.* 17, 840–862. doi:10.1128/CMR.17.4.840–862.2004
- Conlon, B.P., Rowe, S.E., Gandt, A.B., Nuxoll, A.S., Donegan, N.P., Zalis, E.A., Clair, G., Adkins, J.N., Cheung, A.L., Lewis, K., 2016. Persister formation in *Staphylococcus aureus* is associated with ATP depletion. *Nat. Microbiol.* 1, 16051. doi:10.1038/nmicrobiol.2016.51
- Corr, S.C., Li, Y., Riedel, C.U., O’Toole, P.W., Hill, C., Gahan, C.G., 2007. Bacteriocin production as a mechanism for the anti-infective activity of *Lactobacillus salivarius* UCC118. *Proc. Natl. Acad. Sci. USA.* 104, 7617–7621. doi:10.1073/pnas.0700440104
- Costello, E.K., Lauber, C.L., Hamady, M., Fierer, N., Gordon, J.I., Knight, R., 2009. Bacterial community variation in human body habitats across space and time. *Science* 326, 1694–1697. doi:10.1126/science.1177486
- Cox, L.M., Yamanishi, S., Sohn, J., Alekseyenko, A.V., Leung, J.M., Cho, I., Kim, S., Li, H., Gao, Z., Mahana, D., Zarate Rodriguez, J.G., Rogers, A.B., Robine, N., Loke, P., Blaser, M.J., 2014.

- Altering the intestinal microbiota during a critical developmental window has lasting metabolic consequences. *Cell* 158, 705–721. doi:10.1016/j.cell.2014.05.052
- David, L.A., Maurice, C.F., Carmody, R.N., Gootenberg, D.B., Button, J.E., Wolfe, B.E., Ling, A.V., Devlin, A.S., Varma, Y., Fischbach, M.A., Biddinger, S.B., Dutton, R.J., Turnbaugh, P.J., 2014. Diet rapidly and reproducibly alters the human gut microbiome. *Nature* 505, 559–563. doi:10.1038/nature12820
- de Lastours, V., Fantin, B., 2015. Impact of fluoroquinolones on human microbiota. Focus on the emergence of antibiotic resistance. *Future Microbiol.* 10, 1241–1255. doi:10.2217/fmb.15.40
- Deeds, M.C., Anderson, J.M., Armstrong, A.S., Gastineau, D.A., Hiddinga, H.J., Jahangir, A., Eberhardt, N.L., Kudva, Y.C., 2011. Single dose streptozotocin-induced diabetes: considerations for study design in islet transplantation models. *Lab Anim.* 45, 131–140. doi:10.1258/la.2010.010090
- Deng, Z.-L., Sztajer, H., Jarek, M., Bhujju, S., Wagner-Döbler, I., 2018. Worlds Apart – Transcriptome Profiles of Key Oral Microbes in the Periodontal Pocket Compared to Single Laboratory Culture Reflect Synergistic Interactions. *Front. Microbiol.* 9, 1–15. doi:10.3389/fmicb.2018.00124
- Desai, M.S., Seekatz, A.M., Koropatkin, N.M., Kamada, N., Hickey, C.A., Wolter, M., Pudlo, N.A., Kitamoto, S., Terrapon, N., Muller, A., Young, V.B., Henrissat, B., Wilmes, P., Stappenbeck, T.S., Núñez, G., Martens, E.C., 2016. A Dietary Fiber-Deprived Gut Microbiota Degrades the Colonic Mucus Barrier and Enhances Pathogen Susceptibility. *Cell* 167, 1339–1353.e1321. doi: 10.1016/j.cell/2016.10.043
- Dethlefsen, L., Relman, D.A., 2011. Incomplete recovery and individualized responses of the human distal gut microbiota to repeated antibiotic perturbation. *Proc. Natl. Acad. Sci. USA.* 108, 4551–4561. doi:10.1073/pnas.1000087107
- Devaraj, S., Hemarajata, P., Versalovic, J., 2013. The human gut microbiome and body metabolism: implications for obesity and diabetes. *Clin. Chem.* 59, 617–628. doi:10.1373/clinchem.2012.187617
- Devkota, S., Wang, Y., Musch, M.W., Leone, V., Fehlner-Peach, H., Nadimpalli, A., Antonopoulos, D.A., Jabri, B., Chang, E.B., 2012. Dietary-fat-induced taurocholic acid promotes pathobiont expansion and colitis in *Il10^{-/-}* mice. *Nature* 487, 104–108. doi:10.1038/nature11225
- Dominguez-Bello, M.G., Costello, E.K., Contreras, M., Magris, M., Hidalgo, G., Fierer, N., Knight, R., 2010. Delivery mode shapes the acquisition and structure of the initial microbiota across multiple body habitats in newborns. *Proc. Natl. Acad. Sci. USA.* 107, 11971–11975. doi:10.1073/pnas.1002601107
- Donohoe, D.R., Garge, N., Zhang, X., Sun, W., O'Connell, T.M., Bunker, M.K., Bultman, S.J., 2011. The Microbiome and Butyrate Regulate Energy Metabolism and Autophagy in the Mammalian Colon. *Cell Metab.* 13, 517–526. doi:10.1016/j.cmet.2011.02.018
- Douglas, G.M., Maffei, V.J., Zaneveld, J.R., Yurgel, S.N., Brown, J.R., Taylor, C.M., Huttenhower, C., Langille, M.G., 2020. PICRUSt2 for prediction of metagenome function. *Nature Biotechnol.* 38, 685–688. doi:10.1038/s41587-020-0548-6
- Ducarmon, Q.R., Zwiittink, R.D., Hornung, B.V.H., van Schaik, W., Young, V.B., Kuijper, E.J., 2019. Gut Microbiota and Colonization Resistance against Bacterial Enteric Infection. *Microbiol. Mol. Biol. Rev.* 83, e00007-19. doi:10.1128/MMBR.00007-19

- Duncan, K., Carey-Ewend, K., Vaishnava, S., 2021. Spatial analysis of gut microbiome reveals a distinct ecological niche associated with the mucus layer. *Gut Microbes* 13, 1–22. doi:10.1080/19490976.2021.1874815
- Dwyer, D.J., Belenky, P.A., Yang, J.H., MacDonald, I.C., Martell, J.D., Takahashi, N., Chan, C.T.Y., Lobritz, M.A., Braff, D., Schwarz, E.G., Ye, J.D., Pati, M., Vercruyse, M., Ralifo, P.S., Allison, K.R., Khalil, A.S., Ting, A.Y., Walker, G.C., Collins, J.J., 2014. Antibiotics induce redox-related physiological alterations as part of their lethality. *Proc. Natl. Acad. Sci. USA*. 111, E2100–E2109. doi:10.1073/pnas.1401876111
- Eckburg, P.B., Bik, E.M., Bernstein, C.N., Purdom, E., Dethlefsen, L., Sargent, M., Gill, S.R., Nelson, K.E., Relman, D.A., 2005. Diversity of the human intestinal microbial flora. *Science* 1635–1658. doi: 10.1126/science.1110591
- Ewaschuk, J.B., Diaz, H., Meddings, L., Diederichs, B., Dmytrash, A., Backer, J., Looijer-van Langen, M., Madsen, K.L., 2008. Secreted bioactive factors from *Bifidobacterium infantis* enhance epithelial cell barrier function. *Am. J. Gastrointest. Liver Physiol.* 295, 1025–1034. doi:10.1152/ajpgi.90227.2008
- Fabbiano, S., Suarez-Zamorano, N., Trajkovski, M., 2017. Host–Microbiota Mutualism in Metabolic Diseases. *Front. Endocrinol.* 8, 1–9. doi:10.3389/fendo.2017.00267
- Faith, J.J., Guruge, J.L., Charbonneau, M., Subramanian, S., Seedorf, H., Goodman, A.L., Clemente, J.C., Knight, R., Heath, A.C., Leibel, R.L., Rosenbaum, M., Gordon, J.I., 2013. The long-term stability of the human gut microbiota. *Science* 341, 1237439. doi:10.1126/science.1237439
- Falla, T.J., Chopra, I., 1998. Joint tolerance to β -lactam and fluoroquinolone antibiotics in *Escherichia coli* results from overexpression of *hipA*. *Antimicrob. Agents and Chemother.* 42, 3282–3284. doi:10.1128/AAC.42.12.3282
- Falony, G., Joossens, M., Vieira-Silva, S., Wang, J., Darzi, Y., Faust, K., Kurilshikov, A., Bonder, M.J., Valles-Colomer, M., Vandeputte, D., Tito, R.Y., Chaffron, S., Rymenans, L., Verspecht, C., Sutter, L.D., Lima-Mendez, G., D'hoë, K., Jonckheere, K., Homola, D., Garcia, R., Tigchelaar, E.F., Eeckhaut, L., Fu, J., Henckaerts, L., Zhernakova, A., Wijmenga, C., Raes, J., 2016. Population-level analysis of gut microbiome variation. *Science* 352, 560–564. doi:10.1126/science.aad3503
- Feng, Y., Huang, Y., Wang, Y., Wang, P., Song, H., Wang, F., 2019. Antibiotics induced intestinal tight junction barrier dysfunction is associated with microbiota dysbiosis, activated NLRP3 inflammasome and autophagy. *PLoS ONE* 14, 1–19. doi:10.1371/journal.pone.0218384
- Ferrándiz, M.J., Martín-Galiano, A.J., Aranz, C., Zimmerman, T., la Campa, de, A.G., 2016. Reactive Oxygen Species Contribute to the Bactericidal Effects of the Fluoroquinolone Moxifloxacin in *Streptococcus pneumoniae*. *Antimicrob. Agents. Chemother.* 60, 409–417. doi:10.1128/AAC.02299-15
- Ferrer, M., Méndez-García, C., Rojo, D., Barbas, C., Moya, A., 2017. Antibiotic use and microbiome function. *Biochem. Pharmacol.* 134, 114–126. doi:10.1016/j.bcp.2016.09.007
- Fleming, A. 1929. On the antibacterial action of cultures of a penicillium, with special reference to their use in the isolation of *B. influenzae*. *Brit. J. of Exp. Pathol.* 10, 226–236.
- Franzosa, E.A., McIver, L.J., Rahnavard, G., Thompson, L.R., Schirmer, M., Weingart, G., Lipson, K.S., Knight, R., Caporaso, J.G., Segata, N., Huttenhower, C., 2018. Species-level functional profiling of metagenomes and metatranscriptomes. *Nat. Methods* 15, 962–968. doi:10.1038/s41592-018-0176-y

- Furuta, G.T., Turner, J.R., Taylor, C.T., Hershberg, R.M., Comerford, K., Narravula, S., Podolsky, D.K., Colgan, S.P., 2001. Hypoxia-inducible Factor 1–dependent Induction of Intestinal Trefoil Factor Protects Barrier Function during Hypoxia. *J. Exper. Med.* 193, 1027–1034. doi:10.1084/jem.193.9.1027
- Gaboriau-Routhiau, V., Rakotobe, S., LEcuyer, E., Mulder, I., Lan, A., Bridonneau, C., Rochet, V., Pisi, A., De Paepe, M., Brandi, G., Eberl, G., Snel, J., Kelly, D., Cerf-Bensussan, N., 2009. The key role of segmented filamentous bacteria in the coordinated maturation of gut helper T cell responses. *Immunity* 31, 677–689. doi:10.1016/j.immuni.2009.08.020
- Ganesh, B.P., Klopffleisch, R., Loh, G., Blaut, M., 2013. Commensal Akkermansia muciniphila Exacerbates Gut Inflammation in Salmonella Typhimurium-Infected Gnotobiotic Mice. *PLoS ONE* 8, 1–15. doi:10.1371/journal.pone.0074963
- Gao, H., Shu, Q., Chen, J., Fan, K., Xu, P., Zhou, Q., Li, C., Zheng, H., 2019. Antibiotic Exposure Has Sex-Dependent Effects on the Gut Microbiota and Metabolism of Short-Chain Fatty Acids and Amino Acids in Mice. *mSystems* 4, 1262–16. doi:10.1128/mSystems.00048-19
- Ghosh, S., Whitley, C.S., Haribabu, B., Jala, V.R., 2021. Regulation of Intestinal Barrier Function by Microbial Metabolites. *Cell. Mol. Gastroenterol. Hepatol.* 11, 1463–1482. doi:10.1016/j.jcmgh.2021.02.007
- Gilbert, J.A., Blaser, M.J., Caporaso, J.G., Jansson, J.K., Lynch, S.V., Knight, R., 2018. Current understanding of the human microbiome. *Nat. Med.* 24, 392–400. doi:10.1038/nm.4517
- Gilbert, J.A., Lynch, S.V., 2019. Community ecology as a framework for human microbiome research. *Nat. Med.* 25, 884–889. doi:10.1038/s41591-019-0464-9
- Gill, S.R., Pop, M., DeBoy, R.T., Eckburg, P.B., Turnbaugh, P.J., Samuel, B.S., Gordon, J.I., Relman, D.A., Fraser-Liggett, C.M., Nelson, K.E., 2006. Metagenomic Analysis of the Human Distal Gut Microbiome. *Science* 312, 1355–1359. doi:10.1126/science.1124234
- Gilmore, M.S., Rauch, M., Ramsey, M.M., Himes, P.R., Varahan, S., Manson, J.M., Lebreton, F., Hancock, L.E., 2015. Pheromone killing of multidrug-resistant Enterococcus faecalis V583 by native commensal strains. *Proc. Natl. Acad. Sci. USA.* 112, 7273–7278. doi:10.1073/pnas.1500553112
- Gray, M.W., Sankoff, D., Cedergren, R.J., 1984. On the evolutionary descent of organisms and organelles: a global phylogeny based on highly conserved structural core in small subunit ribosomal RNA. *Nucleic Acids Res.* 12, 5837–5852. doi:10.1093/nar/12.14.5837
- Greathouse, K.L., Harris, C.C., Bultman, S.J., 2015. Dysfunctional families: Clostridium scindens and secondary bile acids inhibit the growth of Clostridium difficile. *Cell Metab.* 21, 9–10. doi:10.1016/j.cmet.2014.12.016
- Greulich, P., Scott, M., Evans, M.R., Allen, R.J., 2015. Growth-dependent bacterial susceptibility to ribosome-targeting antibiotics. *Mol. Syst. Biol.* 11, 1–11. doi:10.15252/msb.20145949
- Grice, E.A., Kong, H.H., Conlan, S., Deming, C.B., Davis, J., Young, A.C., NISC Comparative Sequencing Program, Bouffard, G.G., Blakesley, R.W., Murray, P.R., Green, E.D., Turner, M.L., Segre, J.A., 2009. Topographical and Temporal Diversity of the Human Skin Microbiome. *Science* 324, 1190–1192. doi:10.1126/science.1171700
- Gusarov, I., Shatalin, K., Starodubtseva, M., Nudler, E., 2009. Endogenous nitric oxide protects bacteria against a wide spectrum of antibiotics. *Science* 325, 1380–1384. doi:10.1126/science.1175439
- Han, S., Treuren, W., Fischer, C.R., Merrill, B.D., DeFelice, B.C., Sanchez, J.M., Higginbottom, S.K., Guthrie, L., Fall, L.A., Dodd, D., Fischbach, M.A., Sonnenburg, J.L., 2021. A

- metabolomics pipeline for the mechanistic interrogation of the gut microbiome. *Nature* 595, 1–33. doi:10.1038/s41586-021-03707-9
- Hartstra, A.V., Bouter, K.E.C., Bäckhed, F., Nieuwdorp, M., 2015. Insights Into the Role of the Microbiome in Obesity and Type 2 Diabetes. *Diabetes Care* 38, 159–165. doi:10.2337/dc14-0769
- Hernandez, E., Bargiela, R., Diez, M.S., Friedrichs, A., Perez-Cobas, A.E., Gosalbes, M.J., Knecht, H., Martinez-Martinez, M., Seifert, J., Bergen, von, M., Artacho, A., Ruiz, A., Campoy, C., Latorre, A., Ott, S.J., Moya, A., Suarez, A., Martins dos Santos, V.A.P., Ferrer, M., 2013. Functional consequences of microbial shifts in the human gastrointestinal tract linked to antibiotic treatment and obesity. *Gut Microbes* 4, 306–315. doi:10.4161/gmic.25321
- Herrema, H., Niess, J.H., 2020. Intestinal microbial metabolites in human metabolism and type 2 diabetes. *Diabetologia* 63, 2533–2547. doi:10.1007/s00125-020-05268-4
- Hitch, T.C.A., Afrizal, A., Riedel, T., Kioukis, A., Haller, D., Lagkouvardos, I., Overmann, J., Clavel, T., 2021. Recent advances in culture-based gut microbiome research. *Int. J. Med. Microbiol.* 311, 151485. doi:10.1016/j.ijmm.2021.151485
- Hollenbeck, B.L., Rice, L.B., 2012. Intrinsic and acquired resistance mechanisms in enterococcus. *Virulence* 3, 421–569. doi:10.4161/viru.21282
- Hong, Y., Zeng, J., Wang, X., Drlica, K., Zhao, X., 2019. Post-stress bacterial cell death mediated by reactive oxygen species. *Proc. Natl. Acad. Sci. USA.* 116, 10064–10071. doi:10.1073/pnas.1901730116
- Hooper, L.V., Stappenbeck, T.S., Hong, C.V., Gordon, J.I., 2003. Angiogenins: a new class of microbicidal proteins involved in innate immunity. *Nat. Immunol.* 4, 269–273. doi:10.1038/ni888
- Hooper, L.V., Wong, M.H., Thelin, A., Hansson, L., Falk, P.G., Gordon, J.I., 2001. Molecular analysis of commensal host-microbial relationships in the intestine. *Science* 291, 881–884. doi: 10.1126/science.291.5505.881
- Hrala, M., Bosak, J., Micenkova, L., Krenova, J., Lexa, M., Pirkova, V., Tomastikova, Z., Kolackova, I., Smajs, D., 2021. Escherichia coli Strains Producing Selected Bacteriocins Inhibit Porcine Enterotoxigenic Escherichia coli (ETEC) under both *In Vitro* and *In Vivo* Conditions. *Appl. Environ. Microbiol.* 87, 1–12. doi:10.1128/AEM.03121-20
- Iizumi, T., Battaglia, T., Ruiz, V., Perez, G.I.P., 2017. Gut Microbiome and Antibiotics. *Arch. Med. Res.* 48, 727–734. doi:10.1016/j.arcmed.2017.11.004
- Isaac, N.I., Philippe, D., Nicholas, A., Raoult, D., Eric, C., 2019. Metaproteomics of the human gut microbiota: Challenges and contributions to other OMICS. *Clin. Mass Spectrom.* 14, 18–30. doi:10.1016/j.clinms.2019.06.001
- Ivanov, I.I., Atarashi, K., Manel, N., Brodie, E.L., Shima, T., Karaoz, U., Wei, D., Goldfarb, K.C., Santee, C.A., Lynch, S.V., Tanoue, T., Imaoka, A., Itoh, K., Takeda, K., Umesaki, Y., Honda, K., Littman, D.R., 2009. Induction of intestinal Th17 cells by segmented filamentous bacteria. *Cell* 139, 485–498. doi:10.1016/j.cell.2009.09.033
- Ives, A.R., Carpenter, S.R., 2007. Stability and Diversity of Ecosystems. *Science* 317, 58–62. doi:10.1126/science.1133258
- Jakobsson, H.E., Rodriguez-Pineiro, A.M., Schutte, A., Ermund, A., Boysen, P., Bemark, M., Sommer, F., Bäckhed, F., Hansson, G.C., Johansson, M.E., 2015. The composition of the gut microbiota shapes the colon mucus barrier. *EMBO Rep.* 16, 164–177. doi:10.15252/embr.201439263

- Jandhyala, S.M., Talukdar, R., Subramanyam, C., Vuyyuru, H., Sasikala, M., Reddy, D.N., 2015. Role of the normal gut microbiota. *World J. Gastroenterol.* 21, 8787–8803. doi:10.3748/wjg.v21.i29.8787
- Johnson, A.J., Vangay, P., Al-Ghalith, G.A., Hillmann, B.M., Ward, T.L., Shields-Cutler, R.R., Kim, A.D., Shmagel, A.K., Syed, A.N., Walter, J., Menon, R., Koecher, K., Knights, D., Students8, P.M.C., 2019. Daily Sampling Reveals Personalized Diet- Microbiome Associations in Humans. *Cell Host Microbe* 25, 789–802.e5. doi:10.1016/j.chom.2019.05.005
- Jones, R.B., Zhu, X., Moan, E., Murff, H.J., Ness, R.M., Seidner, D.L., Sun, S., Yu, C., Dai, Q., Fodor, A.A., Azcarate-Peril, M.A., Shrubsole, M.J., 2018. Inter-niche and inter-individual variation in gut microbial community assessment using stool, rectal swab, and mucosal samples. *Sci. Rep.* 8, 4139. doi:10.1038/s41598-018-22408-4
- Kamada, N., Núñez, G., 2013. Role of the gut microbiota in the development and function of lymphoid cells. *J. Immunol.* 190, 1389–1395. doi:10.4049/jimmunol.1203100
- Kanehisa, M., Goto, S., 1999. KEGG: Kyoto Encyclopedia of Genes and Genomes. *Nucleic Acids Res.* 28, 27–30. doi:10.1093/nar/28.1.27
- Kanoski, S.E., Hsu, T.M., Pennell, S., 2014. Obesity, Western Diet Intake, and Cognitive Impairment. Omega-3 Fatty Acids in Brain and Neurological Health. Elsevier Academic Press 57-62.
- Kaoutari, El, A., Armougom, F., Gordon, J.I., Raoult, D., Henrissat, B., 2013. The abundance and variety of carbohydrate-active enzymes in the human gut microbiota. *Nat. Rev. Microbiol.* 11, 497–504. doi:10.1038/nrmicro3050
- Karp, P.D., Riley, M., Saier, M., Paulsen, I.T., Paley, S.M., Pellegrini-Toole, A., 2000. The EcoCyc and MetaCyc databases. *Nucleic Acids Res.* 28, 56–59. doi:10.1093/nar/28.1.56
- Kim, S., Covington, A., Pamer, E.G., 2018. The intestinal microbiota: Antibiotics colonization resistance, and enteric pathogens. *Immunol. Rev.* 279, 90–105. doi:10.1111/imr.12563
- Koepsell, H., 2020. Glucose transporters in the small intestine in health and disease. *Eur. J. Physiol.* 472, 1207–1248. doi:10.1007/s00424-020-02439-5
- Kohanski, M.A., Dwyer, D.J., Collins, J.J., 2010. How antibiotics kill bacteria: from targets to networks. *Nat. Rev. Microbiol.* 8, 423-435. doi:10.1038/nrmicro2333
- Kohanski, M.A., Dwyer, D.J., Hayete, B., Lawrence, C.A., Collins, J.J., 2007. A Common Mechanism of Cellular Death Induced by Bactericidal Antibiotics. *Cell* 130, 797–810. doi:10.1016/j.cell.2007.06.049
- Koo, H., Hakim, J.A., Crossman, D.K., Kumar, R., Lefkowitz, E.J., Morrow, C.D., 2019. Individualized recovery of gut microbial strains post antibiotics. *NPJ Biofilms Microbiomes* 5, 1–6. doi:10.1038/s41522-019-0103-8
- Korry, B.J., Belenky, P., Cabral, D.J., 2020. Metatranscriptomics Reveals Antibiotic-Induced Resistance Gene Expression in the Murine Gut Microbiota. *Front. Microbiol.* 11, 1–10. doi:10.3389/fmicb.2020.00322
- Kostic, A.D., Gevers, D., Siljander, H., Vatanen, T., Hyötyläinen, T., Hamalainen, A.-M., Peet, A., Tillmann, V., Poho, P., Mattila, I., Lahdesmaki, H., Franzosa, E.A., Vaarala, O., de Goffau, M., Harmsen, H., Ilonen, J., Virtanen, S.M., Clish, C.B., Orešič, M., Huttenhower, C., Knip, M., on behalf of the DIABIMMUNE Study Group, Xavier, R.J., 2015. The Dynamics of the Human Infant Gut Microbiome in Development and in Progression towards Type 1 Diabetes. *Cell Host Microbe* 17, 260–273. doi:10.1016/j.chom.2015.01.001

- Kriss, M., Hazleton, K.Z., Nusbacher, N.M., Martin, C.G., Lozupone, C.A., 2018. Low diversity gut microbiota dysbiosis: drivers, functional implications and recovery. *Curr. Opin. Microbiol.* 44, 34–40. doi:10.1016/j.mib.2018.07.003
- Kuang, E., Marney, M., Cuevas, D., Edwards, R.A., Forsberg, E.M., 2020. Towards Predicting Gut Microbial Metabolism: Integration of Flux Balance Analysis and Untargeted Metabolomics. *Metabolites* 10, 1–11. doi:10.3390/metabo10040156
- Kuczma, M.P., Szurek, E.A., Cebula, A., Chassaing, B., Jung, Y.-J., Kang, S.-M., Fox, J.G., Stecher, B., Ignatowicz, L., 2020. Commensal epitopes drive differentiation of colonic Tregs. *Sci. Adv.* 6, 1–13. doi:10.1126/sciadv.aaz3186
- Kuhn, K.A., Stappenbeck, T.S., 2013. Peripheral education of the immune system by the colonic microbiota. *Semin. Immunol.* 25, 364–369. doi:10.1016/j.smim.2013.10.002
- Lam, P.L., Wong, R.S.M., Lam, K.H., Hung, L.K., Wong, M.M., Yung, L.H., Ho, Y.W., Wong, W.Y., Hau, D.K.P., Gambari, R., Chui, C.H., 2020. The role of reactive oxygen species in the biological activity of antimicrobial agents: An updated mini review. *Chem. Biol. Interact.* 320, 109023. doi:10.1016/j.cbi.2020.109023
- Lebreton, F., van Schaik, W., Manson McGuire, A., Godfrey, P., Griggs, A., Mazumdar, V., Corander, J., Cheng, L., Saif, S., Young, S., Zeng, Q., Wortman, J., Birren, B., Willems, R.J.L., Earl, A.M., Gilmore, M.S., 2013. Emergence of Epidemic Multidrug-Resistant *Enterococcus faecium* from Animal and Commensal Strains. *mBio* 4, e00534–13–e00534–13. doi:10.1128/mBio.00534-13
- Lee, A.J., Wang, S., Meredith, H.R., Zhuang, B., Dai, Z., You, L., 2018. Robust, linear correlations between growth rates and β -lactam-mediated lysis rates. *Proc. Natl. Acad. Sci. USA.* 115, 4069–4074. doi:10.1073/pnas.1719504115
- Lei, Z., Huhman, D.V., Sumner, L.W., 2011. Mass Spectrometry Strategies in Metabolomics. *J. Biol. Chem.* 286, 25435–25422. doi:10.1074/jbc.R111.238691
- Lelie, D., Oka, A., Taghavi, S., Umeno, J., Fan, T.-J., Merrell, K.E., Watson, S.D., Ouellette, L., Liu, B., Awoniyi, M., Lai, Y., Chi, L., Lu, K., Henry, C.S., Sartor, R.B., 2021. Rationally designed bacterial consortia to treat chronic immune-mediated colitis and restore intestinal homeostasis. *Nat. Comm.* 12, 1–17. doi:10.1038/s41467-021-23460-x
- Ley, R.E., Bäckhed, F., Turnbaugh, P., Lozupone, C.A., Knight, R.D., Gordon, J.I., 2005. Obesity alters gut microbial ecology. *Proc. Natl. Acad. Sci. USA.* 102, 11070–11075. doi:10.1073/pnas.0504978102
- Litvak, Y., Byndloss, M.X., Bäumler, A.J., 2018. Colonocyte metabolism shapes the gut microbiota. *Science* 362, 1–15. doi:10.1126/science.aat9076
- Litvak, Y., Byndloss, M.X., Tsohis, R.M., Bäumler, A.J., 2017. Dysbiotic Proteobacteria expansion: a microbial signature of epithelial dysfunction. *Curr. Opin. Microbiol.* 39, 1–6. doi:10.1016/j.mib.2017.07.003
- Liu, B., Pop, M., 2009. ARDB-Antibiotic Resistance Genes Database. *Nucleic Acids Res.* 37, D443–D447. doi:10.1093/nar/gkn656
- Liu, S., Qin, P., Wang, J., 2019. High-Fat Diet Alters the Intestinal Microbiota in Streptozotocin-Induced Type 2 Diabetic Mice. *Microorganisms* 7, 1–12. doi:10.3390/microorganisms7060176
- Liu, Y., Wang, Y., Ni, Y., Cheung, C.K.Y., Lam, K.S.L., Wang, Y., Xia, Z., Ye, D., Guo, J., Tse, M.A., Panagiotou, G., Xu, A., 2020. Gut Microbiome Fermentation Determines the Efficacy of Exercise for Diabetes Prevention. *Cell Metab.* 31, 77–91.e5. doi:10.1016/j.cmet.2019.11.001

- Liu, Y.-X., Qin, Y., Chen, T., Lu, M., Qian, X., Guo, X., Bai, Y., 2021. A practical guide to amplicon and metagenomic analysis of microbiome data. *Protein Cell* 12, 315–330. doi:10.1007/s13238-020-00724-8
- Livanos, A.E., Greiner, T.U., Vangay, P., Pathmasiri, W., Stewart, D., McRitchie, S., Li, H., Chung, J., Sohn, J., Kim, S., Gao, Z., Barber, C., Kim, J., Ng, S., Rogers, A.B., Sumner, S., Zhang, X.-S., Cadwell, K., Knights, D., Alekseyenko, A., Bäckhed, F., Blaser, M.J., 2016. Antibiotic-mediated gut microbiome perturbation accelerates development of type 1 diabetes in mice. *Nat. Microbiol.* 1, 857–32. doi:10.1038/nmicrobiol.2016.140
- Lloyd-Price, J., Mahurkar, A., Rahnavard, G., Crabtree, J., Orvis, J., Hall, A.B., Brady, A., Creasy, H.H., McCracken, C., Giglio, M.G., McDonald, D., Franzosa, E.A., Knight, R., White, O., Huttenhower, C., 2017. Strains, functions and dynamics in the expanded Human Microbiome Project. *Nature* 550, 61–66. doi:10.1038/nature23889
- Lobritz, M.A., Belenky, P., Porter, C.B.M., Gutierrez, A., Yang, J.H., Schwarz, E.G., Dwyer, D.J., Khalil, A.S., Collins, J.J., 2015. Antibiotic efficacy is linked to bacterial cellular respiration. *Proc. Natl. Acad. Sci. USA.* 112, 8173–8180. doi:10.1073/pnas.1509743112
- Lopatkin, A.J., Stokes, J.M., Zheng, E.J., Yang, J.H., Takahashi, M.K., You, L., Collins, J.J., 2019. Bacterial metabolic state more accurately predicts antibiotic lethality than growth rate. *Nat. Microbiol.* 4, 2109–2117. doi:10.1038/s41564-019-0536-0
- Lozupone, C.A., Stombaugh, J.I., Gordon, J.I., Jansson, J.K., Knight, R., 2012. Diversity, stability, and resilience of the human gut microbiota. *Nature* 489, 220–230. doi:10.1038/nature11550
- Luan, G., Hong, Y., Drlica, K., Zhao, X., 2018. Suppression of Reactive Oxygen Species Accumulation Accounts for Paradoxical Bacterial Survival at High Quinolone Concentration. *Antimicrob. Agents Chemother.* 62, e01622-17. doi:10.1128/AAC.01622-17
- Luan, H., Wang, X., Cai, Z., 2019. Mass spectrometry-based metabolomics: Targeting the crosstalk between gut microbiota and brain in neurodegenerative disorders. *Mass Spectrom. Rev.* 38, 22–33. doi:10.1002/mas.21553
- Lynch, S.V., Boushey, H.A., 2016. The microbiome and development of allergic disease. *Curr. Opin. Allerg. Clin. Immunol.* 16, 165–171. doi:10.1097/ACI.0000000000000255
- Ma, F., Xu, S., Tang, Z., Li, Z., Zhang, L., 2021. Use of antimicrobials in food animals and impact of transmission of antimicrobial resistance on humans. *Biosafety and Health* 3, 32–38. doi:10.1016/j.bsheal.2020.09.004
- Ma, Q., Li, Y., Wang, J., Li, P., Duan, Y., Dai, H., An, Y., Cheng, L., Wang, T., Wang, C., Wang, T., Zhao, B., 2020. Investigation of gut microbiome changes in type 1 diabetic mellitus rats based on high-throughput sequencing. *Biomed. Pharmacother.* 124, 109873. doi:10.1016/j.biopha.2020.109873
- Manyi-Loh, C., Mamphweli, S., Meyer, E., Okoh, A., 2018. Antibiotic Use in Agriculture and Its Consequential Resistance in Environmental Sources: Potential Public Health Implications. *Molecules* 23, 1–48. doi:10.3390/molecules23040795
- Mazmanian, S.K., Liu, C.H., Tzianabos, A.O., Kasper, D.L., 2005. An immunomodulatory molecule of symbiotic bacteria directs maturation of the host immune system. *Cell* 122, 107–118. doi:10.1016/j.cell.2005.05.007
- McIver, L.J., Abu-Ali, G., Franzosa, E.A., Schwager, R., Morgan, X.C., Waldron, L., Segata, N., Huttenhower, C., 2018. bioBakery: a meta’omic analysis environment. *J. Bioinform.* 34, 1235–1237. doi:10.1093/bioinformatics/btx754
- Meylan, S., Porter, C.B.M., Yang, J.H., Belenky, P., Gutierrez, A., Lobritz, M.A., Park, J., Kim, S.H., Moskowitz, S.M., Collins, J.J., 2017. Carbon Sources Tune Antibiotic Susceptibility in

- Pseudomonas aeruginosa* via Tricarboxylic Acid Cycle Control. *Cell Chem. Biol.* 24, 195–206. doi:10.1016/j.chembiol.2016.12.015
- Modi, S.R., Lee, H.H., Spina, C.S., Collins, J.J., 2013. Antibiotic treatment expands the resistance reservoir and ecological network of the phage metagenome. *Nature* 499, 219–222. doi:10.1038/nature12212
- Mok, W.W.K., Park, J.O., Rabinowitz, J.D., Brynildsen, M.P., 2015. RNA Futile Cycling in Model Persisters Derived from MazF Accumulation. *mBio* 6, e01588–15. doi:10.1128/mBio.01588-15
- Monleon-Getino, T., Frias-Lopez, J., 2020. A priori estimation of sequencing effort in complex microbial metatranscriptomes. *Ecol. Evol.* 10, 13382–13394. doi:10.1002/ece3.6941
- Mori, K., Kamagata, Y., 2014. The Challenges of Studying the Anaerobic Microbial World. *Microbes Environ.* 29, 335–337. doi:10.1264/jsme2.ME2904rh
- Moya, A., Ferrer, M., 2016. Functional Redundancy- Induced Stability of Gut Microbiota Subjected to Disturbance. *Trends in Microbiol.* 24, 402–413. doi:10.1016/j.tim.2016.02.002
- Naeem, S., Li, S., 1997. Biodiversity enhances ecosystem reliability. *Nature* 390, 507-509. doi:10.1038/37348
- Naeem, S., Thompson, L.J., Lawler, S.P., Lawton, J.H., Woodfin, R.M., 1994. Declining biodiversity can alter the performance of ecosystems. *Nature* 368, 1–4. doi:10.1038/368734a0
- Neish, A.S., 2014. Mucosal Immunity and the Microbiome. *Annals. ATS* 11, 1–5. doi:10.1513/AnnalsATS.201306-161MG
- Ng, K.M., Aranda-Díaz, A., Tropini, C., Frankel, M.R., Van Treuren, W., O’Loughlin, C.T., Merrill, B.D., Yu, F.B., Pruss, K.M., Oliveira, R.A., Higginbottom, S.K., Neff, N.F., Fischbach, M.A., Xavier, K.B., Sonnenburg, J.L., Huang, K.C., 2019. Recovery of the Gut Microbiota after Antibiotics Depends on Host Diet, Community Context, and Environmental Reservoirs. *Cell Host Microbe* 26, 650–665.e4. doi:10.1016/j.chom.2019.10.011
- Nguyen, D., Joshi-Datar, A., Lepine, F., Bauerle, E., Olakanmi, O., Beer, O., McKay, G., Siehnel, R., Schafhauser, J., Wang, Y., Britigan, B.E., Singh, P.K., 2011. Active starvation responses mediate antibiotic tolerance in biofilms and nutrient-limited bacteria. *Science* 334, 982–986. doi:10.1126/science.1211037
- Ni, J., Friedman, H., Boyd, B.C., McGurn, A., Babinski, P., Markossian, T., Dugas, L.R., 2019. Early antibiotic exposure and development of asthma and allergic rhinitis in childhood. *BMC Pediatr.* 19, 225–8. doi: 10.1186/s12887-019-1594-4
- Nusbaum, D.J., Sun, F., Ren, J., Zhu, Z., Ramsy, N., Pervolarakis, N., Kunde, S., England, W., Gao, B., Fiehn, O., Michail, S., Whiteson, K., 2018. Gut microbial and metabolomic profiles after fecal microbiota transplantation in pediatric ulcerative colitis patients. *FEMS Microbiol. Ecol.* 94, 1–11. doi:10.1093/femsec/fiy133
- Obrenovich, M.E., Tima, M., Polinkovsky, A., Zhang, R., Emancipator, S.N., Donskey, C.J., 2017. Targeted Metabolomics Analysis Identifies Intestinal Microbiota-Derived Urinary Biomarkers of Colonization Resistance in Antibiotic-Treated Mice. *Antimicrob. Agents and Chemother.* 61, 1–7. doi:10.1128/AAC.00477-17
- Oliphant, K., Allen-Vercoe, E., 2019. Macronutrient metabolism by the human gut microbiome: major fermentation by- products and their impact on host health. *Microbiome* 7, 1–15. doi:10.1186/s40168-019-0704-8
- Org, E., Blum, Y., Kasela, S., Mehrabian, M., Kuusisto, J., Kangas, A.J., Soininen, P., Wang, Z., Ala-Korpela, M., Hazen, S.L., Laakso, M., Lusis, A.J., 2017. Relationships between gut

- microbiota, plasma metabolites, and metabolic syndrome traits in the METSIM cohort. *Genome Biol.* 18, 1–14. doi:10.1186/s13059-017-1194-2
- Ostman, S., Rask, C., Wold, A.E., Hultkrantz, S., Telemo, E., 2006. Impaired regulatory T cell function in germ-free mice. *Eur. J. of Immunol.* 36, 2336–2346. doi:10.1002/eji.200535244
- Overbeek, R., Olson, R., Pusch, G.D., Olsen, G.J., Davis, J.J., Disz, T., Edwards, R.A., Gerdes, S., Parrello, B., Shukla, M., Vonstein, V., Wattam, A.R., Xia, F., Stevens, R., 2014. The SEED and the Rapid Annotation of microbial genomes using Subsystems Technology (RAST). *Nucleic Acids Res.* 42, D206–D214. doi:10.1093/nar/gkt1226
- Pace, N.R., 1997. A Molecular View of Microbial Diversity and the Biosphere. *Science* 276, 734–740. doi:10.1126/science.276.5313.734
- Patterson, E., Stanton, C., Cryan, J.F., Fitzgerald, G.F., Ross, R.P., Dinan, T.G., Fitzgerald, P., Marques, T.M., Cotter, P.D., O’Sullivan, O., 2015. Streptozotocin-induced type-1-diabetes disease onset in Sprague–Dawley rats is associated with an altered intestinal microbiota composition and decreased diversity. *Microbiology* 161, 182–193. doi:10.1099/mic.0.082610-0
- Patwardhan, A., Ray, S., Roy, A., 2014. Molecular Markers in Phylogenetic Studies – A review. *J. Phylog. Evol. Biol.* 2, 1–9. doi:10.4172/2329-9002.1000131
- Penders, J., Stobberingh, E.E., Savelkoul, P.H.M., Wolffs, P.F.G., 2013. The human microbiome as a reservoir of antimicrobial resistance. *Front. Microbiol.* 4, 1–7. doi:10.3389/fmicb.2013.00087/abstract
- Piccolo, B.D., Graham, J.L., Stanhope, K.L., Hookey, I., Mercer, K.E., Chintapalli, S.V., Wankhade, U.D., Shankar, K., Havel, P.J., Adams, S.H., 2018. Diabetes-associated alterations in the cecal microbiome and metabolome are independent of diet or environment in the UC Davis Type 2 Diabetes Mellitus Rat model. *Am. J. of Phys. Endocrinol. Metab.* 315, 1–12. doi:10.1152/ajpendo.00203.2018
- Poretsky, R., Rodriguez-R, L.M., Luo, C., Tsementzi, D., Konstantinidis, K.T., 2014. Strengths and Limitations of 16S rRNA Gene Amplicon Sequencing in Revealing Temporal Microbial Community Dynamics. *PLoS ONE* 9, e93827–12. doi:10.1371/journal.pone.0093827
- Qi, L., Cornelis, M.C., Zhang, C., van Dam, R.M., Hu, F.B., 2009. Genetic predisposition, Western dietary pattern, and the risk of type 2 diabetes in men. *Am. J. Clin. Nutr.* 89, 1453–1458. doi:10.3945/ajcn.2008.27249
- Qin, J., Li, R., Raes, J., Arumugam, M., Burgudorf, K.S., Manichanh, C., Nielsen, T., Pons, N., Levenez, F., Yamada, T., Mende, D.R., Li, J., Xu, J., Li, S., Li, D., Cao, J., Wang, B., Liang, J., Zheng, H., Xie, Y., Tap, J., Lepage, P., Bertalan, M., Batto, J.-M., Hansen, T., Le Paslier, D., Linneberg, A., Nielsen, H.B., Pelletier, E., Renault, P., Sicheritz-Ponten, T., Turner, K., Zhu, H., Yu, C., Li, S., Jian, M., Zhou, Y., Li, Y., Zhang, X., Li, S., Qin, N., Yang, H., Wang, J., Brunak, S., Doré, J., Guarner, F., Kristiansen, K., Pedersen, O., Parkhill, J., Weissenbach, J., MetaHIT Consortium, Bork, P., Ehrlich, S.D., Wang, J., 2010. A human gut microbial gene catalog established by metagenomic sequencing. *Nature* 464, 59–65. doi:10.1038/nature08821
- Qin, J., Li, Y., Cai, Z., Li, S., Zhu, J., Zhang, F., Liang, S., Zhang, W., Guan, Y., Shen, D., Peng, Y., Zhang, D., Jie, Z., Wu, W., Qin, Y., Xue, W., Li, J., Han, L., Lu, D., Wu, P., Dai, Y., Sun, X., Li, Z., Tang, A., Zhong, S., Li, X., Chen, W., Xu, R., Wang, M., Feng, Q., Gong, M., Yu, J., Zhang, Y., Zhang, M., Hansen, T., Sanchez, G., Raes, J., Falony, G., Okuda, S., Almeida, M., LeChatelier, E., Renault, P., Pons, N., Batto, J.-M., Zhang, Z., Chen, H., Yang, R., Zheng, W., Li, S., Yang, H., Wang, J., Ehrlich, S.D., Nielsen, R., Pedersen, O., Kristiansen, K., Wang,

- J., 2012. A metagenome-wide association study of gut microbiota in type 2 diabetes. *Nature* 490, 55–60. doi:10.1038/nature11450
- Quail, M.A., Smith, M., Coupland, P., Otto, T.D., Harris, S.R., Connor, T.R., Bertoni, A., Swerdlow, H.P., Gu, Y., 2012. A tale of three next generation sequencing platforms: comparison of Ion Torrent, Pacific Biosciences and Illumina MiSeq sequencers. *BMC Genom.* 13, 1–13. doi:10.1186/1471-2164-13-341
- Raes, J., Korbil, J.O., Lercher, M.J., Mering, von, C., Bork, P., 2007. Prediction of effective genome size in metagenomic samples. *Genome Biol.* 8, 1–11. doi:10.1186/gb-2007-8-1-r10
- Rajpal, D.K., Klein, J.-L., Mayhew, D., Boucheron, J., Spivak, A.T., Kumar, V., Ingraham, K., Paulik, M., Chen, L., Van Horn, S., Thomas, E., Sathe, G., Livi, G.P., Holmes, D.J., Brown, J.R., 2015. Selective Spectrum Antibiotic Modulation of the Gut Microbiome in Obesity and Diabetes Rodent Models. *PLoS ONE* 10, e0145499–19. doi:10.1371/journal.pone.0145499
- Rea, M.C., Sit, C.S., Clayton, E., OConnor, P.M., Whittall, R.M., Zheng, J., Vederas, J.C., Ross, R.P., Hill, C., 2010. Thuricin CD, a posttranslationally modified bacteriocin with a narrow spectrum of activity against *Clostridium difficile*. *Proc. Natl. Acad. Sci. USA.* 107, 9352–9357. doi:10.1073/pnas.0913554107
- Reese, A.T., Carmody, R.N., 2019. Thinking Outside the Cereal Box: Noncarbohydrate Routes for Dietary Manipulation of the Gut Microbiota. *Appl. Environ. Microbiol.* 85, 1–17. doi:10.1128/AEM.02246-18
- Ridlon, J.M., Kang, D.J., Hylemon, P.B., Bajaj, J.S., 2014. Bile acids and the gut microbiome. *Curr. Opin. Gastroenter.* 30, 332–338. doi:10.1097/MOG.000000000000057
- Riiser, A., 2015. The human microbiome, asthma, and allergy. *Allergy Asthma Clin. Immunol.* 11, 1–7. doi:10.1186/s13223-015-0102-0
- Roberts, S.A., Morris, A.J., 2020. Surgical antibiotic prophylaxis: more is not better. *Lancet Infect. Dis.* 20, 1110–1111. doi:10.1016/S1473-3099(20)30290-5
- Rodríguez, J.M., Murphy, K., Stanton, C., Ross, R.P., Kober, O.I., Juge, N., Avershina, E., Rudi, K., Narbad, A., Jenmalm, M.C., Marchesi, J.R., Collado, M.C., 2015. The composition of the gut microbiota throughout life, with an emphasis on early life. *Microb. Ecol. Health Dis.* 26, 1–17. doi:10.3402/mehd.v26.26050
- Romano-Keeler, J., Moore, D.J., Wang, C., Brucker, R.M., Fannesbeck, C., Slaughter, J.C., Li, H., Curran, D.P., Meng, S., Correa, H., Lovvorn, H.N., III, Tang, Y.-W., Bordenstein, S., George, A.L., Jr, Weitkamp, J.-H., 2014. Early life establishment of site-specific microbial communities in the gut. *Gut Microbes* 5, 192–201. doi:10.4161/gmic.28442
- Rotimi, C.N., 2020. Gut Microbiome Profiles Are Associated With Type 2 Diabetes in Urban Africans. *Front. Cell. Infect. Microbiol.* 1–13. doi:10.3389/fcimb.2020.00063
- Round, J.L., Mazmanian, S.K., 2009. The gut microbiota shapes intestinal immune responses during health and disease. *Nature Rev. Immunol.* 9, 313–323. doi:10.1038/nri2515
- Sabatino, A., Regolisti, G., Cosola, C., Gesualdo, L., Fiaccadori, E., 2017. Intestinal Microbiota in Type 2 Diabetes and Chronic Kidney Disease. *Curr. Diab. Rep.* 1–9. doi:10.1007/s11892-017-0841-z
- Salking, A.R., Rao, K.C., 2011. Antibiotic Prophylaxis to Prevent Surgical Site Infections. *Am. Fam. Physician* 83, 585–590. PMID: 21391526
- Salvato, F., Hettich, R.L., 2021. Five key aspects of metaproteomics as a tool to understand functional interactions in host-associated microbiomes. *PLoS Pathog.* 17, 1–10. doi:10.1371/journal.ppat.1009245

- Scheithauer, T.P.M., Rampanelli, E., Nieuwdorp, M., Vallance, B.A., Verchere, C.B., van Raalte, D.H., Herrema, H., 2020. Gut Microbiota as a Trigger for Metabolic Inflammation in Obesity and Type 2 Diabetes. *Front. in Immunol.* 11, 571731. doi:10.3389/fimmu.2020.571731
- Schloissnig, S., Arumugam, M., Sunagawa, S., Mitreva, M., Tap, J., Zhu, A., Waller, A., Mende, D.R., Kultima, J.R., Martin, J., Kota, K., Sunyaev, S.R., Weinstock, G.M., Bork, P., 2013. Genomic variation landscape of the human gut microbiome. *Nature* 493, 45–50. doi:10.1038/nature11711
- Schloss, P.D., Iverson, K.D., Petrosino, J.F., Schloss, S.J., 2014. The dynamics of a family's gut microbiota reveal variations on a theme. *Microbiome* 2, 1–13. doi:10.1186/2049-2618-2-25
- Schoeler, M., Caesar, R., 2019. Dietary lipids, gut microbiota and lipid metabolism. *Rev. Endocr. Metab. Disord.* 20, 461–472. doi:10.1007/s11154-019-09512-0
- Sender, R., Fuchs, S., Milo, R., 2016. Revised Estimates for the Number of Human and Bacteria Cells in the Body. *PLoS Biol.* 14, e1002533–14. doi:10.1371/journal.pbio.1002533
- Sharma, P., Rashid, M., Kaur, S., 2020. Novel enterocin E20c purified from *Enterococcus hirae* 20c synergised with β -lactams and ciprofloxacin against *Salmonella enterica*. *Microb. Cell. Fact.* 19, 1–11. doi:10.1186/s12934-020-01352-x
- Shaw, L.P., Bassam, H., Barnes, C.P., Walker, A.S., Klein, N., Balloux, F., 2019. Modelling microbiome recovery after antibiotics using a stability landscape framework. *ISME J.* 13, 1845–1856. doi:10.1038/s41396-019-0392-1
- Shaw, S.Y., Blanchard, J.F., Bernstein, C.N., 2010. Association between the use of antibiotics in the first year of life and pediatric inflammatory bowel disease. *Am. J. Gastroenter.* 105, 2687–2692. doi:10.1038/ajg.2010.398
- Singh, R., Chandrashekarappa, S., Bodduluri, S.R., Baby, B.V., Hegde, B., Kotla, N.G., Hiwale, A.A., Saiyed, T., Patel, P., Vijay-Kumar, M., Langille, M.G.I., Douglas, G.M., Cheng, X., Rouchka, E.C., Waigel, S.J., Dryden, G.W., Alatassi, H., Zhang, H.-G., Haribabu, B., Vemula, P.K., Jala, V.R., 2019. Enhancement of the gut barrier integrity by a microbial metabolite through the Nrf2 pathway. *Nat. Comm.* 10, 1–18. doi:10.1038/s41467-018-07859-7
- Singh, R., Lemire, J., Mailloux, R.J., Chénier, D., Hamel, R., Appanna, V.D., 2009. An ATP and oxalate generating variant tricarboxylic acid cycle counters aluminum toxicity in *Pseudomonas fluorescens*. *PLoS ONE* 4, e7344. doi:10.1371/journal.pone.0007344
- Skovsø, S., 2014. Modeling type 2 diabetes in rats using high fat diet and streptozotocin. *J. Diabetes Investig.* 5, 349–358. doi:10.1111/jdi.12235
- Smith, K., McCoy, K.D., Macpherson, A.J., 2007. Use of axenic animals in studying the adaptation of mammals to their commensal intestinal microbiota. *Semin. Immunol.* 19, 59–69. doi:10.1016/j.smim.2006.10.002
- Smits, S.A., Leach, J., Sonnenburg, E.D., Gonzalez, C.G., Lichtman, J.S., Reid, G., Knight, R., Manjurano, A., Changalucha, J., Elias, J.E., Dominguez-Bello, M.G., Sonnenburg, J.L., 2017. Seasonal cycling in the gut microbiome of the Hadza hunter-gatherers of Tanzania. *Science* 357, 802–806. doi:10.1126/science.aan4834
- Smits, S.A., Marcobal, A., Higginbottom, S., Sonnenburg, J.L., Kashyap, P.C., 2016. Individualized Responses of Gut Microbiota to Dietary Intervention Modeled in Humanized Mice. *mSystems* 1, 105–6. doi:10.1128/mSystems.00098-16
- Sonnenburg, E.D., Sonnenburg, J.L., 2014. Starving our Microbial Self: The Deleterious Consequences of a Diet Deficient in Microbiota-Accessible Carbohydrates. *Cell Metab.* 20, 779–786. doi:10.1016/j.cmet.2014.07.003

- Sonnenburg, J.L., Xu, J., Leip, D.D., Chen, C.-H., Westover, B.P., Weatherford, J., Buhler, J.D., Gordon, J.I., 2005. Glycan foraging in vivo by an intestine-adapted bacterial symbiont. *Science* 307, 1952–1955. doi:10.1126/science.1109051
- Stewart, C.J., Ajami, N.J., O’Brien, J.L., Hutchinson, D.S., Smith, D.P., Wong, M.C., Ross, M.C., Lloyd, R.E., Doddapaneni, H., Metcalf, G.A., Muzny, D., Gibbs, R.A., Vatanen, T., Huttenhower, C., Xavier, R.J., Rewers, M., Hagopian, W., Toppari, J., Ziegler, A.-G., She, J.-X., Akolkar, B., Lernmark, A., Hyoty, H., Vehik, K., Krischer, J.P., Petrosino, J.F., 2018. Temporal development of the gut microbiome in early childhood from the TEDDY study. *Nature* 562, 583–588. doi:10.1038/s41586-018-0617-x
- Stokes, J.M., Lopatkin, A.J., Lobritz, M.A., Collins, J.J., 2019. Bacterial Metabolism and Antibiotic Efficacy. *Cell Metab.* 30, 251–259. doi:10.1016/j.cmet.2019.06.009
- Tasse, L., Bercovici, J., Pizzut-Serin, S., Robe, P., Tap, J., Klopp, C., Cantarel, B.L., Coutinho, P.M., Henrissat, B., Leclerc, M., Doré, J., Monsan, P., Remaud-Simeon, M., Potocki-Veronese, G., 2010. Functional metagenomics to mine the human gut microbiome for dietary fiber catabolic enzymes. *Genome Res.* 20, 1605–1612. doi:10.1101/gr.108332.110
- Thaiss, C.A., Levy, M., Grosheva, I., Zheng, D., Soffer, E., Blacher, E., Braverman, S., Tengeler, A.C., Barak, O., Elazar, M., Ben-Zeev, R., Lehavi-Regev, D., Katz, M.N., Pevsner-Fischer, M., Gertler, A., Halpern, Z., Harmelin, A., Amar, S., Serradas, P., Grosfeld, A., Shapiro, H., Geiger, B., Elinav, E., 2018. Hyperglycemia drives intestinal barrier dysfunction and risk for enteric infection. *Science* 359, 1376–1383. doi:10.1126/science.aar3318
- The Human Microbiome Project Consortium. 2012. Structure, function and diversity of the healthy human microbiome. *Nature* 486, 207–214. doi:10.1038/nature11234
- Theriot, C.M., Bowman, A.A., Young, V.B., 2016. Antibiotic-Induced Alterations of the Gut Microbiota Alter Secondary Bile Acid Production and Allow for *Clostridium difficile* Spore Germination and Outgrowth in the Large Intestine. *mSphere* 1, e00045–15–16. doi:10.1128/mSphere.00045-15
- Thingholm, L.B., Rühlemann, M.C., Koch, M., Fuqua, B., Laucke, G., Boehm, R., Bang, C., Franzosa, E.A., Hübenthal, M., Rahnavard, A., Frost, F., Lloyd-Price, J., Schirmer, M., Lusi, A.J., Vulpe, C.D., Lerch, M.M., Homuth, G., Kacprowski, T., Schmidt, C.O., Nöthlings, U., Karlsen, T.H., Lieb, W., Laudes, M., Franke, A., Huttenhower, C., 2019. Obese Individuals with and without Type 2 Diabetes Show Different Gut Microbial Functional Capacity and Composition. *Cell Host Microbe* 26, 252–264. doi:10.1016/j.chom.2019.07.004
- Thomas, V.C., Kinkead, L.C., Janssen, A., Schaeffer, C.R., Woods, K.M., Lindgren, J.K., Peaster, J.M., Chaudhari, S.S., Sadykov, M., Jones, J., Mohamadi AbdelGhani, S.M., Zimmerman, M.C., Bayles, K.W., Somerville, G.A., Fey, P.D., 2013. A Dysfunctional Tricarboxylic Acid Cycle Enhances Fitness of *Staphylococcus* β -Lactam Stress. *mBio* 4, e00437–13. doi:10.1128/mBio.00437-13
- Tian, L., Wang, X.-W., Wu, A.-K., Fan, Y., Friedman, J., Dahlin, A., Waldor, M.K., Weinstock, G.M., Weiss, S.T., Liu, Y.-Y., 2020. Deciphering functional redundancy in the human microbiome. *Nat. Comm.* 1–11. doi:10.1038/s41467-020-19940-1
- Turnbaugh, P.J., Bäckhed, F., Fulton, L., Gordon, J.I., 2008. Diet-Induced Obesity Is Linked to Marked but Reversible Alterations in the Mouse Distal Gut Microbiome. *Cell Host Microbe* 3, 213–223. doi:10.1016/j.chom.2008.02.015
- Turnbaugh, P.J., Ley, R.E., Mahowald, M.A., Magrini, V., Mardis, E.R., Gordon, J.I., 2006. An obesity-associated gut microbiome with increased capacity for energy harvest. *Nature* 444, 1027–1031. doi:10.1038/nature05414

- Turnbaugh, P.J., Ridaura, V.K., Faith, J.J., Rey, F.E., Knight, R., Gordon, J.I., 2009. The Effect of Diet on the Human Gut Microbiome: A Metagenomic Analysis in Humanized Gnotobiotic Mice. *Sci. Transl. Med.* 1, 6ra14. doi:10.1126/scitranslmed.3000322
- Ursell, L.K., Metcalf, J.L., Parfrey, L.W., Knight, R., 2012. Defining the human microbiome. *Nutr. Rev.* 70, S38–S44. doi:10.1111/j.1753-4887.2012.00493.x
- Van Acker, H., Coenye, T., 2017. The Role of Reactive Oxygen Species in Antibiotic-Mediated Killing of Bacteria. *Trends Microbiol.* 25, 456–466. doi:10.1016/j.tim.2016.12.008
- Vemuri, R., Shankar, E.M., Chieppa, M., Eri, R., Kavanagh, K., 2020. Beyond Just Bacteria: Function Biomes in the Gut Ecosystem Including Virome, Mycobiome, Archaeome and Helminths. *Microorganisms* 8, 1–24. doi:10.3390/microorganisms8040483
- Ventola, C.L., 2015. The Antibiotic Resistance Crisis. *P.T.* 40, 277–283. PMID: 25859123
- Walker, A.W., Ince, J., Duncan, S.H., Webster, L.M., Holtrop, G., Ze, X., Brown, D., Stares, M.D., Scott, P., Bergerat, A., Louis, P., McIntosh, F., Johnstone, A.M., Lobley, G.E., Parkhill, J., Flint, H.J., 2011. Dominant and diet-responsive groups of bacteria within the human colonic microbiota. *ISME J.* 5, 220–230. doi:10.1038/ismej.2010.118
- Walker, B.H., 1992. Biodiversity and Ecological Redundancy. *Biol. Conserv.* 6, 18–23. doi:10.1046/j.1523-1739.1992.610018.x
- Wang, C.-Y., Liao, J.K., 2011. A Mouse Model of Diet-Induced Obesity and Insulin Resistance, in: Allen, I.C. (Ed.), *Mouse Models of Innate Immunity, Methods in Molecular Biology (Methods and Protocols)*, vol 821. Humana Press, Totowa, NJ, pp. 421–433. ISBN: 978-62703-408-7
- Wang, W.-L., Xu, S.-Y., Ren, Z.-G., Tao, L., Jiang, J.-W., Zheng, S.-S., 2015. Application of metagenomics in the human gut microbiome. *World J. Gastroenterol.* 21, 803–814. doi:10.3748/wjg.v21.i3.803
- Weinstock, G.M., 2012. Genomic approaches to studying the human microbiota. *Nature* 489, 250–256. doi:10.1038/nature11553
- Wikoff, W.R., Anfora, A.T., Liu, J., Schultz, P.G., Lesley, S.A., Peters, E.C., Siuzdak, G., 2009. Metabolomics analysis reveals large effects of gut microflora on mammalian blood metabolites. *Proc. Natl. Acad. Sci. USA.* 106, 1–6. doi:10.1073/pnas.0812874106
- Wilkins, L.J., Monga, M., Miller, A.W., 2019. Defining Dysbiosis for a Cluster of Chronic Diseases. *Sci. Rep.* 9, 1–10. doi:10.1038/s41598-019-49452-y
- Wlodarska, M., Willing, B., Keeney, K.M., Menezes, A., Bergstrom, K.S., Gill, N., Russell, S.L., Vallance, B.A., Finlay, B.B., 2011. Antibiotic Treatment Alters the Colonic Mucus Layer and Predisposes the Host to Exacerbated *Citrobacter rodentium*-induced Colitis. *Infect. Immun.* 79, 1536–1545. doi:10.1128/IAI.01104-10
- Woo, V., Eshleman, E.M., Hashimoto-Hill, S., Whitt, J., Wu, S.-E., Engleman, L., Rice, T., Karns, R., Qualls, J.E., Haslam, D.B., Vallance, B.A., Alenghat, T., 2021. Commensal segmented filamentous bacteria- derived retinoic acid primes host defense to intestinal infection. *Cell Host Microbe* S1931-3128(21)00426-1. doi:10.1016/j.chom.2021.09.010
- Woolhouse, M., Ward, M., van Bunnik, B., Farrar, J., 2015. Antimicrobial resistance in humans, livestock and the wider environment. *Philosoph. Trans. Royal Soc. B* 370, 1–7. doi:10.1098/rstb.2014.0083
- Wu, H., Tremaroli, V., Schmidt, C., Lundqvist, A., Olsson, L.M., Krämer, M., Gummesson, A., Perkins, R., Bergström, G., Bäckhed, F., 2020. The Gut Microbiota in Prediabetes and Diabetes: A Population-Based Cross-Sectional Study. *Cell Metab.* 32, 379–390.e3. doi:10.1016/j.cmet.2020.06.011

- Xu, Z., Knight, R., 2015. Dietary effects on human gut microbiome diversity. *Br. J. Nutr.* 113, S1–S5. doi:10.1017/S0007114514004127
- Yachi, S., Loreau, M., 1999. Biodiversity and ecosystem productivity in a fluctuating environment: The insurance hypothesis. *Proc. Natl. Acad. Sci. USA.* 96, 1463–1468. doi:10.1073/pnas.96.4.1463
- Yasuda, S., Okahashi, N., Tsugawa, H., Ogata, Y., Ikeda, K., Suda, W., Arai, H., Hattori, M., Arita, M., 2020. Elucidation of Gut Microbiota-Associated Lipids Using LC-MS/MS and 16S rRNA Sequence Analyses. *iScience* 23, 101841. doi:10.1016/j.isci.2020.101841
- Yatsunencko, T., Rey, F.E., Manary, M.J., Trehan, I., Dominguez-Bello, M.G., Contreras, M., Magris, M., Hidalgo, G., Baldassano, R.N., Anokhin, A.P., Heath, A.C., Warner, B., Reeder, J., Kuczynski, J., Caporaso, J.G., Lozupone, C.A., Lauber, C., Clemente, J.C., Knights, D., Knight, R., Gordon, J.I., 2012. Human gut microbiome viewed across age and geography. *Nature* 486, 222–227. doi:10.1038/nature11053
- Yoon, M.Y., Yoon, S.S., 2018. Disruption of the Gut Ecosystem by Antibiotics. *Yonsei Med. J.* 59, 4–12. doi:10.3349/ymj.2018.59.1.4
- Yu, L.-M., Zhao, K.-J., Wang, S.-S., Wang, X., Bin Lu, 2018. Gas chromatography/mass spectrometry based metabolomic study in a murine model of irritable bowel syndrome. *World J. Gastroenter.* 24, 894–904. doi:10.3748/wjg.v24.i8.894
- Zarepour, M., Bhullar, K., Montero, M., Ma, C., Huang, T., Velcich, A., Xia, L., Vallance, B.A., 2013. The Mucin Muc2 limits pathogen burdens and epithelial barrier dysfunction during *Salmonella enterica* serovar Typhimurium colitis. *Infect. Immun.* 81, 3672–3683. doi:10.1128/IAI.00854-13
- Zarrinpar, A., Chaix, A., Xu, Z.Z., Chang, M.W., Marotz, C.A., Saghatelian, A., Knight, R., Panda, S., 2018. Antibiotic-induced microbiome depletion alters metabolic homeostasis by affecting gut signaling and colonic metabolism. *Nat. Comm.* 9, 1–13. doi:10.1038/s41467-018-05336-9
- Zhang, Y., Thompson, K.N., Branck, T., Yan, Y., Nguyen, L.H., Franzosa, E.A., Huttenhower, C., 2021. Metatranscriptomics for the Human Microbiome and Microbial Community Functional Profiling. *Ann. Rev. Biomed. Data Sci.* 4, 279–311. doi:10.1146/annurev-biodatasci-031121-103035
- Zhao, X., Hong, Y., Drlica, K., 2015. Moving forward with reactive oxygen species involvement in antimicrobial lethality. *J. Antimicrob. Chemother.* 70, 639–642. doi:10.1093/jac/dku463
- Zheng, P., Li, Z., Zhou, Z., 2018. Gut microbiome in type 1 diabetes: A comprehensive review. *Diabetes Metab. Res. Rev.* 34, e3043–33. doi:10.1002/dmrr.3043
- Zheng, X., Huang, F., Zhao, A., Lei, S., Zhang, Y., Xie, G., Chen, T., Qu, C., Rajani, C., Dong, B., Li, D., Jia, W., 2017. Bile acid is a significant host factor shaping the gut microbiome of diet-induced obese mice. *BMC Biol.* 15, 1–15. doi:10.1186/s12915-017-0462-7
- Zhou, W., Sailani, M.R., Contrepois, K.X.V., Zhou, Y., Ahadi, S., Leopold, S.R., Zhang, M.J., Rao, V., Avina, M., Mishra, T., Johnson, J., Lee-McMullen, B., Chen, S., Metwally, A.A., Tran, T.D.B., Nguyen, H., Zhou, X., Albright, B., Hong, B.-Y., Petersen, L., Bautista, E., Hanson, B., Chen, L., Spakowicz, D., Bahmani, A., Salins, D., Leopold, B., Ashland, M., Dagan-Rosenfeld, O., Rego, S., Limcaoco, P., Colbert, E., Allister, C., Perelman, D., Craig, C., Wei, E., Chaib, H., Hornburg, D., Dunn, J., Liang, L., Rose, S.M.S.X.S.-F., Kukurba, K., Piening, B., Rost, H., Tse, D., McLaughlin, T., Sodergren, E., Weinstock, G.M., Snyder, M., 2019. Longitudinal multi-omics of host–microbe dynamics in prediabetes. *Nature* 569, 1–28. doi:10.1038/s41586-019-1236-x

Zinöcker, M., Lindseth, I., 2018. The Western Diet–Microbiome-Host Interaction and Its Role in Metabolic Disease. *Nutrients* 10, 365–15. doi:10.3390/nu10030365

Chapter 2:
**Consumption of a Western-Style Diet Modulates the
Response of the Murine Gut Microbiome to
Ciprofloxacin**

Originally published in *mSystems*, 28 July 2020, Vol 5, No. 4.
DOI: 10.1128/mSystems.00317-20

Consumption of a Western-Style Diet Modulates the Response of the Murine Gut Microbiome to Ciprofloxacin

Damien J. Cabral^{1,+}, Jenna I. Wurster^{1,+}, Benjamin J. Korry¹, Swathi Penumutthu¹, Peter Belenky^{1,#}

Running Title: Impact of antibiotics and diet on the gut microbiome

¹ Department of Molecular Microbiology and Immunology, Brown University, Providence, RI 02906, USA

⁺ Damien J. Cabral and Jenna I. Wurster contributed equally to this work. Author order was determined both by seniority and involvement in study planning.

[#] Address correspondence to Peter Belenky, peter_belenky@brown.edu

Abstract

Dietary composition and antibiotic use have major impacts on the structure and function of the gut microbiome, often resulting in dysbiosis. Despite this, little research has been done to explore the role of host diet as a determinant of antibiotic-induced microbiome disruption. Here, we utilize a multi-omic approach to characterize the impact of Western-style diet consumption on ciprofloxacin-induced changes to gut microbiome structure and transcriptional activity. We found that Western diet consumption dramatically increased *Bacteroides* abundances and shifted the community toward the metabolism of simple sugars and mucus glycoproteins. Mice consuming a Western-style diet experienced a greater expansion of *Firmicutes* following ciprofloxacin treatment than those eating a control diet. Transcriptionally, we found that ciprofloxacin reduced the abundance of tricarboxylic acid (TCA) cycle transcripts on both diets, suggesting that carbon metabolism plays a key role in the response of the gut microbiome to this antibiotic. Despite this, we observed extensive diet-dependent differences in the impact of ciprofloxacin on microbiota function. In particular, at the whole-community level, we detected an increase in starch degradation, glycolysis, and pyruvate fermentation following antibiotic treatment in mice on the Western diet, which we did not observe in mice on the control diet. Similarly, we observed diet-specific changes in the transcriptional activity of two important commensal bacteria, *Akkermansia muciniphila* and *Bacteroides thetaiotaomicron*, involving diverse cellular processes such as nutrient acquisition, stress responses, and capsular polysaccharide (CPS) biosynthesis. These findings demonstrate that host diet plays a role in determining the impacts of ciprofloxacin on microbiome composition and microbiome function.

Importance

Due to the growing incidence of disorders related to antibiotic- induced dysbiosis, it is essential to determine how our “Western”-style diet impacts the response of the microbiome to antibiotics. While diet and antibiotics have profound impacts on gut microbiome composition, little work has been done to ex- amine their combined effects. Previous work has shown that nutrient availability, influenced by diet, plays an important role in determining the extent of antibiotic- induced disruption to the gut microbiome. Thus, we hypothesize that the Western diet will shift microbiota metabolism toward simple sugar and mucus degradation and away from polysaccharide utilization. Because of bacterial metabolism’s critical role in antibiotic susceptibility, this change in baseline metabolism will impact how the structure and function of the microbiome are impacted by ciprofloxacin expo- sure. Understanding how diet modulates antibiotic-induced microbiome disruption will allow for the development of dietary interventions that can alleviate many of the microbiome-dependent complications of antibiotic treatment.

Keywords

Diet, Antibiotics, Metagenomics, Metatranscriptomics, Dysbiosis

List of Abbreviations

CAZyme	Carbohydrate-Active Enzymes
CPS	Capsular Polysaccharide
LPS	Lipopolysaccharide
MAC	Microbiota-Accessible Carbohydrates
PCoA	Principal Coordinates Analysis
PERMANOVA	Permutational ANOVA
PTS	Phosphotransferase system
SCFA	Short-Chain Fatty Acids
TCA	Tricarboxylic Acid

Introduction

The gut microbiome includes the trillions of largely commensal bacteria, archaea, and fungi that inhabit the gastrointestinal tract (Gilbert et al., 2018; Rowan-Nash et al., 2019; Ursell et al., 2012). These communities play an important role in numerous biological processes such as digestion, neurological development, colonization resistance, and immune function (De Luca and Shoenfeld, 2019; Dickerson et al., 2017; Foster and Neufeld, 2013; Hartstra et al., 2015; Leong et al., 2018; Lynch and Boushey, 2016; Mukherjee et al., 2014; Peleg et al., 2010; Riiser, 2015; Rea et al., 2011; Tremlett et al., 2017; Vieira et al., 2014; Blaser, 2011; Stiemsma and Michels, 2018). Consequently, it is unsurprising that disruption of microbial homeostasis, termed dysbiosis, has numerous harmful impacts to the host. The gut microbiome is highly sensitive to perturbations such as broad-spectrum antibiotic usage. Within hours of treatment, antibiotics induce dramatic reductions in both bacterial load and diversity within the microbiome, both of which are common indicators of dysbiosis (Cabral et al., 2019; Dethlefsen and Relman, 2011).

While compositional changes are typically transient and recover following the cessation of a perturbation, oftentimes the structure and diversity of the microbiota never return to their original levels. The resulting dysbiosis often has numerous acute and chronic impacts on host health. In the case of antibiotic usage, this may increase the risk of infection with opportunistic fungal and bacterial pathogens by reducing colonization resistance (Blaser, 2011; Chang et al., 2008; Mukherjee et al., 2014; Peleg et al., 2010; Preidis and Versalovic, 2009; Rafii et al., 2008; Rea et al., 2011; Rowan-Nash et al., 2019; Theriot et al., 2016). Most notably, broad-spectrum antibiotic treatment is a major risk factor in *Clostridioides difficile* infection (Chang et al., 2008; Hryckowian et al., 2018; Lessa et al., 2015; Theriot et al., 2016). Persistent dysbiosis is correlated with many chronic conditions with considerable morbidity and mortality, such as asthma, obesity, and

inflammatory bowel disease (Blaser, 2011; De Luca and Shoenfeld, 2019; Dickerson et al., 2017; Foster and Neufeld, 2013; Hartstra et al., 2015; Hryckowian et al., 2018; Lynch and Boushey, 2016; Rea et al., 2011; Tremlett et al., 2017).

Interestingly, antibiotic-induced disruption of the microbiome may be influenced by the metabolic environment of the gut. A large body of *in vitro* data indicates that the rate of metabolic activity for bacteria correlates positively with antimicrobial susceptibility, such that metabolically active, ATP-producing processes such as respiration promote toxicity, whereas less efficient or quiescent metabolism induces tolerance (Belenky et al., 2015; Dwyer et al., 2014; Lobritz et al., 2015). A similar trend is observed in the context of bacteria responding to antibiotics in the gut microbiome, where nutrient availability and bacterial metabolism are closely linked to host diet. Recent work has demonstrated that antibiotic exposure changes both the composition of the gut microbiome and its metabolic capacity, such that the surviving microbiome is overall less metabolically active (Cabral et al., 2019). Further, amoxicillin treatment was shown to increase the expression of polysaccharide utilization genes, while simultaneously decreasing the abundance of transcripts involved in simple sugar utilization (Cabral et al., 2019). Reflecting these changes, amoxicillin also decreased the total concentration of glucose within the ceca of mice (Cabral et al., 2019). These transcriptional changes have significant impacts on the response of specific bacteria to the treatment. In the case of *Bacteroides thetaiotaomicron*, polysaccharide utilization promoted tolerance to amoxicillin, and simple sugar utilization increased toxicity. Accordingly, the response of the microbiota to antibiotics can be impacted by dietary nutrient modulation (Schnizlein et al., 2020). For example, Cabral et al. found that glucose supplementation impacts the response of the total community and reduces the absolute abundance of bacteria, particularly *B. thetaiotaomicron*, following amoxicillin treatment in mice (Cabral et al., 2019). Together these findings suggest that

dietary composition may act as an additional perturbation that drives the severity of the microbiome's response to antibiotic treatment.

Dietary composition is known to have a profound impact on microbiome diversity and overall gut health (Argueta and DiPatrizio, 2017; Bisanz et al., 2019; Kanoski et al., 2014; Ley et al., 2005; Smits et al., 2017; Turnbaugh et al., 2009; Xu and Knight, 2015). Diets high in fat and simple sugars, typically referred to as “Western” diets, have been associated with a number of negative health states including obesity, diabetes mellitus, allergies, and inflammatory bowel disease (Argueta and DiPatrizio, 2017; Arpaia et al., 2013; Cotillard et al., 2013; Kanoski et al., 2014; Qi et al., 2009; Sami et al., 2017; E. D. Sonnenburg and J. L. Sonnenburg, 2019; 2014; J. L. Sonnenburg et al., 2005; Trompette et al., 2014; Turnbaugh, 2017). Such diets have very low levels of microbiota-accessible carbohydrates (MACs), which are typically found in complex plant polysaccharides and are indigestible and unabsorbable by the host (Fischbach and J. L. Sonnenburg, 2011; Kashyap et al., 2013; E. D. Sonnenburg and J. L. Sonnenburg, 2014; Trompette et al., 2014; Walker et al., 2011). MACs are typically fermented by the colonic microbiota to produce short-chain fatty acids (SCFAs), which play important roles in regulating energy homeostasis and inflammation within the host (Arpaia et al., 2013; E. D. Sonnenburg and J. L. Sonnenburg, 2014; Topping and Clifton, 2001; J. M. W. Wong et al., 2006; Yatsunenکو et al., 2012) (Cani et al., 2019; Chambers et al., 2018; S. Macfarlane and G. T. Macfarlane, 2003). High-MAC diets have also been shown to increase microbial diversity, a classic benchmark for gut microbiota health. Conversely, low-MAC diets are known to reduce both microbiome diversity and SCFA production (Cotillard et al., 2013; David et al., 2014; Kashyap et al., 2013; Trompette et al., 2014). MAC starvation enriches for mucinophilic microbes that are capable of degrading the mucosal lining of the gut, such as *Akkermansia muciniphila* (Desai et al., 2016; Fischbach and J.

L. Sonnenburg, 2011; E. D. Sonnenburg and J. L. Sonnenburg, 2014; J. L. Sonnenburg et al., 2005). Degradation of the mucosal layer over time may result in compromised gut barrier function and lead to increased inflammation, colitis, and susceptibility to infection by enteric pathogens (Schoeler and Caesar, 2019).

Individually, antibiotic usage and the consumption of Western-style diets are known to negatively impact the microbiota, impacting host health. Despite this, little work has explored the impact of diet on the response of the microbiota to antibiotics. Previous work has suggested that dietary composition may play an important role in determining the extent of antibiotic-induced microbiome disruption (Cabral et al., 2019). Thus, we hypothesize that the consumption of a Western-style diet will significantly modify the metabolic activity of the microbiome toward simple sugar and mucus glycoprotein degradation rather than dietary polysaccharide utilization. This will be characterized by differential utilization of carbohydrate-active enzymes (CAZymes) along with changes in respiratory activity and central carbon metabolism. Given that respiratory activity plays a key role in drug susceptibility *in vitro*, when this community is treated with a bactericidal antibiotic like ciprofloxacin, its compositional and functional responses to the drug would be different due to the altered metabolic state. Overall, we anticipate that the diet-related metabolic state of the microbiome before treatment will have a larger impact on drug disruption than the metabolic changes that are induced during the drug exposure. In this study, we use a combined metagenomic and metatranscriptomic approach to characterize the impact of a Western-style diet on the taxonomic and functional disruption of the microbiome during ciprofloxacin treatment. Using shotgun metagenomics, we found that ciprofloxacin elicited differential impacts on community composition in mice at both the phylum and species level in a diet-dependent manner. Using metatranscriptomics, we observed that consumption of a Western diet induced

profound transcriptional changes within the gut microbiomes of mice. Furthermore, consumption of this diet modulated the transcriptional response of these communities to antibiotic treatment. Specifically, dietary composition had a major impact on the abundance of transcripts containing key metabolic genes. Lastly, we were able to detect unique species-specific transcriptional changes in response to both diet and ciprofloxacin treatment in two important commensal bacteria, *A. muciniphila* and *B. thetaiotaomicron*.

Results

To determine the impact of dietary composition and antibiotic exposure on the structure and function of the murine gut microbiome, female C57BL/6J mice were randomly assigned to either a high-fat, high-sugar “Western”-style (Western) diet or a low-fat control diet for 7 days in multiple cages (Table 1). At this point, mice from each diet were again randomly split between ciprofloxacin and vehicle control groups and treated for 24 h in multiple cages ($n = 8$ to 12 per group). Previously it has been shown that 24 h of ciprofloxacin treatment was sufficient to induce changes in community structure and transcriptional activity (Cabral et al., 2019). This time frame also allowed for profiling the acute response of the microbiota to ciprofloxacin exposure, rather than characterizing a post-antibiotic state of equilibrium. Following treatment, the mice were sacrificed to harvest their cecal contents for taxonomic profiling and transcriptional analysis (Figure 1A). Overall, we found that diet and ciprofloxacin treatment had a significant impact on gut microbiome structure (Figure 1B-1D; see also Figure S1 in the supplemental material).

We first assessed the effects that diet and ciprofloxacin have on the diversity of the gut microbiome using 16S rRNA sequencing. Mice consuming the Western diet had significantly less diverse gut microbiomes than those fed the control diet (Figure S1A). Interestingly, we also

observed that the Western diet was associated with a reduction in α -diversity during ciprofloxacin treatment (Figure S1A). Next, we performed Principal Coordinates Analysis (PCoA) using Bray-Curtis dissimilarity paired with permutational multivariate analysis of variance (PERMANOVA) to profile the degree of dissimilarity between our samples and the significance of this distance. Our samples formed four distinct clusters driven by both diet and ciprofloxacin treatment (Figure 1B).

Due to the limited phylogenetic resolution provided by 16S rRNA sequencing and inability to provide functional information about sequenced communities, we opted to perform shotgun metagenomic and metatranscriptomic analyses on a subset of our samples, representing mice from multiple cages ($n = 4$ per treatment group) (Cabral et al., 2019; Clooney et al., 2016; Poretsky et al., 2014; Ranjan et al., 2016; Tessler et al., 2017). Interestingly, we observed that Western diet consumption reduced community diversity while ciprofloxacin did not have a statistically significant impact on the α -diversity of the community (Figure 1C). However, the metagenomic data exhibited a similar trend in unique taxonomic structures being associated with each treatment group, supporting a model wherein diet and antibiotic treatment are distinct perturbations (Figure 1D). However, to evaluate if diet modifies the response to ciprofloxacin, we had to untangle diet-induced changes from antibiotic-induced changes. First, we characterized the impact of the Western diet consumption.

Consumption of a Western diet modifies the metabolic activity of the microbiome. Mice fed a Western diet displayed elevated levels of the phyla *Verrucomicrobia* and *Bacteroidetes* and a reduction of *Firmicutes* (Figure 1D). At the species level, these shifts appear to be largely driven by an expansion of members of the *Bacteroides* genus (Figure 2A, Figure S1B, Data Set S1).

Additionally, the Western diet-fed mice displayed an elevated abundance of several species from the *Proteobacteria* phylum, suggestive of dysbiosis (Shin et al., 2015). Two important bacterial species found in the gut microbiomes of both mice and humans, *B. thetaiotaomicron* and *A. muciniphila*, were observed at significantly elevated levels in the mice fed a Western diet (Figure 2A, Figure S1B). Notably, both species are known to utilize host-produced mucins; thus, this observation is consistent with earlier studies suggesting that the consumption of a low-MAC Western diet enriches for muciniphilic bacteria (Fischbach and J. L. Sonnenburg, 2011; E. D. Sonnenburg and J. L. Sonnenburg, 2014; J. L. Sonnenburg et al., 2005).

Given this expansion, we anticipated that the transcriptional activity of these communities would exhibit an increased capacity for mucus degradation and simple sugar utilization. Due to the potential limitations of using a single pipeline, we analyzed our metatranscriptomic data set with SAMSA2 in parallel with HUMAnN2 (Franzosa et al., 2018; Westreich et al., 2018). The SAMSA2 pipeline generates unnormalized transcript abundances and thus is representative of overall transcript levels (Westreich et al., 2018). SAMSA2 is advantageous in its capacity for annotation against multiple databases and enables differential abundance testing of individual transcripts in addition to pathway- and subsystem-level analysis (Westreich et al., 2018). Conversely, the HUMAnN2 pipeline normalizes the abundance of RNA transcripts against their corresponding gene abundance in the metagenomic data set, thus normalizing for differences in community composition between experimental groups and facilitating comparisons of metabolic pathway expression at the whole-community level (Franzosa et al., 2018). When paired, these pipelines facilitate a more robust examination of microbiome transcriptional activity.

We observed an increased abundance of transcripts related to respiration at the SEED subsystem level in the microbiota of the mice consuming the Western diet, which was mirrored in

our HUMAnN2 data set as increased tricarboxylic acid (TCA) cycle expression (Figure 2B, Figure S2A, Data Sets S2 and S3). The Western diet-fed mouse microbiota also displayed increased abundance of transcripts involving fatty acid metabolism and terpenoid biosynthesis, likely reflecting altered nutrient availability and increased respiratory activity, respectively (Figure 2B, Data Set S3) (Gill et al., 2006; Odom, 2011). Interestingly, we also detected large increases in the abundance of two different sialidase transcripts, which play a key role in the utilization of host-produced mucins (Figure S2B, Data Set S4) (Corfield et al., 1992). While other studies have shown that the consumption of a Western diet enriches for muciniphilic taxa, this observation suggests that this diet also increases transcriptional activity related to mucin degradation within the microbiome (E. D. Sonnenburg and J. L. Sonnenburg, 2014; J. L. Sonnenburg et al., 2005).

Additionally, the Western diet-fed mouse microbiota had reduced expression of nucleotide biosynthesis, glycolysis, gluconeogenesis, starch degradation, and pyruvate fermentation compared to control diet-fed mice (Figure S2A, Data Set S2). We also observed relative reduction in the expression of the *Bifidobacterium* shunt, which is known to play a role in SCFA production and may provide mechanistic insight into the reduced SCFA levels observed on the Western diet in other studies (Figure S2A, Data Set S2) (E. D. Sonnenburg and J. L. Sonnenburg, 2014; J. M. W. Wong et al., 2006). Examination of CAZyme activity provided further evidence of significant transcriptional reprogramming in response to diet. Specifically, we observed that Western diet consumption decreased transcript abundances of multiple enzymes involved in polysaccharide breakdown (Figure 2C, Data Set S5) (Eckardt, 2008; Hii et al., 2012; Kaur et al., 2020; Knoch et al., 2014). Simultaneously, there was a significant increase in α -amylases, lysozyme C, and α -lactalbumin breakdown (Figure 2C, Data Set S5) (Layman et al., 2018; Zhou et al., 2019). Given the content of the Western diet, a shift toward utilization of these carbon sources was not

unexpected. However, the robust loss of complex polysaccharide breakdown was surprising and complements the SEED and HUMAN2 data sets. Together these data suggest that Western diet alone is sufficient to restructure the metabolic activity of the gut microbiome, due to significant changes in nutrient availability.

Ciprofloxacin elicits unique shifts in gene expression on Western and control diets. Given the significant body of literature that links microbial metabolism with antimicrobial susceptibility both *in vitro* and within the microbiome, we hypothesized that the metabolic restructuring induced by the Western diet would result in differential susceptibility to ciprofloxacin (Belenky et al., 2015; Cabral et al., 2019; Dwyer et al., 2014; Lobritz et al., 2015). Although ciprofloxacin did not induce a significant reduction in α -diversity in the time frame tested, we found that diet drove differential community composition following antibiotic exposure (Figure 1C, Figure 1D). At the phylum level, we observed a significant expansion in the relative abundance of *Firmicutes* following ciprofloxacin treatment on the Western diet (adjusted P value = 0.0388) but not on the control diet (adjusted P value = 0.8718) (Figure 1D, Figure S1B). To determine which species displayed a differential response to ciprofloxacin on the Western and control diets, we utilized DESeq2 to analyze the interaction between diet and antibiotic treatment to determine which species displayed differential responses to ciprofloxacin between the diets (Love et al., 2014). While most species responded similarly to ciprofloxacin therapy on both diets, there were several notable exceptions. For example, the expansion of several *Clostridium* species (such as *Clostridium saccharolyticum*, *Clostridium sphenoides*, and *Clostridium scindens*) following ciprofloxacin was higher on the Western diet than the control (positive interaction values, Figure 3A, Data Set S1). Conversely,

the reduction of several *Bacteroides* species following antibiotic treatment tended to be exacerbated on the Western diet (negative interaction values, Figure 3A, Data Set S1).

We detected clear differences in ciprofloxacin susceptibility between the two diets and hypothesized that diet-induced differences in metabolism would both alter susceptibility and be reflected in unique transcriptional signatures. An all-by-all comparison of experimental groups demonstrated that the microbiota of Western diet-consuming mice displayed elevated expression of TCA cycle and fatty acid degradation pathways in both vehicle and ciprofloxacin treatments, likely reflective of the increased fat and sugar content of this diet (Figure 3B, Data Set S2). Additionally, we found elevated expression of glycogen degradation genes that was specific to Western diet-fed mice receiving ciprofloxacin (Figure 3B, Data Set S2). Conversely, the microbiota of control diet-consuming mice had elevated expression of amino acid biosynthesis pathways (isoleucine, aspartate, asparagine, lysine, and histidine) regardless of antibiotic treatment (Figure 3B, Data Set S2). We also observed elevated levels of several different nucleotide biosynthesis pathways in the vehicle-treated control diet mice while the Western diet mice displayed elevated levels of adenosine and guanosine nucleotide degradation (Figure 3B, Data Set S2). Overall, these data support that our experimental groups could be characterized by unique transcriptional signatures.

We found key differences in the overall transcriptional profiles in response to ciprofloxacin on each diet. On the Western diet, ciprofloxacin treatment was associated with an increased abundance of transcripts from glycogen and starch degradation, glycolysis, and pyruvate fermentation (Figure S3C, Data Set S2). Notably, the expression of glycogen degradation was elevated in vehicle-treated samples on the control diet, suggesting that the utilization of this pathway during ciprofloxacin treatment is diet dependent (Figure S3C, Data Set S2). We observed

that TCA cycle expression was reduced in ciprofloxacin-treated mice compared to the vehicle treatment—the lone commonality between diets (Figure S3C, Data Set 2). Previous work has demonstrated that TCA cycle elevation increases sensitivity to bactericidal antibiotics (Belenky et al., 2015; Lobritz et al., 2015; Meylan et al., 2017). Thus, this result suggests that TCA cycle activity may play a key role in the response of the microbiota to ciprofloxacin treatment *in vivo*, though more work is required to understand its impact.

Interestingly, comparatively few subsystems were changed following ciprofloxacin treatment on either diet (Figure 3C, Figure 3D, Data Set S3), suggesting that the pretreatment metabolic state affects the antibiotic response more than the drug-induced transcriptional changes. Most notably, we observed a decrease in transcripts related to dormancy and sporulation in response to ciprofloxacin on both diets (Figure 3C, Figure 3D, Data Set S3). A similar finding was observed in a recent study, suggesting that these transcripts may play a key role in the response of the microbiota to this antibiotic (Cabral et al., 2019). Furthermore, ciprofloxacin increased the abundance of sialidase transcripts in mice on the control diet, suggesting that this effect may be exacerbated by antibiotic treatment (Figure S3A, Data Set S4). Reflecting the overall reduction in sporulation seen at the subsystem level, we found that several sporulation-related transcripts were reduced on the control diet following ciprofloxacin treatment (Figure S3A, Data Set S4).

We also examined the interaction of diet and antibiotic treatment on transcript abundance within the microbiome. Notably, we found that several sporulation genes were significantly higher on the Western diet than the control following ciprofloxacin treatment (Data Set S4), which was reflected in the SEED subsystem level (Figure 3C, Figure 3D). Additionally, transcripts encoding phosphotransferase system (PTS) transporters of various substrates were also found to be higher on the Western diet following ciprofloxacin treatment (Data Set S4). Conversely, Western diet

consumption significantly reduced the change in transcript abundance of both pectate lyase and a hemin receptor following ciprofloxacin therapy. Together, these findings demonstrate that dietary composition significantly impacts the transcriptional response of the microbiome to ciprofloxacin.

Recent studies have shown CAZyme activity to be a significant component of the microbiome's response to antibiotic stress (Cabral et al., 2019). In our study, over 75 CAZymes exhibited differential abundance during ciprofloxacin treatment (Data Set S5). Interestingly, these changes were exclusive to the control diet-fed microbiota, as the Western diet-fed communities displayed no significant difference in CAZyme abundance (Data Set S5). The microbiota of mice on the control diet exhibited increases in CAZymes involved in starch, glycogen, xylose, pectin, rhamnogalacturonan, and arabinofuranose degradation (Data Set S5) (Lapébie et al., 2019; Mäkelä et al., 2018). Additionally, these communities exhibited a significant increase in trehalose phosphorylase and synthase activity, both of which have been associated with transient antibiotic tolerance in pathogenic species (Data Set S5) (Collins et al., 2018; Lee et al., 2019). Loss of these CAZyme shifts may be directly involved in the increased toxicity of ciprofloxacin on the Western diet; however, more work is required to elucidate the mechanism. These data, in conjunction with our SEED and HUMAnN2 data sets, provide evidence for unique transcriptional signatures during ciprofloxacin challenge that are diet dependent. Overall, this supports a model in which diet-driven differences in baseline metabolism directly impact taxonomic and functional responses to ciprofloxacin treatment.

Diet and ciprofloxacin alter gene expression within *B. thetaiotaomicron* and *A. muciniphila*.

Next, we sought to profile how diet and drug treatment impacted the transcriptional response of

individual species within the microbiota. In order to have sufficient genome coverage and sequencing depth, we ranked all taxa that were differentially abundant in the Western diet by average RNA reads, further analyzing only those with 500,000 or greater (Data Set S6). With this criterion, we used a previously published pipeline to interrogate the impact of diet and antibiotic treatment on three individual species: *B. thetaiotaomicron*, *A. muciniphila*, and *C. scindens* (Cabral et al., 2019; Deng et al., 2018). We focused on these bacteria because they are known human gut commensals, were found at relatively high levels in all samples analyzed and were differentially abundant in a diet-dependent manner. Unfortunately, *C. scindens* had relatively few transcriptional changes across all comparisons, and those genes that were differentially regulated were almost exclusively hypothetical proteins (Data Set S6).

The Western diet significantly elevated the relative abundance of *A. muciniphila* (Figure 4A). Interestingly, on this diet *A. muciniphila* displayed increased expression of several known stress response genes: catalase HPII, ATP-dependent chaperone ClpB, a universal stress protein, superoxide dismutase, and a UvrB/UvrC protein (Figure 4B, Data Set S7). Additionally, we observed numerous changes in respiration and central carbon metabolism, including increased terminal oxidases, TCA cycle, glycolysis, and pyruvate metabolism, suggesting broad metabolic changes in response to the Western diet (Figure 4B, Data Set 7). No CAZymes were differentially expressed on this diet, suggesting that the changes in *A. muciniphila* that facilitate its expansion are not driven by CAZyme activity (Data Set S7).

Ciprofloxacin treatment had a relatively minor impact on *A. muciniphila* gene expression (Data Set S7), likely due to the relatively low impact on the relative abundance of *A. muciniphila* (Figure 4A). In total, ciprofloxacin significantly altered the expression of 2 and 17 genes on the control and Western diets, respectively (Data Set S7). On the control diet, *A. muciniphila* increased

the expression of the molecular chaperone protein DnaK, which is known to play a role in stress responses (Anglès et al., 2017; Ogata et al., 1996; Susin et al., 2006; K. S. Wong and Houry, 2012). On the Western diet, several genes related to tryptophan biosynthesis and metabolism were elevated following ciprofloxacin treatment; however, their biological significance is unclear at this time (Data Set S7). Additionally, ciprofloxacin induced the differential expression of a sole chitin or lysozyme glycoside hydrolase, and only on the control diet (Figure S3F, Data Set S7). Lastly, an examination of the interaction between diet and ciprofloxacin treatment indicated that only three genes were significantly altered. Overall, these data suggest that diet does not have a major impact on the response of this bacterium to ciprofloxacin within the microbiome (Data Set 7).

In contrast to *A. muciniphila*, diet had a relatively minor impact on *B. thetaiotaomicron* gene expression while ciprofloxacin induced extensive changes. Of note, *B. thetaiotaomicron* bloomed in response to the Western diet and was significantly perturbed by ciprofloxacin on this diet but not on the control (Figure 4C). In total, 42 genes were altered in *B. thetaiotaomicron* in response to Western diet consumption (Data Set S7). Of note, this diet increased the expression of an aminoglycoside efflux pump and a hemin receptor. However, more than half of the genes (52.4%) that changed in response to diet are of unknown function and are classified as “hypothetical proteins;” making interpretation difficult. Interestingly, *B. thetaiotaomicron* did not exhibit robust changes in CAZyme transcription in response to the Western diet. Like *A. muciniphila*, *B. thetaiotaomicron* did not exhibit any differentially abundant CAZymes, suggesting that carbohydrate utilization does not drive the diet-induced changes in *B. thetaiotaomicron* abundance (Data Set S7). Ultimately, a description of this change will be dependent on improved functional annotations going forward.

On the control diet, we observed an increased abundance of transcripts encoding proteins involved in capsular polysaccharide (CPS) biosynthesis and export (Figure 4D, Data Set S7). Within *B. thetaiotaomicron*, CPS production is encoded by a total of 182 genes distributed among eight loci (typically termed *cps1* to -8) (Coyne and Comstock, 2008; Porter et al., 2017). It is hypothesized that an individual bacterium expresses one of these CPS configurations at any given time and that these structures play key roles in processes such as nutrient acquisition and immune evasion (Porter et al., 2017). Additionally, the two genes with the greatest increase in expression during ciprofloxacin treatment encoded UDP-glucose 6-dehydrogenase, which plays a key role in the biosynthesis of glycan precursors that are essential for capsule production in other bacteria (Dougherty and van de Rijn, 1993; Petit et al., 1995; van Selm et al., 2002). Together, these findings may suggest a role for CPS state as a determinant of ciprofloxacin susceptibility *in vivo*.

On the Western diet, ciprofloxacin elicited profound changes in transcriptional activity, altering the expression of 278 different genes (Figure 4E, Data Set S7), and this robust response may be related to the reduction in *B. thetaiotaomicron* under this condition (Figure 4C). Interestingly, expression of many genes involved in the utilization of host-derived carbohydrates (sialic acid-specific 9-*O*-acetyltransferase, endo- β -*N*-acetylglucosaminidase F1, β -hexosaminidase) and stress responses (universal stress protein UspA, thioredoxin) was reduced, mirroring changes seen at the whole- community level (Figure 4E, Data Set S7) in response to ciprofloxacin. Conversely, we observed increased expression of several genes that encode molecular chaperones or are involved in DNA replication or damage repair (Figure 4E, Data Set S7). Ciprofloxacin triggers DNA damage via inhibition of DNA gyrase and topoisomerase IV. Thus, these changes in gene expression may be reflective of the primary mechanism of action of this antibiotic, are

consistent with previously published data, and serve as a validation for our analysis (Cabral et al., 2019).

Diet appears to have a significant impact on ciprofloxacin-induced transcriptional changes in *B. thetaiotaomicron*, modulating the response of 71 genes (Data Set S7). Of note, Western diet consumption in the context of ciprofloxacin treatment had a negative impact on several genes involved in the acquisition of nutrients, such as vitamin B12 and hemin receptors, and transporters of glucose/galactose, hexuronate, arabinose, and Na⁺ (Data Set S7). Thus, it is likely that the availability of nutrients within the gut plays a role in the response of these bacteria to antibiotics. Lastly, we examined the impact that nutrient availability has on the response of *B. thetaiotaomicron* CAZyme abundance to ciprofloxacin. We observed notable differences in CAZyme levels between the diets as well as differences in substrate targets (Figure S3DE, Data Set S7). On the control diet, *B. thetaiotaomicron* exhibits an increase in polysaccharide CAZymes, including those targeting pectin, rhamnogalacturonan, α -glucans, and hemicelluloses, with a simultaneous decrease in β -fucosidases (Figure S3D, Data Set S7). On the Western diet, *B. thetaiotaomicron* exhibits an increase in lipopolysaccharide (LPS) biosynthesis and heparan degradation (Figure S3E, Data Set S7). While interesting, more work will be required to elucidate mechanisms driving these phenotypes.

Discussion

Previous work has demonstrated that host diet, particularly with respect to sugar and fiber content, plays a major role in antibiotic-induced microbiome disruption (Cabral et al., 2019; Schnizlein et al., 2020). In Western societies, many people consume a diet high in added sugars and fat but low in host-indigestible fiber. Such a composition is thought to promote the

development of metabolic syndrome, heart disease, diabetes, and a number of other chronic conditions (Argueta and DiPatrizio, 2017; Arpaia et al., 2013; Cotillard et al., 2013; Kanoski et al., 2014; Qi et al., 2009; Sami et al., 2017; E. D. Sonnenburg and J. L. Sonnenburg, 2019; 2014; J. L. Sonnenburg et al., 2005; Trompette et al., 2014; Turnbaugh, 2017). Furthermore, broad-spectrum antibiotic use and resulting micro- biome dysbiosis have been associated with a number of similar comorbidities along with increased susceptibility to opportunistic infections (Blaser, 2011; Chang et al., 2008; Lessa et al., 2015; Mukherjee et al., 2014; Peleg et al., 2010; Preidis and Versalovic, 2009; Rafii et al., 2008; Rowan-Nash et al., 2019; Theriot et al., 2016). Despite this connection, little work has been done examining how host dietary composition impacts the response of the microbiota to antibiotic perturbation. Nutrient availability and metabolic state are known to be major determinants of antibiotic susceptibility of bacteria *in vitro* (Adolfson and Brynildsen, 2015; Allison et al., 2011; Belenky et al., 2015; Cabral et al., 2019; 2018; Cho et al., 2014; Dwyer et al., 2014; Kohanski et al., 2007; Lobritz et al., 2015; Meylan et al., 2017; Thomas et al., 2013). Thus, modulating diet and subsequently nutrient availability to the microbiota would likely alter the sensitivity of bacteria in these communities to antibiotic therapy.

Using a combined metagenomic and metatranscriptomic approach, we demonstrate that diet composition has a major impact on the response of the murine gut microbiome to ciprofloxacin therapy. By utilizing these tools in parallel, we are able to link transcriptional changes to observed shifts in community structure on each diet. Using metagenomics, we observed that ciprofloxacin had a differential impact on community composition in a diet-dependent manner. Specifically, we observed a significant expansion of the *Firmicutes* phylum following ciprofloxacin treatment only on the Western diet. Metatranscriptomic data showed decreased abundance of transcripts from the TCA cycle after antibiotic treatment in both diets, suggesting that this response is diet independent,

which is consistent with previous *in vitro* findings that demonstrate a key role for bacterial respiration as a determinant of fluoroquinolone susceptibility (Adolfson and Brynildsen, 2015; Belenky et al., 2015; Elderman et al., 2018; Johnson et al., 2019; Lapébie et al., 2019; Lobritz et al., 2015; Singh et al., 2017). Conversely, the impact of ciprofloxacin on the abundance of various iron and mucin utilization transcripts differed between diets. Lastly, we detected species-specific transcriptional changes in two important commensal bacteria, *B. thetaiotaomicron* and *A. muciniphila*. In addition to detecting changes in transcript levels that were reflective of stress responses, we also observed differential expression in transcripts involved in diverse cellular processes such as nutrient acquisition, carbon metabolism, and CPS biosynthesis. Together, our findings supported our hypothesis that the Western diet would modify the metabolic capacity of the gut microbiome and that this change would directly translate to differential activity in response to ciprofloxacin treatment.

Despite the advantages of a multi-omic approach, there are several drawbacks to these techniques that complicate interpretation of the results. First, our study was performed only in female mice. It is now understood that sex-dependent differences exist in diet metabolism, mucosal immunity, and gut microbiome antibiotic responses, and as such our findings may not be generalizable to males (Elderman et al., 2018; Gao et al., 2019; Ingvorsen et al., 2017). Another critical drawback is that the analytical pipelines used to analyze microbiome data are reliant on existing databases that are largely incomplete: approximately half of all genes within the human gut microbiome are hypothesized to have no functional annotation, limiting the ability to accurately profile the transcriptional activity of these communities (The Human Microbiome Project Consortium, 2012). Additionally, inferring biological significance of taxonomic changes is often difficult in many microbiome analyses. 16S amplicon sequencing and shotgun

metagenomics are inherently limited to reporting relative abundances and thus may fail to fully characterize changes in absolute abundance. Thus, we cannot comment on how diet or antibiotics change the total number of bacteria found in the gut, nor can we determine if the bloom in *Firmicutes* is a result of an increase in colony-forming units or a reduction of other bacteria relative to *Firmicutes*. Due to the complex nature of these communities, it is challenging to ascertain if the observed transcriptional changes are the result of the direct action of the antibiotic or the indirect effect of changes in host physiology, nutrient availability, or the disruption of ecological networks within the microbiome. For example, our transcriptional analysis of *B. thetaiotaomicron* showed that this bacterium differentially expressed receptors for both heme and vitamin B₁₂, which may suggest that these nutrients play a role in ciprofloxacin toxicity. Alternatively, it is possible that these transcriptional changes are reflective of increased availability of these nutrients due to decreased competition from other members of the microbiota. Further, dietary composition could play a significant role in antibiotic absorption or sequestration in the gut, which in turn would impact the extent of the damage caused to the microbiota.

This study builds on recent work that demonstrates that the availability of metabolites plays an important role in determining the extent of antibiotic-induced microbiome disruption (Cabral et al., 2019). Taken together, these results demonstrate the need to consider dietary composition in the design and interpretation of experiments focused on understanding the impact of antibiotics on the microbiota. Previous studies have demonstrated that dietary changes induce rapid shifts in gut microbiome composition (Bisanz et al., 2019; David et al., 2014; Johnson et al., 2019; Singh et al., 2017; Turnbaugh, 2017; Turnbaugh et al., 2009; 2008; 2006). Therefore, in the long term, dietary modulation could represent an attractive strategy to reduce the collateral damage to commensal bacteria and the resulting complications from dysbiosis caused by clinical therapy.

Despite these promising applications, considerable work is required before these findings have direct clinical relevance. In particular, the considerable differences in physiology, microbiome composition, and diet between humans and rodents complicate the direct clinical relevance of these findings. Furthermore, it is unclear whether short-term dietary modulation has any long-term consequences on either the host or the microbiome. Thus, additional research is warranted to fully elucidate how host diet impacts antibiotic-induced microbiome disruption in humans and how specific dietary formulation will impact these disruptions.

Acknowledgements

D.J.C., J.I.W., B.J.K., and S.P. were supported by the Graduate Research Fellowship Program from the National Science Foundation under award number 1644760. P.B. was supported by the U.S. Department of Defense through the Peer Reviewed Medical Research Program under award number W81XWH-18-1-0198, by the National Center for Complementary & Integrative Health of the NIH under award number R21AT010366, and by institutional development awards P20GM121344 and P20GM109035 received from the National Institute of General Medical Sciences. The funding agencies had no role in the design of the study or the collection, analysis, and interpretation of data. The authors would like to specifically thank Caroline Keroack for her thoughtful feedback during the editing process.

Author Contributions

D.J.C planned the study, performed mouse experiments, extracted nucleic acids from cecal samples, conducted analysis of 16S rRNA amplicon, metagenomic, and metatranscriptomic data, and co-wrote the manuscript. J.I.W assisted with mouse experiments, prepared DNA and RNA

into sequencing libraries for metagenomics and metatranscriptomics, conducted analysis of metatranscriptomic data, assisted in the interpretation of results, and co-wrote the manuscript. B.J.K. assisted with the analysis of metatranscriptomic data. S.P. assisted in the interpretation of results. P.B. conceptualized and planned the study, contributed to the writing of the manuscript, and secured funding. All authors have read and approved of the final manuscript.

Declarations of Interest

The authors declare no competing interests.

Materials and Methods

Resource Availability

Lead Contact

Further information and requests for resources and reagents should be directed to and will be fulfilled by the Lead Contact, Peter Belenky (peter_belenky@brown.edu).

Materials Availability

This study did not generate new, unique reagents

Data and Code Availability

- The data sets generated and analyzed during this study are available from the NCBI Sequence Read Archive (SRA) under BioProject accession numbers PRJNA563913 (metagenomics and metatranscriptomics) and PRJNA594642 (16S rRNA amplicon sequences). Data are publicly available as of the date of publication.
- This paper does not report original code
- Any additional information required to reanalyze the data reported in this paper is available from the lead contact upon request

Method Details

Animal Procedures

All animal work was approved by Brown University's Institutional Animal Care and Use Committee (IACUC) under protocol number 1706000283. Four-week-old female C57BL/6J mice

were purchased from Jackson Laboratories (Bar Harbor, ME, USA) and given a 2-week habituation period immediately following arrival at Brown University's Animal Care Facility. After habituation, mice were switched from standard chow (Laboratory Rodent Diet 5001; St. Louis, MO, USA) to either a Western diet (D12079B; Research Diets Inc., New Brunswick, NJ, USA) or a macronutrient-defined control diet (D12450B; Research Diets Inc., New Brunswick, NJ, USA) for 1 week (see Table 1 and Data Set S7:Sheet 41, in the supplemental material). On the 8th day of dietary intervention, mice were given acidified ciprofloxacin (12.5 mg/kg of body weight/day), or a pH-adjusted vehicle, via filter-sterilized drinking water *ad libitum* for 24 h ($n = 8$ to 12 per treatment group). Water consumption was monitored to ensure equal consumption across cages. Mice were then sacrificed and dissected in order to collect cecal contents. Cecal contents were immediately transferred to ZymoBIOMICS DNA/RNA Miniprep kit (Zymo Research, Irvine, CA, USA) collection tubes containing DNA/RNA Shield. Tubes were processed via vortex at maximum speed for 5 min to homogenize cecal contents and then placed on ice until permanent storage at -80°C .

Nucleic Acid Extraction & Purification

Total nucleic acids (DNA and RNA) were extracted from samples using the ZymoBIOMICS DNA/RNA Miniprep kit from Zymo Research (R2002; Irvine, CA, USA) using the parallel extraction protocol per the manufacturer's instructions. Total RNA and DNA were eluted in nuclease-free water and quantified using the dsDNA-HS and RNA-HS kits on a Qubit 3.0 fluorometer (Thermo Fisher Scientific, Waltham, MA, USA) before use in library preparations.

16S rRNA Amplicon Preparation & Sequencing

The 16S rRNA V4 hypervariable region was amplified from total DNA using the barcoded 518F forward primer and the 816Rb reverse primers from the Earth Microbiome Project (Thompson et al., 2017). Amplicons were generated using 5X Phusion high-fidelity DNA polymerase under the following cycling conditions: initial denaturation at 98°C for 30 s, followed by 25 cycles of 98°C for 10 s, 57°C for 30 s, and 72°C for 30 s, and then a final extension at 72°C for 5 min. After amplification, samples were pooled in equimolar amounts and visualized via gel electrophoresis. The pooled amplicon library was submitted to the Rhode Island Genomics and Sequencing Center at the University of Rhode Island (Kingston, RI, USA) for sequencing on the Illumina MiSeq platform. Amplicons were pair-end sequenced (2 X 250 bp) using the 500-cycle kit with standard protocols. We obtained an average of $106,135 \pm 49,789$ reads per sample.

Analysis of 16S rRNA Sequencing Reads

Raw 16S rRNA reads were subjected to quality filtering, trimming, denoising, and merging using the DADA2 package (version 1.8.0) in R (version 3.5.0). Ribosomal sequence variants were assigned taxonomy using the RDP Classifier algorithm with RDP Training set 16 using the *assignTaxonomy* function in DADA2 (Wang et al., 2007). α -diversity (Shannon) and β -diversity (Bray-Curtis dissimilarity) were calculated using the phyloseq package (version 1.24.2) in R (version 3.5.0).

Metagenomic & Metatranscriptomic Library Preparation

Metagenomic libraries were prepared from DNA (100 ng) using the NEBNext Ultra II FS DNA library prep kit (New England BioLabs, Ipswich, MA, USA) >100-ng input protocol per the manufacturer's instructions. This yielded a pool of 200- to 1,000-bp fragments where the average

library was 250 to 500 bp. Metatranscriptomic libraries were prepared from total RNA using the NEBNext Ultra II Directional RNA sequencing prep kit (New England BioLabs, Ipswich, MA, USA) in conjunction with the NEBNext rRNA depletion kit for human/mouse/rat (New England BioLabs, Ipswich, MA, USA) and the MICROBExpress kit (Invitrogen, Carlsbad, CA, USA). First, up to 1 μ g of total RNA was treated with recombinant DNase I (rDNase I) and subsequently depleted of bacterial rRNAs using MICROBExpress per the manufacturer's instructions. This depleted RNA was then used to prepare libraries with the NEBNext Ultra II Directional RNA sequencing prep and rRNA depletion kits per the manufacturer's instructions. This yielded libraries that averaged between 200 and 450 bp. Once library preparation was complete, both metagenomic and metatranscriptomic libraries were sequenced as paired-end 150-bp reads on an Illumina HiSeq X Ten. We sequenced an average of 2,278,948,631 (\pm 2,309,494,556) bases per metagenomic sample and 14,751,606,319 (\pm 3,089,205,166) bases per metatranscriptomic sample. One metagenomic sample from the Western diet + vehicle group had an abnormally low number of bases sequenced (165,000 bp) and was excluded from all subsequent analyses. Following the removal of this sample, we obtained an average of 2,430,867,540 (\pm 2,306,317,898) bases per metagenomic sample.

Processing of Raw Metagenomic and Metatranscriptomic Reads

Raw metagenomic reads were trimmed and decontaminated using the kneaddata utility (version 0.6.1) (McIver et al., 2018). In brief, reads were first trimmed to remove low-quality bases and Illumina TruSeq3 adapter sequences using Trimmomatic (version 0.36) using a SLIDINGWINDOW value of 4:20 and an ILLUMINACLIP value of 2:20:10, respectively (Bolger et al., 2014). Trimmed reads shorter than 75 bases were discarded. Reads passing quality control

were subsequently decontaminated by removing those that mapped to the genome of C57BL/6J mice using bowtie2 (version 2.2) (Langmead and Salzberg, 2012). Additionally, preliminary work by our group detected high levels of reads mapping to two murine retroviruses found in our animal facility: murine mammary tumor virus (MMTV, accession NC_001503) and murine osteosarcoma viruses (MOV, accession NC_001506.1) (Cabral et al., 2019). Raw metatranscriptomic reads were trimmed and decontaminated using the same parameters. However, in addition to removing reads that mapped to the C57BL/6J, MMTV, and MOV genomes, we also decontaminated sequences that aligned to the SILVA 128 LSU and SSU Parc rRNA databases (Pruesse et al., 2007).

Taxonomic Classification of Metagenomic Reads

Trimmed and decontaminated metagenomic reads were taxonomically classified against a database containing all bacterial and archaeal genomes found in NCBI RefSeq using Kraken2 (version 2.0.7-beta) with a default k-mer length of 35 (Wood and Salzberg, 2014). Phylum- and species-level abundances were subsequently calculated from Kraken2 reports using Bracken (version 2.0.0) with default settings (Lu et al., 2017). The phyloseq package (version 1.28.0) in R (version 3.6.0) was used to calculate α -diversity using the Shannon diversity index (McMurdie and Holmes, 2013). Metagenomic data were not sub-sampled prior to analysis.

To perform differential abundance testing, species-level taxonomic output was first filtered to remove taxa that were not observed in >1,000 reads (corresponding to approximately 0.1% of all reads) in at least 20% of all samples using phyloseq in R. Differential abundance testing was subsequently performed on filtered counts using the DESeq2 package (version 1.24.0) using default parameters (Love et al., 2014). All *P* values were corrected for multiple hypothesis testing using the Benjamini-Hochberg method (Benjamini and Hochberg, 1995).

Annotation of Metatranscriptomic Reads Using SAMSA2

Trimmed and decontaminated meta- transcriptomic reads were annotated using a modified version of the Simple Annotation of Metatranscriptomes by Sequence Analysis 2 (SAMSA2) pipeline as described previously (Cabral et al., 2019; Westreich et al., 2018; 2016). First, the Paired-End Read Merger (PEAR) utility was used to merge forward and reverse reads (Zhang et al., 2014). Merged reads were then aligned to databases containing entries from the RefSeq, SEED Subsystems, and CAZyme databases using DIAMOND (version 0.9.12) (Buchfink et al., 2014; Cantarel et al., 2009; Overbeek et al., 2014). The resulting alignment counts were subsequently analyzed using DESeq2 (version 1.24.0) using the Benjamini-Hochberg method to perform multiple hypothesis testing correction (Benjamini and Hochberg, 1995; Cabral et al., 2019; Westreich et al., 2018). Features with an adjusted P value of less than 0.05 were considered to be statistically significant.

Metatranscriptomic Analysis using HUMAnN2

To determine the impact of dietary modulation and ciprofloxacin treatment on gene expression within the gut microbiome, we used the HMP Unified Metabolic Analysis Network 2 (HUMAnN2, version 0.11.1) pipeline (Franzosa et al., 2018). First, metagenomic reads were taxonomically annotated using MetaPhlan2 (version 2.6.0) and functionally annotated against the UniRef90 database to generate gene family and MetaCyc pathway-level abundances. To ensure consistent assignment between paired samples, the taxonomic profile generated from the metagenomic reads was supplied to the HUMAnN2 algorithm during the analysis of the corresponding metatranscriptomic reads. Metatranscriptomic reads were subsequently annotated as done for metagenomic reads. The resulting gene family and pathway-level abundance data from the

metatranscriptomic reads were normalized against the metagenomic data from the corresponding sample and smoothed using the Witten-Bell method (Witten and Bell, 1991). Lastly, the resulting RPKM (reads per kilobase per million) values were unstratified to obtain whole-community level data, converted into relative abundances, and analyzed using LEfSe (version 1) hosted on the Galaxy web server (Segata et al., 2011).

Transcriptional Analysis of *A. muciniphila* and *B. thetaiotaomicron*

A modified version of a previously published pipeline from Deng et al. was utilized to perform transcriptional analysis of individual species within the murine microbiome during dietary modulation and antibiotic treatment (Cabral et al., 2019; Deng et al., 2018). First, Kraken2 (version 2.0.7-beta) was used to identify the 50 most prevalent bacterial species present within the metatranscriptomic samples (Wood and Salzberg, 2014). Next, the BBSplit utility within the BBSplit package (version 37.96) was used to extract reads within our metatranscriptomic data set that mapped to these 50 most abundant species (Bushnell, 2014). Reads from *B. thetaiotaomicron*, *A. muciniphila*, and *C. scindens* were subsequently aligned to their corresponding reference genomes using the BWA-MEM algorithm (version 0.7.15) (Li and Durbin, 2010). Lastly, the featureCounts command within the subread program (version 1.6.2) was used to analyze the resulting alignment files to generate a count table for differential expression analysis with DESeq2 (Love et al., 2014). All *P* values were corrected for multiple hypothesis testing with the Benjamini-Hochberg method (Benjamini and Hochberg, 1995). Features with an adjusted *P* value of less than 0.05 were considered to be statistically significant.

Main Figures, Titles, Tables, and Legends

Table 1. Diet formulation used in this study. Diets were purchased from Research Diets Incorporated (New Brunswick, New Jersey, USA)

Formulation	Gram % (Control Diet)	Kcal % (Control Diet)	Gram (Western Diet)	Kcal (Western Diet)
Proteins	19.2	20	20	17
Carbohydrates	67.3	70	50	43
Fats	4.3	10	21	40
Formulation	Gram % (Control Diet)	Kcal % (Control Diet)	Gram (Western Diet)	Kcal (Western Diet)
Casein (30 mesh)	200	800	-	-
Casein (80 mesh)	-	-	195	780
L-cystine	3	12	-	-
D/L-Methionine	-	-	3	12
Corn Starch	315	2160	50	200
Maltodextrin	35	140	100	400
Sucrose	350	1400	341	1364
Cellulose BW200	50	0	50	0
Anhydrous Milk Fat	-	-	200	1800
Corn Oil	-	-	10	90
Soybean Oil	25	225	-	-
Lard	20	180	-	-
Mineral Mix S10026	10	0	-	-
Mineral Mix S10001	-	-	35	0
DiCalcium Phosphate	13	0	-	-
Calcium Carbonate	5.5	0	4	0
Potassium Citrate	16.5	0	-	-
Vitamin Mix V10001	10	40	10	40
Choline Bicarbonate	2	0	2	0
Cholesterol USP	-	-	1.5	0
Ethoxyquin	-	-	0.04	0
FD&C Yellow Dye No. 5	0.05	0	-	-
Total	1055.5	4057	1001.54	4686

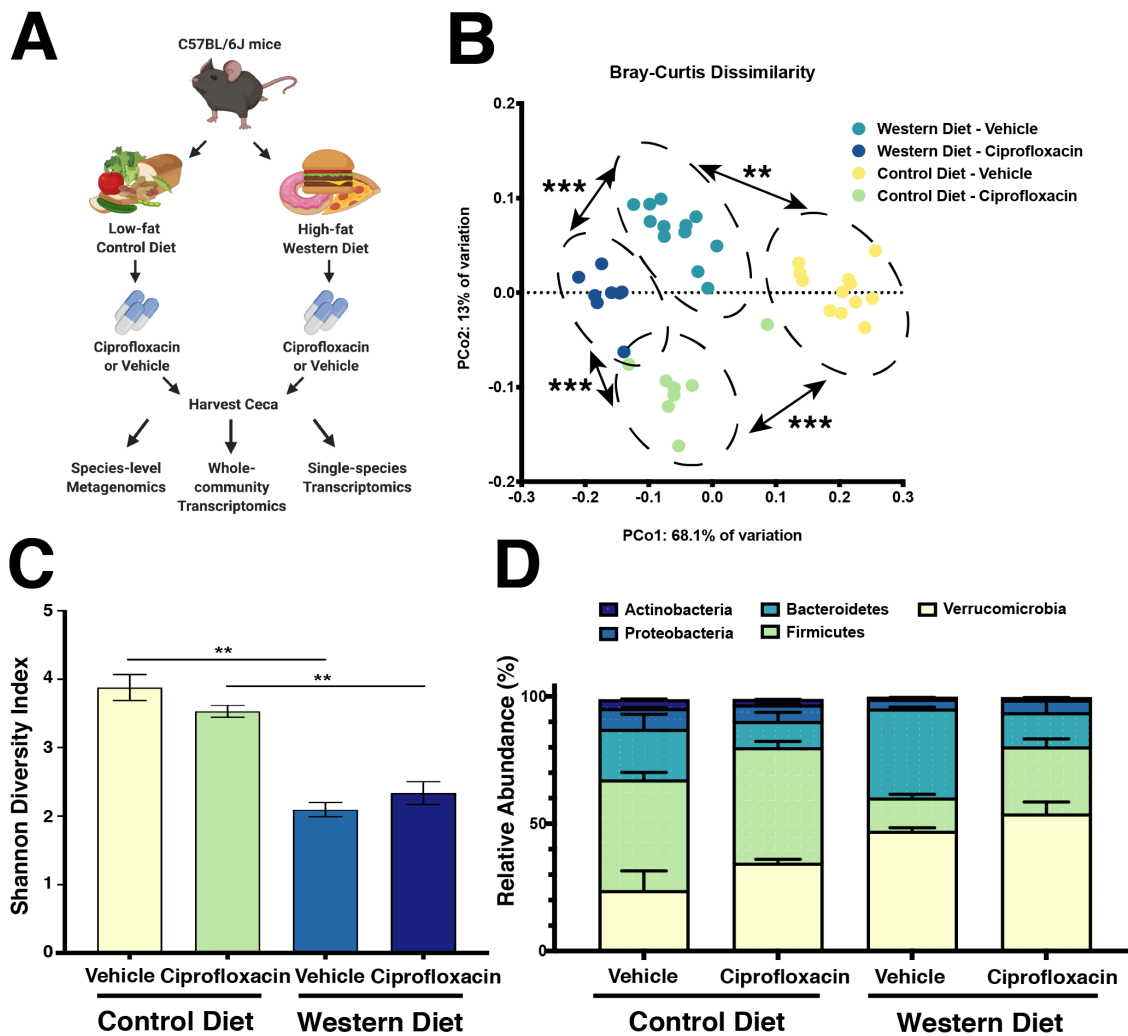


Figure 1: Impact of diet and ciprofloxacin administration on murine gut microbiome composition

- Experimental workflow used in this study. Figure was created with Biorender.com.
- Principle Coordinates Analysis of experimental groups as measured by Bray-Curtis dissimilarity of 16S rRNA amplicons. Dashed lines indicate 95% confidence intervals (**p<0.01, ***p<0.001, Permutational ANOVA).
- α -diversity of experimental groups as measured by the Shannon Diversity Index. Data are represented as mean \pm standard error of the mean (SEM). (**p<0.01, Welch ANOVA with Dunnett T3 test for multiple hypothesis testing).
- Stacked barplot of the five most abundant bacterial phyla in our dataset. Data are represented as mean \pm SEM for each phylum.

For all analyses, n = 4.

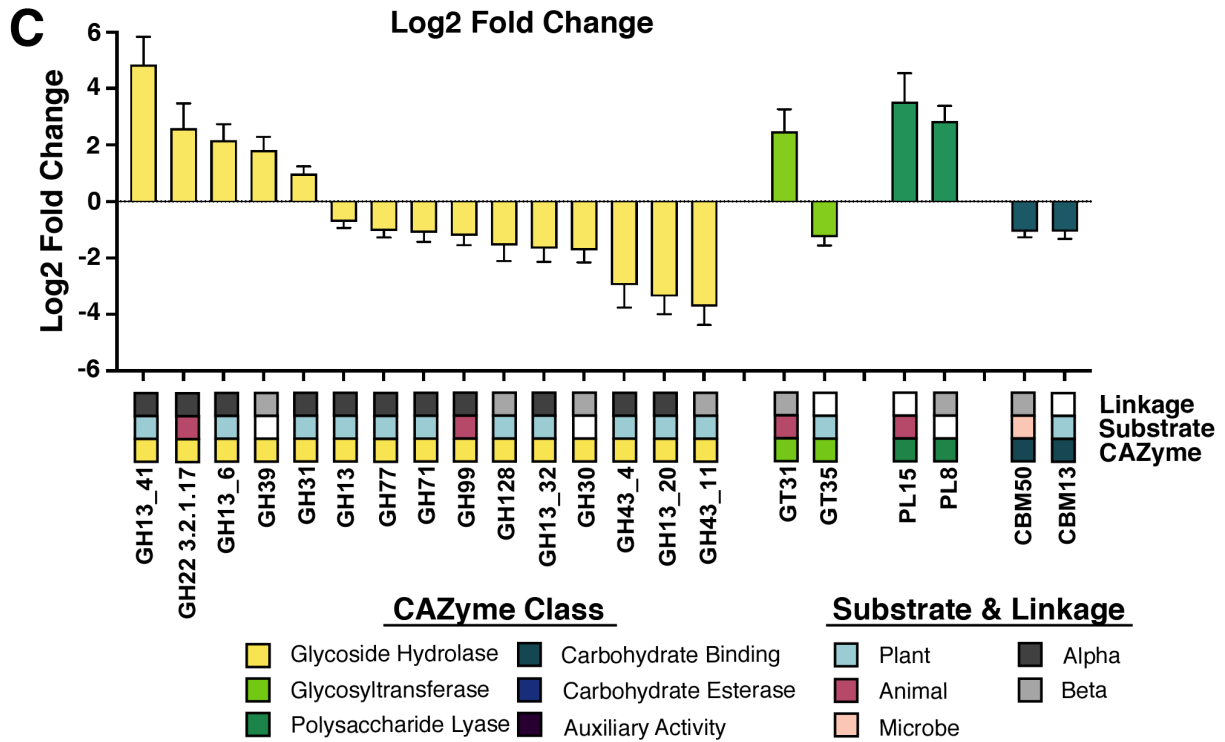
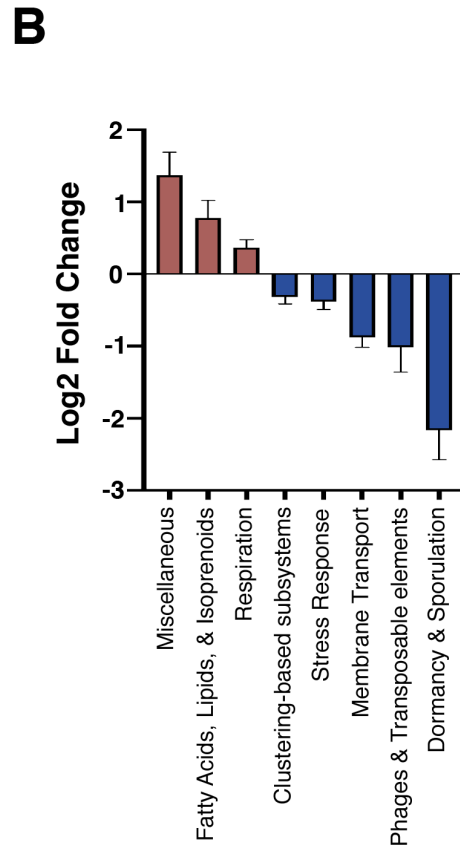
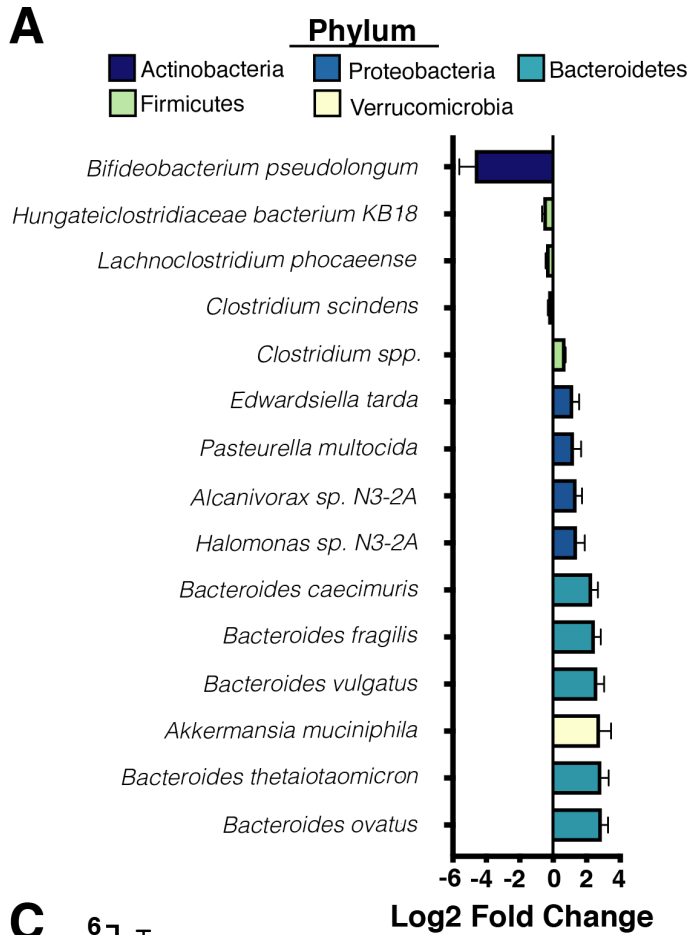


Figure 2: Consumption of a Western diet induces broad taxonomic and transcriptional changes at the community level

- A. Differentially abundant (Benjamini-Hochberg adjusted p-value ≤ 0.05) bacterial species (within the 45-most abundant taxa) as detected in mice consuming the Western diet (WD). Data are represented as \log_2 fold change relative to control diet \pm standard error. Bar color and left legend denotes phylum level taxonomic classification (yellow – *Verrucomicrobia*, green – *Firmicutes*, teal – *Bacteroidetes*, blue – *Proteobacteria*, navy – *Actinobacteria*). See Additional File 1 for full results.
- B. Differentially expressed (Benjamini-Hochberg adjusted p-value ≤ 0.05) level 1 SEED subsystems in the murine cecal metatranscriptome in mice consuming the Western diet. Data are represented as \log_2 fold change relative to control diet \pm standard error. Only features with a base mean ≥ 100 were plotted. See Additional File 3 for full results.
- C. Differentially expressed (Benjamini-Hochberg adjusted p-value ≤ 0.05) CAZyme transcripts in the murine cecal metatranscriptome in mice consuming the Western diet. Data are represented as \log_2 fold change relative to control diet \pm standard error. CAZyme class (yellow – glycoside hydrolase, lime – glycosyl transferase, green – polysaccharide lyase, teal – carbohydrate binding modules, blue – carbohydrate esterase, purple – auxillary activity), source of the target substrate (blue – plant derived, magenta – animal derived, peach – microbially derived), and linkages targeted by the CAZyme (dark grey – α , light grey – β) are listed below the data and color-coded. White values represent either a lack of singular substrate/linkage or a lack of enough information available to make a definitive call. See Additional File 5 for full results.

For all analyses, n = 4.

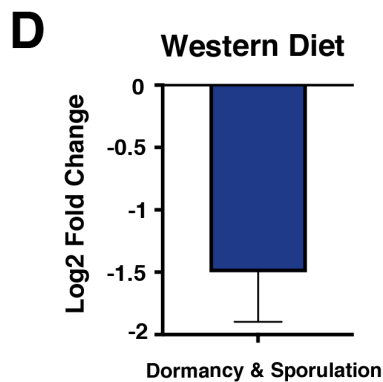
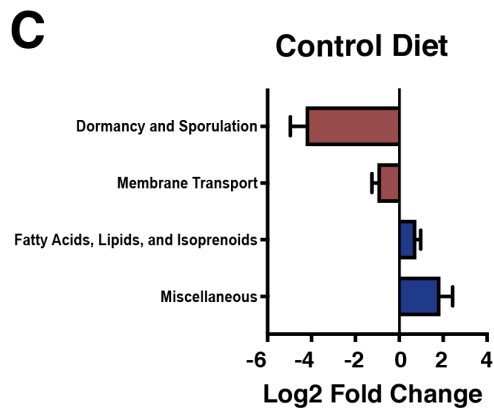
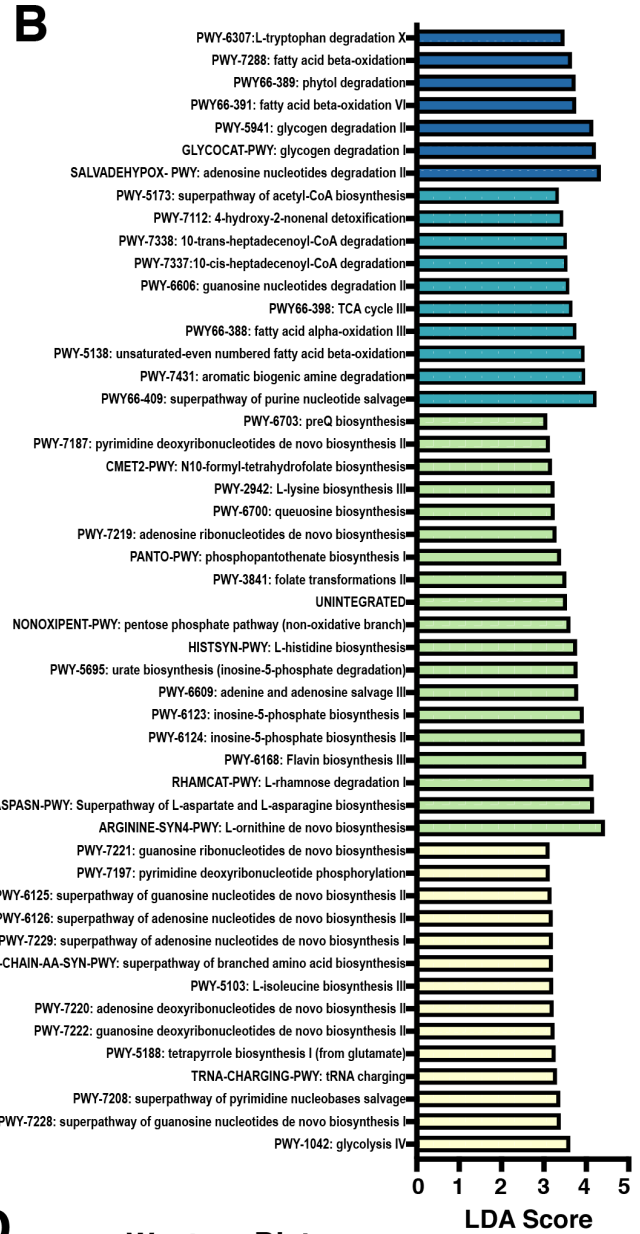
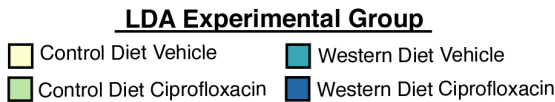
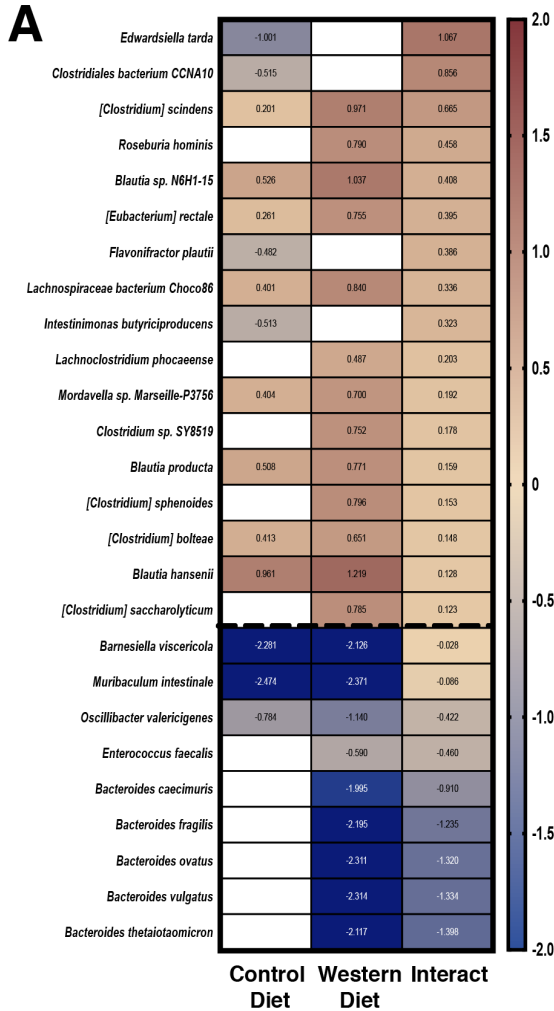


Figure 3: Ciprofloxacin elicits unique shifts in gene expression on Western and control diets at the community level

- A. Heatmap of the change in abundance of the top 45 bacterial species in response to ciprofloxacin on control and Western diets. The Interaction column represents the interaction term generated by DESeq2, denoting the impact of diet on the change in abundance of each species to ciprofloxacin. Cell color denotes \log_2 fold change of a particular species in response to ciprofloxacin (white represents failure to meet statistical significance: Benjamini-Hochberg adjusted p-value ≤ 0.05). Heatmap rows were sorted by interaction term value from highest to lowest, and taxa with no differential abundance (failure to meet statistical significance) in either group were removed. See Additional File 1 for full DESeq2 results.
- B. Linear discriminant analysis (LDA) of MetaCyc pathways that were differentially associated with each experimental group. Bar size indicates LDA score and color indicates the experimental group that a MetaCyc pathway was significantly associated with. All LDA scores were generated using LEfSe on unstratified pathway outputs from HUMAnN2. For full pathway names and statistics, see Additional File 2.
- C. Differentially expressed (Benjamini-Hochberg adjusted p-value ≤ 0.05) level 1 SEED subsystems in the murine cecal metatranscriptome after ciprofloxacin treatment in mice consuming the control diet. Data are represented as \log_2 fold change relative to vehicle controls \pm standard error. Only features with a base mean ≥ 100 were plotted. See Additional File 3 for full results.
- D. Differentially expressed (Benjamini-Hochberg adjusted p-value ≤ 0.05) level 1 SEED subsystems in the murine cecal metatranscriptome after ciprofloxacin treatment in mice consuming the Western diet. Data are represented as \log_2 fold change relative to vehicle controls \pm standard error. Only features with a base mean ≥ 100 were plotted. See Additional File 3 for full results.

For all analyses, $n = 4$.

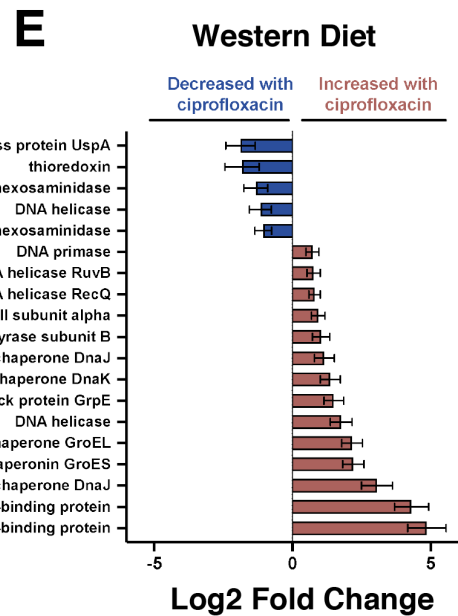
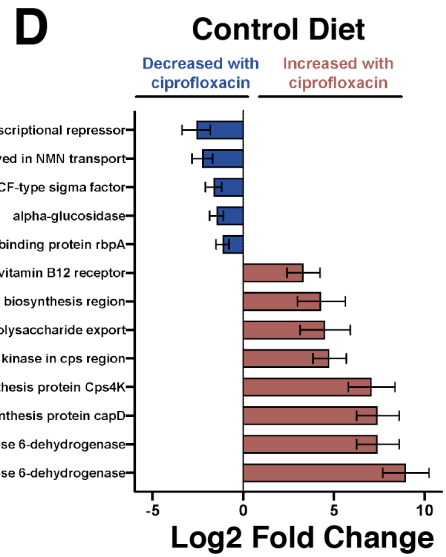
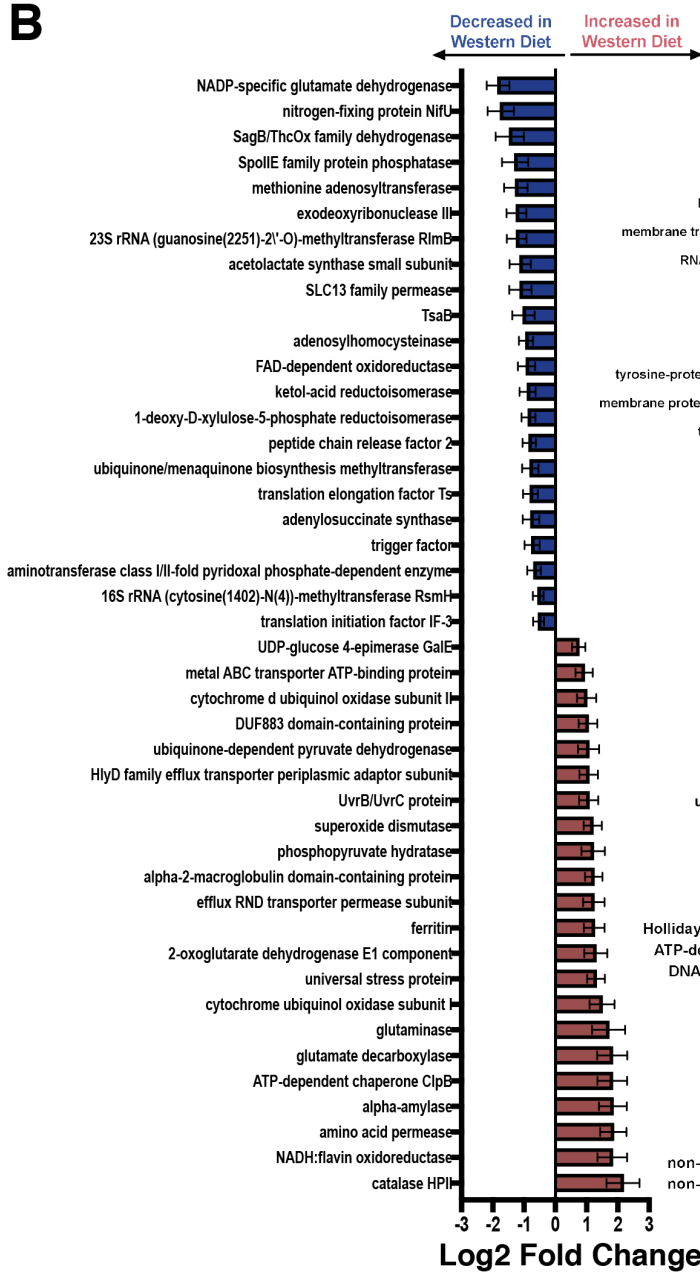
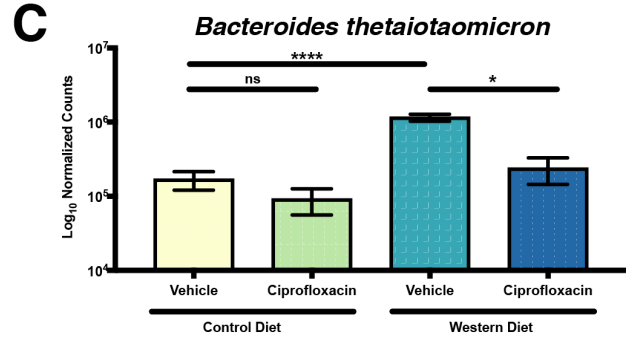
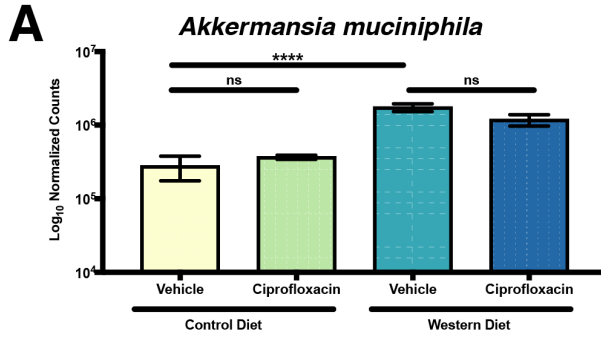


Figure 4: Diet and ciprofloxacin alter gene expression within *B. thetaiotaomicron* and *A. muciniphila*

- A. Normalized counts of *A. muciniphila* in each experimental group. Data are represented as mean \pm SEM. Normalized counts were generated with DESeq2 and subsequently used to perform differential abundance testing. (* $p < 0.05$, **** $p < 0.0001$, Wald test with Benjamini and Hochberg correction). See Additional File 1 for full results.
- B. Select differentially expressed (Benjamini-Hochberg adjusted p -value ≤ 0.05) genes of interest in *A. muciniphila* within the cecum of vehicle-treated mice consuming the Western diet. Data are represented as \log_2 fold change relative to control diet \pm standard error. See Additional File 7 for full results.
- C. Normalized counts of *B. thetaiotaomicron* in each experimental group. Data are represented as mean \pm SEM. Normalized counts were generated with DESeq2 and subsequently used to perform differential abundance testing. (* $p < 0.05$, **** $p < 0.0001$, Wald test with Benjamini and Hochberg correction). See Additional File 1 for full results.
- D. Select differentially expressed (Benjamini-Hochberg adjusted p -value ≤ 0.05) genes of interest in *B. thetaiotaomicron* within the cecum of ciprofloxacin-treated mice consuming the control diet. Data are represented as \log_2 fold change relative to control diet \pm standard error. See Additional File 7 for full results.
- E. Select differentially expressed (Benjamini-Hochberg adjusted p -value ≤ 0.05) genes of interest in *B. thetaiotaomicron* within the cecum of vehicle-treated mice consuming the Western diet. Data are represented as \log_2 fold change relative to control diet \pm standard error. See Additional File 7 for full results.

For all analyses, $n = 4$.

Supplemental Figures, Titles, and Legends

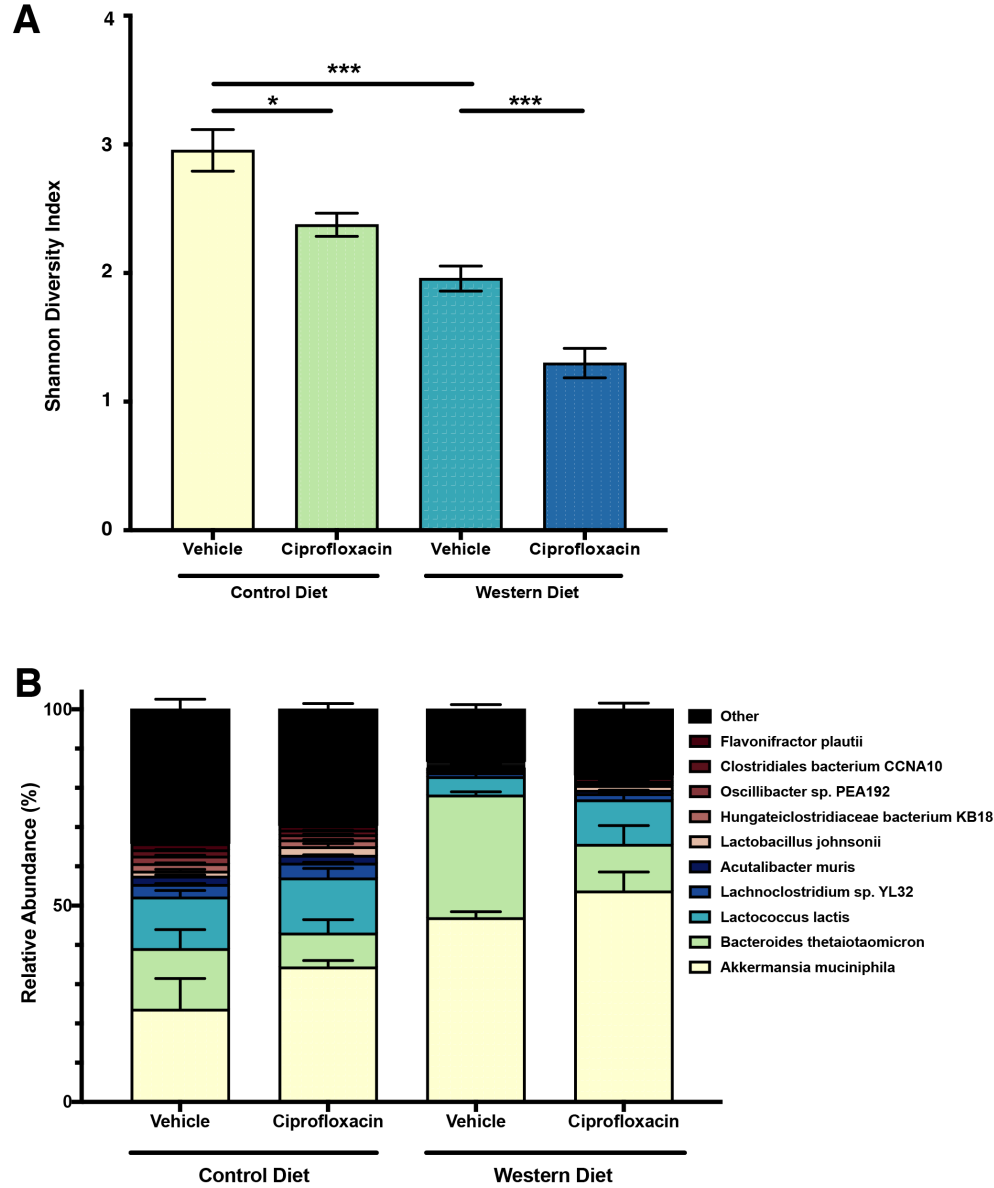


Figure S1: Dietary composition and antibiotic treatment impact the diversity of the gut microbiome

A. α -diversity of experimental groups as measured by the Shannon Diversity Index of 16S rRNA amplicons. Data are represented as mean \pm standard error of the mean (SEM). (* $p < 0.05$, ** $p < 0.01$, *** $p < 0.001$, Welch ANOVA with Dunnett T3 test for multiple hypothesis testing).

B. Stacked bar plot of the ten most abundant bacterial species in our dataset. Data are represented as mean \pm SEM for each species.

For 16S rRNA amplicons, $n = 8-12$. For metagenomics, $n = 4$.

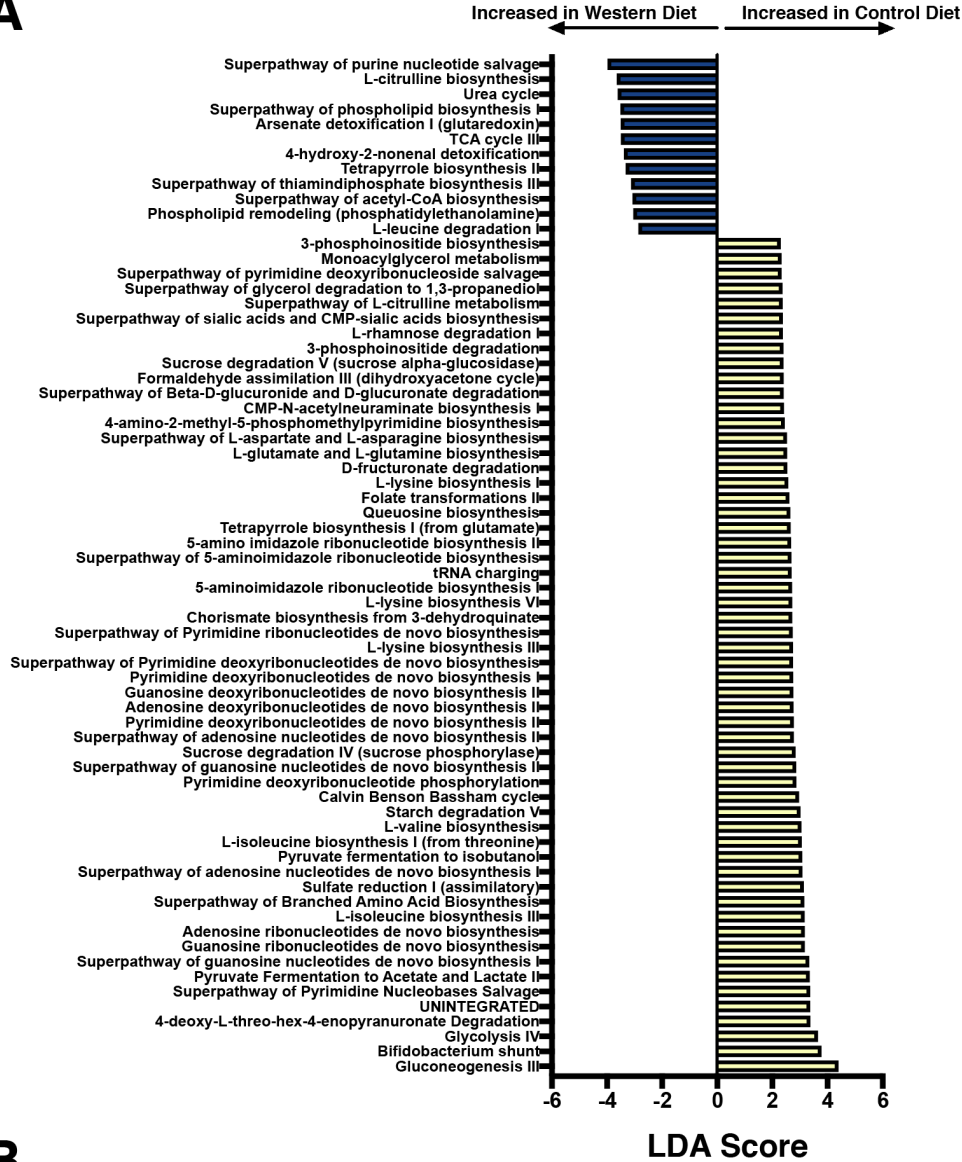
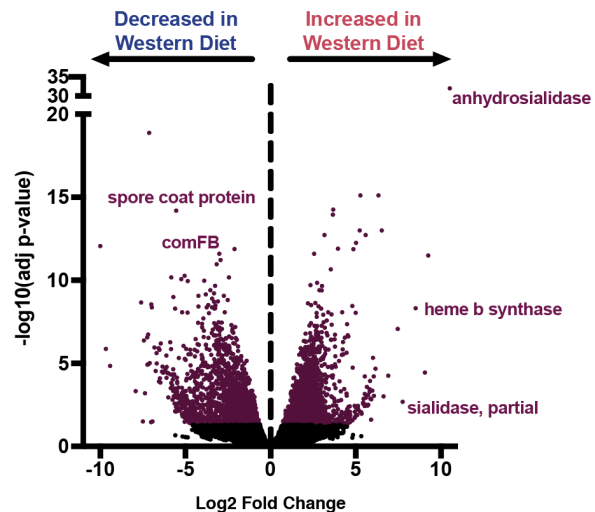
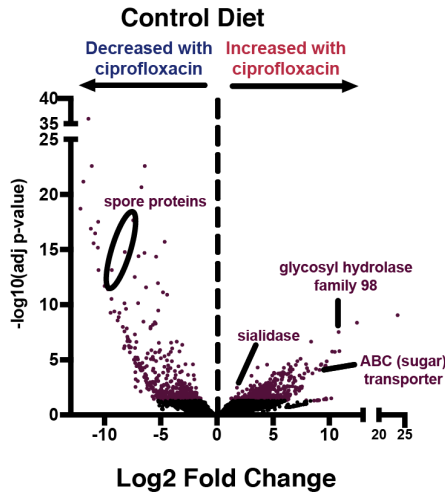
A**B**

Figure S2: Consumption of a Western diet induces broad taxonomic and transcriptional changes at the community and species level

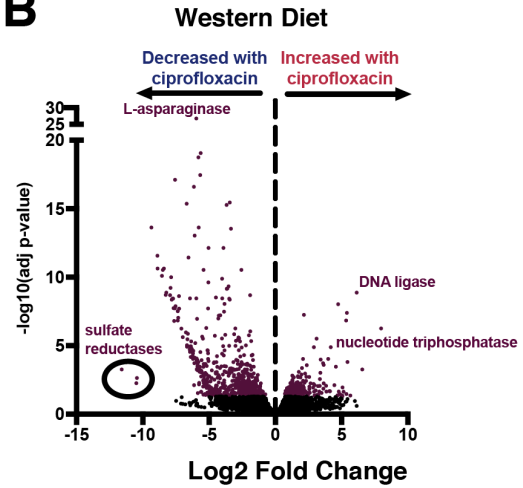
- A. Linear discriminant analysis (LDA) of MetaCyc pathways that were differentially associated with either the control or Western diet. Bar size indicates LDA score and color indicates the experimental group (blue – Western diet, yellow – control diet) that a MetaCyc pathway was significantly associated with. All LDA scores were generated using LEfSe on unstratified pathway outputs from HUMAnN2. For full pathway names and statistics, see Additional File 2.
- B. Volcano plot of the metatranscriptomic profile of the murine cecal microbiome in vehicle-treated mice consuming Western diet. Data was generated by aligning metatranscriptomic reads to RefSeq using SAMSA2 and analyzing using DESeq2. Points in purple represent transcripts for which a statistically significant change in expression was detected (Benjamini-Hochberg adjusted p-value ≤ 0.05). Select genes of interest are labeled. See Additional File 4 for full results.

For all analyses, n = 4.

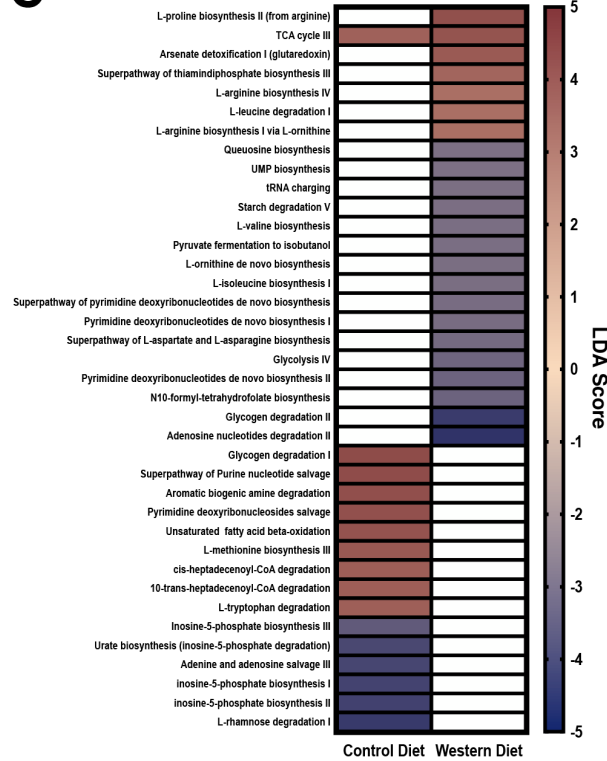
A



B



C



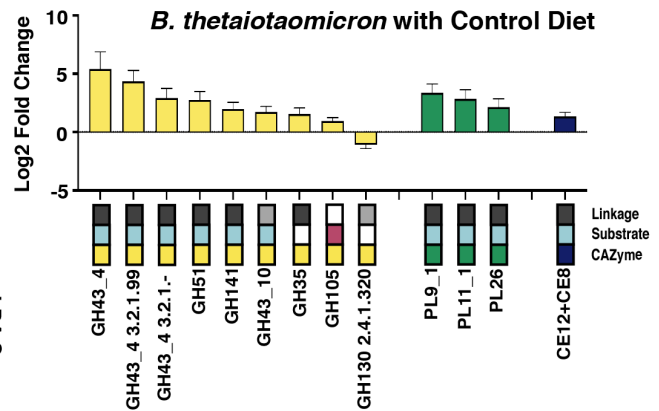
CAZyme Class

- Glycoside Hydrolase
- Glycosyltransferase
- Polysaccharide Lyase
- Carbohydrate Binding
- Carbohydrate Esterase
- Auxiliary Activity

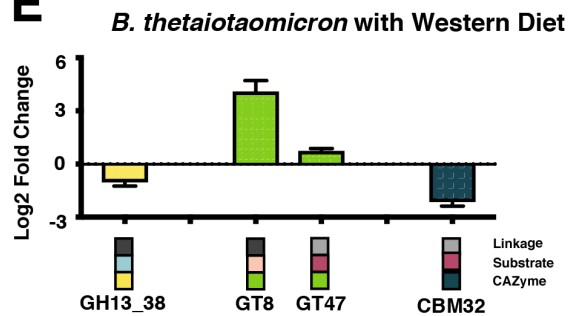
Substrate & Linkage

- Plant
- Animal
- Microbe
- Alpha
- Beta

D



E



F

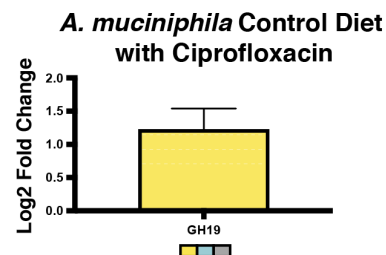


Figure S3: Ciprofloxacin elicits unique shifts in gene expression on Western and control diets at the community and species level

- A. Volcano plot of the metatranscriptomic profile of the murine cecal microbiome in ciprofloxacin-treated mice on the control diet. Data was generated by aligning metatranscriptomic reads to RefSeq using SAMSA2 and analyzing using DESeq2. Points in purple represent transcripts for which a statistically significant change in expression was detected (Benjamini-Hochberg adjusted p-value ≤ 0.05). Select genes of interest are labeled. See Additional File 4 for full results.
- B. Volcano plot of the metatranscriptomic profile of the murine cecal microbiome in ciprofloxacin-treated mice on the Western diet. Data generation, point labeling, and statistical cutoffs are the same as (A). See Additional File 4 for full results.
- C. Linear discriminant analysis (LDA) of MetaCyc pathways that were differentially associated with either the control or Western diet during ciprofloxacin treatment. LDA score indicates the experimental group that a MetaCyc pathway was significantly associated with (negative values – vehicle treatment, positive values – ciprofloxacin treatment). All LDA scores were generated using LEfSe on unstratified pathway outputs from HUMAnN2. (White represents failure to meet statistical significance). For full pathway names and statistics, see Additional File 2.
- D. Differentially expressed. Differentially expressed (Benjamini-Hochberg adjusted p-value ≤ 0.05) CAZyme transcripts in *B. thetaiotaomicron* within mice consuming the control diet during ciprofloxacin treatment. Data are represented as log₂ fold change relative to control diet \pm standard error. CAZyme class (yellow – glycoside hydrolase, lime – glycosyl transferase, green – polysaccharide lyase, teal – carbohydrate binding modules, blue – carbohydrate esterase, purple – auxillary activity), source of the target substrate (blue – plant derived, magenta – animal derived, peach – microbially derived), and linkages targeted by the CAZyme (dark grey – α , light grey – β) are listed to the left of the data and color-coded. White values represent either a lack of singular substrate/linkage or a lack of enough information available to make a definitive call. See Additional File 7 for full results.
- E. Differentially expressed. Differentially expressed (Benjamini-Hochberg adjusted p-value ≤ 0.05) CAZyme transcripts in *B. thetaiotaomicron* within mice consuming the Western diet during ciprofloxacin treatment. Data are represented as log₂ fold change relative to control diet \pm standard error. CAZyme class, source of target substrate, and linkages targeted by the CAZyme are listed below the data and color-coded as described in (D). See Additional File 7 for full results.
- F. Differentially expressed. Differentially expressed (Benjamini-Hochberg adjusted p-value ≤ 0.05) CAZyme transcripts in *A. muciniphila* within mice consuming either diet during ciprofloxacin treatment. Data are represented as log₂ fold change relative to control diet \pm standard error. CAZyme class, source of target substrate, and linkages targeted by the CAZyme are listed below the data and color-coded as described in (D). See Additional File 7 for full results.

For all analyses, n = 4.

Supplemental Files

Data Set 1: Full DESeq2 results of differential abundance testing of top 45 species detected by shotgun metagenomics

Sheet 1 – Differential abundance testing of the impact of Western diet (WD) consumption on the abundance of the top 45 bacterial species detected in our dataset. Log₂ fold change values were calculated relative to control diet samples.

Sheet 2 – Differential abundance testing of the impact of ciprofloxacin treatment on the abundance of the top 45 bacterial species in mice consuming the Western diet (WD). Log₂ fold change values were calculated relative to vehicle-treated samples on the WD.

Sheet 3 - Differential abundance testing of the impact of ciprofloxacin treatment on the abundance of the top 45 bacterial species in mice consuming the control diet (NC). Log₂ fold change values were calculated relative to vehicle-treated samples on the NC.

Sheet 4 – Interaction term analysis generated by DESeq2 for the impact of host diet consumption on changes in species abundance following ciprofloxacin therapy. Log₂ fold change values were calculated relative to vehicle-treated samples on the NC.

Data Set 2: Full LEfSe results from the analysis of MetaCyc pathway abundance generated by HUMAnN2. “Class” denotes the experimental group a particular pathway was associated with.

Sheet 5 – LEfSe analysis of all experimental groups.

Sheet 6 – Pairwise LEfSe analysis of vehicle-treated samples from mice consuming either the Western (WD) or control (NC) diet.

Sheet 7– Pairwise LEfSe analysis of ciprofloxacin- and vehicle-treated samples from mice consuming the control diet (NC)

Sheet 8 – Pairwise LEfSe analysis of ciprofloxacin- and vehicle-treated samples from mice consuming the Western diet (WD)

Data Set 3: Full DESeq2 results of SEED subsystem abundance generated by SAMSA2

Sheet 9 – Differential abundance testing of the impact of Western diet (WD) consumption on the abundance of SEED subsystems in the murine cecal metatranscriptome. Log₂ fold change values were calculated relative to control diet samples.

Sheet 10 – Differential abundance testing of the impact of ciprofloxacin treatment on the abundance of SEED subsystems in the murine cecal metatranscriptome in animals consuming the Western diet (WD). Log₂ fold change values were calculated relative to vehicle-treated samples on the WD.

Sheet 11 - Differential abundance testing of the impact of ciprofloxacin treatment on the abundance of SEED subsystems in the murine cecal metatranscriptome in animals consuming the control diet (NC). Log₂ fold change values were calculated relative to vehicle-treated samples on the NC.

Data Set 4: Full DESeq2 results of RefSeq transcript abundance generated by SAMSA2

Sheet 12 – Differential abundance testing of the impact of Western diet (WD) consumption on the abundance of RefSeq transcripts in the murine cecal metatranscriptome. Log₂ fold change values were calculated relative to control diet samples.

Sheet 13 – Differential abundance testing of the impact of ciprofloxacin treatment on the abundance of RefSeq transcripts in the murine cecal metatranscriptome in animals consuming the

Western diet (WD). Log₂ fold change values were calculated relative to vehicle-treated samples on the WD.

Sheet 14 - Differential abundance testing of the impact of ciprofloxacin treatment on the abundance of RefSeq transcripts in the murine cecal metatranscriptome in animals consuming the control diet (NC). Log₂ fold change values were calculated relative to vehicle-treated samples on the NC.

Sheet 15 – Interaction term analysis generated by DESeq2 for the impact of host diet consumption on changes in RefSeq transcripts abundance following ciprofloxacin therapy. Log₂ fold change values were calculated relative to vehicle-treated samples on the NC.

Data Set 5: Full DESeq2 results of CAZyme transcript abundance generated by SAMSA2

Sheet 16 – Differential abundance testing of the impact of Western diet (WD) consumption on the abundance of CAZyme transcripts in the murine cecal metatranscriptome. Log₂ fold change values were calculated relative to control diet samples

Sheet 17 – Differential abundance testing of the impact of ciprofloxacin treatment on the abundance of CAZyme transcripts in the murine cecal metatranscriptome in animals consuming the Western diet (WD). Log₂ fold change values were calculated relative to vehicle-treated samples on the WD. Table

Sheet 18 – Differential abundance testing of the impact of ciprofloxacin treatment on the abundance of CAZyme transcripts in the murine cecal metatranscriptome in animals consuming the control diet (NC). Log₂ fold change values were calculated relative to vehicle-treated samples on the NC.

Sheet 19 – Interaction term analysis generated by DESeq2 for the impact of host diet consumption on changes in CAZyme transcripts abundance following ciprofloxacin therapy. Log₂ fold change values were calculated relative to vehicle-treated samples on the NC.

Data Set 6: Selection criteria for single species sequencing and full DESeq2 results of transcript abundance analysis of *C. scindens* during dietary intervention and ciprofloxacin treatment

Sheet 20 – Total and average counts for metagenomic and metatranscriptomic read assignments generated via Kraken2.

Sheet 21 – Differential abundance testing of the impact of Western diet (WD) consumption on the abundance of *C. scindens* transcripts within the murine cecal metatranscriptome. Log₂ fold change values were calculated relative to control diet samples.

Sheet 22 - Differential abundance testing of the impact of ciprofloxacin treatment on the abundance of *C. scindens* transcripts within the murine cecal metatranscriptome in animals consuming the Western diet (WD). Log₂ fold change values were calculated relative to vehicle-treated samples on the WD.

Sheet 23 - Differential abundance testing of the impact of ciprofloxacin treatment on the abundance of *C. scindens* transcripts within the murine cecal metatranscriptome in animals consuming the control diet (NC). Log₂ fold change values were calculated relative to vehicle-treated samples on the NC.

Sheet 24 - Interaction term analysis generated by DESeq2 for the impact of host diet consumption on changes in *C. scindens* transcript abundance following ciprofloxacin therapy. Log₂ fold change values were calculated relative to vehicle-treated samples on the NC.

Data Set 7: Full DESeq2 results of transcript abundance analysis of *A. muciniphila* and *B. thetaiotaomicron* during dietary intervention and ciprofloxacin treatment and dietary formulation.

Sheet 25 – Differential abundance testing of the impact of Western diet (WD) consumption on the abundance of *A. muciniphila* transcripts within the murine cecal metatranscriptome. Log₂ fold change values were calculated relative to control diet samples.

Sheet 26 – Differential abundance testing of the impact of ciprofloxacin treatment on the abundance of *A. muciniphila* transcripts within the murine cecal metatranscriptome in animals consuming the Western diet (WD). Log₂ fold change values were calculated relative to vehicle-treated samples on the WD.

Sheet 27 - Differential abundance testing of the impact of ciprofloxacin treatment on the abundance of *A. muciniphila* transcripts within the murine cecal metatranscriptome in animals consuming the control diet (NC). Log₂ fold change values were calculated relative to vehicle-treated samples on the NC.

Sheet 28 – Interaction term analysis generated by DESeq2 for the impact of host diet consumption on changes in *A. muciniphila* transcript abundance following ciprofloxacin therapy. Log₂ fold change values were calculated relative to vehicle-treated samples on the NC.

Sheet 29 – Differential abundance testing of the impact of Western diet (WD) consumption on the abundance of *A. muciniphila* CAZyme transcripts within the murine cecal metatranscriptome. Log₂ fold change values were calculated relative to control diet samples.

Sheet 30 – Differential abundance testing of the impact of ciprofloxacin treatment on the abundance of *A. muciniphila* CAZyme transcripts within the murine cecal metatranscriptome in animals consuming the Western diet (WD). Log₂ fold change values were calculated relative to vehicle-treated samples on the WD.

Sheet 31 – Differential abundance testing of the impact of ciprofloxacin treatment on the abundance of *A. muciniphila* CAZyme transcripts within the murine cecal metatranscriptome in animals consuming the control diet (NC). Log₂ fold change values were calculated relative to vehicle-treated samples on the NC.

Sheet 32 – Interaction term analysis generated by DESeq2 for the impact of host diet consumption on changes in *A. muciniphila* CAZyme transcript abundance following ciprofloxacin therapy. Log₂ fold change values were calculated relative to vehicle-treated samples on the NC.

Sheet 33 – Differential abundance testing of the impact of Western diet (WD) consumption on the abundance of *B. thetaiotaomicron* transcripts within the murine cecal metatranscriptome. Log₂ fold change values were calculated relative to control diet samples.

Sheet 34 – Differential abundance testing of the impact of ciprofloxacin treatment on the abundance of *B. thetaiotaomicron* transcripts within the murine cecal metatranscriptome in animals consuming the Western diet (WD). Log₂ fold change values were calculated relative to vehicle-treated samples on the WD.

Sheet 35 - Differential abundance testing of the impact of ciprofloxacin treatment on the abundance of *B. thetaiotaomicron* transcripts within the murine cecal metatranscriptome in animals consuming the control diet (NC). Log₂ fold change values were calculated relative to vehicle-treated samples on the NC.

Sheet 36 – Interaction term analysis generated by DESeq2 for the impact of host diet consumption on changes in *B. thetaiotaomicron* transcript abundance following ciprofloxacin therapy. Log₂ fold change values were calculated relative to vehicle-treated samples on the NC.

Sheet 37 – Differential abundance testing of the impact of Western diet (WD) consumption on the abundance of *B. thetaiotaomicron* CAZyme transcripts within the murine cecal metatranscriptome. Log₂ fold change values were calculated relative to control diet samples.

Sheet 38 – Differential abundance testing of the impact of ciprofloxacin treatment on the abundance of *B. thetaiotaomicron* CAZyme transcripts within the murine cecal metatranscriptome in animals consuming the Western diet (WD). Log₂ fold change values were calculated relative to vehicle-treated samples on the WD.

Sheet 39 – Differential abundance testing of the impact of ciprofloxacin treatment on the abundance of *B. thetaiotaomicron* CAZyme transcripts within the murine cecal metatranscriptome in animals consuming the control diet (NC). Log₂ fold change values were calculated relative to vehicle-treated samples on the NC.

Sheet 40 – Interaction term analysis generated by DESeq2 for the impact of host diet consumption on changes in *B. thetaiotaomicron* CAZyme transcript abundance following ciprofloxacin therapy. Log₂ fold change values were calculated relative to vehicle-treated samples on the NC.

Sheet 41 – Catalog number, macronutrient breakdown, and ingredient formulation of both the Control Diet and Western Diet (Research Diets, Inc., New Brunswick, NJ) used in this study.

References

- Adolfsen, K.J., Brynildsen, M.P., 2015. Futile cycling increases sensitivity toward oxidative stress in *Escherichia coli*. *Metab. Eng.* 29, 26–35. doi:10.1016/j.ymben.2015.02.006
- Allison, K.R., Brynildsen, M.P., Collins, J.J., 2011. Metabolite-enabled eradication of bacterial persisters by aminoglycosides. *Nature* 473, 216–220. doi:10.1038/nature10069
- Anglès, F., Castanié-Cornet, M.-P., Slama, N., Dinclaux, M., Cirinesi, A.-M., Portais, J.-C., Létisse, F., Genevaux, P., 2017. Multilevel interaction of the DnaK/DnaJ(HSP70/HSP40) stress-responsive chaperone machine with the central metabolism. *Sci. Rep.* 7, 1–16. doi:10.1038/srep41341
- Argueta, D.A., DiPatrizio, N.V., 2017. Peripheral endocannabinoid signaling controls hyperphagia in western diet-induced obesity. *Physiol. Behav.* 171, 32–39. doi:10.1016/j.physbeh.2016.12.044
- Arpaia, N., Campbell, C., Fan, X., Dikiy, S., van der Veeken, J., deRoos, P., Liu, H., Cross, J.R., Pfeffer, K., Coffey, P.J., Rudensky, A.Y., 2013. Metabolites produced by commensal bacteria promote peripheral regulatory T-cell generation. *Nature* 504, 451–455. doi:10.1038/nature12726
- Belenky, P., Ye, J.D., Porter, C.B.M., Cohen, N.R., Lobritz, M.A., Ferrante, T., Jain, S., Korry, B.J., Schwarz, E.G., Walker, G.C., Collins, J.J., 2015. Bactericidal Antibiotics Induce Toxic Metabolic Perturbations that Lead to Cellular Damage. *Cell Rep.* 13, 968–980. doi:10.1016/j.celrep.2015.09.059
- Benjamini, Y., Hochberg, Y., 1995. Controlling the false discovery rate: a practical and powerful approach to multiple testing. *J. R. Statist. Soc.* 57, 289–300. doi: 10.2307/2346101
- Bisanz, J.E., Upadhyay, V., Turnbaugh, J.A., Ly, K., Turnbaugh, P.J., 2019. Meta-Analysis Reveals Reproducible Gut Microbiome Alterations in Response to a High-Fat Diet. *Cell Host Microbe* 26, 265–272. doi:10.1016/j.chom.2019.06.013
- Blaser, M., 2011. Antibiotic overuse: Stop the killing of beneficial bacteria. *Nature* 476, 393–394. doi:10.1038/476393a
- Bolger, A.M., Lohse, M., Usadel, B., 2014. Trimmomatic: a flexible trimmer for Illumina sequence data. *J. Bioinform.* 30, 2114–2120. doi:10.1093/bioinformatics/btu170
- Buchfink, B., Xie, C., Huson, D.H., 2014. Fast and sensitive protein alignment using DIAMOND. *Nat. Methods* 12, 59–60. doi:10.1038/nmeth.3176
- Bushnell, B., 2014. BBMap: A fast, accurate, splice-aware aligner, in: Presented at the 9th Annual Genomics of Energy Environment Meeting, Walnut Creek, CA.
- Cabral, D.J., Penumutthu, S., Reinhart, E.M., Zhang, C., Korry, B.J., Wurster, J.I., Nilson, R., Guang, A., Sano, W.H., Rowan-Nash, A.D., Li, H., Belenky, P., 2019. Microbial Metabolism Modulates Antibiotic Susceptibility within the Murine Gut Microbiome. *Cell Metab.* 30, 800–823. doi:10.1016/j.cmet.2019.08.020
- Cabral, D.J., Wurster, J.I., Belenky, P., 2018. Antibiotic Persistence as a Metabolic Adaptation: Stress, Metabolism, the Host, and New Directions. *Pharmaceuticals* 11, 1–19. doi:10.3390/ph11010014
- Cani, P.D., Van Hul, M., Lefort, C., Depommier, C., Rastelli, M., Everard, A., 2019. Microbial regulation of organismal energy homeostasis. *Nat. Metab.* 1, 34–46. doi:10.1038/s42255-018-0017-4
- Cantarel, B.L., Coutinho, P.M., Rancurel, C., Bernard, T., Lombard, V., Henrissat, B., 2009. The Carbohydrate-Active EnZymes database (CAZy): an expert resource for Glycogenomics. *Nucleic Acids Res.* 37, D233–D238. doi:10.1093/nar/gkn663

- Chambers, E.S., Preston, T., Frost, G., Morrison, D.J., 2018. Role of Gut Microbiota-Generated Short-Chain Fatty Acids in Metabolic and Cardiovascular Health. *Cardiovasc. Dis.* 7, 198–206. doi:10.1007/s13668-018-0248-8
- Chang, J.Y., Antonopoulos, D.A., Kalra, A., Tonelli, A., Khalife, W.T., Schmidt, T.M., Young, V.B., 2008. Decreased diversity of the fecal microbiome in recurrent *Clostridium difficile*-associated diarrhea. *J. Infect. Dis.* 197, 435–438. doi:10.1086/525047
- Cho, H., Uehara, T., Bernhardt, T.G., 2014. Beta-lactam antibiotics induce a lethal malfunctioning of the bacterial cell wall synthesis machinery. *Cell* 159, 1300–1311. doi:10.1016/j.cell.2014.11.017
- Clooney, A.G., Fouhy, F., Sleator, R.D., O’ Driscoll, A., Stanton, C., Cotter, P.D., Claesson, M.J., 2016. Comparing Apples and Oranges?: Next Generation Sequencing and Its Impact on Microbiome Analysis. *PLoS ONE* 11, e0148028–16. doi:10.1371/journal.pone.0148028
- Collins, J., Robinson, C., Danhof, H., Knetsch, C.W., van Leeuwen, H.C., Lawley, T.D., Auchtung, J.M., Britton, R.A., 2018. Dietary trehalose enhances virulence of epidemic *Clostridium difficile*. *Nature* 553, 291–294. doi:10.1038/nature25178
- Corfield, A.P., Wagner, S.A., Clamp, J.R., Kriaris, M.S., Hoskins, L.C., 1992. Mucin Degradation in the Human Colon: Production of Sialidase, Sialate O-Acetyltransferase, N-Acetylneuraminase Lyase, Arylesterase, and Glycosulfatase Activities by Strains of Fecal Bacteria. *Infect. Immun.* 60, 3971–3978. doi:10.1128/IAI.60.10.3971-3978.1992
- Cotillard, A., Kennedy, S.P., Kong, L.C., Prifti, E., Pons, N., Le Chatelier, E., Almeida, M., Quinquis, B., Levenez, F., Galleron, N., Gougis, S., Rizkalla, S., Batto, J.-M., Renault, P., ANR MicroObes consortium members, Doré, J., Zucker, J.-D., Clément, K., Ehrlich, S.D., 2013. Dietary intervention impact on gut microbial gene richness. *Nature* 500, 585–588. doi:10.1038/nature12480
- Coyne, M.J., Comstock, L.E., 2008. Niche-Specific Features of the Intestinal Bacteroidales. *J. Bacteriol.* 190, 736–742. doi:10.1128/JB.01559-07
- David, L.A., Maurice, C.F., Carmody, R.N., Gootenberg, D.B., Button, J.E., Wolfe, B.E., Ling, A.V., Devlin, A.S., Varma, Y., Fischbach, M.A., Biddinger, S.B., Dutton, R.J., Turnbaugh, P.J., 2014. Diet rapidly and reproducibly alters the human gut microbiome. *Nature* 505, 559–563. doi:10.1038/nature12820
- De Luca, F., Shoefeld, Y., 2019. The microbiome in autoimmune diseases. *Clin. Exp. Immunol.* 195, 74–85. doi:10.1111/cei.13158
- Deng, Z.-L., Sztajer, H., Jarek, M., Bhujju, S., Wagner-Döbler, I., 2018. Worlds Apart – Transcriptome Profiles of Key Oral Microbes in the Periodontal Pocket Compared to Single Laboratory Culture Reflect Synergistic Interactions. *Front. Microbiol.* 9, 1–15. doi:10.3389/fmicb.2018.00124
- Desai, M.S., Seekatz, A.M., Koropatkin, N.M., Kamada, N., Hickey, C.A., Wolter, M., Pudlo, N.A., Kitamoto, S., Terrapon, N., Muller, A., Young, V.B., Henrissat, B., Wilmes, P., Stappenbeck, T.S., Núñez, G., Martens, E.C., 2016. A Dietary Fiber-Deprived Gut Microbiota Degrades the Colonic Mucus Barrier and Enhances Pathogen Susceptibility. *Cell* 167, 1339–1353.e1321. doi: 10.1016/j.cell/2016.10.043
- Dethlefsen, L., Relman, D.A., 2011. Incomplete recovery and individualized responses of the human distal gut microbiota to repeated antibiotic perturbation. *Proc. Natl. Acad. Sci. USA.* 108, 4551–4561. doi:10.1073/pnas.1000087107
- Dickerson, F., Severance, E., Yolken, R., 2017. The microbiome, immunity, and schizophrenia and bipolar disorder. *Brain Behav. Immun.* 62, 46–52. doi:10.1016/j.bbi.2016.12.010

- Dougherty, B.A., van de Rijn, I., 1994. Molecular characterization of hasB from an operon required for hyaluronic acid synthesis in group A streptococci. *J. Biol. Chem.* 269, 169–175. PMID: 8276791
- Dwyer, D.J., Belenky, P.A., Yang, J.H., MacDonald, I.C., Martell, J.D., Takahashi, N., Chan, C.T.Y., Lobritz, M.A., Braff, D., Schwarz, E.G., Ye, J.D., Pati, M., Vercruyse, M., Ralifo, P.S., Allison, K.R., Khalil, A.S., Ting, A.Y., Walker, G.C., Collins, J.J., 2014. Antibiotics induce redox-related physiological alterations as part of their lethality. *Proc. Natl. Acad. Sci. USA.* 111, E2100–E2109. doi:10.1073/pnas.1401876111
- Eckardt, N.A., 2008. Role of xyloglucan in primary cell walls. *Plant Cell* 20, 1421–1422. doi:10.1105/tpc.108.061382
- Elderman, M., Hugenholtz, F., Belzer, C., Boekschoten, M., van Beek, A., de Haan, B., Savelkoul, H., de Vos, P., Faas, M., 2018. Sex and strain dependent differences in mucosal immunology and microbiota composition in mice. *Biol. Sex Differ.* 9, 1–18. doi:10.1186/s13293-018-0186-6
- Fischbach, M.A., Sonnenburg, J.L., 2011. Eating for two: how metabolism establishes interspecies interactions in the gut. *Cell Host Microbe* 10, 336–347. doi:10.1016/j.chom.2011.10.002
- Foster, J.A., Neufeld, K.-A.M., 2013. Gut–brain axis: how the microbiome influences anxiety and depression. *Trends Neurosci.* 36, 305–312. doi:10.1016/j.tins.2013.01.005
- Franzosa, E.A., McIver, L.J., Rahnavard, G., Thompson, L.R., Schirmer, M., Weingart, G., Lipson, K.S., Knight, R., Caporaso, J.G., Segata, N., Huttenhower, C., 2018. Species-level functional profiling of metagenomes and metatranscriptomes. *Nat. Methods* 15, 962–968. doi:10.1038/s41592-018-0176-y
- Gao, H., Shu, Q., Chen, J., Fan, K., Xu, P., Zhou, Q., Li, C., Zheng, H., 2019. Antibiotic Exposure Has Sex-Dependent Effects on the Gut Microbiota and Metabolism of Short-Chain Fatty Acids and Amino Acids in Mice. *mSystems* 4, 1262–16. doi:10.1128/mSystems.00048-19
- Gilbert, J.A., Blaser, M.J., Caporaso, J.G., Jansson, J.K., Lynch, S.V., Knight, R., 2018. Current understanding of the human microbiome. *Nat. Med.* 24, 392–400. doi:10.1038/nm.4517
- Gill, S.R., Pop, M., DeBoy, R.T., Eckburg, P.B., Turnbaugh, P.J., Samuel, B.S., Gordon, J.I., Relman, D.A., Fraser-Liggett, C.M., Nelson, K.E., 2006. Metagenomic Analysis of the Human Distal Gut Microbiome. *Science* 312, 1355–1359. doi:10.1126/science.1124234
- Hartstra, A.V., Bouter, K.E.C., Bäckhed, F., Nieuwdorp, M., 2015. Insights Into the Role of the Microbiome in Obesity and Type 2 Diabetes. *Diabetes Care* 38, 159–165. doi:10.2337/dc14-0769
- Hii, S.L., Tan, J.S., Ling, T.C., Ariff, A.B., 2012. Pullulanase: role in starch hydrolysis and potential industrial applications. *Enzyme Res.* 2012, 1–14. doi:10.1155/2012/921362
- Hryckowian, A.J., Van Treuren, W., Smits, S.A., Davis, N.M., Gardner, J.O., Bouley, D.M., Sonnenburg, J.L., 2018. Microbiota-accessible carbohydrates suppress *Clostridium difficile* infection in a murine model. *Nat. Microbiol.* 3, 662–669. doi:10.1038/s41564-018-0150-6
- Ingvorsen, C., Karp, N.A., Lelliott, C.J., 2017. The role of sex and body weight on the metabolic effects of high-fat diet in C57BL/6N mice. *Nutr. Diabetes* 7, e261–7. doi:10.1038/nutd.2017.6
- Johnson, A.J., Vangay, P., Al-Ghalith, G.A., Hillmann, B.M., Ward, T.L., Shields-Cutler, R.R., Kim, A.D., Shmagel, A.K., Syed, A.N., Personalized Microbiome Class Students, Walter, J., Menon, R., Koecher, K., Knights, D., 2019. Daily Sampling Reveals Personalized Diet-Microbiome Associations in Humans. *Cell Host Microbe* 25, 789–802.e5. doi:10.1016/j.chom.2019.05.005

- Kanoski, S.E., Hsu, T.M., Pennell, S., 2014. Obesity, Western Diet Intake, and Cognitive Impairment. *Omega-3 Fatty Acids in Brain and Neurological Health*. Elsevier Academic Press 57-62.
- Kashyap, P.C., Marcobal, A., Ursell, L.K., Smits, S.A., Sonnenburg, E.D., Costello, E.K., Higginbottom, S., Domino, S.E., Holmes, S.P., Relman, D.A., Knight, R., Gordon, J.I., Sonnenburg, J.L., 2013. Genetically dictated change in host mucus carbohydrate landscape exerts a diet-dependent effect on the gut microbiota. *Proc. Natl. Acad. Sci. USA*. 110, 17059–17064. doi:10.1073/pnas.1306070110
- Kaur, R., Sharma, M., Ji, D., Xu, M., Agyei, D., 2020. Structural Features, Modification, and Functionalities of Beta-Glucan. *Fibers* 8, 1–29. doi:10.3390/fib8010001
- Knoch, E., Dilokpimol, A., Geshi, N., 2014. Arabinogalactan proteins: focus on carbohydrate active enzymes. *Front. Plant Sci.* 5, 1–9. doi:10.3389/fpls.2014.00198
- Kohanski, M.A., Dwyer, D.J., Hayete, B., Lawrence, C.A., Collins, J.J., 2007. A Common Mechanism of Cellular Death Induced by Bactericidal Antibiotics. *Cell* 130, 797–810. doi:10.1016/j.cell.2007.06.049
- Langmead, B., Salzberg, S.L., 2012. Fast gapped-read alignment with Bowtie 2. *Nat. Methods* 9, 357–359. doi:10.1038/nmeth.1923
- Lapébie, P., Lombard, V., Drula, E., Terrapon, N., Henrissat, B., 2019. Bacteroidetes use thousands of enzyme combinations to break down glycans. *Nat. Comm.* 10, 1–7. doi:10.1038/s41467-019-10068-5
- Layman, D.K., Lönnerdal, B., Fernstrom, J.D., 2018. Applications for α -lactalbumin in human nutrition. *Nutr. Rev.* 76, 444–460. doi:10.1093/nutrit/nuy004
- Lee, J.J., Lee, S.-K., Song, N., Nathan, T.O., Swarts, B.M., Eum, S.-Y., Ehrt, S., Cho, S.-N., Eoh, H., 2019. Transient drug-tolerance and permanent drug-resistance rely on the trehalose-catalytic shift in *Mycobacterium tuberculosis*. *Nat. Comm.* 10, 1–12. doi:10.1038/s41467-019-10975-7
- Leong, K.S.W., Derraik, J.G.B., Hofman, P.L., Cutfield, W.S., 2018. Antibiotics, gut microbiome and obesity. *Clin. Endocrinol.* 88, 185–200. doi:10.1111/cen.13495
- Lessa, F.C., Mu, Y., Bamberg, W.M., Beldavs, Z.G., Dumyati, G.K., Dunn, J.R., Farley, M.M., Holzbauer, S.M., Meek, J.I., Phipps, E.C., Wilson, L.E., Winston, L.G., Cohen, J.A., Limbago, B.M., Fridkin, S.K., Gerding, D.N., McDonald, L.C., 2015. Burden of *Clostridium difficile* infection in the United States. *N. Engl. J. Med.* 372, 825–834. doi:10.1056/NEJMoa1408913
- Ley, R.E., Bäckhed, F., Turnbaugh, P., Lozupone, C.A., Knight, R.D., Gordon, J.I., 2005. Obesity alters gut microbial ecology. *Proc. Natl. Acad. Sci. USA*. 102, 11070–11075. doi:10.1073/pnas.0504978102
- Li, H., Durbin, R., 2010. Fast and accurate long-read alignment with Burrows–Wheeler transform. *Bioinformatics* 26, 589–595. doi:10.1093/bioinformatics/btp698
- Lobritz, M.A., Belenky, P., Porter, C.B.M., Gutierrez, A., Yang, J.H., Schwarz, E.G., Dwyer, D.J., Khalil, A.S., Collins, J.J., 2015. Antibiotic efficacy is linked to bacterial cellular respiration. *Proc. Natl. Acad. Sci. USA*. 112, 8173–8180. doi:10.1073/pnas.1509743112
- Love, M.I., Huber, W., Anders, S., 2014. Moderated estimation of fold change and dispersion for RNA-seq data with DESeq2. *Genome Biol.* 15, 31–21. doi:10.1186/s13059-014-0550-8
- Lu, J., Breitwieser, F.P., Thielen, P., Salzberg, S.L., 2017. Bracken: estimating species abundance in metagenomics data. *PeerJ Comput. Sci.* 3, 1–17. doi:10.7717/peerj-cs.104
- Lynch, S.V., Boushey, H.A., 2016. The microbiome and development of allergic disease. *Curr. Opin. Allerg. Clin. Immunol.* 16, 165–171. doi:10.1097/ACI.0000000000000255

- Macfarlane, S., Macfarlane, G.T., 2003. Regulation of short-chain fatty acid production. *Proc. Nutr. Soc.* 62, 67–72. doi:10.1079/PNS2002207
- Mäkelä, M.R., DiFalco, M., McDonnell, E., Nguyen, T.T.M., Wiebenga, A., Hildén, K., Peng, M., Grigoriev, I.V., Tsang, A., de Vries, R.P., 2018. Genomic and exoproteomic diversity in plant biomass degradation approaches among *Aspergilli*. *Stud. Mycol.* 91, 79–99. doi:10.1016/j.simyco.2018.09.001
- McIver, L.J., Abu-Ali, G., Franzosa, E.A., Schwager, R., Morgan, X.C., Waldron, L., Segata, N., Huttenhower, C., 2018. bioBakery: a meta’omic analysis environment. *J. Bioinform.* 34, 1235–1237. doi:10.1093/bioinformatics/btx754
- McMurdie, P.J., Holmes, S., 2013. phyloseq: An R Package for Reproducible Interactive Analysis and Graphics of Microbiome Census Data. *PLoS ONE* 8, e61217–11. doi:10.1371/journal.pone.0061217
- Meylan, S., Porter, C.B.M., Yang, J.H., Belenky, P., Gutierrez, A., Lobritz, M.A., Park, J., Kim, S.H., Moskowicz, S.M., Collins, J.J., 2017. Carbon Sources Tune Antibiotic Susceptibility in *Pseudomonas aeruginosa* via Tricarboxylic Acid Cycle Control. *Cell Chem. Biol.* 24, 195–206. doi:10.1016/j.chembiol.2016.12.015
- Mukherjee, P.K., Chandra, J., Retuerto, M., Sikaroodi, M., Brown, R.E., Jurevic, R., Salata, R.A., Lederman, M.M., Gillevet, P.M., Ghannoum, M.A., 2014. Oral Mycobiome Analysis of HIV-Infected Patients: Identification of *Pichia* as an Antagonist of Opportunistic Fungi. *PLoS Pathog.* 10, e1003996–17. doi:10.1371/journal.ppat.1003996
- Odom, A.R., 2011. Five Questions about Non-Mevalonate Isoprenoid Biosynthesis. *PLoS Pathog.* 7, e1002323–3. doi:10.1371/journal.ppat.1002323
- Ogata, Y., Mizushima, T., Kataoka, K., Kita, K., Miki, T., Sekimizu, K., 1996. DnaK Heat Shock Protein of *Escherichia coli* Maintains the Negative Supercoiling of DNA against Thermal Stress*. *J. Biol. Chem.* 271, 1–9. doi: 10.1074/jbc.271.46.29407
- Overbeek, R., Olson, R., Pusch, G.D., Olsen, G.J., Davis, J.J., Disz, T., Edwards, R.A., Gerdes, S., Parrello, B., Shukla, M., Vonstein, V., Wattam, A.R., Xia, F., Stevens, R., 2014. The SEED and the Rapid Annotation of microbial genomes using Subsystems Technology (RAST). *Nucleic Acids Res.* 42, D206–D214. doi:10.1093/nar/gkt1226
- Peleg, A.Y., Hogan, D.A., Mylonakis, E., 2010. Medically important bacterial–fungal interactions. *Nat. Rev. Micro.* 8, 340–349. doi:10.1038/nrmicro2313
- Petit, C., Rigg, G.P., Pazzani, C., Smith, A., Sieberth, V., Stevens, M., Boulnois, G., Jahn, K., Roberts, I.S., 1995. Region 2 of the *Escherichia coli* K5 capsule gene cluster encoding proteins for the biosynthesis of the K5 polysaccharide. *Mol. Microbiol.* 17, 611–620. doi:10.1111/j.1365-2958.1995.mmi_17040611
- Poretzky, R., Rodriguez-R, L.M., Luo, C., Tsementzi, D., Konstantinidis, K.T., 2014. Strengths and Limitations of 16S rRNA Gene Amplicon Sequencing in Revealing Temporal Microbial Community Dynamics. *PLoS ONE* 9, e93827–12. doi:10.1371/journal.pone.0093827
- Porter, N.T., Canales, P., Peterson, D.A., Martens, E.C., 2017. A Subset of Polysaccharide Capsules in the Human Symbiont *Bacteroides thetaiotaomicron* Promote Increased Competitive Fitness in the Mouse Gut. *Cell Host Microbe* 22, 494–506.e8. doi:10.1016/j.chom.2017.08.020
- Preidis, G.A., Versalovic, J., 2009. Targeting the Human Microbiome with Antibiotics, Probiotics, and Prebiotics: Gastroenterology Enters the Metagenomics Era. *Gastroenterology* 136, 2015–2031. doi: 10.1053/j.gastro.2009.01.072

- Pruesse, E., Quast, C., Knittel, K., Fuchs, B.M., Ludwig, W., Peplies, J., Glockner, F.O., 2007. SILVA: a comprehensive online resource for quality checked and aligned ribosomal RNA sequence data compatible with ARB. *Nucleic Acids Research* 35, 7188–7196. doi:10.1093/nar/gkm864
- Qi, L., Cornelis, M.C., Zhang, C., van Dam, R.M., Hu, F.B., 2009. Genetic predisposition, Western dietary pattern, and the risk of type 2 diabetes in men. *Am. J. Clin. Nutr.* 89, 1453–1458. doi:10.3945/ajcn.2008.27249
- Raffi, F., Sutherland, J.B., Cerniglia, C.E., 2008. Effects of treatment with antimicrobial agents on the human colonic microflora. *Ther. Clin. Risk Manag.* 4, 1343–1357. doi:10.2147/tcrm.s4328
- Ranjan, R., Rani, A., Metwally, A., McGee, H.S., Perkins, D.L., 2016. Analysis of the microbiome: Advantages of whole genome shotgun versus 16S amplicon sequencing. *Biochem. Biophys. Res. Commun.* 469, 967–977. doi:10.1016/j.bbrc.2015.12.083
- Rea, M.C., Dobson, A., O’Sullivan, O., Crispie, F., Fouhy, F., Cotter, P.D., Shanahan, F., Kiely, B., Hill, C., Ross, P.R., 2011. Effect of broad- and narrow-spectrum antimicrobials on *Clostridium difficile* and microbial diversity in a model of the distal colon. *Proc. Natl. Acad. Sci. USA.* 108, 4639–4644. doi:10.1073/pnas.1001224107
- Riiser, A., 2015. The human microbiome, asthma, and allergy. *Allergy Asthma Clin. Immunol.* 11, 1–7. doi:10.1186/s13223-015-0102-0
- Rowan-Nash, A.D., Korry, B.J., Mylonakis, E., Belenky, P., 2019. Cross-Domain and Viral Interactions in the Microbiome. *Microbiol. Mol. Biology Rev.* 83, 51–63. doi:10.1128/MMBR.00044-18
- Sami, W., Ansar, T., Butt, N.S., Hamid, M.R.A., 2017. Effect of diet on type 2 diabetes mellitus: A review. *Int. J. Health Sci. (Qassim)* 11, 1–7.
- Schnizlein, M.K., Vendrov, K.C., Edwards, S.J., Martens, E.C., Young, V.B., 2020. Dietary xanthan gum alters antibiotic efficacy against the murine gut microbiota and attenuates *Clostridioides difficile* colonization. *mSphere* 5, e00708–19. doi:10.1128/mSphere.00708-19
- Schoeler, M., Caesar, R., 2019. Dietary lipids, gut microbiota and lipid metabolism. *Rev. Endocr. Metab. Disord.* 20, 461–472. doi:10.1007/s11154-019-09512-0
- Segata, N., Izard, J., Waldron, L., Gevers, D., Miropolsky, L., Garrett, W.S., Huttenhower, C., 2011. Metagenomic biomarker discovery and explanation. *Genome Biol.* 12, R60. doi:10.1186/gb-2011-12-6-r60
- Shin, N.-R., Whon, T.W., Bae, J.-W., 2015. Proteobacteria: microbial signature of dysbiosis in gut microbiota. *Trends Biotechnol.* 33, 496–503. doi:10.1016/j.tibtech.2015.06.011
- Singh, R.K., Chang, H.-W., Di Yan, Lee, K.M., Ucmak, D., Wong, K., Abrouk, M., Farahnik, B., Nakamura, M., Zhu, T.H., Bhutani, T., Liao, W., 2017. Influence of diet on the gut microbiome and implications for human health. *J. Transl. Med.* 15, 1–17. doi:10.1186/s12967-017-1175-y
- Smits, S.A., Leach, J., Sonnenburg, E.D., Gonzalez, C.G., Lichtman, J.S., Reid, G., Knight, R., Manjurano, A., Changalucha, J., Elias, J.E., Dominguez-Bello, M.G., Sonnenburg, J.L., 2017. Seasonal cycling in the gut microbiome of the Hadza hunter-gatherers of Tanzania. *Science* 357, 802–806. doi:10.1126/science.aan4834
- Sonnenburg, E.D., Sonnenburg, J.L., 2019. The ancestral and industrialized gut microbiota and implications for human health. *Nat. Rev. Micro.* 17, 1–8. doi:10.1038/s41579-019-0191-8
- Sonnenburg, E.D., Sonnenburg, J.L., 2014. Starving our Microbial Self: The Deleterious Consequences of a Diet Deficient in Microbiota-Accessible Carbohydrates. *Cell Metab.* 20, 779–786. doi:10.1016/j.cmet.2014.07.003

- Sonnenburg, J.L., Xu, J., Leip, D.D., Chen, C.-H., Westover, B.P., Weatherford, J., Buhler, J.D., Gordon, J.I., 2005. Glycan foraging in vivo by an intestine-adapted bacterial symbiont. *Science* 307, 1952–1955. doi:10.1126/science.1109051
- Stiemsma, L.T., Michels, K.B., 2018. The Role of the Microbiome in the Developmental Origins of Health and Disease. *Pediatrics* 141, e20172437–22. doi:10.1542/peds.2017-2437
- Susin, M.F., Baldini, R.L., Gueiros-Filho, F., Gomes, S.L., 2006. GroES/GroEL and DnaK/DnaJ Have Distinct Roles in Stress Responses and during Cell Cycle Progression in *Caulobacter crescentus*. *J. Bacteriol.* 188, 8044–8053. doi:10.1128/JB.00824-06
- Tessler, M., Neumann, J.S., Afshinnekoo, E., Pineda, M., Hersch, R., Velho, L.F.M., Segovia, B.T., Lansac-Toha, F.A., Lemke, M., DeSalle, R., Mason, C.E., Brugler, M.R., 2017. Large-scale differences in microbial biodiversity discovery between 16S amplicon and shotgun sequencing. *Sci. Rep.* 7, 1–14. doi:10.1038/s41598-017-06665-3
- The Human Microbiome Project Consortium, 2012. A framework for human microbiome research. *Nature* 486, 215–221. doi:10.1038/nature11209
- Theriot, C.M., Bowman, A.A., Young, V.B., 2016. Antibiotic-Induced Alterations of the Gut Microbiota Alter Secondary Bile Acid Production and Allow for *Clostridium difficile* Spore Germination and Outgrowth in the Large Intestine. *mSphere* 1, e00045–15–16. doi:10.1128/mSphere.00045-15
- Thomas, V.C., Kinkead, L.C., Janssen, A., Schaeffer, C.R., Woods, K.M., Lindgren, J.K., Peaster, J.M., Chaudhari, S.S., Sadykov, M., Jones, J., Mohamadi AbdelGhani, S.M., Zimmerman, M.C., Bayles, K.W., Somerville, G.A., Fey, P.D., 2013. A Dysfunctional Tricarboxylic Acid Cycle Enhances Fitness of *Staphylococcus* β -Lactam Stress. *mBio* 4, e00437–13. doi:10.1128/mBio.00437-13
- Thompson, L.R., Sanders, J.G., McDonald, D., Amir, A., Ladau, J., Locey, K.J., Prill, R.J., Tripathi, A., Gibbons, S.M., Ackermann, G., Navas-Molina, J.A., Janssen, S., Kopylova, E., Vázquez-Baeza, Y., González, A., Morton, J.T., Mirarab, S., Zech Xu, Z., Jiang, L., Haroon, M.F., Kanbar, J., Zhu, Q., Jin Song, S., Kosciulek, T., Bokulich, N.A., Leffler, J., Brislawn, C.J., Humphrey, G., Owens, S.M., Hampton-Marcell, J., Berg-Lyons, D., McKenzie, V., Fierer, N., Fuhrman, J.A., Clauset, A., Stevens, R.L., Shade, A., Pollard, K.S., Goodwin, K.D., Jansson, J.K., Gilbert, J.A., Knight, R., The Earth Microbiome Project Consortium, 2017. A communal catalogue reveals Earth’s multiscale microbial diversity. *Nature* 551, 457–463. doi:10.1038/nature24621
- Topping, D.L., Clifton, P.M., 2001. Short-chain fatty acids and human colonic function: roles of resistant starch and nonstarch polysaccharides. *Physiol. Rev.* 81, 1–34. doi:10.1152/physrev.2001.81.3.1031
- Tremlett, H., Bauer, K.C., Appel-Cresswell, S., Finlay, B.B., Waubant, E., 2017. The gut microbiome in human neurological disease: A review. *Ann. Neurol.* 81, 369–382. doi:10.1002/ana.24901
- Trompette, A., Gollwitzer, E.S., Yadava, K., Sichelstiel, A.K., Sprenger, N., Ngom-Bru, C., Blanchard, C., Junt, T., Nicod, L.P., Harris, N.L., Marsland, B.J., 2014. Gut microbiota metabolism of dietary fiber influences allergic airway disease and hematopoiesis. *Nat. Med.* 20, 159–166. doi:10.1038/nm.3444
- Turnbaugh, P.J., 2017. Microbes and Diet-Induced Obesity: Fast, Cheap, and Out of Control. *Cell Host Microbe* 21, 278–281. doi:10.1016/j.chom.2017.02.021

- Turnbaugh, P.J., Bäckhed, F., Fulton, L., Gordon, J.I., 2008. Diet-Induced Obesity Is Linked to Marked but Reversible Alterations in the Mouse Distal Gut Microbiome. *Cell Host Microbe* 3, 213–223. doi:10.1016/j.chom.2008.02.015
- Turnbaugh, P.J., Ley, R.E., Mahowald, M.A., Magrini, V., Mardis, E.R., Gordon, J.I., 2006. An obesity-associated gut microbiome with increased capacity for energy harvest. *Nature* 444, 1027–1031. doi:10.1038/nature05414
- Turnbaugh, P.J., Ridaura, V.K., Faith, J.J., Rey, F.E., Knight, R., Gordon, J.I., 2009. The Effect of Diet on the Human Gut Microbiome: A Metagenomic Analysis in Humanized Gnotobiotic Mice. *Sci. Transl. Med.* 1, 6ra14. doi:10.1126/scitranslmed.3000322
- Ursell, L.K., Metcalf, J.L., Parfrey, L.W., Knight, R., 2012. Defining the human microbiome. *Nutr. Rev.* 70, S38–S44. doi:10.1111/j.1753-4887.2012.00493.x
- van Selm, S., Kolkman, M.A.B., van der Zeijst, B.A.M., Zwaagstra, K.A., Gaastra, W., van Putten, J.P.M., 2002. Organization and characterization of the capsule biosynthesis locus of *Streptococcus pneumoniae* serotype 9V. The GenBank accession number for the sequence reported in this paper is AF402095. *Microbiology* 148, 1747–1755. doi:10.1099/00221287-148-6-1747
- Vieira, S.M., Pagovich, O.E., Kriegel, M.A., 2014. Diet, microbiota and autoimmune diseases. *Lupus* 23, 518–526. doi:10.1177/0961203313501401
- Walker, A.W., Ince, J., Duncan, S.H., Webster, L.M., Holtrop, G., Ze, X., Brown, D., Stares, M.D., Scott, P., Bergerat, A., Louis, P., McIntosh, F., Johnstone, A.M., Lobley, G.E., Parkhill, J., Flint, H.J., 2011. Dominant and diet-responsive groups of bacteria within the human colonic microbiota. *ISME J.* 5, 220–230. doi:10.1038/ismej.2010.118
- Wang, Q., Qiong, Garrity, G.M., Tiedje, J.M., Cole, J.R., 2007. Naïve bayesian classifier for rapid assignment of rRNA sequences into the new bacterial taxonomy. *Appl. Environ. Microbiol.* 73, 5261–5267. doi:10.1128/AEM.00062-07
- Westreich, S.T., Korf, I., Mills, D.A., Lemay, D.G., 2016. SAMSA: a comprehensive metatranscriptome analysis pipeline. *BMC Bioinform.* 17, 1–12. doi:10.1186/s12859-016-1270-8
- Westreich, S.T., Treiber, M.L., Mills, D.A., Korf, I., Lemay, D.G., 2018. SAMSA2: a standalone metatranscriptome analysis pipeline. *BMC Bioinform.* 19, 1–11. doi:10.1186/s12859-018-2189-z
- Witten, I.H., Bell, T.C., 1991. The Zero-Frequency Problem: Estimating the Probabilities of Novel Events in Adaptive Text Compression. *IEEE Trans. Inf. Theor.* 137, 1–10. doi:10.1109/18.87000
- Wong, J.M.W., de Souza, R., Kendall, C.W.C., Emam, A., Jenkins, D.J.A., 2006. Colonic Health: Fermentation and Short Chain Fatty Acids. *J. Clin. Gastroenterol.* 40, 1–9. doi:10.1097/00004836-200603000-00015
- Wong, K.S., Houry, W.A., 2012. Novel structural and functional insights into the MoxR family of AAA+ ATPases. *J. Struct. Biol.* 179, 211–221. doi:10.1016/j.jsb.2012.03.010
- Wood, D.E., Salzberg, S., 2014. Kraken: ultrafast metagenomic sequence classification using exact alignments. *Genome Biol.* 15, 1–12. doi:10.1186/gb-2014-15-r46
- Xu, Z., Knight, R., 2015. Dietary effects on human gut microbiome diversity. *Br. J. Nutr.* 113, S1–S5. doi:10.1017/S0007114514004127
- Yatsunencko, T., Rey, F.E., Manary, M.J., Trehan, I., Dominguez-Bello, M.G., Contreras, M., Magris, M., Hidalgo, G., Baldassano, R.N., Anokhin, A.P., Heath, A.C., Warner, B., Reeder, J., Kuczynski, J., Caporaso, J.G., Lozupone, C.A., Lauber, C., Clemente, J.C., Knights, D.,

- Knight, R., Gordon, J.I., 2012. Human gut microbiome viewed across age and geography. *Nature* 486, 222–227. doi:10.1038/nature11053
- Zhang, J., Kobert, K., Flouri, T., Stamatakis, A., 2014. PEAR: a fast and accurate Illumina Paired-End reAd mergeR. *Bioinformatics* 30, 614–620. doi:10.1093/bioinformatics/btt593
- Zhou, J., Xiong, X., Yin, J., Zou, L., Wang, K., Shao, Y., Yin, Y., 2019. Dietary Lysozyme Alters Sow's Gut Microbiota, Serum Immunity, and Milk Metabolite Profile. *Front. Microbiol.* 10, 1–14. doi:10.3389/fmicb.2019.00177

Chapter 3:
**Streptozotocin-Induced Hyperglycemia Alters the
Cecal Metabolome and Exacerbates Antibiotic-
Induced Dysbiosis**

Originally published in *Cell Reports*, 14 Dec 2021, Vol 37, No. 110113
DOI: 10.1016/j.celrep.2021.110113

Copyright © Cell Press

Streptozotocin-Induced Hyperglycemia Alters the Cecal Metabolome and Exacerbates Antibiotic-Induced Dysbiosis

Jenna I. Wurster¹, Rachel L. Peterson¹, Claire E. Brown¹, Swathi Penumutthu¹, Douglas V. Guzior^{2,3}, Kerri Neugebauer³, William H. Sano⁴, Manu M. Sebastian⁵, Robert A. Quinn³, Peter Belenky^{1,6,*}

¹ Department of Molecular Microbiology and Immunology, Brown University, Providence, RI 02906, USA

² Department of Microbiology and Molecular Genetics, Michigan State University, East Lansing, MI 48824, USA

³ Department of Biochemistry and Molecular Biology, Michigan State University, East Lansing, MI 48824, USA

⁴ Department of Biology, University of Washington, Seattle, WA 98195, USA

⁵ Department of Epigenetics and Molecular Carcinogenesis, Division of Basic Science Research, The University of Texas MD Anderson Cancer Center, Smithville, TX 78957, USA

⁶ Lead Contact

* Address correspondence to Peter Belenky: peter_belenky@brown.edu

Abstract

It is well established in the microbiome field that antibiotic (ATB) use and metabolic disease both impact the structure and function of the gut microbiome. But how host and microbial metabolism interacts with ATB susceptibility to affect the resulting dysbiosis remains poorly understood. In a streptozotocin-induced model of hyperglycemia (HG), we use a combined metagenomic, metatranscriptomic, and metabolomic approach to profile changes in microbiome taxonomic composition, transcriptional activity, and metabolite abundance both pre- and post-ATB challenge. We find that HG impacts both microbiome structure and metabolism, ultimately increasing susceptibility to amoxicillin. HG exacerbates drug-induced dysbiosis and increases both phosphotransferase system activity and energy catabolism compared to controls. Finally, HG and ATB co-treatment increases pathogen susceptibility and reduces survival in a *Salmonella enterica* infection model. Our data demonstrate that induced HG is sufficient to modify the cecal metabolite pool, worsen the severity of ATB dysbiosis, and decrease colonization resistance.

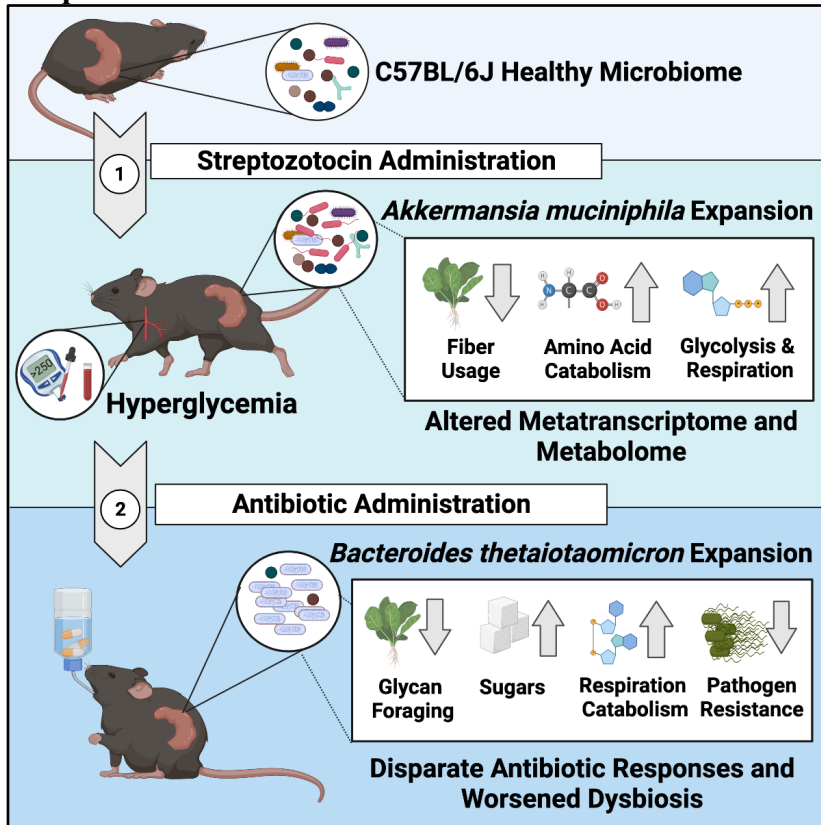
Keywords:

Hyperglycemia, Streptozotocin, Antibiotics, Microbiome, Dysbiosis, Metagenomics, Metatranscriptomics, Metabolomics

List of Abbreviations

AA	Amino Acid
AAA	Aromatic Amino Acid
AMX	Amoxicillin
ATB	Antibiotic
B. theta	<i>Bacteroides thetaiotaomicron</i>
CAZyme	Carbohydrate-Active Enzyme
GI	Gastrointestinal Tract
HG	Hyperglycemia / Hyperglycemic
LC-MS/MS	Liquid Chromatography Tandem Mass Spectrometry
NG	Normoglycemia / Normoglycemic
PTS	Phosphotransferase System
Q-TOF-MS	Quadrupole Time of Flight Mass Spectrometry
SCFA	Short-Chain Fatty Acid
STZ	Streptozotocin
WMGS	Whole Metagenomic Sequencing

Graphical Abstract



Introduction

Exposure to antibiotics (ATB) is one of the most significant known microbiome perturbations. Drug-induced dysbiosis occurs within hours of treatment, and is characterized by loss of total bacterial load, taxonomic diversity, and significant transcriptional changes (Cabral et al., 2019; 2020; Dethlefsen and Relman, 2011). This alters the intestinal metabolome, placing the host at a higher risk for opportunistic infection (Bäumler and Sperandio, 2016; Buffie et al., 2012; Chang et al., 2008; Croswell et al., 2009; Kaiko and Stappenbeck, 2014; Rivera-Chávez et al., 2016; Theriot et al., 2016; Theriot and Young, 2015). Given the severity of ATBs on the microbiome and the near ubiquitous use of these drugs, it is critical to mechanistically understand ATB activity within the gut and the external factors that dictate susceptibility.

Microbial metabolism is a key determinant of ATB susceptibility (Stokes et al., 2019). Microbes performing ATP-generating processes like aerobic respiration have increased bactericidal drug sensitivity and experience a lethal respiratory burst during *in vitro* exposure (Adolfsen and Brynildsen, 2015; Belenky et al., 2015; Dwyer et al., 2014; Kohanski et al., 2007; Lam et al., 2020; Lobritz et al., 2015). Meanwhile, fermentation, diversion away from the tricarboxylic acid (TCA) cycle, or overall reduction in metabolism can confer drug tolerance in some species (Ahn et al., 2016; Conlon et al., 2016; Lobritz et al., 2015; Meylan et al., 2017; Thomas et al., 2013). We demonstrated that this trend holds true within the context of the microbiome, where ATB exposure dramatically reduces community metabolic capacity (Cabral et al., 2019). Surviving taxa like *Bacteroides thetaiotaomicron* (*B. theta*) can endure amoxicillin (AMX) exposure by transcriptional adaptation that prioritizes fiber fermentation over the utilization of simple sugars (Cabral et al., 2019). When considering mechanisms of *in vivo* susceptibility, it is important to consider the role of local nutrients on microbial metabolism. Host

diet is likely one of the largest factors shaping the cecal nutrient pool; dietary changes can perturb microbiome diversity and activity, and thus may impact ATB susceptibility (Albenberg and Wu, 2014; Bisanz et al., 2019; Collins et al., 2018; David et al., 2014; Ley, 2014; Smits et al., 2017; Tanes et al., 2021). Congruently, we showed that added dietary glucose potentiates AMX toxicity within the cecum, reducing total bacterial load and *B. theta*'s drug tolerance phenotype (Cabral et al., 2019). This also occurs with the bactericidal drug ciprofloxacin, where consumption of a high fat/sugar diet increases mucus and simple sugar breakdown, increases gut glycolysis, and enhances microbiome drug susceptibility (Cabral et al., 2020). This suggests that the local nutrient pool can drive the severity of ATB activity in the microbiome by altering the metabolic rate of resident taxa.

Diet composition is not the sole determinant of nutrient availability within the gut. Normally, a small fraction of digested material reaches the dense communities of the lower gastrointestinal tract (GI). The composition of dietary molecules presented to the lower GI is impacted by multiple small intestinal digestive gradients and pancreaticobiliary secretions (Reese and Carmody, 2019; Shin et al., 2019). For example, the host controls colonic sugar concentrations via a combination of small intestinal transporter expression, gastric emptying rate, and enteroendocrine function (L. Chen et al., 2016; Holst et al., 2016; Koepsell, 2020; Holst et al., 2016; Ussar et al., 2017). Disruptions of host metabolism, like digestive and metabolic disorders, are correlated with microbial dysbiosis, highlighting the connection between host and microbial systems in the GI (Brestoff and Artis, 2013; Westfall et al., 2015; Qin et al., 2012; Sabatino et al., 2017). For example, dysglycemic patients demonstrate bacterial infiltration of the intestinal epithelial mucosa, suggesting that dysglycemia triggers an inflammatory intestinal phenotype by prompting microbial breakdown of mucus glycoproteins (Chassaing et al., 2017).

Host hyperglycemia (HG) may cause potent modulation of the lower GI metabolic environment. Currently, the relationship between dysregulated host metabolism, the local metabolite environment of the GI, and the severity of ATB-induced dysbiosis remains relatively understudied. *We hypothesize that changes in host metabolism associated with induced HG will alter the microbiota-accessible cecal metabolite pool and place the community in a metabolically permissive state that increases susceptibility to bactericidal ATBs.* To test this, we used the single-dose streptozotocin (STZ) model rather than a diet- or genetically-based model of glucose dysregulation (Deeds et al., 2011; Kobayashi et al., 2000; C.-Y. Wang and Liao, 2012). STZ is a glucosamine nitrosourea compound that induces HG via the selective and irreversible destruction of insulin-producing pancreatic β cells; (Eleazu et al., 2013; Wu and Yan, 2015). STZ is quickly metabolized by the host, with a serum clearance time of about 15 minutes (Lee et al., 2010; Eleazu et al., 2013). Thus, STZ provides the benefit of rapidly-induced and irreversible HG without potentially microbiome-confounding factors like diet and host genetics (Deeds et al., 2011; Xiao et al., 2017; Yang et al., 2019). Existing research on glucose dysregulation and the microbiome is impacted by the use of dietary metabolic animal models like the high-fat diet-induced diabetes mouse (Fujisaka et al., 2016). In this study we used a multi-omic approach that profiled the taxonomic composition, transcriptional activity, and small molecule repertoire of the cecum to characterize the impact of STZ-induced HG on microbiome disruption during AMX treatment. We then profiled the effects of HG on AMX-induced pathogen susceptibility by challenging mice with *Salmonella enterica*. Our data show that HG is sufficient to modulate the cecal metabolite pool, and that these changes both potentiate ATB-induced dysbiosis and worsen the dysbiosis-related complication of opportunistic infection.

Results

To examine the combined effect of HG and ATBs on microbiome structure and function, male C57BL/6J mice were given an intraperitoneal injection of either STZ or a sham (control). Mice were assessed for HG 48 hours post-injection then randomized. The next day, animals were given AMX or a sham (vehicle) for 24 hours *ad libitum*, which is sufficient to profile acute microbiome ATB responses without encountering significant extinction events (Cabral et al., 2020; 2019). After AMX delivery, mice were sacrificed and cecal contents were harvested for multi-omic profiling (Figure 1A).

STZ caused significant and sustained HG (Figure 1B, Figure S1A). Because STZ's mechanism of action involves organ cytotoxicity, we quantified plasma cytokines to evaluate systemic inflammation (Eleazu et al., 2013). We found no statistical difference in cytokine levels prior to ATB administration (Figure S1B, Figure S1C), but did observe an increase in IFN- γ 24 hours later (Figure S1D) that is likely correlated with the early stages of disease progression in this model (Hanafusa and Imagawa, 2008). We then assessed GI histopathology and quantified GI lipocalin-2 to profile for localized inflammation. STZ-treated mice had minimal to no edema or inflammation compared to controls (Figure S1E), and no difference in lipocalin-2 levels (Figure S1F). Together these data show minimal differences in inflammatory phenotypes between STZ-treated and control mice during the time frame used in this study.

We profiled the effect of HG and AMX on microbiome structure using 16S rRNA sequencing. STZ treatment did not reduce diversity (Figure S1G) but did alter community composition when combined with AMX (Figure 1C, Figure S1H, Figure S1I). Because 16S sequencing has limited phylogenetic resolution, we conducted the remaining analyses with whole metagenomic sequencing (WMGS) (Cabral et al., 2020; 2019; Clooney et al., 2016; Poretsky et

al., 2014; Ranjan et al., 2016). WMGS showed that STZ alone did not impact α -diversity but bolstered the reduction in diversity and taxonomic shifts caused by AMX (Figure 1D, Figure 1E).

Since STZ ablates insulin synthesis, and insulin helps regulate intestinal glucose absorption (Ussar et al., 2017), we asked if GI-localized glucose levels were altered by HG. However, we found that STZ-treated mice and controls had no significant difference in cecal glucose levels (Figure 1F). Therefore, glucose availability cannot explain the changes in community composition between experimental groups. Thus, we profiled the metabolome using quadrupole time-of-flight mass spectrometry (Q-TOF-MS) and liquid chromatography tandem mass spectrometry (LC-MS/MS) (Table S1, Table S2). By assessing cecal metabolite diversity using Principal Coordinates Analysis, we found that both STZ and AMX significantly impacted the cecal metabolome's composition (Figure 2A). We hypothesized that STZ-induced HG establishes a transcriptional and metabolic environment that alters the microbiome's response to ATB exposure. To confirm this, we assessed the impact of HG on microbiome function both pre- and post-AMX treatment.

Hyperglycemia Significantly Modifies the Cecal Metabolome and Metatranscriptome.

Unlike diet-induced models of HG, STZ was associated with a single significant phylum-level change: the expansion of Verrucomicrobia (Figure 1E, Figure S1I) (Xiao et al., 2017; Yang et al., 2019). We confirmed that this expansion was driven by *Akkermansia muciniphila* using differential abundance testing (Figure 2B) (Love et al., 2014). *A. muciniphila* forages carbon from epithelial mucins and has been proposed to breakdown gut lining integrity, which may contribute to cecal metabolome divergence via imbalances in the local carbon pool that impact microbial cross-feeding networks (Belzer et al., 2017; Cabral et al., 2020; Desai et al., 2016; T. Zhang et al., 2019). For example, we observed a reduction in the abundance of *Blautia* sp. YL58 after STZ

(Figure 2B). Members of this genus are short-chain fatty acid (SCFA) producers that use mucin as a carbon substrate (Bui et al., 2019; Oliphant and Allen-Vercoe, 2019; Rey et al., 2010; Vacca et al., 2020). *A. muciniphila* may outcompete *Blautia* for mucins in the HG host, which would disrupt any syntropic reactions *Blautia* participates in. Because the pre-AMX community structure was similar between hosts, we felt that the disparity in ATB susceptibility was due to modified metabolic and transcriptional activity, rather than baseline taxonomic differences.

We paired differential abundance testing (Love et al., 2014) and pathway-level projection (Aggio et al., 2010) of our Q-TOF-MS data with random forest classification of LC-MS/MS features to identify distinctive metabolites between HG mice and controls (Figure S2A-C, Table S1-S3). We then paired these findings with community- and species-level transcriptomics to better profile the microbiome's functional capacity prior to ATB exposure. Despite consuming identical diets, HG and normoglycemic (NG) mice had varied levels of metabolites related to polysaccharide processing. We saw STZ-specific enrichment of the flavones apigenin, schaftoside, and daidzein, and significant reduction of major metabolites from apigenin breakdown such as 3-hydroxyphenyl propanoate (Figure 2C, Table S1). These metabolites can generate either hydroxyphenylacetic acids or phenolic intermediates that are converted to SCFAs by Firmicutes (Braune and Blaut, 2016), and their accumulation may indicate diminished SCFA generation. To that end, STZ-treatment reduced valerate levels (Figure 2C). HG also lowered phytate degradation and multiple polysaccharide-targeted carbohydrate-active enzymes (CAZymes) (Figure 2C, Figure 2D, Figure S2D, Table S1, Table S4, Table S6). Polysaccharide-fermenting taxa like *B. theta* (Martens et al., 2008; Sonnenburg et al., 2005) had reduced expression of targeted fiber import loci (Figure S2E: BT3086, BT3087, BT3090, and BT4581, Table S5). These data suggest

that STZ may impair microbial fiber fermentation and alter the level of polysaccharide-derived carbon sources.

Amino acids (AA) are another significant bacterial carbon source (X. Wang et al., 2019) that was impacted by STZ treatment. Multiple metabolites related to aromatic amino acid (AAA) generation, like 3-(3-hydroxyphenyl)propanoic acid and phenylethyl alcohol, were reduced by STZ (Figure 2C, Table S1). We saw enrichment of metabolites involved in AA catabolism like 6-methylnicotinamide, 2-ketoisocaproate and α -ketovaline, as well as pathway enrichment of AAA degradation and protein digestion, suggesting a shift towards AA catabolism rather than *de novo* synthesis (Figure S2A, Figure S2B, Table S1, Table S3). Shikimate pathway intermediates like 3-dehydroquinate, 3-dehydroshikimate, and shikimate were enriched after STZ treatment, and likely caused by a block in a terminal component of the pathway, as transcription of both AAA and chorismate synthesis were reduced (Figure 2C, Figure 2D, Table S1, Table S6). The shikimate pathway feeds directly into AAA generation via chorismate; thus, reduced transcription and accumulation of metabolic intermediates suggests a shift from anabolic to catabolic AA metabolism.

The shikimate pathway is also involved in B-vitamin generation and impacts the availability of energy carriers like coenzyme A (CoA) (Tzin and Galili, 2010). We observed enrichment of metabolites involved in pantothenate and CoA biosynthesis coupled with reduced pathway transcription (Figure 2D, Figure S2B, Table S3, Table S6). STZ increased expression of thiazole biosynthesis, which is critical for generating vitamin B1- and thus key metabolic enzymes like pyruvate dehydrogenase, pyruvate decarboxylase, and α -ketoglutarate dehydrogenase (Andersen et al., 2015; Allaway et al., 2020; Yoshii et al., 2019) (Figure 2D, Table S6). We observed increased pyruvate, glycolysis, and gluconeogenesis-related metabolites, including

glutamine and glycerol-3-phosphate (Figure S2A, Figure S2B). This enrichment was coupled with elevated ATPase, phosphoenolpyruvate hydratase, and succinate dehydrogenase transcription (Figure 2E, Table S8), that, when considered in tandem with increased inosine and tRNA processing (Figure 2D, Table S1, Table S6), suggests that STZ bolsters respiration within the microbiome.

These data describe community-level changes to microbiome function. To identify species-specific contributors to metabolome variation, we taxon stratified our Q-TOF-MS data using MIMOSA (Figure 2F) (Noecker et al., 2016). *A. muciniphila* had the largest contribution to community metabolism, followed by *B. theta* (Figure 2F, Table S9). *A. muciniphila* significantly contributed to acetate variation between hosts, speaking to STZ-related difference in SCFAs. Metabolic signatures of increased metabolism, including glutamine, inosine, and glycerol-3-phosphate accumulation, could be explained by synthesis and degradation from *A. muciniphila* (glutamate & inosine) and synthesis from *B. theta* (inosine and glycerol-3-phosphate). Finally, variation in phosphatidylethanolamine, a major component of microbial cell walls, could be somewhat explained by *A. muciniphila* (Figure 2F), suggesting increased cell wall synthesis by this taxon. These data highlight that these two taxa are key in HG-specific changes to microbiome function. STZ has robust impacts on cecal microbiome function. While *A. muciniphila* and *B. theta* are involved in this phenotype, it is important to consider that there is redundancy in species function and in substrate utilization across biochemical pathways (Tian et al., 2020). Thus, it is likely that the cumulative effect of multiple metabolic disruptions incurred from STZ increases metabolic demand on the community and leads to increased AMX susceptibility.

Hyperglycemia Modifies the Composition of Bacteroidetes and Firmicutes after Amoxicillin Exposure. Given the connection between microbial metabolism and ATB susceptibility (Belenky et al., 2015; Cabral et al., 2019; Lobritz et al., 2015; Stokes et al., 2019), we hypothesized that STZ-induced metabolic disruption bolstered AMX susceptibility. HG mice had a highly divergent microbial composition after ATB exposure compared to controls (Figure 3A, Figure S3). Specifically, HG exacerbated the AMX-related reduction in α -diversity (Figure 1D). Only HG mice had a reduction in Verrucomicrobia, although this may be due to the pre-AMX expansion of *A. muciniphila* (Figure 1E, Figure 3B). Interestingly, the loss of Actinobacteria, Firmicutes, and Proteobacteria, and the bloom in Bacteroidetes that was expected after AMX were greater in HG mice (Figure 3C-F) (Cabral et al., 2019). Consistent with our previous work (Cabral et al., 2019), the Bacteroidetes bloom was driven by the expansion of *B. theta* in both hosts (Figure 3G).

We calculated the interaction of HG and AMX to examine host-specific changes in species abundance (Love et al., 2014). In addition to *B. theta*, many members of the *Bacteroides* genus increased after AMX, with significantly elevated abundance in HG mice (Figure 3H, Figure S3A). Meanwhile, the species with reduced abundance in HG mice after AMX treatment were primarily within the order Clostridiales (Figure 3H, Figure S3B-I). These taxa are key starch degraders and SCFA producers, and their reduction suggests an increased dysbiotic state in STZ and AMX co-treated mice (Bui et al., 2016; Iino et al., 2007; Kazemian et al., 2020; Newman et al., 2018). Overall, these data show that STZ-induced metabolic shifts can exacerbate the post-AMX bloom of *Bacteroides* and significantly worsen the loss of key SCFA-producing Firmicutes. This likely impacts the local metabolome and metatranscriptome, and thus AMX susceptibility, given the syntrophic nature of *Bacteroides* and Firmicutes metabolism (Fischbach and Sonnenburg, 2011).

Hyperglycemia Exacerbates Antibiotic-Induced Dysbiosis and Shifts Microbial Metabolism.

As with taxonomic changes, the majority of detected functional AMX responses were highly host dependent. We used the same interaction calculation to profile host-specific changes in CAZyme and SEED subsystem transcript abundances (Figure 4A, Figure 4B). Interestingly, HG animals lack the reduction in glycoside hydrolase (GH) 43 seen in controls, suggesting modified processing of hemicelluloses, pectins, xylans, and arabinose (Figure 4A, Table S4) (Mewis et al., 2016). Given the reduced polysaccharide foraging in the STZ baseline, it is likely that the HG microbiota is unable to adapt its CAZyme expression in response to AMX. HG communities had overall fewer GH transcripts at the SEED subsystem level, and a greater loss of GH abundance relative to controls (Figure S4A, Figure S4B, Table S4, Table S7). We saw STZ-specific accumulation of polyphenols and polysaccharides, providing further support for host-dependent modifications in polysaccharide metabolism (Figure 5A, Table S1). HG mice had accumulation of multiple phenylpropanoids, phenylacetic acids, polyphenols, alkaloids, flavonoids, and isoprenoids (Figure 5A, Table S1) and pathway-level enrichment of metabolites related to flavonoid/isoflavonoid synthesis after AMX treatment (Table S3). Because fiber metabolism can confer a protective phenotype to select gut microbes (Cabral et al., 2019) we anticipated that reduced fiber and polyphenol metabolism may directly contribute to the severity of AMX-induced dysbiosis in HG mice.

Mucus foraging by the microbiota after AMX was also perturbed. In our CAZyme dataset, HG mice had a loss of GHs that target the chitobiose core of mucins (GH115), and did not upregulate GH84, GH129, and GH89 which target N-acetylglucosamine, class-III mucins, and mucus glycoproteins, respectively (Figure 4A, value, Table S4). Simultaneously, STZ and AMX co-treatment downregulated expression of multiple pathways involved in mucin-derived carbon

metabolism, including the Leloir pathway (foraging of mucus galactose residues), 4-deoxy-L-theo-hex-4-enopyranuronate degradation (breakdown of heparin and hyaluron into pyruvate), and D-galacturonate degradation (Figure 4C, Figure 4D, Table S6) (Tang et al., 2016). The sialic acid residue N-acetylneuraminic acid (NANA) was enriched in NG but not HG animals after AMX (Table S1). Because NANA is liberated by mucus breakdown (Crost et al., 2016), this suggested reduced muciniphilic activity by STZ and AMX co-treated communities. Ultimately, HG-related modifications in glycan foraging occur both before and after AMX, indicating that STZ-induced HG impacts the composition of the cecal carbon pool.

Further evidence of perturbed carbon foraging in the HG AMX-treated microbiome arose from examination of host and ATB interaction for SEED subsystem transcript abundances (Figure 4B, Table S7). We found a STZ-specific increase in phosphotransferase system (PTS) transcripts (Figure 4B, Table S7) as well as enrichment of PTS metabolites like mannitol 1-phosphate (Figure 5A, Table S1). PTS systems function to rapidly import target saccharides into bacterial cells, and increased PTS activity may be the result of higher environmental sugar concentrations (McCoy, Levin, and Zhou, 2015). Although AMX reduced cecal glucose concentrations in both hosts, HG mice had significantly higher glucose levels than controls (Figure 1F) and we observed STZ-specific enrichment of sugars like acetylated maltose (Figure 5A, Table S1).

Elevated sugars and PTS likely also increased catabolism. To that end, we observed significant HG-specific increases in glycolysis and gluconeogenesis (Figure 4B, Table S7) and pyruvate fermentation transcripts compared to controls (Figure S4A, Figure S4B Table S7). The metabolome of HG AMX-treated mice was specifically enriched in catabolism and catabolism-supporting pathways like 2-oxocarboxylic acid metabolism, glycolysis, starch/sucrose utilization, nicotinate/nicotinamide, and propanoate generation (Figure 5B, Table S3). The abundance of

vitamin co-factors was also impacted; in our LC-MS/MS dataset we saw HG-specific enrichment in riboflavin (Figure S4C: Cluster 699, Figure S4D, Table S2) (Steinert et al., 2020). The enrichment of nicotinate/nicotinamide, propanoate generation, and cofactor-related metabolites may impact the abundance of energy carriers (Belenky et al., 2007). Together these data suggest that carbon metabolism is disturbed in the HG AMX-treated microbiome, in part due to higher environmental concentrations of readily metabolized sugars.

We stratified our metabolomics and transcriptional data with MIMOSA to identify taxonomic drivers of community behavior during AMX treatment (Figure 5C, Figure 5D, Table S9). Regardless of host, *B. theta* was the major metabolome-contributing taxa, which is congruent with its dominance of the microbiome during AMX perturbation (Figure 3A, Figure 3G, Figure 5C, Figure 5D, Table S9). Of the metabolites correlated with differential community activity in HG mice, *B. theta* was responsible for enrichment of B-vitamins like riboflavin (via synthesis) and pantothenate (via synthesis and degradation). Additionally, sucrose and glycerol-3-phosphate levels could be partially explained by synthetic reactions from *B. theta* (Figure 5D, Table S9).

The fact that *B. theta* significantly shapes the metabolic function of the microbiome after AMX in both hosts prompted us to compare the post-ATB transcriptome and metabolome (Figure 6). We found that HG AMX-treated metabolomes were significantly enriched for metabolites involved in multiple AA generation pathways, nucleotide biosynthesis, and linoleic acids (Figure 6A, Table S3). Additionally, we saw significant enrichment of metabolites related to carbon processing (fructose/mannose metabolism, ABC transporters, PTS) and metabolic homeostasis (pyruvate metabolism, ubiquinone/terpenoid-quinone biosynthesis, and glutathione metabolism) (Figure 6A). At the MetaCyc pathway level, we observed HG-related increases in pyruvate fermentation and nucleotide biosynthesis (Figure 6B, Table S6). Unsurprisingly, *B. theta* was the

major contributing taxon to this variation (Figure 6C, Table S9). Thus, we performed single-species transcriptomics on *B. theta* during AMX challenge in HG and NG mice. Interestingly, *B. theta* downregulated the expression of multiple polysaccharide utilization loci (BT4293-BT4299, BT4296-4298, BT3025, BT1761, and BT1762) and sugar import systems for fructose (BT1759-1763, and BT1759), ribose (BT2804), and fucose (BT3665) (Figure 6D, Table S5) only in HG mice (Figure 6D, Table S5) (Lynch and Sonnenburg, 2012; Mardo et al., 2017; Mimee et al., 2015; Townsend et al., 2020). The combination of STZ and AMX treatment also coincided with significant upregulation of the NADH dehydrogenase complex (BT4058-4067) which is a primary redox balance locus (Fischbach and Sonnenburg, 2011). We also saw elevation of another NADH ubiquinone reductase operon (BT0616) (Goodman et al., 2009), and ATPase (BT1746) (Figure 6D, Table S5). Our community-level metabolomics indicated HG-specific loss of phosphoenolpyruvate (Table S1), which may be related to the differential regulation of respiration-related complexes in *B. theta*. Together these data show that HG, and the resultant changes in environmental metabolites, are sufficient to dramatically modify the transcriptional and metabolic behavior of *B. theta* during AMX treatment. This change ultimately impacts the AMX susceptibility of other taxa within the community and greatly perturbs the functional response of the larger community to ATB pressure.

Streptozotocin and Amoxicillin Co-treatment Increases Susceptibility to *Salmonella enterica*

Infection. We noticed that fatty acid metabolism was differentially impacted by STZ and AMX treatment. Specifically, co-treated communities were enriched for multiple N-acylethanolamines (Figure 5A, Table S1) and the precursor phosphatidylethanolamine (Table S1). Higher ethanolamine concentrations may suggest more fatty acid epoxidation and dysbiosis-associated

inflammation within the GI (Ormsby et al., 2019; Thiennimitr et al., 2011). Ethanolamines are naturally generated by phosphatidylethanolamine breakdown during cell turnover, however, most of the microbiota is unable to ferment ethanolamines, and these compounds can increase the colonization and virulence of multiple enteric pathogens (Anderson et al., 2018; 2015; Nawrocki et al., 2018; Rowley et al., 2018; Garsin, 2010). Specifically, some *Enterobacteriaceae* are enriched for the genetic machinery required to use ethanolamines, and can funnel their breakdown products into both nitrogen metabolism and respiration (Anderson et al., 2015; Garsin, 2010; Srikumar and Fuchs, 2011; Thiennimitr et al., 2011). In *Salmonella*, exogenous ethanolamine signals a cascade of metabolic and virulence genes that promote intestinal colonization (Anderson and Kendall, 2016). ATB-induced dysbiosis is also associated with increased *S. enterica* colonization, likely through the induction of a respiratory-favorable environment and disruption of the endogenous microbiota (M. Y. Yoon and S. S. Yoon, 2018; Zeng et al., 2017). The transcriptional changes we observed in *B. theta* are highly indicative of a respiratory-favorable environment in the HG AMX-treated GI (Figure 6D). Thus, we asked if the microbiome modifications in HG AMX-treated mice would increase infection susceptibility to *S. enterica* (Figure 7A).

We found that co-treatment with STZ and AMX lowered the infective dose required to establish *S. enterica* colonization and significantly increased intestinal, hepatic, and splenic pathogen burden (Figure 7B, Figure S5A). Host HG increased lethality by day 7 of infection (Figure 7C, Figure 7D). In the control group, all vehicle-treated mice survived, and AMX-treated mice in the high dosage groups (1×10^4 and 1×10^5) experienced 75 and 50 percent survival respectively (Figure 7C). In the STZ group, vehicle-treated mice in the highest dosage groups

(1×10^5 and 1×10^6) had 75 and 40 percent survival, while the AMX-treated mice experienced between 25 to 80 percent survival with lethality events starting as early as 24 hours (Figure 7D).

To check for any significant differences in GI physiology or immunocompetence, we assessed GI edema and inflammation between HG and control mice (Figure S5B). We saw no differences in GI physiology, but we noticed slight differences in some serum cytokines (Figure S5C-I). For IL-1 α , IL-6, and IL-12p70, variation was between vehicle-treated mice and may represent progression of the STZ model rather than responses to infection. For GM-CSF, IFN- β , IL-10, and IL-17A, plasma concentrations are only elevated in HG AMX-treated mice after infection and thus may be the result of differential susceptibility (Figure S5C-I).

Infection with *S. enterica* represents another form of microbiome dysbiosis in conjunction with ATBs. Thus, we profiled the fecal microbiome during the first 4 days of infection to assess if HG worsened infection-related dysbiosis (Figure 7E-G, Figure S5J-L). The initial infection significantly impacted microbiome β -diversity (Figure S5). However, diversity remained divergent in accordance with pre-infection experimental treatment (Figure 7E). This indicates that regardless of infective dose, the microbiome changes induced by STZ or AMX remain the drivers of β -diversity. Interestingly, we noticed that only HG mice experienced a significant reduction in α -diversity (Figure S5K). During the 4-day period following infection, *Salmonella* expansion was only detected in AMX-treated animals (Figure 7F). We then quantified the difference in *Salmonella*- reads between control and HG mice after AMX and found that HG mice had notably higher levels of *Salmonella* (Figure 7G). Together, these data suggest that the combination of STZ and AMX severely reduces the probability of survival after *S. enterica* challenge and increases pathogen burden and microbiome dysbiosis relative to NG controls. It is possible that the enrichment of favorable metabolites or change in respiratory potential in HG AMX-treated

communities promotes the expansion and virulence of *S. enterica*, although more work is required to confirm this hypothesis.

Discussion

Recent estimates of HG global prevalence suggest that metabolic disruption occurs in approximately ten percent of all people, with incidence increasing annually (Saeedi et al., 2019). Thus, understanding how host metabolism impacts ATB-induced dysbiosis is key to the development of microbiome-protective therapeutic strategies. To address this knowledge gap, we used an integrated multi-omic strategy to examine how HG modifies the microbiome's response to AMX. Specifically, we combined WMGS, metatranscriptomics, and untargeted metabolomics to examine differences in microbiome composition and function both pre- and post-ATB treatment and characterized the severity of dysbiosis-related complications like enteric infection.

A key goal of this study was to profile the impact of altered host metabolism, and the microbiota-accessible metabolite pool, on microbiome function during ATB treatment. Since dietary modulation has inherent limitations involved in restructuring microbiome composition, we opted for a rapid-chemotherapeutic method to perturb the GI metabolite pool. We chose STZ, in part, due to its widespread use and quick onset of changes. However, it is critical to address limitations of the model as it does not perfectly replicate the pathology of clinical HG. STZ has been used to replicate both type-I and type-II diabetic phenotypes in animals since the mid-1960s (Deeds et al., 2011; Eleazu et al., 2013). Models of STZ administration vary widely in their dosage concentration, injection frequency, and inclusion or exclusion of high-fat feed typically due to differences in research goals (Deeds et al., 2011; Furman, 2021). Because STZ does not perfectly mimic type-II diabetes, the inclusion of a high-fat feeding period before injection was recently

proposed as a method to induce hyperinsulinemia and insulin resistance in STZ-treated animals (Furman, 2021; Chao et al., 2018). Regardless, STZ consistently induces the characteristic symptoms of HG, insulin deficiency, polydipsia and polyurea (Furman, 2021; Kolb, 1987). Although there is conservation of immunological responses to β cell ablation (Eleazu et al., 2013), one must consider that microbiome-related phenotypes derived from STZ-induced HG are likely specific to the sub-model and may not readily translate across studies. For example, the only taxonomic changes we found after STZ treatment were the expansion of *A. muciniphila* and collapse of *Blautia* sp YL58. This contrasts with the many taxonomic shifts seen in existing work examining STZ-treated rats, but this may be due to inherent differences between mice and rats, use of multiple STZ doses, sample collection, sequencing depth, use of a diet in combination with STZ, or the time-frame of weeks rather than days (S. Liu et al., 2019; Ma et al., 2020; Patterson et al., 2015; Yin et al., 2020).

Interestingly, serum metabolomics in multiple low-dose STZ treated mice found enrichment of AAAs, bile acids, dipeptides, fatty acids, nucleotides, sphingolipids, and vitamins (Ugarte et al., 2012). These results are congruent with our pre-AMX metabolomics data and may represent true HG-related changes. Metabolomic studies focused on pre-diabetic patients have found shifts in AA catabolism as a potential biomarker of progression to type-I diabetes, and spikes in both aromatic and branched-chain AA as predictive of type-II diabetes (T. Wang, et al., 2011; Neis et al., 2015), supporting our observed AA changes as a true HG phenotype. A potential explanation for this enrichment is that fiber use within the GI impacts the production of several AA-based metabolites by members of the Firmicutes phylum (Neis et al., 2015; Tanes et al., 2021), suggesting an intrinsic link between metabolic dysregulation and shifts in gut AA metabolism.

We found that STZ initiated a cascade of changes related to fiber and SCFA generation. Specifically, the loss of SCFA-producing Firmicutes may perturb syntrophic reactions involved in fiber-fermentation (Bui et al., 2016; Oliphant and Allen-Vercoe, 2019; Rey et al., 2010; Vacca et al., 2020). Because the microbiome is responsible for this fermentation (Holscher, 2017), we anticipate that disturbances in polysaccharide processing are microbially-driven rather than host-derived. In the case of polyphenol substrates and metabolites, bacteria can coopt and liberate sugars from these compounds for use in their own metabolism (Fraser and Chapple, 2011; Braune and Blaut, 2016; Moore et al., 2002; M. Wang et al., 2019; Lundgren and Thaiss, 2020; Vollmer et al., 2018) For example, some taxa can directly utilize flavones as a carbon source, fueling them into their respiratory cycle (Burlingame and Chapman, 1983). Thus, shifts in the abundance of dietary-derived polyphenols could modify microbial metabolism in GI.

Reduced fiber use by the microbiota may be partially explained by a side-effect of STZ treatment. Rodents receiving a multiple low-dose regime (i.e. 50 mg/kg/day for 5 days) of STZ exhibit an initial reduction in food consumption (Motyl and McCabe, 2009). However animals exhibit hyperphagia one week post-injection (Motyl and McCabe, 2009; M. Zhang et al., 2008). It is possible that our experimental time point for AMX administration and sample collection (3 and 4 days-post injection, respectively) is associated with reduced food intake, which would lower the availability of fiber. Regardless, reduced fiber and polyphenol intake has been recognized as a form of dysbiosis, increasing susceptibility to bactericidal ATBs via modification of microbial metabolism (Cabral et al., 2020; 2019; Makki et al., 2018; Ng et al., 2019), and we propose that a similar disruption of the microbiome occurs here.

We observed that the HG microbiome was enriched for transcripts and metabolites involved in pyruvate metabolism and glycolysis. It is likely that the overall enrichment of AA

catabolism directly contributes to increased community respiration because many of the observed AAs are glucogenic (Berg, 2002). A key consideration of any ecological network is its taxonomic composition (Coyte and Rakoff-Nahoum, 2019). Polymicrobial interactions are a significant component of the microbiome's ecology and changes to taxonomic structure or function will directly impact the overall activity (Coyte and Rakoff-Nahoum, 2019; Layeghifard et al., 2017; Boon et al., 2014). Because Firmicutes have been characterized to perform a bulk of AA, nitrogen, and sulfur metabolism reactions within the GI, it is possible that these taxa are driving the increased metabolic rate. This may prime the microbiome as a whole for increased AMX susceptibility, but more work is needed to confirm this hypothesis (Bernal et al., 2007; Böttcher et al., 2014; Gao et al., 2018; Meadows and Wargo, 2015). Overall, these data make a strong argument for the degree of control that changes in the baseline function of the microbiome have on compositional restructuring after ATB perturbation.

When comparing HG and NG communities during and after AMX treatment, the increased dysbiosis in HG mice was expected given both the increased basal metabolic rate and the elevation of simple sugars and PTS activity during AMX exposure. Increased sugar availability and decreased polysaccharide utilization have been demonstrated to potentiate ATB toxicity within the GI (Cabral et al., 2019; 2020). The most striking finding to us was how divergent the transcriptional behavior of *B. theta* was between hosts. We previously identified that polysaccharide fermentation by *B. theta* functions as an amoxicillin tolerance response in NG animals (Cabral et al., 2019). However, this study complicates that understanding, as STZ-specific reductions in *B. theta*'s polysaccharide and mucus foraging suggests that these may not be universal amoxicillin tolerance responses. There may be non-mucosal or non-polysaccharide metabolite species that induce a protective phenotype to members of the *Bacteroides* genus.

Alternatively, members of this genus possess β -lactamases, and differences in the expression of these resistance genes may be involved in the observed enrichment of *Bacteroides* in HG AMX-treated mice (Edwards, 1997). Regardless, reduction in fiber fermentation by *Bacteroides* disrupts the balance of nutrients available for syntrophic metabolism with Firmicutes and Actinobacteria (Fischbach and Sonnenburg, 2011). These changes may induce a proinflammatory state and contribute to the increased dysbiosis experienced by HG mice during ATB exposure. Given the total ecological complexity of the gut microbiome, a more robust understanding of cross-feeding networks will be integral to the full characterization of a given perturbation's impact on the microbiome.

Lastly, we examined if the increased severity of AMX toxicity in HG mice would increase susceptibility to enteric infection. Overall, HG AMX-treated animals had both increased susceptibility to *S. enterica* and reduced overall survival after one-week of infection (Figure 7). Recent work by Thaiss et al. has shown that decreased barrier function caused by STZ increases *S. enterica* susceptibility (Thaiss et al., 2018). However, this study used a multiple-dose STZ model and did not infect mice until a few weeks after STZ treatment, thus these results may not translate to our study. For example, we found that, at low infective doses, STZ treatment had no impact on susceptibility in the absence of ATBs. Thus, it is possible that the HG ATB co-treated microbiome is structurally, functionally, and metabolically perturbed in a way that promotes pathogen colonization and expansion. For example, we found enrichment of multiple ethanolamines, which are a carbon source that cannot be used by the microbiota but can be utilized by *Salmonella* (Anderson et al. 2015; Srikumar and Fuchs, 2011; Thiennimitr et al., 2011). *S. enterica* has flexible metabolism compared to the bulk of the microbiota (Taylor and Winter, 2020), and can use non-accessible carbon sources like ethanolamines to promote colonization and

niche adaptation in mammals (Anderson et al. 2015). Other metabolites that may have impacted *S. enterica* infection severity include acetyl-maltose, as *Salmonella* are equipped with tightly controlled maltose import systems and readily fuel this carbon source into their respiratory cycle (Erhardt and Dersch, 2015; Jain et al., 2020; Miller et al., 2013). Another metabolite of interest was pantetheine, which *Salmonella* can shunt into its CoA synthesis, potentially providing a fitness advantage through competitor exclusion (Ernst and Downs, 2015) (Table S1). An alternate explanation for the increased expansion of *Salmonella* is an overall increase in ATB-induced intestinal oxygenation. *Salmonella* are facultative anaerobes and can readily switch to aerobic respiration when needed (Rhen, 2019). Additionally, *Salmonella* can use inflammation-related metabolites like tetrathionate as terminal electron acceptors, and can coopt the oxygenated and inflamed gut for growth (Winter et al., 2010). Although more work is required to parse what components of the HG microbiome provide a competitive advantage to *Salmonella* after AMX treatment, our data provides strong preliminary evidence that STZ-induced HG can directly impact the acute consequences of ATB dysbiosis. Ultimately, our study shows that host-related physiology and metabolic state must be a key consideration of any current and future therapeutic strategy aimed at mitigating ATB-induced microbiome damage.

Limitations of the Study. While our multi-omic approach robustly characterizes the cecal microbiome during dysglycemia and ATB perturbation, there are limitations in the study design and methodology that complicate the interpretation of the results. First, our study exclusively uses male mice. Female mice are partially resistant to STZ-induced HG and require significantly higher doses and (or) repetitive dosing regimens compared to males to induce a metabolic phenotype (Deeds et al., 2011; Goyal et al., 2016). An additional consideration is that STZ's mechanism of

action involves organ cytotoxicity (Deeds et al., 2011). Although STZ is rapidly eliminated from the host, it is nearly impossible to guarantee that off-target effects of pancreatic toxicity are not contributing to some microbiome phenotypes.

A key consideration of our metagenomic and metatranscriptomic-reliant analyses is the dependence on existing databases that possess annotation-based limitations and the need for imperfect alignment algorithms (Consortium, 2012). While WMGS provides increased resolution over 16S rRNA sequencing, the taxonomic classification of sequencing reads is still subject to currently available reference genomes, which are biased towards some taxa over others (Consortium, 2012; McLaren et al., 2019). Further, WMGS data is complicated by the fact that taxonomic levels are reported as relative abundances. Even metabolomic-focused pipelines like MIMOSA are limited by their reference databases. Specifically, full reaction annotations within the KEGG database are required for this pipeline (Noecker et al., 2016).

For untargeted metabolomics, ion annotation is still considered the primary bottleneck of analysis (Gertsman and Barshop, 2018; Schrimpe-Rutledge et al., 2016). The diversity in chemical modification, polarity, solubility, and ionization of chemical structures from complex biological samples often requires multiple analytical modes (i.e. positive versus negative ion mode) to be run in order to characterize all structures, and that can subsequently complicate ion identification (Gertsman and Barshop, 2018; Lei et al., 2011; Luan et al., 2019). While metabolomics offers a powerful examination of the small molecule repertoire of the cecum, it does not distinguish between bacterially-derived, fungal-derived and host-derived metabolites (Gertsman and Barshop, 2018). While pairing these data with metatranscriptomics and using networking models like MIMOSA helps improve inference of metabolite origin it does not eliminate the possibility of host-derived metabolites being mistaken for bacterially derived compounds and vice versa.

Additionally, our metabolomics preparation is unable to separate intracellular from extracellular-derived metabolites, potentially complicating biological interpretations. Ultimately, further work will be required to correlate STZ and AMX-induced metabolomic changes with individual taxa, and greater annotation of metabolic syntrophy in the gut will aid in the biological interpretation of subsequent metabolomic analyses.

Acknowledgements

P.B. was supported by the U.S. Department of Defense through the Peer Reviewed Medical Research Program (W81XWH-18-1-0198), the National Institute of General Medical Sciences (P20GM121344), and the National Institute of Diabetes and Digestive and Kidney Diseases of the National Institutes of Health (R01DK125382). J.I.W. and S.P. were supported by the National Science Foundation Graduate Research Fellowship (1644760). This study made use of the Research Histology, Pathology, and Imaging core supported by the DHHS/NCI Cancer Center (P30CA16672) and computational resources from the Center for Computation and Visualization at Brown University. The funding agencies had no role in the study design, data collection, analysis, or interpretation. The opinions and interpretations presented here are not representative of the standing of the funding agencies.

Author Contributions

Conceptualization: J.I.W and P.B.; Methodology: J.I.W. and P.B.; Formal Analysis: J.I.W., D.V.G., and K.N.; Investigation: J.I.W., R.L.P., C.E.B, S.P., D.V.G., K.N., W.H.S., and M.M.S.; Data Curation: J.I.W.; Writing- Original Draft: J.I.W., D.V.G., and P.B.; Writing- Review and

Editing: J.I.W., R.L.P., S.P., D.V.G., R.A.Q., and P.B.; Visualization: J.I.W; Supervision: R.A.Q. and P.B.; Funding Acquisition: P.B.

Declarations of Interests

The authors declare no competing interests.

Materials and Methods

Resource Availability

Lead Contact

Further information and requests for resources and reagents should be directed to and will be fulfilled by the Lead Contact, Peter Belenky (peter_belenky@brown.edu).

Materials Availability

This study did not generate new, unique reagents.

Data and Code Availability

- Illumina sequencing read data have been deposited at the NCBI Short Read Archive (SRA) under the BioProject Accession numbers PRJNA720755 (16S rRNA reads) and PRJNA72012 (WMGS and metatranscriptomic reads), and are publicly available as of the date of publication. LC-MS/MS and GNPS data have been deposited to massive.ucsd.edu (MSV000087093) and gnps.ucsd.edu (<https://gnps.ucsd.edu/ProteoSAFe/status.jsp?task=e4efce0c33fb4ada96e373d53460f2d5>) and are publicly available as of the date of publication.
- This paper does not report original code.
- Any additional information required to reanalyze the data reported in this paper is available from the lead contact upon request.

Experimental Model And Subject Details

Animal Housing

Experimental procedures involving mice were conducted in accordance with protocols approved by the Institutional Animal Care and Use Committee (IACUC) of Brown University. Five-week-old male C57BL/6J mice were purchased from the Jackson Laboratories (Bar Harbor, ME, USA) and given a two-week habituation period immediately following their arrival at Brown University. All animals were cohoused together in specific-pathogen-free (SPF), temperature controlled (21 ± 1.1 °C), and 12-hour light/dark cycling conditions within Brown University's animal care facility, while being fed a standard chow (Laboratory Rodent Diet 5001, LabDiet, St. Louis, MO, USA). After habituation, mice were randomized into new cages to reduce potential cage effects.

Bacterial Strains

S. enterica Typhimurium SL1344 (GFP⁺, Amp^R) was generously donated by Dr. Venessa Sperandio (University of Texas, Southwestern). Cells were grown at 37°C under shaking aerobic conditions in Luria-Bertani (LB) broth containing ampicillin (100 µg/mL). Colony forming units (CFU) were quantified on LB agar plates containing ampicillin (100 µg/mL). Because *S. enterica* Typhimurium SL1344 constitutively expresses green-fluorescent protein, CFU counts were confirmed by UV-imaging using the ChemiDoc Imaging System (Bio-Rad, Hercules, CA, USA).

Method Details

Animal Experiments

All animal work was conducted in accordance with protocols approved by the Institutional Animal Care and Use Committee (IACUC) of Brown University. To induce HG, 7-week-old male C57BL/6J mice were fasted for 4-6 hours, then given an intraperitoneal injection of either Na-Citrate buffered streptozotocin (STZ) (150 mg/kg, pH 4.5) or a Na-Citrate sham (pH 4.5). All mice

were given overnight supplementation of 10% sucrose water to avoid post-procedural hypoglycemia. Sucrose water was then replaced with standard filter-sterilized water the following morning. Two days post-injection, fasting blood glucose was assessed in all mice using the CONTOUR®NEXT blood glucose monitoring system (Bayer AG, Whippany, NJ, USA). Mice with HG (fasting blood glucose ≥ 250 mg/dL) were selected for subsequent ATB treatment along with NG controls. 24-hours after glyceemic assessment, all mice were randomized again to reduced potential cage effects and given either amoxicillin (25 mg/kg/day) or a pH-adjusted vehicle via filter-sterilized drinking water *ad libitum* for 24 hours (Cabral et al., 2019). Mice were subsequently sacrificed and dissected to collect blood, tissues, and cecal contents. Cecal contents were weighed then divided to be processed according to their downstream application (nucleic acid extraction, Q-TOF-MS, or LC-MS/MS). Exact processing methods are described in each application section below.

The 16S ribosomal RNA sequencing, whole metagenome sequencing, metatranscriptomic sequencing, metabolomics, and infection studies are the result of independent biological replicates conducted several months apart from one another. The 16S rRNA sequencing results were derived from two independent animal experiments performed in 2017 and 2018. Whole metagenomic sequencing results were derived from two independent animal experiments performed in 2018 and 2019. Metatranscriptomic results were paired from respective metagenomic samples. Metabolomics data were acquired from a separate animal experiment performed in 2020. Finally, infection data were acquired from two independent animal experiments performed in 2020 and 2021.

Multi-omic Analysis: Pipelines/Purpose/Scope

Our multi-omic approach to microbiome analysis features the combinatory usage of the *Kraken2* and *Bracken* annotation pipelines for whole metagenomic sequencing (Lu et al., 2017; Wood et al., 2019), and the *HMP Unified Metabolic Analysis Network* (HUMAN2) (Franzosa et al., 2018) and *Simple Annotation of Metatranscriptomes by Sequencing Analysis* (SAMSA2) pipelines for metatranscriptomics (Westreich et al., 2018). Combined utilization of these pipelines facilitates examination of species-level taxonomic shifts (Kraken2/Bracken), community-level changes in transcript abundances (SAMSA2) and community-level gene expression that is normalized to the abundance of each taxon (HUMAN2). We also used the pipeline developed by Deng et al. (Deng et al., 2018) to examine species-level transcriptional responses to STZ and amoxicillin challenge for high-abundance and transcriptionally active members of the microbiota.

Sequencing pipelines were used in conjunction with both *quadrupole flow injection electrospray time-of-flight mass spectrometry* (Q-TOF-MS) (Fuhrer et al., 2011) and *liquid chromatography tandem mass spectrometry* (LC-MS/MS) paired with spectral annotation and networking analysis via the *Global Natural Products Social Metabolic Network* (GNPS; <http://gnps.ucsd.edu>) (M. Wang et al., 2016). While recent advances in mass spectrometry methods have vastly increased the range and accuracy of metabolite detection, no single analytical method is currently capable of capturing the entirety of small molecules in a complex biological sample (Luan et al., 2019). Thus, we opted to increase our metabolite coverage through the combinatory use of a tandem (LC-MS/MS) and a high-resolution (Q-TOF-MS) method (M. X. Chen et al., 2019). The Q-TOF-MS data is presented at the metabolite level where unknown features are ignored. For pathway-level comparisons, available Kyoto Encyclopedia of Genes and Genomes compound identifiers were used to perform Pathway Activity Profiling (Aggio et al., 2010) of known features (Figure S1E, Table S3). A deeper metabolome analysis including unknown

molecules or related metabolites to known compounds is presented with the and data originating from our LC-MS/MS dataset using GNPS cluster identification.

Finally, integration of transcriptomic (HUMAN2) and metabolomic (Q-TOF-MS) data was performed using the R implementation of *Model-based Integration of Metabolite Observations and Species Abundances* (Noecker et al. 2019). This software calculates the potential metabolic capacity of a microbiome by examining which enzymatic reactions are present in a community (i.e., the sum of all synthetic and degradation machinery present). This output is then compared against observed metabolite variations from KEGG-annotated metabolomics data.

Nucleic Acid Extraction & Purification

For nucleic acid extraction, cecal contents were transferred to ZymoBIOMICS DNA/RNA Miniprep Kit (Zymo Research, Irvine, CA, USA) Collection Tubes containing DNA/RNA Shield. These tubes were then processed via vortex at maximum speed for 5 minutes to homogenize cecal contents, which were subsequently placed on ice until permanent storage at -80°C. Using the parallel extraction protocol as per the manufacturer's instructions, the ZymoBIOMICS DNA/RNA Miniprep Kit was used to isolate total nucleic acids (DNA and RNA) from cecal slurry. Total DNA/RNA were eluted in nuclease-free water and quantified using the dsDNA-HS and RNA-HS kits on the Qubit™ 3.0 fluorometer (Thermo Fisher Scientific, Waltham, MA, USA).

16S rRNA Amplicon Generation and Sequencing

The V4 hypervariable region of the 16S ribosomal RNA was amplified from extracted total DNA using the 515F and 806R barcoded primers published under the Earth Microbiome Project (Caporaso et al. 2012; Thompson et al., 2017). Amplicons were generated using Phusion high-

fidelity polymerase and the following cycling protocol: 98°C for 30 seconds initial denaturation, then 25 cycles of 98°C for 10 seconds (denaturation), 57°C for 30 seconds (annealing), and 72°C for 30 seconds (extension). This was followed by a final extension of 72°C for 5 minutes. Amplicon libraries were submitted to the Rhode Island Genomics and Sequencing Center at the University of Rhode Island (Kingston, RI, USA) for pair-end sequencing (2x250 bp) on the Illumina MiSeq platform using the 500-cycle kit with standard protocols. We obtained an average of $11,511 \pm 10,632$ reads per sample for sequences related to Figure 1 and Figure S1, and an average of $6,167 \pm 3,498$ reads per sample for sequences related to Figures 7 and S5.

16S rRNA Read Processing & Analysis

Raw reads underwent quality filtering, trimming, de-noising and merging using the R (version 3.5.0) package implementation of DADA2 (version 1.8.0) (Cabral et al., 2020; 2019; Callahan et al., 2016). The resulting ribosomal sequence variants underwent taxonomic assignment by using the *assignTaxonomy* function in DADA2 with the RDP Classifier algorithm with RDP training set 18 (Wang, Q., 2007). Both α (Shannon) and β (Bray-Curtis Dissimilarity) diversity were calculated using the R package phyloseq (version 1.24.2) (McMurdie and Holmes, 2013).

Metagenomic/transcriptomic Library Preparation

Libraries for metagenomics and metatranscriptomics were prepared as described in our recent work (Cabral et al., 2020). We prepared metagenomic libraries from DNA (100 ng) using the NEBNext® Ultra II FS DNA Library Prep Kit (New England BioLabs, Ipswich, MA, USA) and the > 100 ng input protocol as per the manufacturer's instructions, which generated a pool of fragments whose average size was between 250 and 500 bp. Meanwhile, we prepared

metatranscriptomic libraries from total RNA (≤ 1 ug) using a combination of the MICROBExpress kit (Invitrogen, Carlsbad, CA, USA), NEBNext® rRNA Depletion Kit for Human/Mouse/Rat (New England BioLabs, Ipswich, MA, USA), and the NEBNext® Ultra II Direction RNA Sequencing Prep Kit as per the manufacturers' instructions. This generated a pool of fragments with an average size between 200 and 450 bp. Both metagenomic and metatranscriptomic libraries were pair-end sequenced (2x150 bp) on the Illumina HiSeq X Ten platform, yielding an average of $1,464,061 \pm 728,330$ reads per metagenomic sample and $35,884,874 \pm 27,059,402$ reads per metatranscriptomic sample.

Metagenomic/transcriptomic Read Processing

Raw metagenomic and metatranscriptomic reads underwent trimming and decontamination using KneadData (version 0.6.1) as previously described (Cabral et al., 2020; 2019; McIver et al., 2018). Illumina adapter sequences were removed using Trimmomatic (version 0.36), then depleted of reads that mapped to C57BL/6J, murine mammary tumor virus (MMTV, accession NC_001503) and murine osteosarcoma virus (MOV, accession NC_001506.1) using Bowtie2 (version 2.2) (Bolger et al., 2014; Cabral et al., 2020; Langmead and Salzberg, 2012). Metatranscriptomic reads were additionally depleted of sequences that aligned to the SILVA 128 LSU and SSU Parc ribosomal RNA databases as previously described (Cabral et al., 2020; 2019; Pruesse et al., 2007).

Taxonomic Classification of Reads

We taxonomically classified trimmed and decontaminated metagenomic reads against a database of all completed bacterial, archaeal, and viral genomes contained within NCBI RefSeq using Kraken2 (version 2.0.7-beta, "Kraken2 Standard Database") with a k-mer length of 35 (Wood et

al., 2019). Bracken (version 2.0.0) was then used to calculate phylum- and species-level abundances from Kraken2 reports, and the R package phyloseq (version 1.28.0) was used to calculate α - and β -diversity metrics (Lu et al., 2017; McMurdie and Holmes, 2013).

We then performed differential abundance testing on species-level taxonomic assignments (Cabral et al., 2020; 2019). First, low-abundance taxa (< 1,000 reads in \geq 20% of samples) were removed, then differential abundance testing of filtered counts was performed with the DESeq2 package (version 1.24.0) using default parameters (Love et al., 2014). All p-values were corrected for multiple hypothesis testing using the Benjamini-Hochberg method (Benjamini and Hochberg, 1995). Features with an adjusted p-value of less than 0.05 were considered statistically significant.

Metatranscriptomic Analysis: SAMSA2

We used a modified version of the Simple Annotation of Metatranscriptomes by Sequences Analysis 2 (SAMSA2) pipeline to annotate trimmed and decontaminated metatranscriptomics reads as previously described (Cabral et al., 2020; 2019; Westreich et al., 2018). This modified pipeline involves implementation of the Paired-End Read Merger (PEAR) utility to generate merged reads and DIAMOND (version 0.9.12) aligner algorithm (Buchfink et al., 2014; J. Zhang et al., 2014) to generate alignments against RefSeq, SEED Subsystem, and CAZyme databases (Cantarel et al., 2009; Overbeek et al., 2014). The resulting alignments were subjected to differential abundance testing using DESeq2 (version 1.24.0) with standard parameters and Benjamini-Hochberg multiple hypothesis testing correction (Benjamini and Hochberg, 1995; Love et al., 2014). Features with an adjusted p-value of less than 0.05 were considered statistically significant.

Metatranscriptomic Analysis: HUMAnN2

We used the HMP Unified Metabolic Analysis Network 2 (HUMAnN2, version 0.11.1) pipeline to assess the impact of STZ-based HG and amoxicillin treatment on gene expression within the gut microbiome (Franzosa et al., 2018). We supplied the taxonomic profiles generated for each sample into the HUMAnN2 algorithm in order to assure consistent taxonomic assignment between paired samples (Segata et al., 2012; Cabral et al., 2020; 2019). Then, using HUMAnN2, we generated MetaCyc pathway abundances and used these to estimate community-level gene expression and normalized this to metagenomic abundance using the Witten-Bell method (Witten and Bell, 1991). Unstratified smoothed RPKM values were converted to relative abundances then analyzed using linear discriminant analysis as described (Cabral et al., 2020; 2019). This was performed with the LEfSe (version 1) toolkit hosted on the Huttenhower Galaxy server (Segata et al., 2011).

Single-species Transcriptomics

We performed transcriptional analysis at the individual species level using a modified version of the pipeline developed by Deng et al. (Deng et al., 2018). First, species whose metagenomic abundance was subjected to an interaction between host glycemia and ATB usage were selected. We then calculated total RNA read abundance for each of these species and performed transcriptional analysis only on those with 500,000 or greater reads per sample (Table S5). First, reads that mapped to candidate taxa were extracted from our metatranscriptomes using the BBSplit utility within BBMap (version 37.96) (Bushnell, 2014). Reads from *B. theta*, *O. valericigenes*, and *O. spp.* PEA192 were aligned to their corresponding reference genomes using BWA-MEM (version 0.7.15) (Cabral et al., 2020; H. Li and Durbin, 2010). Then, we used subread program

(version 1.6.2) command *featureCounts* was used to generate a count table from alignments, and this count table was assessed for differential abundance using DESeq2 (Liao et al., 2014; Love et al., 2014). All p-values were corrected for multiple hypothesis testing using the Benjamini-Hochberg method (Benjamini and Hochberg, 1995). Features with an adjusted p-value of less than 0.05 were considered statistically significant.

Metabolite Extraction & Annotation: Q-TOF-MS

For untargeted Q-TOF-MS metabolomics, cecal samples were flash frozen upon collection and stored at -80°C until extraction. To extract metabolites, flash-frozen samples were removed from -80°C and placed on ice. A 10-20 mg sample was taken and submerged in 300 µl of fresh-made LC/MS-grade acetone:isopropanol (2:1) extraction solvent, then homogenized via vortex two times for 15 seconds each at 4°C. Supernatant extraction solvent was transferred to a new tube and was placed at -80°C temporarily. The 300 µl wash and homogenization was repeated, and this supernatant was then added to the original aliquot. Combined samples underwent centrifugation at 4°C for 10 minutes at 13,500 x G. After centrifugation, supernatant was moved to a fresh microcentrifuge tube, sealed with parafilm, and placed on dry ice before immediate delivery to General Metabolics Inc. (Boston, MA, USA) where samples were stored at -80°C.

Extracted metabolites were quantified as described in Fuhrer et al. (Fuhrer et al., 2011) using flow injection Time-of-Flight mass spectrometry on the Agilent G6550A iFunnel Quadrupole Time-of-Flight mass spectrometer (Agilent, Santa Clara, CA, USA) equipped with a dual AJS electrospray ionization source operated in negative ion mode. Samples were injected at a flowrate of 0.15 mL/minute in a mobile phase containing isopropanol and water (60%:40% ratio) buffered in 1mM Ammonium Fluoride, 15nM HP-0921, and 5µM homotaurine. Mass spectra data

was recorded in 4 GHz high-resolution Ms mode at a rate of 1.4 spectra/second. We detected 714.3 ms/spectra and 9652 transients/spectra between 50 and 1000 m/z. Source operating parameters included a temperature of 225°C, drying gas rate of 11 L/min, nebulizer pressure of 20 psi, sheath gas temperature of 350°C and flow of 10 L/min. The source Vcap and Nozzle voltage were 3500V and 2000V. The ms TOF operating parameters include fragmentor, collision, RF peak-to-peak voltages of 350V, 0V, and 750V, respectively and the Skimmer was disabled.

Data processing and analysis was performed as described by Fuhrer et al. in Matlab (The Mathworks, Natick, MA, USA) using functions from the following toolkits: Bioinformatics, Statistics, Database, and Parallel Computing (Fuhrer et al., 2011). Ions were additionally referenced against the Human Metabolome Database in addition to KEGG. Data analyses were run on an automated embedded platform by General Metabolics Inc. then delivered upon run completion. Finally, Principal Coordinate Analysis was performed on ion intensities by using Bray-Curtis dissimilarity paired with PERMANOVA analysis using the phyloseq (version 1.26.1) R package and subsequently visualized in Prism GraphPad (version 9.0.2) (McMurdie and Holmes, 2013).

Metabolite Extraction & Annotation: LC-MS/MS

For untargeted LC-MS/MS metabolomics, cecal samples were placed into 300 µl of LMCS-grade methanol then supplemented with 600 µl of 70% cold LC-MS-grade methanol. Samples were homogenized via vortex for 5 minutes, then placed at 4°C for an overnight incubation. Following incubation, samples were subjected to centrifugation at 1000 x G for 3 minutes. 500 µl of the supernatant was moved to a sterile microcentrifuge tube and stored at -80°C for long-term preservation.

Samples were thawed and diluted 1:1 (v/v) in 50% methanol prior to LC-MS/MS. Liquid chromatography was performed using a Vanquish Autosampler (Thermo Scientific, Waltham, MA, USA) and an Acquity UPLC column (Waters, Milford, MA, USA). Mass spectrometry was performed using a Q Exactive® Hybrid Quadrupole-Orbitrap Mass Spectrometer (Thermo Scientific, Waltham, MA, USA) in positive ion mode. All analysis used a 5 μ L injection volume. Samples were eluted via water-acetonitrile gradient (98:2 to 2:98) containing 0.1% formic acid at a 0.4 mL min⁻¹ flow rate. RAW files were converted via GNPS Vendor Conversion and mined with MZmine (ver. 2.52) prior to submission for feature based molecular networking (Pluskal et al., 2010; Nothias et al., 2020). Briefly, MS1 and MS2 feature extraction was performed for a centroid mass detector with a signal threshold of 5.0×10^5 and 5.0×10^4 respectively. Chromatogram builder was run with an *m/z* tolerance of 0.02 Da or 7 ppm and a minimum height of 1.0×10^5 . Then, chromatograms were deconvoluted utilizing a baseline cut-off algorithm of 1.0×10^5 and a peak duration range of 0 to 1.00 minutes. Following this, isotopic peaks were then grouped with an *m/z* tolerance of 0.02 Da or 7 ppm and a retention time percentage of 0.1. The Join Aligner Module was then utilized with a 0.02 Da or 7 ppm *m/z* tolerance and a retention time tolerance of 0.1 minutes. Feature-based molecular networking on GNPS was performed with the following parameters: precursor and fragment ion mass tolerance 0.02 Da; minimum cosine of 0.7 and minimum matched peaks of 4, all others were defaults. Library searching was performed with the same parameters as described above.

Analysis of Q-TOF-MS Metabolite Data

Differentially abundant metabolites were identified using the DESeq2 package (version 1.22.2) with standard parameters (Love et al., 2014). All p-values were corrected for multiple hypothesis

testing using the Benjamini-Hochberg method (Benjamini and Hochberg, 1995). Features with an adjusted p-value of less than 0.05 were considered statistically significant. KEGG compound identifiers that were feature-matched by the Bioinformatics MATLAB toolkit were used to create a list of all KEGG IDs associated with differentially abundant metabolites. This list (and associated ion intensities) were used to perform KEGG pathway enrichment analysis using the PAPI R package (version 1.22.1) with standard parameters (Aggio et al., 2010). Pathways with an adjusted p-value of less than 0.05 were considered statistically significant.

To link our transcriptional data and metabolomics data, we used the R package implementation of Mimosa (version 2.0.0) and the publicly available KEGG reaction database (circa 2010) (Noecker et al 2016). The configuration table settings were as follows: *File1*) taxon-stratified output from HUMAnN2 based of KEGG Orthology annotation. *File2*) per-sample ion counts of differentially abundant Q-TOF-MS metabolites. *File1_type*) “taxon stratified KO abundance (HUMAnN2 or PICRUST/PICRUST2”. *Ref_choices*) PICRUST KO genomes and KEGG metabolic model. *metType*) KEGG compound ID. *data_prefix*) complete file path to the KEGG reaction database. *Vsearch_path*) complete file path to the vsearch executable (<https://github.com/torognes/vsearch>). The *run_mimosa2* function was used with standard parameters to calculate the community metabolic potential within each sample, score this against the input metabolite table, and calculate the level of metabolic variation attributable to individual taxa using a linear rank regression as described (Noecker, et al., 2016). All data tables produced by the *run_mimosa2* function were then exported and data visualization was performed in Prism GraphPad (version 9.0.2). “Positive” metabolites have observed abundances that match the predictive model. “Negative” metabolites are those whose observed abundance diverges from the predictive model.

Analysis of LC-MS/MS Metabolite Data

First, principal coordinate analysis was performed on ion intensities by using Bray-Curtis dissimilarity paired with PERMANOVA analysis. These analyses were performed using the phyloseq (version 1.26.1) R package and subsequently visualized in Prism GraphPad (version 9.0.2) (McMurdie and Holmes, 2013). Random forest classification models on treatment mouse treatment group were then generated using the randomForest (version 4.6-16) R package (Breiman, 2001). Variable importance plots from the models were used to identify metabolites that best contributed to group classification. Each metabolite feature of interest was then checked for annotation in GNPS, if not directly annotated from MS/MS library searching, the node of interest was identified in the molecular network and assessed for spectral similarity to other annotated nodes. This provided a molecular family annotation of each unknown cluster. Models classifying HG mice treated with amoxicillin and not treated with amoxicillin resulted in out-of-bag prediction error of 2.7%. Classification of nonHG treated with amoxicillin and not treated with amoxicillin resulted in out-of-bag prediction error of 6.25%. Classification of HG mice and nonHG mice, both treated with ATBs, resulted in out-of-bag prediction error of 7.96%. Classification of HG mice and nonHG mice, neither treated with ATBs, resulted in out-of-bag prediction error of 16.67%.

Cecal Glucose Assessment

Cecal glucose levels were assessed using the Abcam Glucose Detection Kit (Abcam, Cambridge, United Kingdom). First, cecal material was weighed out and resuspended in glucose assay buffer at a concentration of 100 mg/mL, then homogenized via vortex until no visible clumps were present. Samples were spun at maximum speed for 1 minute to pellet any residual debris, and 500

µl of supernatant was transferred to a Corning Costar Spin-X 0.22 µM centrifuge tube filter (Corning Brand, Corning, New York, USA). The costar tubes containing supernatant were spun via centrifugation at 15,000 x G for 10 minutes, after which up to 500 µl of flow-through was transferred to an abcam 10kD spin column to deproteinize the samples. Samples were again spun at 15,000 x G for 10 minutes and flow-through was quantified using the Abcam Glucose Assay kit as per the manufacturer's instructions.

Plasma Cytokine Profiling

Upon animal sacrifice, whole blood was collected via cardiac puncture and placed in a microcentrifuge tube containing up to 15µl of 1X heparin. Collection tubes were then spun via centrifugation at 13,000 x G for 10 minutes to isolate plasma. The plasma-containing supernatant was transferred to a new microcentrifuge tube and frozen at -80°C until ready to process. Once ready, samples were thawed on ice, split into a working aliquot and a re-frozen stock aliquot. The working aliquot was assessed for signatures of inflammation in mice using the LEGENDplex Mouse Inflammation Panel (13-plex) (BioLegend, San Diego, CA) flow cytometry kit as per the manufacturer's instructions. Samples were processed on the Attune NxT Flow Cytometer (ThermoFisher, Waltham, MA) and subsequently analyzed using the LegendPlex cloud software cool (BioLegend, San Diego, CA). This panel allows for simultaneous profiling of *IL-1α*, *IL-1β*, *IL-6*, *IL-10*, *IL-12p70*, *IL-17A*, *IL-23*, *MCP-1*, *IFN-β*, *IFN-γ*, *TNF-α*, and *GM-CSF*. Cytokine concentrations were compared across samples using Welch's ANOVA with Dunnett T3 test for multiple hypothesis testing. Only cytokines with a p-value < 0.05 were included in the manuscript discussion.

Lipocalin-2 Quantification

Cecal lipocalin-2 levels were assessed using the Mouse Lipocalin-2/NGAL DuoSet ELISA kit (R&D Systems, Minneapolis, MN). First, flash-frozen cecal contents were weighed and reconstituted into a freshly made working solution of 1X phosphate buffered saline (PBS) and 0.1% Tween 20 at a concentration of 100 mg/mL. This working solution was vigorously pipetted to aid in resuspension. Samples were mixed by vortex at max speed for at 5 minutes until fully homogenized, then spun via centrifugation at 12,000 rpm for 10 minutes. The supernatant was transferred to sterile microcentrifuge tubes and used as input for the DuoSet kit. Lipocalin-2 was quantified from these samples as per the manufacturer's instructions. Concentrations were compared across samples using Welch's ANOVA with Dunnet T3 test for multiple hypothesis testing.

GI Histopathology Assessment

During animal necropsy an approximate 1-inch section of the distal colon was collected and fixed in methacarn. Fixed tissues were incubated at room temperature for 24 hours, then washed twice with a 70% ethanol solution. Samples were placed in 70% ethanol and stored in a light-safe box at 4°C until ready to process. To process, tissues were transferred to histology cassettes, submerged in 70% ethanol, and submitted to the Molecular Pathology Core at Brown University. Core staff embedded the sample cassettes in paraffin, then sectioned the blocks at 4-5 μ M thickness. Tissues sections were mounted on microscopy slides and stained with hematoxylin and eosin. Stained slides were dried for 24 hours before being shipped to the University of Texas MD Anderson Cancer Center for pathology scoring.

Enteric Pathogen Challenge

Salmonella enterica serovar Typhimurium SL1344 was grown overnight in 5 mL Luria-Bertani (LB) broth supplemented with fresh-made ampicillin (100 µg/mL) and grown at 37°C. This culture was diluted 1:1000 into fresh LB+ampicillin (100 µg/mL) the morning of infections and grown until cells were approximately at mid-log phase (OD₆₀₀ = 0.3-0.4).

Rather than sacrificing animals after the 24-hours of amoxicillin treatment as outlined above (See *Animal Procedures*), animals were given an additional 48 hours of *ad libitum* amoxicillin within their drinking water followed by ATB-free filter-sterilized water for 24 hours. Subsequently, animals were moved to clean cages and placed under a 4-hour fast, at which point they were infected with an inoculum between 10² and 10⁶ cells/dose via oral gavage (volume ≤ 200 µl). Animals were transferred to clean cages and weighed daily throughout the course of pathogen challenge. Fecal samples were collected daily then resuspended in 1 mL of 1X PBS and homogenized via vortex at maximum speed for at least 5 minutes. Fecal slurry was then serially diluted and plated onto ampicillin-supplemented (100 µg/mL) LB agar plates and grown at 37°C for 24 hours. After growth, colonies were counted and the total colony forming units (CFU) were quantified per gram of feces to assess pathogen burden. To quantify non-intestinal *S. enterica* burden, fresh liver and spleen were collected during post-sacrifice necropsy, weighed, then placed into 1mL of 1X PBS, mixed via vortex for 5 minutes, serially diluted, and plated onto LB agar plates supplemented with ampicillin (100 mg/mL). CFUs were quantified 24 hours later.

During the course of infection, any animal that experienced a loss of ≥ 20 percent of total body weight was sacrificed as per our IACUC protocol. These qualified as “lethality events” and were logged accordingly.

Quantification and Statistical Analysis

Specific details of the statistical analyses for all experiments are outlined in the figure legends and Results section. Sample numbers represent biological replicates, and instances of technical replicates are specifically stated in corresponding figure legends. LEfSe (version 1.0) was used to analyze MetaCyc pathway abundance data generated by HUMAnN2 on the Galaxy web server using default settings (<http://huttenhower.sph.harvard.edu/galaxy>). Metatranscriptomic outputs generated by SAMSA2 and single-species sequencing, along with Q-TOF-MS abundances were subjected to differential abundance testing using the DESeq2 package (1.24.0) in R (version 3.5.2) under default parameters and included contrast:interaction comparisons (Love et al., 2014). All DESeq2 results were corrected using the Benjamini-Hochberg method (Benjamini and Hochberg, 1995) to account for multiple hypothesis testing and significance was considered when the adjusted p-value was below 0.05. LC-MS/MS Random Forest testing was conducted using the R package implementation (Breiman, 2001). Permutational ANOVA calculations were made using the vegan R package (version 2.5.2). ANOVA, unpaired T tests, and Mann-Whitney U tests were performed in Prism Graphpad (version 9.0) without sample size estimation.

Main Figures, Titles, and Legends

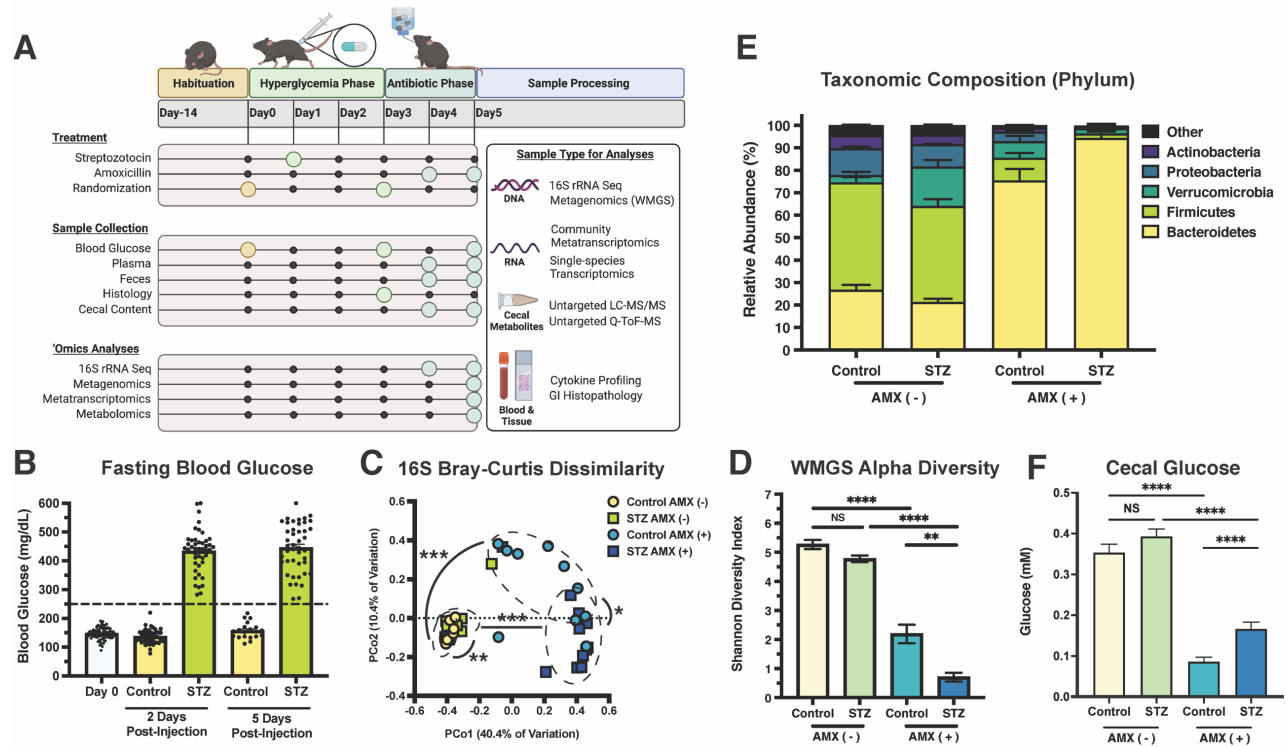


Figure 1. Streptozotocin modifies glucose levels and impacts microbiome composition after amoxicillin.

A. Experimental design of this study. Figure was created with BioRender.com (BioRender, Toronto, Canada).

B. Murine fasting blood glucose pre-STZ injection (Day 0), 2, and 5 days post-injection.

C. Bray-Curtis Dissimilarity between 16S rRNA amplicons.

D. α -diversity of WMGS experimental groups. Data represent mean \pm SEM.

E. Relative abundance of the five most-prominent bacterial phyla. Data represent mean \pm SEM.

F. Quantification of cecal glucose concentrations from experimental groups. Data represent mean \pm SEM.

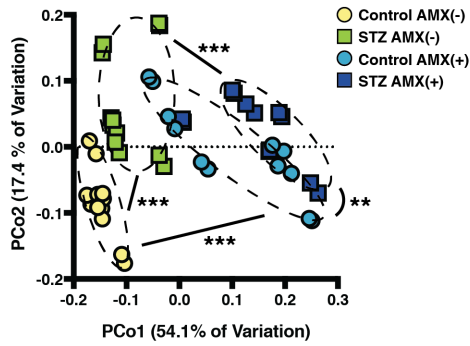
(* , $P < 0.05$; ** , $P < 0.01$; *** , $P < 0.001$; **** , $P < 0.0001$)

For B: N = 44 control and 44 STZ-treated samples per time point

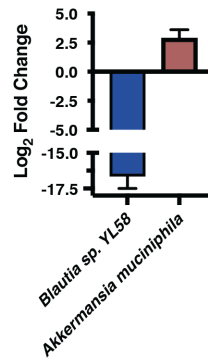
For C: N = 8 to 11 per group; permutational ANOVA

For D-F: N = 5 to 8 per group; Welch's ANOVA with Dunnett T3 test for multiple hypothesis testing

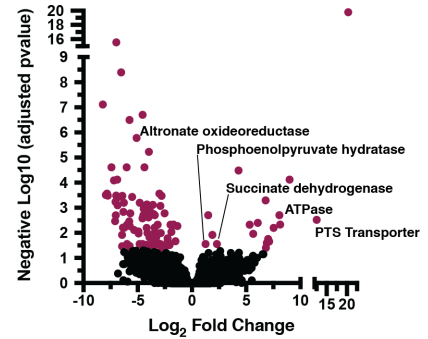
A Q-TOF-MS Bray Curtis Dissimilarity



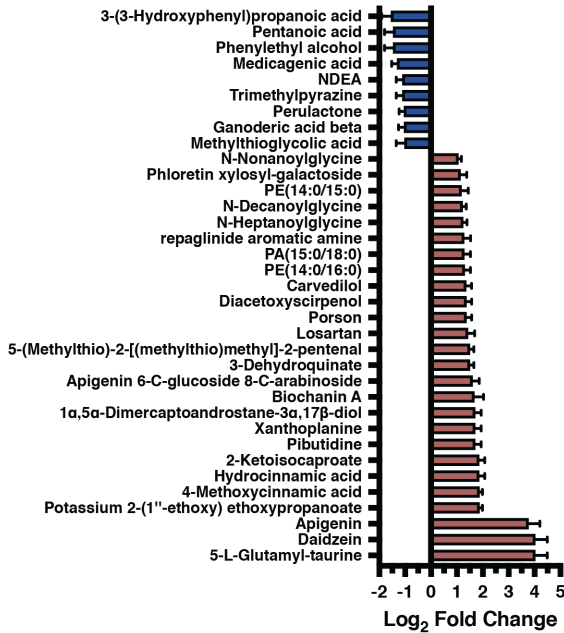
B Taxonomic Shifts



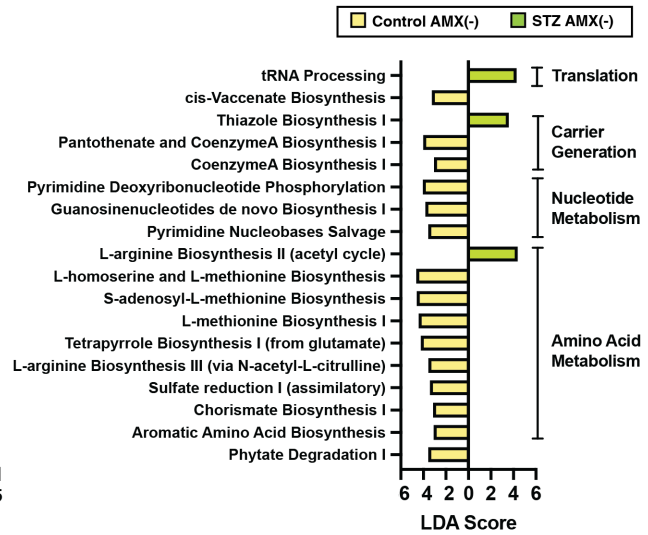
E RefSeq Transcript Abundance



C Q-TOF-MS Metabolite Enrichment



D MetaCyc Pathway Expression



F Community Metabolic Potential - Taxon Stratified

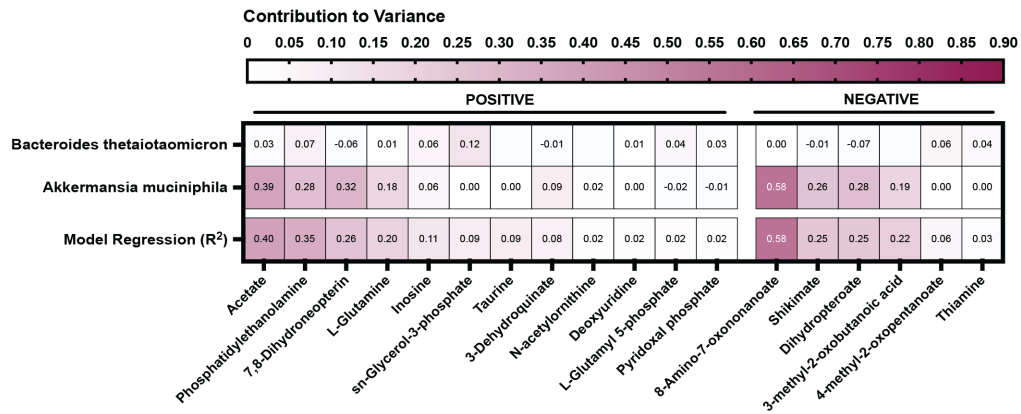


Figure 2. Streptozotocin modifies the cecal metabolome and metatranscriptome

- A. Bray-Curtis Dissimilarity of Q-TOF-MS extracts from experimental groups.
- B. Differentially abundant bacterial species following STZ treatment. Data represent \log_2 fold change \pm SEM versus NG controls.
- C. Differentially abundant Q-TOF-MS metabolites following STZ treatment. Data represent \log_2 fold change \pm SEM. See Table S1 for full results.
- D. Linear discriminant analysis of MetaCyc pathways following STZ treatment. See Table S6 for full results.
- E. Volcano plot of the cecal metatranscriptome following STZ treatment. Purple points represent differentially abundant transcripts. See Table S8 for full results.
- F. Taxon Stratified Community Metabolic Potential as calculated by MIMOSA. See Table S9 for full results.

(* , $P < 0.05$; **, $P < 0.01$; ***, $P < 0.001$)

For A & C: N = 6 per group, 2 replicates per sample

For B: N = 5 to 8 per group

For D-F: N = 4 per group

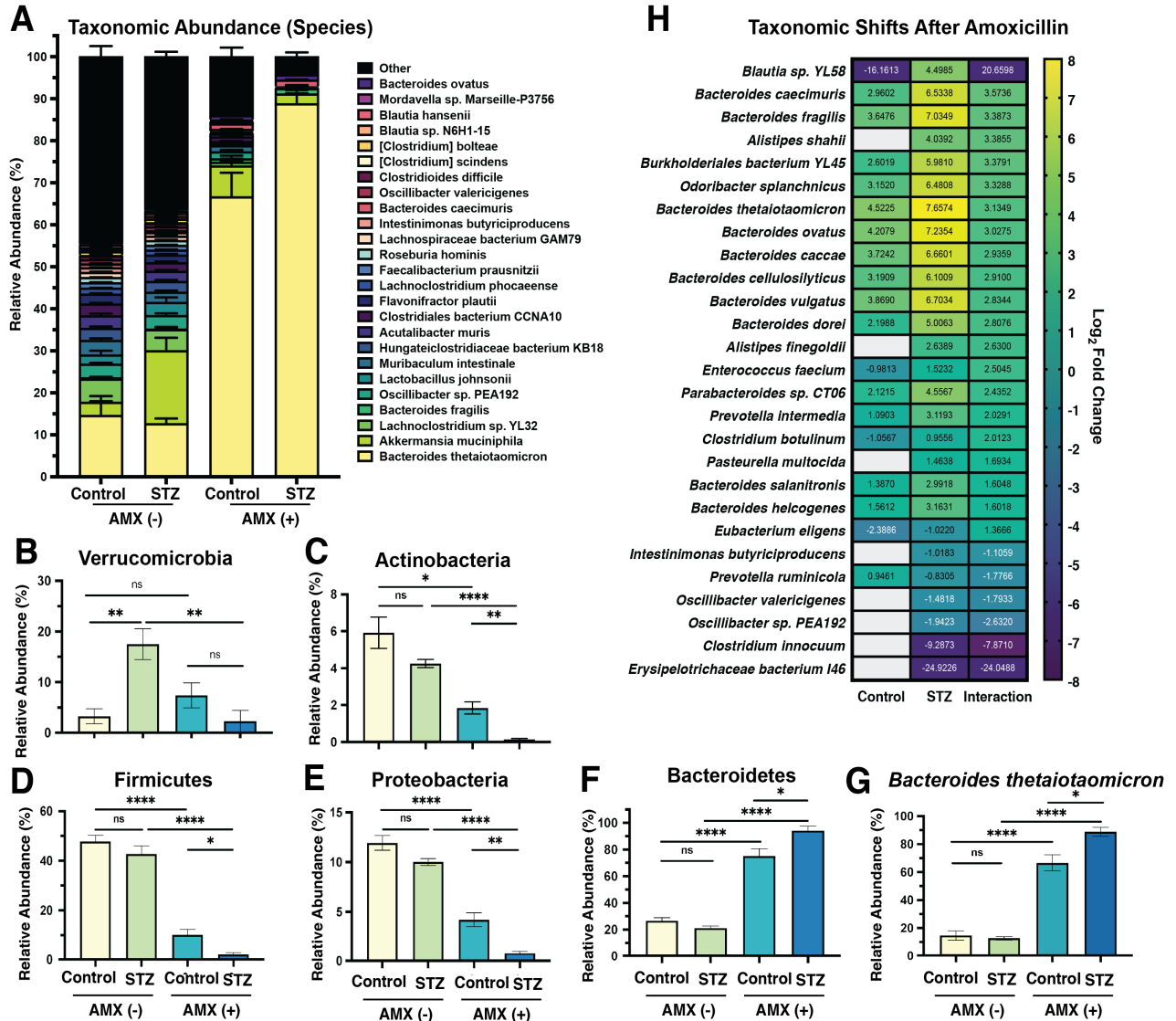


Figure 3. Streptozotocin and amoxicillin treatment modify the composition of the cecal microbiome.

- A. Relative abundance of the 25 most-abundant species in our data set. Data are represented as mean \pm SEM for each species.
- B. Relative abundance of Bacteroidetes.
- C. Relative abundance of Actinobacteria.
- D. Relative abundance of Firmicutes.
- E. Relative abundance of Proteobacteria.
- F. Relative abundance of Verrucomicrobia.
- G. Relative abundance of *B. theta*.
- H. Differentially abundant bacterial species following AMX treatment in control and STZ mice, with interaction value. Data represent log₂ fold change \pm SEM versus vehicle-treated controls.

For all panels: N = 5 to 8 per group.

For B-G: (*, P < 0.05; **, P < 0.01; ***, P < 0.001; ****, P < 0.0001; Welch's ANOVA with Dunnett T3 test for multiple hypothesis testing).

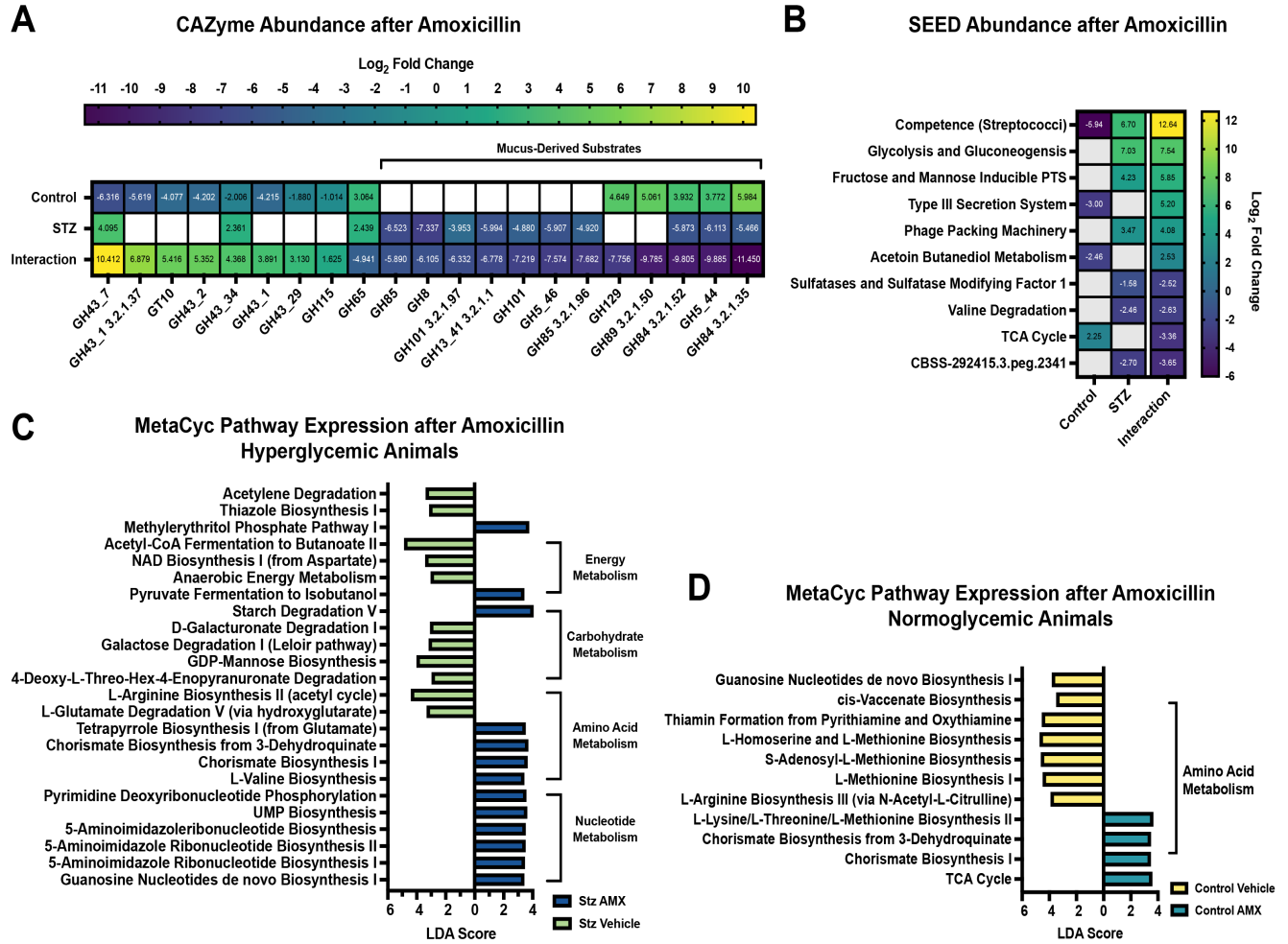


Figure 4. Amoxicillin differentially alters the cecal metatranscriptome.

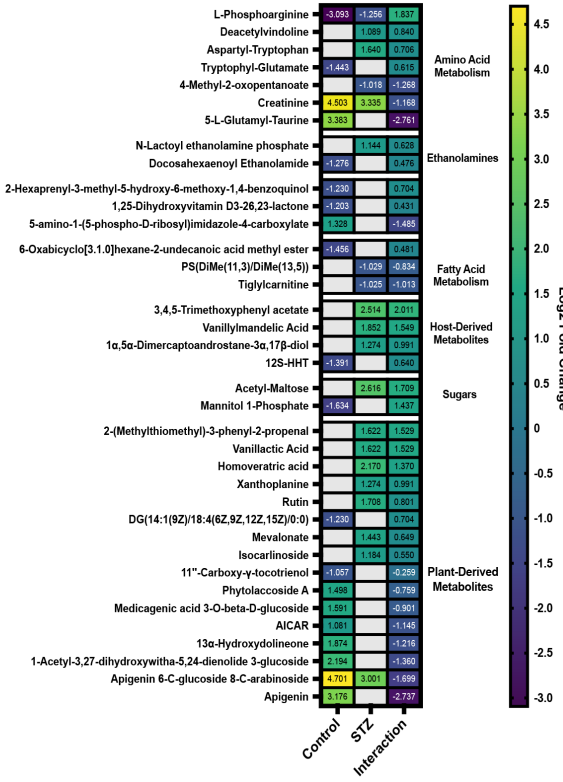
- Differentially abundant CAZyme transcripts in control and STZ mice after AMX, with interaction values. See Table S4 for full results.
- Differentially abundant level 3 SEED Subsystem transcripts in control and STZ mice after AMX, with interaction values. See Table S7 for full results.
- Linear discriminant analysis of MetaCyc pathways following AMX treatment in STZ mice. See Table S6 for full results.
- Linear discriminant analysis of MetaCyc pathways following AMX treatment in control mice. See Table S6 for full results.

For all panels: N = 4 per group

For A & B: Data represent log₂ fold change \pm SEM versus vehicle-treated controls. Blank panels are non-significant.

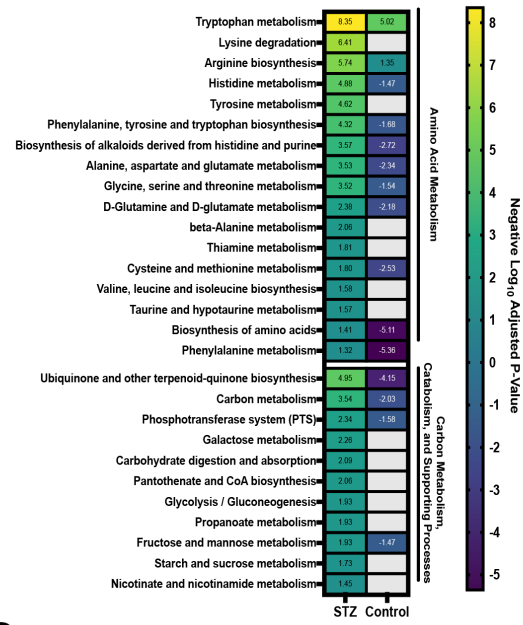
A

O-ToF-MS Metabolite Abundance after Amoxicillin



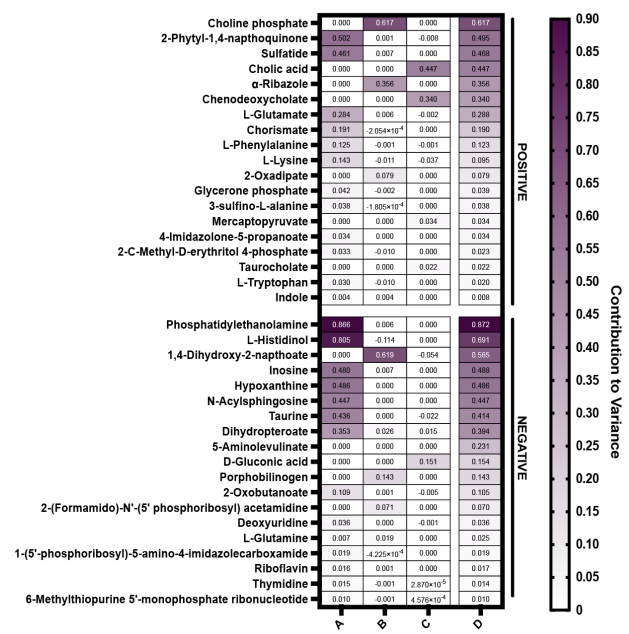
B

Metabolite Pathway Enrichment after Amoxicillin



C

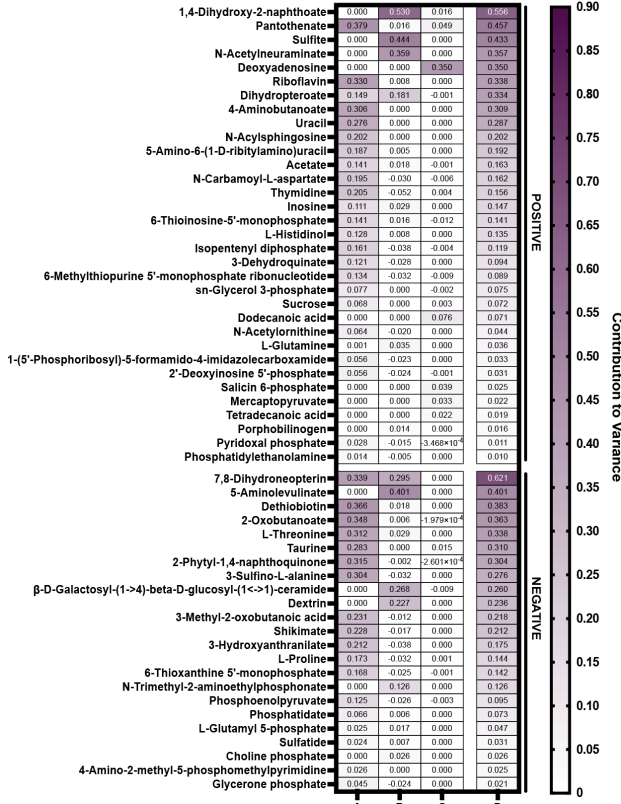
Community Metabolic Potential after Amoxicillin - Taxon Stratified (Control)



A = Bacteroides thetaiotaomicron
B = Akkermansia muciniphila
C = Lactobacillus johnsonii
D = Model Regression (R2 value)

D

Community Metabolic Potential after Amoxicillin - Taxon Stratified (STZ)



A = Bacteroides thetaiotaomicron
B = Akkermansia muciniphila
C = Lactobacillus johnsonii
D = Model Regression (R2 value)

Figure 5. Amoxicillin differentially alters the cecal metabolome.

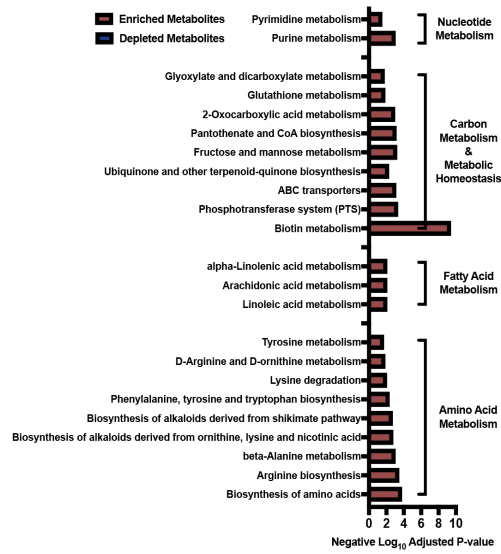
- A. Differentially abundant Q-TOF-MS metabolite features in control and STZ mice after AMX treatment with interaction value. Data represent \log_2 fold change \pm SEM versus vehicle controls. See Table S1 for full results.
- B. KEGG pathway enrichment of differentially abundant Q-TOF-MS metabolites in STZ mice after AMX treatment versus the enrichment score in control and AMX-treated mice. Blank panels represent a lack of statistical significance. See Table S3 for full results.
- C. Taxon Stratified Community Metabolic Potential of control mice after AMX treatment as calculated by MIMOSA. See Table S9 for full results.
- D. Taxon Stratified Community Metabolic Potential of STZ-treated mice after AMX treatment as calculated by MIMOSA. See Table S9 for full results.

For A & B: N = 6 per group, 2 replicates per sample

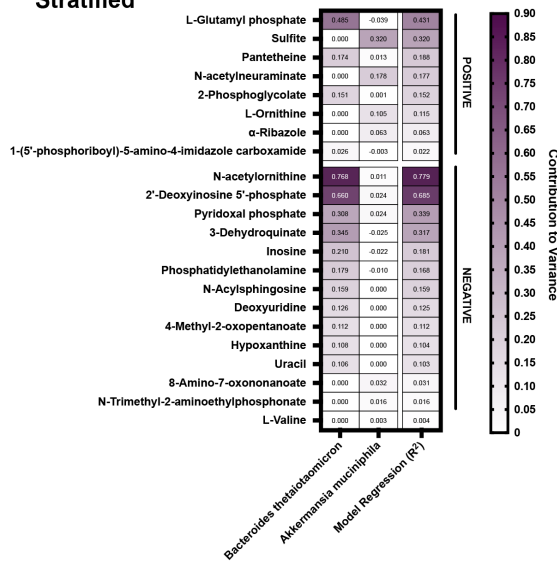
For C & D: N = 4 per group

For B: Significant = $p < 0.05$

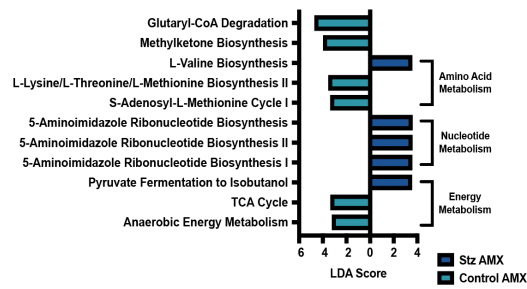
A Metabolite Pathway Enrichment



C Community Metabolic Potential - Taxon Stratified



B MetaCyc Pathway Expression



D B. thetaiotaomicron Gene Expression during Amoxicillin (STZ)

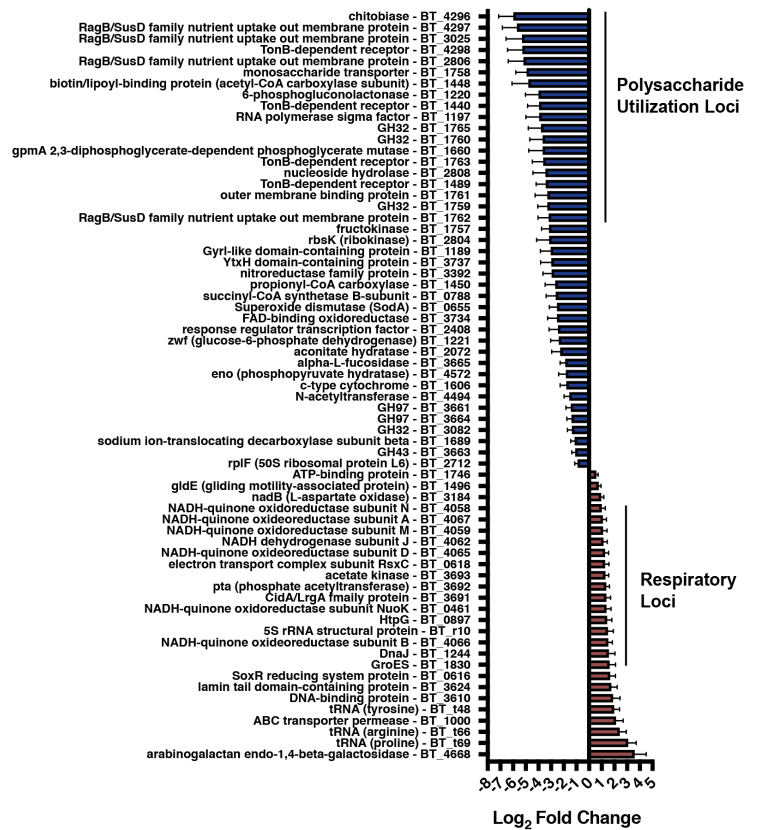


Figure 6. Streptozotocin treatment modifies transcriptomic and metabolomic responses of the microbiome to AMX.

- A. KEGG pathway enrichment of differentially abundant Q-TOF-MS features in STZ AMX (+) mice compared to control AMX (+) mice. See Table S3 for full results.
- B. Linear discriminant analysis score of MetaCyc pathways in STZ AMX (+) mice compared to control AMX (+) mice. See Table S6 for full results.
- C. Taxon Stratified Community Metabolic Potential of STZ AMX (+) mice compared to control AMX (+) mice as calculated by MIMOSA. See Table S9 for full results.
- D. Differentially abundant *B. theta* transcripts after AMX treatment in STZ mice. Data represent log₂ fold change ± SEM of STZ AMX (+) mice versus vehicle controls. See Table S5 for full results.

For A: N = 6 per group with 2 technical replicates per sample; Significant = p < 0.05

For B – D: N = 4 per group

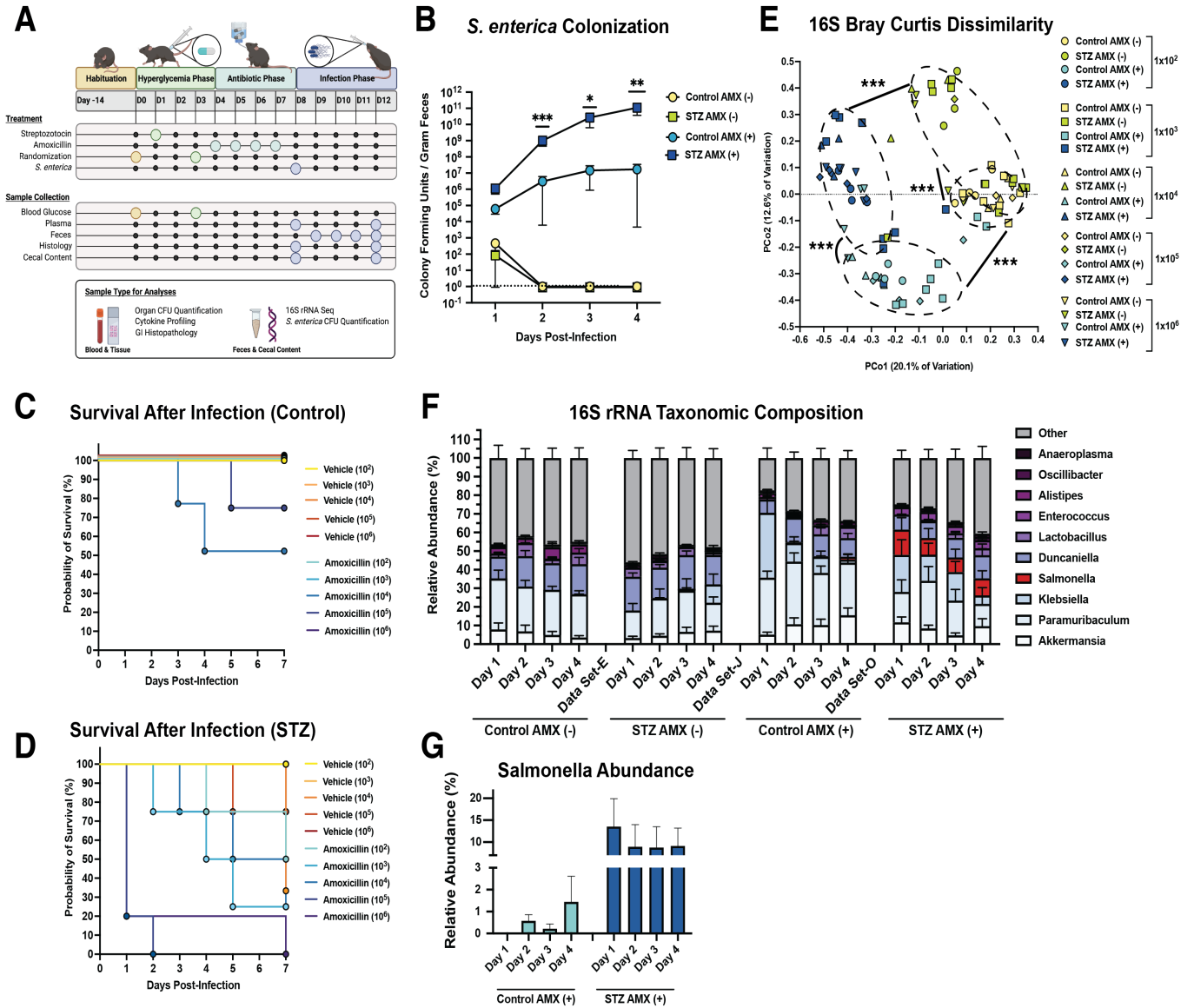


Figure 7. Streptozotocin and Amoxicillin increase susceptibility to *Salmonella enterica* infection.

- Experimental design of pathogen challenge study. Figure was created with BioRender.com (BioRender, Toronto, Canada).
- S. enterica* colony forming units (CFU) per gram of feces in control AMX(+/-), and STZ AMX(+/-) mice after infection with 1×10^3 cells. Data represent mean CFU \pm SEM.
- Kaplan Meier survival curve of NG mice.
- Kaplan Meier survival curve of STZ mice.
- Bray-Curtis Dissimilarity between 16S rRNA amplicons from experimental groups.
- Taxonomic composition of the fecal microbiome based of genus-level 16S rRNA identity between 1 and 4 days post-infection with 1×10^3 cells. Data represented mean \pm SEM.
- Contribution of *Salmonella* assigned reads in STZ AMX(+) and control AMX(+) mice 4 days post-infection. Data represent mean \pm SEM.

(*, $P < 0.05$; **, $P < 0.01$; ***, $P < 0.001$)

For B: $N = 8$ to 10 per group , Mann-Whitney U test of STZ AMX(+) vs Control AMX(+)

For C & D: $N = 4$ to 5 per group

For E – G: $N = 8$ to 10 per group

For E: permutational ANOVA

Supplemental Results

In addition to the results presented in the main-body text, we found that STZ treatment modified other significant macronutrient processing pathways that we will discuss here. Our LC-MS/MS dataset showed STZ-specific enrichment of dipeptides containing either aliphatic or AAAs (Figure S2C: Cluster 713, Cluster 676, Figure S2, Table S2). STZ treatment reduced the abundance of AA-related SEED transcripts, specifically sarcosine oxidase (the generation of N-methylglycine from choline) and selenoprotein processing which are involved in glycine metabolism (Sliwkowski and Stadtman, 1988) (Table S7). We also observed changes in sulfated AA metabolism, specifically reduced sulfur assimilation transcripts (Table S7) and pathway-level reductions in homoserine and methionine biosynthesis (Figure 2D, Table S6). Together, the enrichment of aliphatic AA catabolites and dipeptides, aromatic dipeptides, and arginine synthetic intermediates, coupled with reductions in transcripts related to glycine and sulfated AAs suggests that STZ treatment shifts branched-chain AA metabolism by the gut microbiota (H. Zhang et al., 2018).

STZ treatment was also induced significant dyslipidemia, as characterized by reductions in multiple fatty acid synthetic pathways including sphingolipids (Figure S2C: Clusters 1703, 30, and 2184, Table S2), linoleic, α -linoleic, arachidonic, and unsaturated fatty acids (Figure S2A, Figure S2B, Table S1, Table S3). Our LC-MS/MS data indicated STZ-related enrichment for long-chain fatty acid alcohols, phospholipids, and epoxide derivatives of linoleic acid (Figure S2C: Clusters 2803, 2721, 2851, 2759, Table S2). Coupled with transcriptional reductions in the expression of unsaturated fatty acid biosynthesis pathways like cis-vaccenate (Figure 2D, Table S6), these data suggest that STZ hampers both host and microbial fatty acid processing, likely

enriching for esterification reactions, although we are unable to distinguish between dysregulation of fatty acid uptake and fatty acid storage based off our results (Johnson et al., 2020).

Metabolites involved in primary bile acid biosynthesis and secretion, as well as steroid metabolism (cholesterol sulfate), were depressed in STZ-treated communities (Figure S2A, Figure S2B, Table S1, Table S3). We observed a stark decrease in multiple bile acids including chenodeoxycholate, 7-sulfocholate, and sulfodeoxycholate (Figure S2A, Table S1). Overall, this paints a picture of reduced primary bile acid availability without a detectable change in secondary bile acids in the STZ-treated microbiome. At the species level we noticed that *B. theta* had reduced expression of bile salt efflux systems (Figure S2E: BT2793-2795, Table S5) (H. Liu et al., 2019), perhaps due to overall systemic reductions in the bile acid pool. Both the concentration and composition of the bile acid pool has been demonstrated to exhibit control on the function of the colonic microbiome; bile acid transformations are executed by select community members, and primary bile acids can trigger spore induction in certain Clostridia (Quinn et al., 2020; Staley et al., 2016; Zheng et al., 2017). Thus, reductions in the overall bile acid pool may place the microbiota in a more susceptible state to ATB challenge by reducing sporulation capacity (Cabral et al., 2019). As with fatty acids, changes in bile acid metabolism have been reported in STZ-treated rodent models and are likely a major contributing factor to the larger set of metabolite changes in the cecum, given their involvement in both postprandial nutrient absorption and gut transit time (T. Li et al., 2012; Ugarte et al., 2012).

STZ and AMX co-treatment increased the abundance of multiple *Bacteroides* species relative to normoglycemic controls. This abundance change was also true for other Bacteroidetes including *Odoribacter splanchnicus*, *Parabacteroides* sp. CT06, and *Prevotella intermedia*. We observed a 2-fold and 4-fold increase in the abundances of the Bacteroidetes *Alistipes finegoldii*

and *Alistipes shahii*, respectively, that were unique to STZ-treated mice (Figure S3). Interestingly, these species are heavily enriched for polysaccharide utilization loci, so it is currently unclear how they are involved in community-level polysaccharide foraging (Grondin et al., 2017; Terrapon et al., 2015). Interestingly, in our WMGS dataset, we noticed that the taxa that were more reduced in STZ-treated mice have been correlated with lipid intake, cholesterol, and cholesterol metabolite abundance in other works (Clarke et al., 2014; Wohlgemuth et al., 2011). For example, some species of *Erysipelotrichaceae* are auxotrophic for lipid biosynthesis; thus, the combination of STZ- and AMX-induced dyslipidemia may provide an explanation for the differential abundance of these taxa under HG conditions (Figure 3H) (Kaakoush, 2015; Martínez et al., 2012).

Despite significant host-dependent differences in the impact of AMX, we observed some common ATB responses from the gut microbiota. First, we observed that drug treatment caused enrichment of numerous monosaccharides including deoxyribose, hexose, triose, and pentoses, regardless of host phenotype (Table S1). The availability of these monosaccharides resulted in respiratory microbial metabolism, as indicated by increases in fructose bisphosphate aldolase, succinate dehydrogenase, and ATP synthase transcripts (Table S8). To that end, GNPS Clusters 1020, 883, and 886 which are related to valeryl, palmitoyl, and lauroyl-conjugated carnitine species were elevated (Figure S4C, Figure S4D, Table S3). Carnitines have been identified as possible alternative final electron acceptors in obligate anaerobes (including the *Enterobacteriaceae*), suggesting an increased capacity for anaerobic respiratory activity as a common response to drug challenge (Bernal et al., 2007; Meadows and Wargo, 2015). This respiratory increase is consistent with the model of bactericidal ATB toxicity in which a lethal respiratory burst is a significant contribution to drug susceptibility (Belenky et al., 2015; Cabral et al., 2019; Lobritz et al., 2015).

ATB-induced dysbiosis has been associated with changes in bile acids (Theriot et al., 2015), as well as dyslipidemia in multiple animal models (Sato et al., 2016; Yan et al., 2020) and microbes (Belenky et al., 2015). Thus, we anticipated that signatures of dyslipidemia and bile acid dysregulation would occur in our datasets. AMX reduced the abundance of metabolites involved in primary and secondary bile acid synthesis as well as bile secretion pathways irrespective of host glycemia (Table S3). Specifically, the primary bile acid metabolites 3 α ,7 α -dihydroxycoprostanic acid, cholate, chenodeoxycholate (Figure S4C, Figure S4D: Cluster 376, Table S2), the related GNPS Clusters 915 and 380 (Figure S4C, Figure S4D, Table S2), as well as bile acid alcohols like 6-deoxodolichosterone, 5 β -Cholestane-3 α ,7 α ,12 α ,23S,25-pentol, and 27-norcholestanhexol were all reduced after ATB administration (Table S1). We also observed that STZ-treated communities exhibited typical signatures of ATB stress including increased transcripts related to stress responses, iron metabolism, translation, and quorum sensing/biofilms (Table S7) (Cabral et al., 2020; 2019). Together these data suggest that AMX-induced bile acid dysregulation is not host dependent, while dyslipidemia is, and that STZ-treatment increases the abundance of pro-inflammatory intestinal metabolites and ATB-stress related transcripts.

Supplemental Discussion

When evaluating data that examine host-microbe interactions it is important to acknowledge the influence of host physiology on the system. STZ-mediated insulin dysfunction has been shown to directly modulate intestinal glucose absorption by rapidly increased expression of small intestinal glucose transporters (Koepsell, 2020). Some have suggested that genetic disruption of intestinal insulin signaling increases glucose release from enteroendocrine cells (Ussar et al., 2017). A common clinical feature of metabolic disturbances is delayed gastric transit

time, which is intrinsically linked with proper intestinal glucose absorption (Rayner and Horowitz, 2006). This phenotype has been recapitulated in multiple rodent models, including STZ-treated rats that have significant delays in stomach-to-cecal transit time (Chesta et al., 1990). Delays in gut transit and altered expression of intestinal glucose uptake likely impacts the carbohydrate pool that reaches the cecum, and might explain some of the microbiome disturbances seen in metabolic diseases (Dabke et al., 2019).

We found that a hallmark feature of STZ-induced HG was significant dysregulation of cecal lipid metabolism in both the pre- and post-ATB treatment groups. This finding is in line with existing studies on serum metabolomics in rats, which find perturbation in fatty acid metabolism as a reliable biomarker of STZ-treatment (Fernández-Ochoa et al., 2020; Ugarte et al., 2012). While the host executes significant control of lipid processing via pancreaticobiliary secretions, there is evidence from germ-free animal studies that implicates the gut microbiome as an integral component of fatty acid metabolism, and suggests that microbial dyslipidemia results in negative metabolic phenotypes (Schoeler and Caesar, 2019). Microbial lipid processing (for example the conjugation of linoleic acid) has also been implicated in the generation of metabolite intermediates that increase the integrity of gut epithelial barrier function (Schoeler and Caesar, 2019). Thus, it stands to reason that disruption of lipid homeostasis within the gut, as observed in our datasets, has downstream consequences to gut barrier function and places the cecal microbiota in a more delicate state prior to ATB challenge. Decreases in gut barrier function have also been directly implicated in the susceptibility of the microbiome to enteric pathogen challenge (Christopher A Thaiss et al., 2018), and we observed that the enteric pathogen *S. enterica* was able to infect HG drug-treated animals more readily and caused more lethal disease. These data indicate a potential

link between perturbed lipid metabolism and pathogen colonization, but more work is required to elucidate specific mechanisms.

Beyond disruption to lipid homeostasis, a novel finding in our datasets was that both STZ and AMX treatment reduced the abundance of primary bile acids within the cecum. The microbiota executes a large portion of bile acid conjugation reactions and cross-talks with the host to regulate primary bile acid secretion (Ridlon et al., 2014). Thus, ATB-induced changes were anticipated and were in agreeance with an existing body of work that indicates ATB administration modifies the abundance and composition of the bile acid pool (Ridlon et al., 2014; Sayin et al., 2013; Vrieze et al., 2014). Interestingly, other beta-lactam ATBs have been shown to increase the total bile acid abundance within the colon (Kuribayashi et al., 2012). Meanwhile, vancomycin, clindamycin, cefoperazone, polymyxin B, and the combinatory cocktail of vancomycin/metronidazole/kanamycin/clindamycin reduce the abundance of secondary bile acids but do not modify the primary bile acid pool (Kuno et al., 2018; Theriot et al., 2015). Thus, our data may represent a novel, STZ- and AMX-specific bile acid dysregulation.

Supplemental Figures, Titles, and Legends

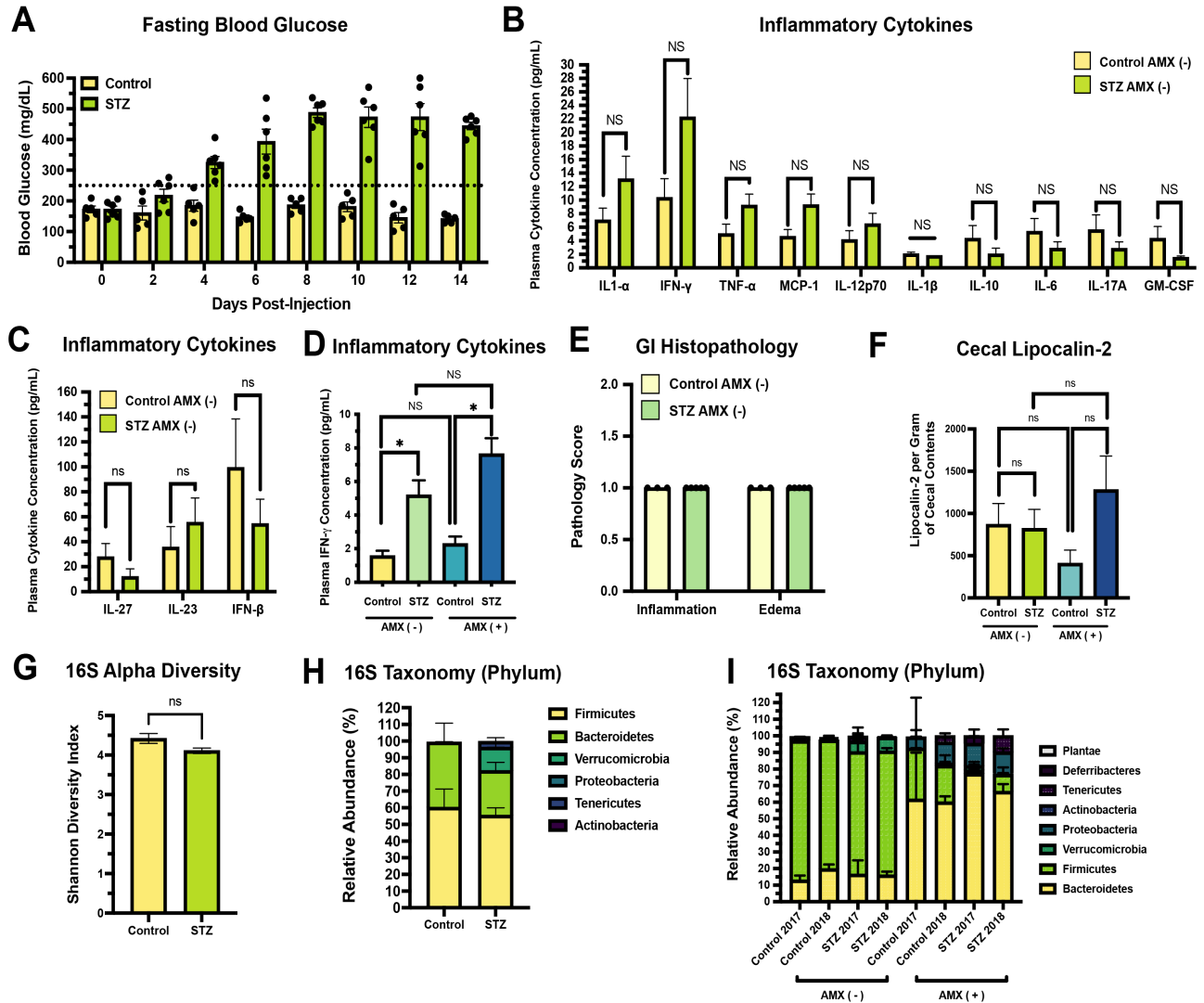


Figure S1. The impact of streptozotocin treatment on host physiology and microbiome composition without additional. (Related to Figure 1)

- Fasting blood glucose of individual mice before STZ injection (Day 0) and on 2 days intervals for up to 14 days post-injection. The Day 14 time-point is representative of the final day of experiments described in Figure 7.
- Plasma cytokine concentrations in STZ-treated and control mice 3 days post-injection. Data represent averaged concentrations \pm SEM for cytokines whose concentration falls between 0 and 23 pg/mL.
- Plasma cytokine concentrations in STZ-treated and control mice 3 days post-injection. Data represent averaged concentrations \pm SEM for cytokines whose concentration falls between 12 and 160 pg/mL.
- Plasma concentration of IFN- γ in STZ-treated and control mice +/- AMX 4 days after STZ injection.
- Pathological assessment of fixed, H&E-stained colon sections 3 days after STZ injection.

- F. Cecal lipocalin-2 concentrations. Data represent average concentrations \pm SEM.
- G. Alpha diversity as measured by the Shannon diversity index for STZ-treated and control animals 3 days post-injection. Data represent average \pm SEM.
- H. Phylum-level taxonomic composition of the cecal microbiome 3 days post STZ-injection. Data represent average abundance + SEM.
- I. Phylum-level taxonomic composition of the cecal microbiome in STZ and control mice +/- AMX treatment. Data represent average abundance + SEM.

For A: N = 5 or 6 per group

For B & C: N = 4 per group; *, P < 0.05; unpaired T-test with Welch's correction

For D & F: N = 4 or 5 per group; *, P < 0.05; Welch's ANOVA with Dunnett T3 test for multiple hypothesis testing

For E: N = 4 to 6 per group. Inflammation (0: absent, 1: minimal, 2: mild affecting mucosa and sub-mucosa, 3: moderate affecting mucosa, 4: severe). Edema (0: < 10%, 1: 10-25%, 2: 25%-50%, 3: 50%-75%, 4: over 75%).

For G -I: N = 3 to 5 per group; ; *, P < 0.05; unpaired T-test with Welch's correction

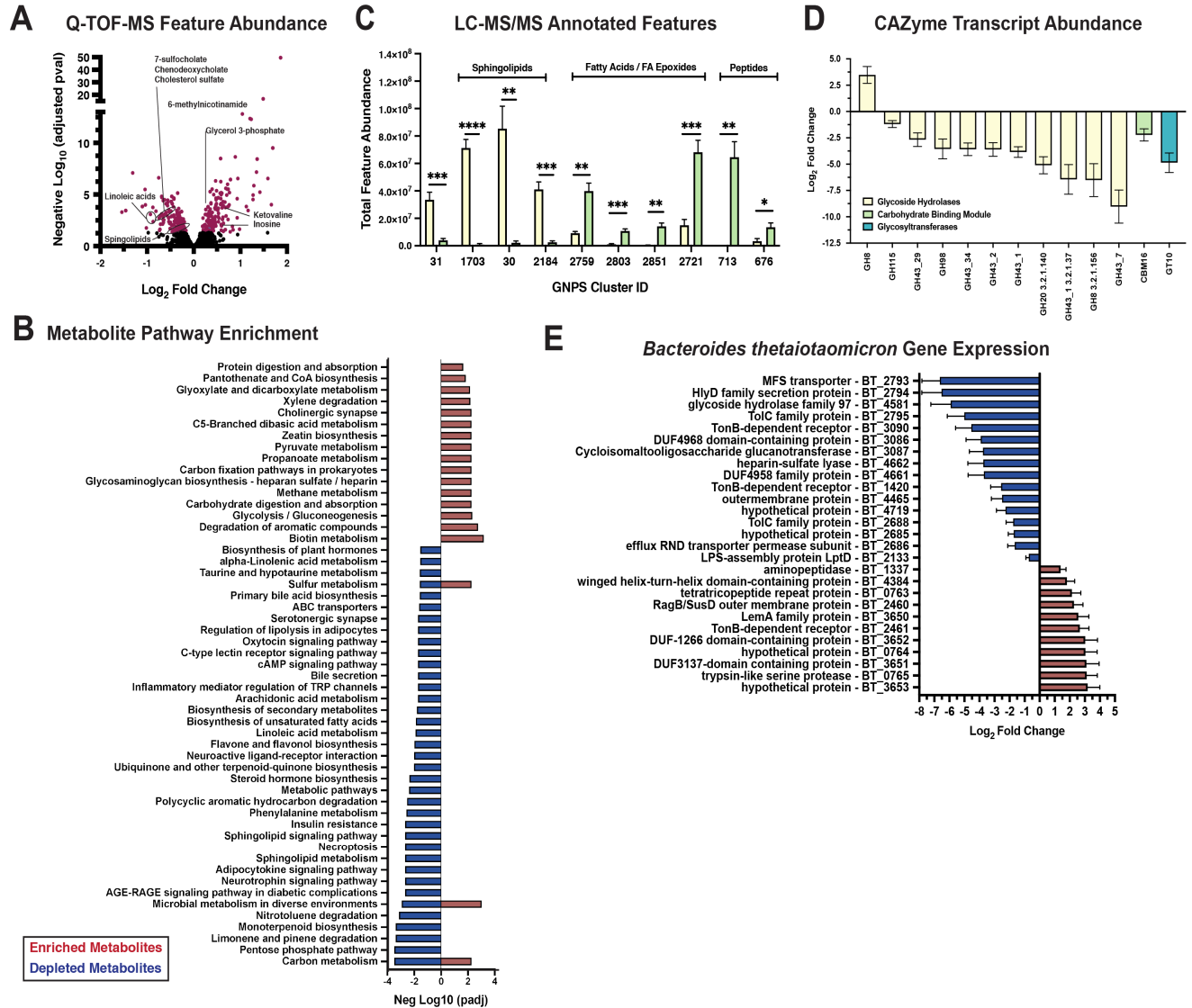


Figure S2. Streptozotocin-induced hyperglycemia modifies both the cecal metabolome and metatranscriptome. (Related to Figure 2)

- Volcano plot of the cecal metabolome in STZ-treated mice relative to normoglycemic controls. Purple points represent differentially abundant metabolite features. Metabolites of interest are labeled. See Table S1 for full results (N = 6 per group, 2 technical replicates per mouse)
- KEGG pathway enrichment of differentially abundant Q-TOF-MS metabolites in STZ-treated mice compared to controls. Colors indicate whether the metabolites contributing to pathway scoring were enriched (red) or depleted (blue) in STZ-treated animals compared to controls. See Table S3 for full results.
- Differentially abundant GNPS-annotated clusters that contain known metabolites within the cluster. Clusters were selected from the top-50 most relevant features via Random Forest Testing. Comparison is between STZ-treated mice and controls. See Table S2 for full results.

D. Differentially abundant CAZyme transcripts in STZ-treated mice. Data represent \log_2 fold change relative to controls \pm SEM. See Table S4 for full results.

E. Differentially abundant *B. thetaiotaomicron* transcripts after STZ treatment. Data represent \log_2 fold change versus controls \pm SEM See Table S5 for full results.

For A – C: N = 6 per group, 2 technical replicates per sample

For D & E : N = 4 per group

For A, D, & E: Differentially abundant = Benjamini-Hochberg adjusted p value < 0.05

For B: Significance = unpaired T-test p value < 0.05

For C: *, P < 0.05; **, P < 0.01; ***, P < 0.001, **** P < 0.0001; unpaired T-test with Welch's correction

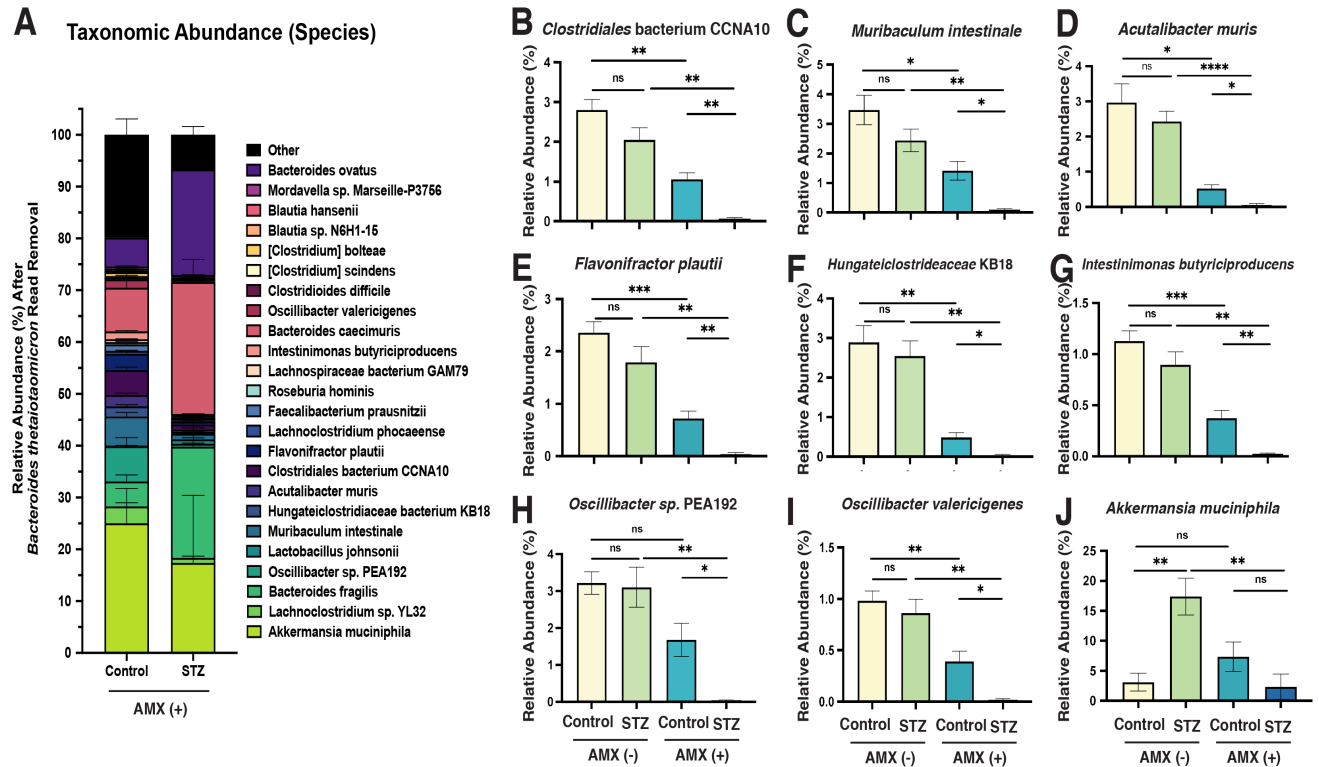


Figure S3. Streptozotocin impacts taxonomic composition after amoxicillin treatment. (Related to Figure 3)

- Average relative abundance of species from A after the removal of reads assigned to *B. thetaiotaomicron*. Data are represented as mean \pm SEM for each species
- Average relative abundance of reads assigned to *Clostridiales* bacterium CCNA10.
- Average relative abundance of reads assigned to *Muribaculum intestinale*.
- Average relative abundance of reads assigned to *Acutalibacter muris*.
- Average relative abundance of reads assigned to *Flavonifractor plautii*.
- Average relative abundance of reads assigned to *Hungateiclostridiaceae* bacterium KB18.
- Average relative abundance of reads assigned to *Intestinimonas butyriciproducens*.
- Average relative abundance of reads assigned to *Oscillibacter* species PEA192.
- Average relative abundance of reads assigned to *Oscillibacter valericigenes*
- Average relative abundance of reads assigned to *Akkermansia muciniphila*.

For all panels: N = 5 to 8 per group

For panels B-J, (*, P < 0.05; **, P < 0.01; ***, P < 0.001; ****, P < 0.0001, Welch's ANOVA with Dunnett T3 test for multiple hypothesis testing).

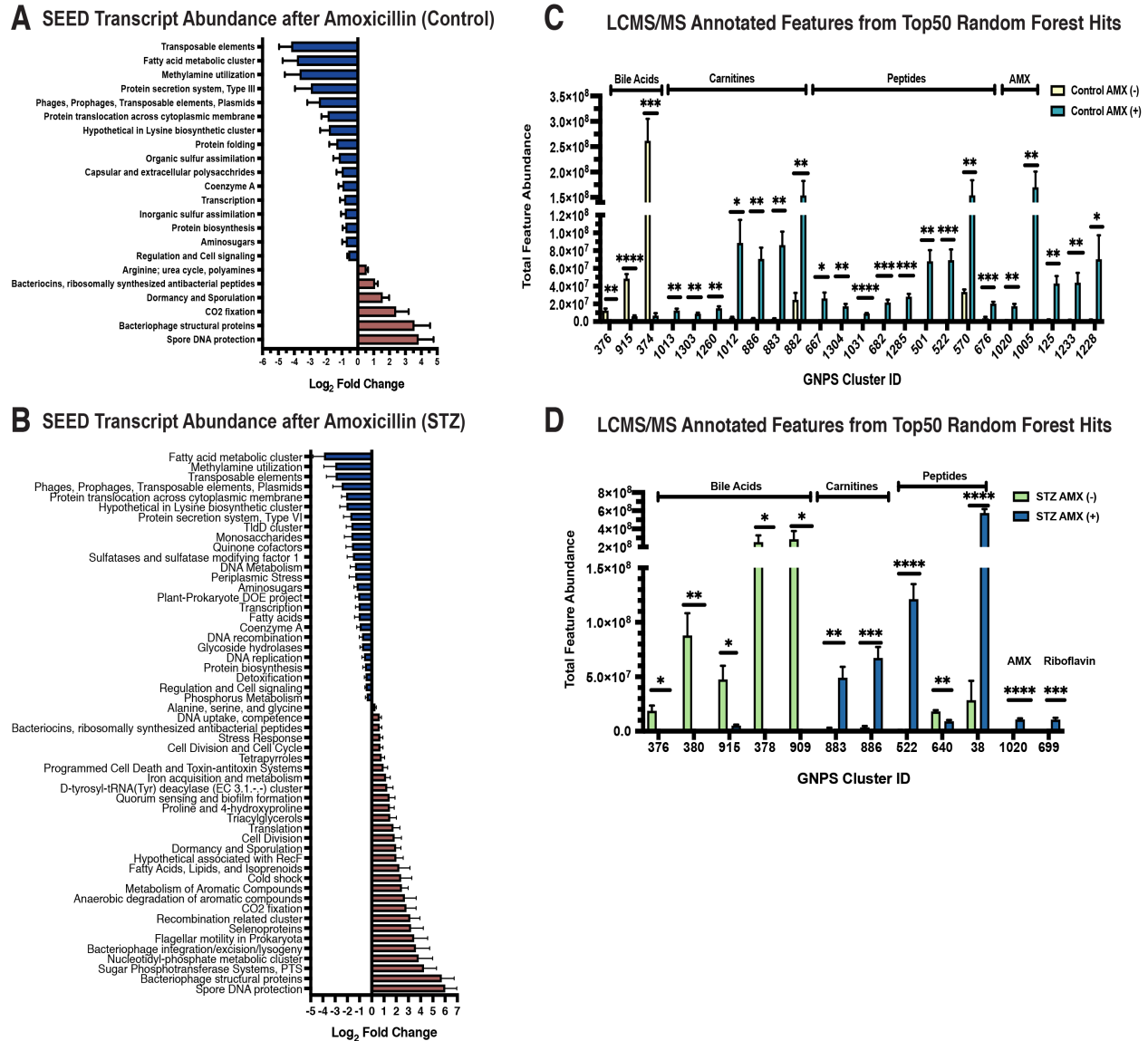


Figure S4: Streptozotocin modifies the metatranscriptomic and metabolomic responses of the gut microbiome to amoxicillin. (Related to Figures 4 & 5)

- Differentially abundant level 2 SEED Subsystem transcripts in normoglycemic control mice after AMX treatment. Data represent \log_2 fold change relative to vehicle controls \pm SEM. See Table S7 for full results.
- Differentially abundant level 2 SEED Subsystem transcripts in STZ-treated mice after AMX treatment. Data represent \log_2 fold change relative to vehicle controls \pm SEM. See Table S7 for full results.
- Differentially abundant GNPS-annotated clusters that contain known metabolites within the cluster. Clusters were selected from the top-50 most relevant features via Random Forest Testing. Comparison is between AMX-treated mice and vehicle-treated mice for normoglycemic controls. See Table S2 for full results.
- Differentially abundant GNPS-annotated clusters that contain known metabolites within the cluster. Clusters were selected from the top-50 most relevant features via Random

Forest Testing. Comparison is between AMX-treated mice and vehicle-treated mice for STZ-treated mice. See Table S2 for full results.

For A & B: N = 4 per group; Differentially abundant = Benjamini-Hochberg adjusted p value < 0.05

For C & D: N = 6 per group, 2 technical replicates per sample; (*, P < 0.05; **, P < 0.01; ***, P < 0.001, **** P < 0.0001); unpaired T-test with Welch's correction

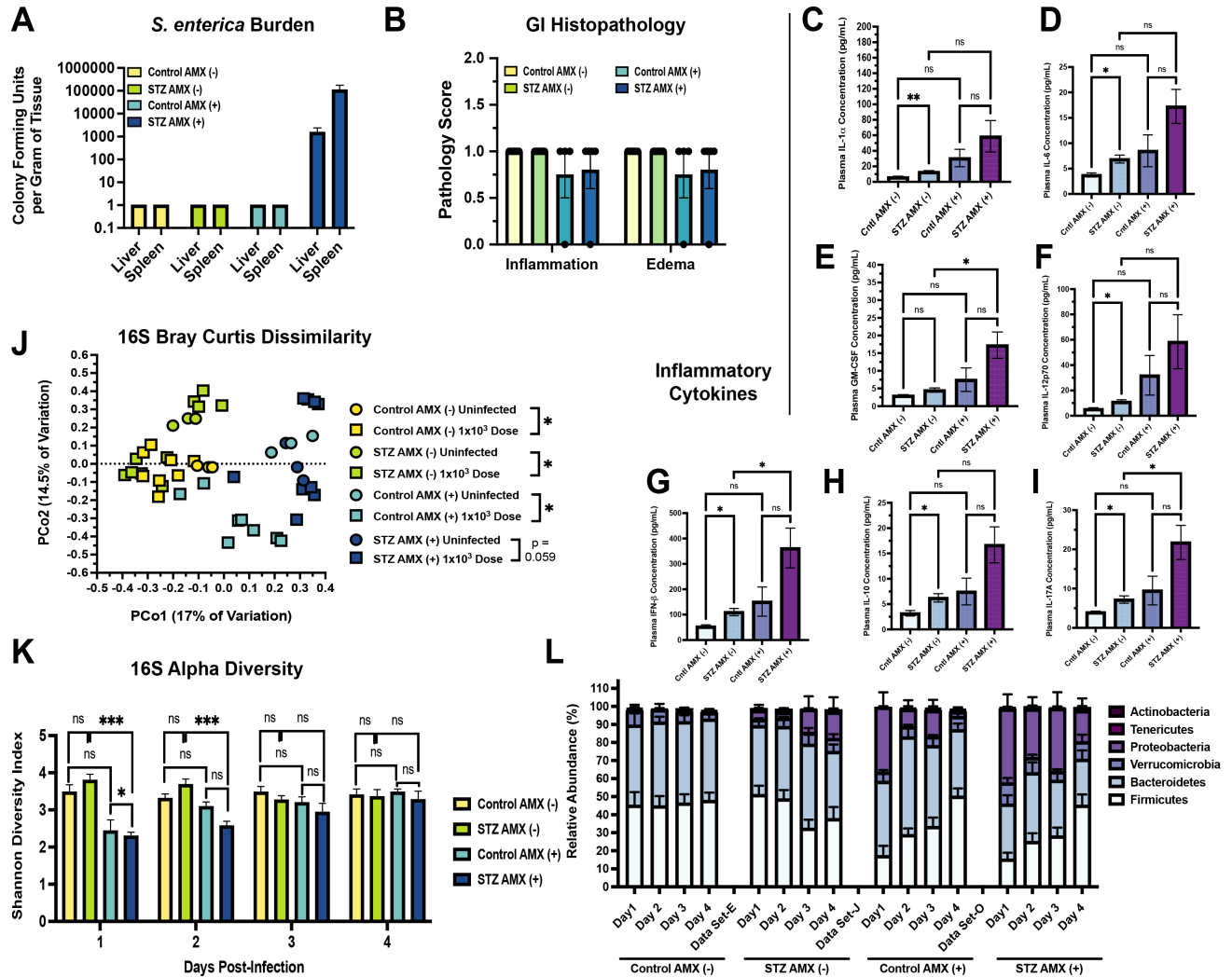


Figure S5: Streptozotocin and amoxicillin dual treatment worsens outcomes during *Salmonella enterica* infection. (Related to Figure 7)

- A. *Salmonella enterica* Typhimurium colony forming units (CFU) per gram of hepatic and splenic tissue in control AMX(+/-), and hyperglycemic AMX(+/-) mice over the course of infection with an inoculum of 1×10^3 cells. Data represent mean CFU \pm SEM.
- B. Pathological assessment of fixed, H&E-stained colon sections 4 days after infection with an inoculum of 1×10^3 cells.
- C. Plasma concentration of IL-1 α in STZ-treated and control mice +/- AMX
- D. Plasma concentration of IL-6 in STZ-treated and control mice +/- AMX
- E. Plasma concentration of GM-CSF in STZ-treated and control mice +/- AMX
- F. Plasma concentration of IL-12p70 in STZ-treated and control mice +/- AMX
- G. Plasma concentration of IFN- β in STZ-treated and control mice +/- AMX
- H. Plasma concentration of IL-10 in STZ-treated and control mice +/- AMX
- I. Plasma concentration of IL-17A in STZ-treated and control mice +/- AMX
- J. Principal Coordinates Analysis of Bray-Curtis Dissimilarity between uninfected controls and mice infected with an inoculum of 1×10^3 cells 24 hours post-infection.

K. Alpha diversity as measured by the Shannon diversity index of fecal 16S rRNA reads. Data represent average score \pm SEM during infection time course after dosage with an inoculum of 1×10^3 cells.

L. Phylum-level taxonomic composition of the fecal microbiome during infection time course after dosage with an inoculum of 1×10^3 cells. Data represent average abundance \pm SEM.

For A - I: N = 4 to 7 per group

For J: N = 3 to 10 per group

For B: Inflammation (0: absent, 1: minimal, 2: mild affecting mucosa and sub-mucosa, 3: moderate affecting mucosa, 4: severe). Edema (0: < 10%, 1: 10-25%, 2: 25%-50%, 3: 50%-75%, 4: over 75%).

For C - I: (*, $P < 0.05$; **, $P < 0.01$; ***, $P < 0.001$; ****, $P < 0.0001$; Welch's ANOVA with Dunnet T3 test for multiple hypothesis testing).

For J: (*, $P < 0.05$; **, $P < 0.01$; ***, $P < 0.001$; permutational ANOVA)

For K: (*, $P < 0.05$; **, $P < 0.01$; ***, $P < 0.001$; ****, $P < 0.0001$; Welch's ANOVA with Dunnet T3 test for multiple hypothesis testing)

Supplemental Files

Table S1: Raw Q-TOF-MS Ion Intensities, annotation guide, and full DESeq2 results of Q-TOF-MS data. Related to Figure 2A, Figure 5A, and Figure S2A.

- A. Raw Q-TOF-MS ion intensities generated by General Metabolics Inc. (Boston, MA, USA)
- B. Annotation guide for Q-TOF-MS ion intensities generated by General Metabolics Inc. (Boston, MA, USA)
- C. Differential abundance testing of the impact of streptozotocin treatment on the abundance of Q-TOF-MS metabolites in the murine cecal microbiome prior to ATB administration. Log₂ fold change values were calculated relative to NG controls samples (STZ AMX - vs Control AMX -)
- D. Differential abundance testing of the impact of amoxicillin treatment on the abundance of Q-TOF-MS metabolites in the NG murine cecal microbiome. Log₂ fold change values were calculated relative to NG vehicle-treated controls samples (Control AMX - vs Control AMX +)
- E. Differential abundance testing of the impact of amoxicillin treatment on the abundance of Q-TOF-MS metabolites in the HG murine cecal microbiome. Log₂ fold change values were calculated relative to HG vehicle-treated controls samples (STZ AMX - vs STZ AMX +)
- F. Differential abundance testing of the impact of streptozotocin treatment on the abundance of Q-TOF-MS metabolites in the murine cecal microbiome after amoxicillin treatment. Log₂ fold change values were calculated relative to NG amoxicillin-treated controls samples (Control AMX + vs STZ AMX +)
- G. Interaction term analysis generated by DESeq2 for the impact of host glycemia on changes in metabolite abundance following amoxicillin therapy. Log₂ fold change values were calculated relative to NG vehicle-treated samples (Control AMX -)

Table S2: Random Forest Classification of GNPS-annotated LC-MS/MS Clusters. Related to Figure S2C, Figure S4C, and Figure S4D.

- A. Full Random Forest results of feature importance distinguishing NG and HG cecal metabolomes before ATB treatment (i.e. STZ AMX - vs. Control AMX -)
- B. Full Random Forest results of feature importance distinguishing vehicle-treated and amoxicillin-treated cecal metabolomes in NG mice (i.e. Control AMX - vs. Control AMX +)
- C. Full Random Forest results of feature importance distinguishing vehicle-treated and amoxicillin-treated cecal metabolomes in HG mice (i.e. STZ AMX - vs. STZ AMX +)
- D. Full Random Forest results of feature importance distinguishing NG and HG cecal metabolomes after ATB treatment (i.e. STZ AMX + vs. Control AMX +)

Table S3: Full KEGG-based Pathway Activity Profiling of enriched and depleted cecal Q-TOF-MS metabolites. Related to Figure 6A and Figure S2B.

- A. Combined results from Pathway Activity Profiling of metabolites that are differentially abundant during streptozotocin treatment (Table S1C).
- B. Combined results from Pathway Activity Profiling of metabolites that are differentially abundant during amoxicillin treatment in NG mice (Table S1D).
- C. Combined results from Pathway Activity Profiling of metabolites that are differentially abundant during amoxicillin treatment in HG mice (Table S1E).

- D. Combined results from Pathway Activity Profiling of metabolites that are differentially abundant after amoxicillin treatment between normo- and HG mice (Table S1F).

Table S4: Full DESeq2 results of CAZyme transcript abundance generated by SAMSA2. Related to Figure 4A and Figure S2D.

- A. Differential abundance testing of the impact of streptozotocin treatment on the abundance of CAZyme transcripts in the murine cecal metatranscriptome. Log₂ fold change values were calculated relative to NG controls (STZ AMX - vs Control AMX -)
- B. Differential abundance testing of the impact of amoxicillin treatment on the abundance of CAZyme transcripts in the murine cecal metatranscriptome in NG animals. Log₂ fold change values were calculated relative to NG vehicle-treated samples (Control AMX - vs Control AMX +)
- C. Differential abundance testing of the impact of amoxicillin treatment on the abundance of CAZyme transcripts in the murine cecal metatranscriptome in HG animals. Log₂ fold change values were calculated relative to HG vehicle-treated samples (STZ AMX - vs STZ AMX +)
- D. Interaction term analysis generated by DESeq2 for the impact of host glycemia on changes in CAZyme transcripts abundance after amoxicillin treatment. Log₂ fold change values were calculated relative to NG vehicle-treated samples (Control AMX-).

Table S5: Full DESeq2 results of transcript abundance analysis of *A. muciniphila* and *B. theta* during dietary intervention and ciprofloxacin treatment and dietary formulation. Related to Figure 6D and Figure S2E.

- A. Total and average counts for Kraken2-generated metatranscriptomic read assignments.
- B. Differential abundance testing of the impact of HG on the abundance of *B. theta* transcripts within the murine cecal metatranscriptome. Log₂ fold change values were calculated relative to NG controls (STZ AMX - vs Control AMX -)
- C. Differential abundance testing of the impact of amoxicillin treatment on the abundance of *B. theta* transcripts within the NG murine cecal metatranscriptome. Log₂ fold change values were calculated relative to NG vehicle-treated controls (Control AMX - vs Control AMX +)
- D. Differential abundance testing of the impact of amoxicillin treatment on the abundance of *B. theta* transcripts within the HG murine cecal metatranscriptome. Log₂ fold change values were calculated relative to HG vehicle-treated controls (STZ AMX - vs STZ AMX +)
- E. Interaction term analysis generated by DESeq2 for the impact of host glycemia on changes in *B. theta* transcripts abundance after amoxicillin treatment. Log₂ fold change values were calculated relative to NG vehicle-treated samples (Control AMX-).
- F. Differential abundance testing of the impact of HG on the abundance of *O. valericigenes* transcripts within the murine cecal metatranscriptome. Log₂ fold change values were calculated relative to NG controls (STZ AMX - vs Control AMX -)
- G. Differential abundance testing of the impact of amoxicillin treatment on the abundance of *O. valericigenes* transcripts within the NG murine cecal metatranscriptome. Log₂ fold change values were calculated relative to NG vehicle-treated controls (Control AMX - vs Control AMX +)

- H. Differential abundance testing of the impact of amoxicillin treatment on the abundance of *O. valericigenes* transcripts within the HG murine cecal metatranscriptome. Log₂ fold change values were calculated relative to HG vehicle-treated controls (STZ AMX - vs STZ AMX +)
- I. Interaction term analysis generated by DESeq2 for the impact of host glycemia on changes in *O. valericigenes* transcripts abundance after amoxicillin treatment. Log₂ fold change values were calculated relative to NG vehicle-treated samples (Control AMX-).
- J. Differential abundance testing of the impact of HG on the abundance of *O. sp.* PEA192 transcripts within the murine cecal metatranscriptome. Log₂ fold change values were calculated relative to NG controls (STZ AMX - vs Control AMX -)
- K. Differential abundance testing of the impact of amoxicillin treatment on the abundance of *O. sp.* PEA192 transcripts within the NG murine cecal metatranscriptome. Log₂ fold change values were calculated relative to NG vehicle-treated controls (Control AMX - vs Control AMX +)
- L. Differential abundance testing of the impact of amoxicillin treatment on the abundance of *O. sp.* PEA192 transcripts within the HG murine cecal metatranscriptome. Log₂ fold change values were calculated relative to HG vehicle-treated controls (STZ AMX - vs STZ AMX +)
- M. Interaction term analysis generated by DESeq2 for the impact of host glycemia on changes in *O. sp.* PEA192 transcripts abundance after amoxicillin treatment. Log₂ fold change values were calculated relative to NG vehicle-treated samples (Control AMX-).

Table S6: Full LEfSe results from the analysis of MetaCyc pathway abundance generated by HUMAnN2. “Class” denotes the experimental group a particular pathway was associated with. Related to Figure 2D, Figure 4C, and Figure 4D.

- A. Pairwise LEfSe analysis of NG and HG samples prior to ATB treatment (STZ AMX - vs Control AMX -)
- B. Pairwise LEfSe analysis of amoxicillin- and vehicle-treated samples from NG mice (Control AMX - vs Control AMX +)
- C. Pairwise LEfSe analysis of amoxicillin- and vehicle-treated samples from HG mice (STZ AMX - vs STZ AMX +)

Table S7: Full DESeq2 results of SEED subsystem abundance generated by SAMSA2. Related to Figure 4B, Figure S4A, and Figure S4D.

- A. Differential abundance testing of the impact of streptozotocin treatment on the abundance of SEED subsystem transcripts in the murine cecal metatranscriptome. Log₂ fold change values were calculated relative to NG controls (STZ AMX- vs Control AMX-)
- B. Differential abundance testing of the impact of amoxicillin treatment on the abundance of SEED subsystem transcripts in the murine cecal metatranscriptome in NG animals. Log₂ fold change values were calculated relative to NG vehicle-treated samples (Control AMX - vs Control AMX +)
- C. Differential abundance testing of the impact of amoxicillin treatment on the abundance of SEED subsystem transcripts in the murine cecal metatranscriptome in HG animals. Log₂ fold change values were calculated relative to HG vehicle-treated samples (STZ AMX - vs STZ AMX +)

- D. Interaction term analysis generated by DESeq2 for the impact of host glycemia on changes in SEED subsystem transcript abundance after amoxicillin treatment. Log₂ fold change values were calculated relative to NG vehicle-treated samples on the (Control AMX-).

Table S8: Full DESeq2 results of RefSeq transcript abundance generated by SAMSA2. Related to Figure 2E.

- A. Differential abundance testing of the impact of streptozotocin treatment on the abundance of RefSeq transcripts in the murine cecal metatranscriptome. Log₂ fold change values were calculated relative to NG controls (STZ AMX- vs Control AMX-)
- B. Differential abundance testing of the impact of amoxicillin treatment on the abundance of RefSeq transcripts in the murine cecal metatranscriptome in NG animals. Log₂ fold change values were calculated relative to NG vehicle-treated samples (Control AMX - vs Control AMX +)
- C. Differential abundance testing of the impact of amoxicillin treatment on the abundance of RefSeq transcripts in the murine cecal metatranscriptome in HG animals. Log₂ fold change values were calculated relative to HG vehicle-treated samples (STZ AMX - vs STZ AMX +)
- D. Interaction term analysis generated by DESeq2 for the impact of host glycemia on changes in RefSeq transcript abundance after amoxicillin treatment. Log₂ fold change values were calculated relative to NG vehicle-treated samples on the (Control AMX-).

Table S9: Full taxon stratification of community metabolic potential generated by MIMOSA. Related to Figure 2F, Figure 5C, Figure 5D, and 6C.

- A. Model Data and Taxon Contribution Results of MIMOSA (version 2.0.0). Data represent STZ-treated vs control mice without AMX.
- B. Model Data and Taxon Contribution Results of MIMOSA (version 2.0.0). Data represent Control AMX-treated vs vehicle-treated controls.
- C. Model Data and Taxon Contribution Results of MIMOSA (version 2.0.0). Data represent STZ- and AMX-treated vs vehicle-treated controls.
- D. Model Data and Taxon Contribution Results of MIMOSA (version 2.0.0). Data represent STZ- and AMX-treated vs Control AMX-treated mice.

References

- Adolfsen, K.J., Brynildsen, M.P., 2015. Futile cycling increases sensitivity toward oxidative stress in *Escherichia coli*. *Metab. Eng.* 29, 26–35. doi:10.1016/j.ymben.2015.02.006
- Aggio, R.B.M., Ruggiero, K., Villas-Bôas, S.G., 2010. Pathway Activity Profiling (PAPi): from the metabolite profile to the metabolic pathway activity. *J. Bioinform.* 26, 2969–2976. doi:10.1093/bioinformatics/btq567
- Ahn, S., Jung, J., Jang, I.-A., Madsen, E.L., Park, W., 2016. Role of Glyoxylate Shunt in Oxidative Stress Response. *J. Biol. Chem.* 291, 11928–11938. doi:10.1074/jbc.M115.708149
- Albenberg, L.G., Wu, G.D., 2014. Diet and the intestinal microbiome: associations, functions, and implications for health and disease. *Gastroenterology* 146, 1564–1572. doi:10.1053/j.gastro.2014.01.058
- Allaway, D., Haydock, R., Lonsdale, Z.N., Deusch, O.D., O'Flynn, C., Hughes, K.R., 2020. Rapid reconstitution of the fecal microbiome after extended diet-induced changes indicates a Stable Gut Microbiome in Healthy Adult Dogs. *Appl. Environ. Microbiol.* 86, e00562-20. doi:10.1128/AEM.00562-20
- Andersen, L.W., Liu, X., Peng, T.J., Giberson, T.A., Khabbaz, K.R., Donnino, M.W., 2015. Pyruvate Dehydrogenase Activity and Quantity Decreases After Coronary Artery Bypass Grafting. *Shock* 43, 250–254. doi:10.1097/SHK.0000000000000306
- Anderson, C.J., Clark, D.E., Mazhar, A., Kendall, M.M., 2015. Ethanolamine Signaling Promotes *Salmonella* Niche Recognition and Adaptation during Infection. *PLoS Pathog.* 11, 1–20. doi:10.1371/journal.ppat.1005278
- Anderson, C.J., Kendall, M.M., 2016. Location, location, location. *Salmonella* senses ethanolamine to gauge distinct host environments and coordinate gene expression. *Microb. Cell* 3, 1–3. doi:10.15698/mic2016.02.479
- Anderson, C.J., Satkovich, J., Lu, V.K.K., Agaisse, H., Kendall, M.M., 2018. The Ethanolamine Permease EutH Promotes Vacuole Adaptation of *Salmonella enterica* and *Listeria monocytogenes* during Macrophage Infection. *Infect. Immun.* 86, e00172-18. doi:10.1128/IAI.00172-18
- Bäumler, A.J., Sperandio, V., 2016. Interactions between the microbiota and pathogenic bacteria in the gut. *Nature* 535, 85–93. doi:10.1038/nature18849
- Belenky, P., Bogan, K.L., Brenner, C., 2007. NAD⁺ metabolism in health and disease. *Trends Biochem. Sci.* 32, 12–9. doi:10.1016/j.tibs.2006.11.006
- Belenky, P., Ye, J.D., Porter, C.B.M., Cohen, N.R., Lobritz, M.A., Ferrante, T., Jain, S., Korry, B.J., Schwarz, E.G., Walker, G.C., Collins, J.J., 2015. Bactericidal Antibiotics Induce Toxic Metabolic Perturbations that Lead to Cellular Damage. *Cell Rep.* 13, 968–980. doi:10.1016/j.celrep.2015.09.059
- Belzer, C., Chia, L.W., Aalvink, S., Chamlagain, B., Piironen, V., Knol, J., De Vos, W.M., 2017. Microbial Metabolic Networks at the Mucus Layer Lead to Diet-Independent Butyrate and Vitamin B12 Production by Intestinal Symbionts. *mBio* 8, 776–14. doi:10.1128/mBio.00770-17
- Benjamini, Y., Hochberg, Y., 1995. Controlling the false discovery rate: a practical and powerful approach to multiple testing. *J. R. Statist. Soc.* 57, 289–300. doi: 10.2307/2346101
- Berg J.M., Tymoczko J.L., Stryer L., 2002. Carbon Atoms of Degraded Amino Acids Emerge as Major Metabolic Intermediates. *Biochemistry*, 5th edition, Section 23.5.
- Bernal, V., Sevilla, Á., Cánovas, M., Iborra, J.L., 2007. Production of L-carnitine by secondary metabolism of bacteria. *Microb. Cell Fact.* 6, 31–17. doi:10.1186/1475-2859-6-31

- Bisanz, J.E., Upadhyay, V., Turnbaugh, J.A., Ly, K., Turnbaugh, P.J., 2019. Meta-Analysis Reveals Reproducible Gut Microbiome Alterations in Response to a High-Fat Diet. *Cell Host Microbe* 26, 265–272. doi:10.1016/j.chom.2019.06.013
- Bolger, A.M., Lohse, M., Usadel, B., 2014. Trimmomatic: a flexible trimmer for Illumina sequence data. *J. Bioinform.* 30, 2114–2120. doi:10.1093/bioinformatics/btu170
- Boon, E., Meehan, C.J., Whidden, C., Wong, D.H.-J., Langille, M.G.I., Beiko, R.G., 2014. Interactions in the microbiome: communities of organisms and communities of genes. *FEMS Microbiol. Rev.* 38, 90–118. doi:10.1111/1574-6976.12035
- Böttcher, C., Chapman, A., Fellermeier, F., Choudhary, M., Scheel, D., Glawischnig, E., 2014. The Biosynthetic Pathway of Indole-3-Carbaldehyde and Indole-3-Carboxylic Acid Derivatives in Arabidopsis. *Plant Physiol.* 165, 841–853. doi:10.1104/pp.114.235630
- Braune, A., Blaut, M., 2016. Bacterial species involved in the conversion of dietary flavonoids in the human gut. *Gut Microbes* 7, 216–234. doi:10.1080/19490976.2016.1158395
- Breiman, L., 2001. Random Forests. *Mach. Learn.* 45, 5–32. doi: 10.1023/A:1010933404324
- Brestoff, J.R., Artis, D., 2013. Commensal bacteria at the interface of host metabolism and the immune system. *Nat. Immunol.* 14, 676–684. doi:10.1038/ni.2640
- Buchfink, B., Xie, C., Huson, D.H., 2014. Fast and sensitive protein alignment using DIAMOND. *Nat. Methods* 12, 59–60. doi:10.1038/nmeth.3176
- Buffie, C.G., Jarchum, I., Equinda, M., Lipuma, L., Gobourne, A., Viale, A., Ubeda, C., Xavier, J., Pamer, E.G., 2012. Profound alterations of intestinal microbiota following a single dose of clindamycin results in sustained susceptibility to Clostridium difficile-induced colitis. *Infect. Immun.* 80, 62–73. doi:10.1128/IAI.05496-11
- Bui, T.P.N., Schols, H.A., Jonathan, M., Stams, A.J.M., de Vos, W.M., Plugge, C.M., 2019. Mutual Metabolic Interactions in Co-cultures of the Intestinal Anaerostipes rhamnosivorans With an Acetogen, Methanogen, or Pectin-Degrader Affecting Butyrate Production. *Front. Microbiol.* 10, 1–12. doi:10.3389/fmicb.2019.02449
- Bui, T.P.N., Shetty, S.A., Lagkouvardos, I., Ritari, J., Chamlagain, B., Douillard, F.P., Paulin, L., Piironen, V., Clavel, T., Plugge, C.M., De Vos, W.M., 2016. Comparative genomics and physiology of the butyrate-producing bacterium Intestinimonas butyriciproducens. *Environ. Microbiol. Rep.* 8, 1024–1037. doi:10.1111/1758-2229.12483
- Burlingame, R., Chapman, P.J., 1983. Catabolism of Phenylpropionic Acid and Its 3-Hydroxy Derivative by *Escherichia coli*. *J. Bacteriol.* 155, 113–121. doi:10.1128/jb.155.1.113-121.1983
- Bushnell, B., 2014. BBMap: A fast, accurate, splice-aware aligner, in: Presented at the 9th Annual Genomics of Energy Environment Meeting, Walnut Creek, CA.
- Cabral, D.J., Penumutchu, S., Reinhart, E.M., Zhang, C., Korry, B.J., Wurster, J.I., Nilson, R., Guang, A., Sano, W.H., Rowan-Nash, A.D., Li, H., Belenky, P., 2019. Microbial Metabolism Modulates Antibiotic Susceptibility within the Murine Gut Microbiome. *Cell Metab.* 30, 800–823. doi:10.1016/j.cmet.2019.08.020
- Cabral, D.J., Wurster, J.I., Belenky, P., 2018. Antibiotic Persistence as a Metabolic Adaptation: Stress, Metabolism, the Host, and New Directions. *Pharmaceuticals* 11, 1–19. doi:10.3390/ph11010014
- Callahan, B.J., McMurdie, P.J., Rosen, M.J., Han, A.W., Johnson, A.J.A., Holmes, S.P., 2016. DADA2: High-resolution sample inference from Illumina amplicon data. *Nat. Methods* 13, 581–583. doi:10.1038/nmeth.3869

- Cantarel, B.L., Coutinho, P.M., Rancurel, C., Bernard, T., Lombard, V., Henrissat, B., 2009. The Carbohydrate-Active EnZymes database (CAZy): an expert resource for Glycogenomics. *Nucleic Acids Res.* 37, D233–D238. doi:10.1093/nar/gkn663
- Caporaso J.G., Lauber, C.L., Walters, W.A., Berg-Lyons, D., Huntley, J., Fierer, N., Owens, S.M., Betley, J., Fraser, L., Bauer, M., Gormley, N., Gilbert, J.A., Smith, G., Knight, R., 2012. Ultra-high-throughput microbial community analysis on the Illumina HiSeq and MiSeq platforms. *IMSE J.* 6, 1621-1624. doi:10.1038/ismej.2012.8
- Chang, J.Y., Antonopoulos, D.A., Kalra, A., Tonelli, A., Khalife, W.T., Schmidt, T.M., Young, V.B., 2008. Decreased diversity of the fecal microbiome in recurrent *Clostridium difficile*-associated diarrhea. *J. Infect. Dis.* 197, 435–438. doi:10.1086/525047
- Chao, P.-C., Li, Y., Chang, C.-H., Shieh, J.P., Cheng, J.-T., Cheng, K.-C., 2018. Investigation of insulin resistance in the popularly used four rat models of type-2 diabetes. *Biomed. Pharmacother.* 101, 155-161. doi:10.1016/j.biopha.2018.02.084
- Chassaing, B., Raja, S.M., Lewis, J.D., Srinivasan, S., Gewirtz, A.T., 2017. Colonic Microbiota Encroachment Correlates with Dysglycemia in Humans. *Cell. Mol. Gastroenterol. Hepatol.* 4, 205–221. doi:10.1016/j.jcmgh.2017.04.001
- Chen, L., Tuo, B., Dong, H., 2016. Regulation of Intestinal Glucose Absorption by Ion Channels and Transporters. *Nutrients* 8, 43–11. doi:10.3390/nu8010043
- Chen, M.X., Wang, S.-Y., Kuo, C.-H., Tsai, I.-L., 2019. Metabolome analysis for investigating host-gut microbiota interactions. *J. Formos. Med. Assoc.* 118, S10–S22. doi:10.1016/j.jfma.2018.09.007
- Chesta, J., Debnam, E.S., Srani, S.K.S., Epstein, O., 1990. Delayed stomach to caecum transit time in the diabetic rat. Possible role of hyperglucagonaemia. *Gut* 31, 660–662. doi:10.1136/gut.31.6.660
- Clarke, S.F., Murphy, E.F., Nilaweera, K., Ross, P.R., Shanahan, F., O’Toole, P.W., Cotter, P.D., 2012. The gut microbiota and its relationship to diet and obesity. *Gut Microbes* 3, 186–202. doi:10.4161/gmic.20168
- Clooney, A.G., Fouhy, F., Sleator, R.D., O’ Driscoll, A., Stanton, C., Cotter, P.D., Claesson, M.J., 2016. Comparing Apples and Oranges?: Next Generation Sequencing and Its Impact on Microbiome Analysis. *PLoS ONE* 11, e0148028–16. doi:10.1371/journal.pone.0148028
- Collins, J., Robinson, C., Danhof, H., Knetsch, C.W., van Leeuwen, H.C., Lawley, T.D., Auchtung, J.M., Britton, R.A., 2018. Dietary trehalose enhances virulence of epidemic *Clostridium difficile*. *Nature* 553, 291–294. doi:10.1038/nature25178
- Conlon, B.P., Rowe, S.E., Gandt, A.B., Nuxoll, A.S., Donegan, N.P., Zalis, E.A., Clair, G., Adkins, J.N., Cheung, A.L., Lewis, K., 2016. Persister formation in *Staphylococcus aureus* is associated with ATP depletion. *Nat. Microbiol.* 1, 16051. doi:10.1038/nmicrobiol.2016.51
- Coyte, K.Z., Rakoff-Nahoum, S., 2019. Understanding Competition and Cooperation within the Mammalian Gut Microbiome. *Curr. Biol.* 29, R583–R544. doi:10.1016/j.cub.2019.04.017
- Crost, E.H., Tailford, L.E., Monestier, M., Swarbreck, D., Henrissat, B., Crossman, L.C., Juge, N., 2016. The mucin-degradation strategy of *Ruminococcus gnavus*: The importance of intramolecular trans-sialidases. *Gut Microbes* 7, 302–312. doi:10.1080/19490976.2016.1186334
- Croswell, A., Amir, E., Tegatz, P., Barman, M., Salzman, N.H., 2009. Prolonged Impact of ATBs on Intestinal Microbial Ecology and Susceptibility to Enteric *Salmonella* Infection. *Infection and Immunity* 77, 2741–2753. doi:10.1128/IAI.00006-09

- Dabke, K., Hendrick, G., Devkota, S., 2019. The gut microbiome and metabolic syndrome. *J. Clin. Invest.* 129, 4050–4057. doi:10.1172/JCI129194
- David, L.A., Maurice, C.F., Carmody, R.N., Gootenberg, D.B., Button, J.E., Wolfe, B.E., Ling, A.V., Devlin, A.S., Varma, Y., Fischbach, M.A., Biddinger, S.B., Dutton, R.J., Turnbaugh, P.J., 2014. Diet rapidly and reproducibly alters the human gut microbiome. *Nature* 505, 559–563. doi:10.1038/nature12820
- Deeds, M.C., Anderson, J.M., Armstrong, A.S., Gastineau, D.A., Hiddinga, H.J., Jahangir, A., Eberhardt, N.L., Kudva, Y.C., 2011. Single dose streptozotocin-induced diabetes: considerations for study design in islet transplantation models. *Lab Anim.* 45, 131–140. doi:10.1258/la.2010.010090
- Deng, Z.-L., Sztajer, H., Jarek, M., Bhujju, S., Wagner-Döbler, I., 2018. Worlds Apart – Transcriptome Profiles of Key Oral Microbes in the Periodontal Pocket Compared to Single Laboratory Culture Reflect Synergistic Interactions. *Front. Microbiol.* 9, 1–15. doi:10.3389/fmicb.2018.00124
- Desai, M.S., Seekatz, A.M., Koropatkin, N.M., Kamada, N., Hickey, C.A., Wolter, M., Pudlo, N.A., Kitamoto, S., Terrapon, N., Muller, A., Young, V.B., Henrissat, B., Wilmes, P., Stappenbeck, T.S., Núñez, G., Martens, E.C., 2016. A Dietary Fiber-Deprived Gut Microbiota Degrades the Colonic Mucus Barrier and Enhances Pathogen Susceptibility. *Cell* 167, 1339–1353.e1321. doi: 10.1016/j.cell/2016.10.043
- Dethlefsen, L., Relman, D.A., 2011. Incomplete recovery and individualized responses of the human distal gut microbiota to repeated antibiotic perturbation. *Proc. Natl. Acad. Sci. USA.* 108, 4551–4561. doi:10.1073/pnas.1000087107
- Dwyer, D.J., Belenky, P.A., Yang, J.H., MacDonald, I.C., Martell, J.D., Takahashi, N., Chan, C.T.Y., Lobritz, M.A., Braff, D., Schwarz, E.G., Ye, J.D., Pati, M., Vercruyse, M., Ralifo, P.S., Allison, K.R., Khalil, A.S., Ting, A.Y., Walker, G.C., Collins, J.J., 2014. Antibiotics induce redox-related physiological alterations as part of their lethality. *Proc. Natl. Acad. Sci. USA.* 111, E2100–E2109. doi:10.1073/pnas.1401876111
- Edwards, R., 1997. Resistance to β -lactam ATBs in *Bacteroides* spp. *J. Med. Microbiol.* 46, 979–986. doi:10.1099/00222615-46-12-979
- Eleazu C.O., Eleazu K.C., Chukwuma S., Essien U.N., 2013. Review of the mechanism of cell death resulting from streptozotocin challenge in experimental animals, its practical use and potential risk to humans. *J. Diabetes Metab. Disord.* 12, 60. doi:10.1186/2251-6581-12-60
- Erhardt, M., Dersch, P., 2015. Regulatory principles governing Salmonella and Yersinia virulence. *Front. Microbiol.* 6, 1–20. doi:10.3389/fmicb.2015.00949
- Ernst, D.C., Downs, D.M., 2015. The STM4195 Gene Product (PanS) Transports Coenzyme A Precursors in *Salmonella enterica*. *J. Bacteriol.* 197, 1–10. doi:10.1128/JB.02506-14
- Fernández-Ochoa, Á., Cázares-Camacho, R., Borrás-Linares, I., Domínguez-Avila, J.A., Segura-Carretero, A., González-Aguilar, G.A., 2020. Evaluation of metabolic changes in liver and serum of streptozotocin-induced diabetic rats after Mango diet supplementation. *J. Funct. Foods* 64, 103695. doi:10.1016/j.jff.2019.103695
- Fischbach, M.A., Sonnenburg, J.L., 2011. Eating for two: how metabolism establishes interspecies interactions in the gut. *Cell Host Microbe* 10, 336–347. doi:10.1016/j.chom.2011.10.002
- Franzosa, E.A., McIver, L.J., Rahnavard, G., Thompson, L.R., Schirmer, M., Weingart, G., Lipson, K.S., Knight, R., Caporaso, J.G., Segata, N., Huttenhower, C., 2018. Species-level functional profiling of metagenomes and metatranscriptomes. *Nat. Methods* 15, 962–968. doi:10.1038/s41592-018-0176-y

- Fraser, C.M., Chapple, C., 2011. The Phenylpropanoid Pathway in Arabidopsis. *Arabidopsis Book* 9, e0152–19. doi:10.1199/tab.0152
- Furman, B.L., 2021. Streptozotocin-induced Diabetic Models in Mice and Rats. *Curr. Prot.*, 1, e78. doi:10.1002/cpz1.78
- Fuhrer, T., Heer, D., Begemann, B., Zamboni, N., 2011. High-Throughput, Accurate Mass Metabolome Profiling of Cellular Extracts by Flow Injection–Time-of-Flight Mass Spectrometry. *Anal. Chem.* 83, 7074–7080. doi:10.1021/ac201267k
- Fujisaka, S., Ussar, S., Clish, C., Devkota, S., Dreyfuss, J.M., Sakaguchi, M., Soto, M., Konishi, M., Softic, S., Altindis, E., Li, N., Gerber, G., Bry, L., Kahn, C.R., 2016. ATB effects on gut microbiota and metabolism are host dependent. *J. Clin. Invest.* 126, 4430–4443. doi:10.1172/JCI86674
- Gao, J., Xu, K., Liu, H., Liu, G., Bai, M., Peng, C., Li, T., Yin, Y., 2018. Impact of the Gut Microbiota on Intestinal Immunity Mediated by Tryptophan Metabolism. *Front. Cell. Infect. Microbiol.* 8, 1010–22. doi:10.3389/fcimb.2018.00013
- Garsin, D.A., 2010. Ethanolamine Utilization in Bacterial Pathogens: Roles and Regulation. *Nat. Rev. Micro.* 8, 290–295. doi:10.1038/nrmicro2334
- Gertsman, I., Barshop, B.A., 2018. Promises and pitfalls of untargeted metabolomics. *J. Inherit. Metab. Dis.* 41, 355–366. doi:10.1007/s10545-017-0130-7
- Goodman, A.L., McNulty, N.P., Zhao, Y., Leip, D., Mitra, R.D., Lozupone, C.A., Knight, R., Gordon, J.I., 2009. Identifying genetic determinants needed to establish a human gut symbiont in its habitat. *Cell Host Microbe* 6, 279–289. doi:10.1016/j.chom.2009.08.003
- Goyal, S.N., Reddy, N.M., Patil, K.R., Nakhate, K.T., Ojha, S., Patil, C.R., Agrawal, Y.O., 2016. Challenges and issues with streptozotocin-induced diabetes - A clinically relevant animal model to understand the diabetes pathogenesis and evaluate therapeutics. *Chem. Biol. Interact.* 244, 49–63. doi:10.1016/j.cbi.2015.11.032
- Grondin, J.M., Tamura, K., Déjean, G., Abbott, D.W., Brumer, H., 2017. Polysaccharide Utilization Loci: Fueling Microbial Communities. *J. Bacteriol.* 199, 237–15. doi:10.1128/JB.00860-16
- Hanafusa, T., Imagawa, A., 2008. Insulinitis in human type 1 diabetes. *Ann. N. Y. Acad. Sci.* 1150, 297–9. doi:10.1196/annals.1447.052
- Holscher, H.D., 2017. Dietary fiber and prebiotics and the gastrointestinal microbiota. *Gut Microbes*, 8, 172–184. doi:1080/19490976.2017.1290756
- Holst, J.J., Gribble, F., Horowitz, M., Rayner, C.K., 2016. Roles of the Gut in Glucose Homeostasis. *Diabetes Care* 39, 884–892. doi:10.2337/dc16-0351
- Iino, T., Mori, K., Tanaka, K., Suzuki, K.-I., Harayama, S., 2007. *Oscillibacter valericigenes* gen. nov., sp. nov., a valerate-producing anaerobic bacterium isolated from the alimentary canal of a Japanese corbicula clam. *Int. J. Syst. Evol. Microbiol.* 57, 1840–1845. doi:10.1099/ijs.0.64717-0
- Jain, N., Mishra, S.K., Shankar, U., Jaiswal, A., Sharma, T.K., Kodgire, P., Kumar, A., 2020. G-quadruplex stabilization in the ions and maltose transporters gene inhibit *Salmonella enterica* growth and virulence. *Genomics* 11, 4863–4874. doi:10.1016/j.ygeno.2020.09.010
- Johnson, E.L., Heaver, S.L., Waters, J.L., Kim, B.I., Bretin, A., Goodman, A.L., Gewirtz, A.T., Worgall, T.S., Ley, R.E., 2020. Sphingolipids produced by gut bacteria enter host metabolic pathways impacting ceramide levels. *Nat. Commun.* 11, 1–11. doi:10.1038/s41467-020-16274-w

- Kaakoush, N.O., 2015. Insights into the Role of Erysipelotrichaceae in the Human Host. *Front. Cell. Infect. Microbiol.* 5, 181–4. doi:10.3389/fcimb.2015.00084
- Kaiko, G.E., Stappenbeck, T.S., 2014. Host–microbe interactions shaping the gastrointestinal environment. *Trends Immunol.* 35, 538–548. doi:10.1016/j.it.2014.08.002
- Kazemian, N., Ramezankhani, M., Sehgal, A., Khalid, F.M., Kalkhoran, A.H.Z., Narayan, A., Wong, G.K.-S., Kao, D., Pakpour, S., 2020. The trans-kingdom battle between donor and recipient gut microbiome influences fecal microbiota transplantation outcome. *Sci. Rep.* 1–10. doi:10.1038/s41598-020-75162-x
- Kobayashi, K., Forte, T.M., Taniguchi, S., Ishida, B.Y., Oka, K., Chan, L., 2000. The *db/db* mouse, a model for diabetic dyslipidemia: molecular characterization and effect of western diet feeding. *Metabolism* 49, 22–31. doi:10.1016/s0026-0495(00)90588-2
- Koepsell, H., 2020. Glucose transporters in the small intestine in health and disease. *Pflugers Arch.* 472, 1207–1248. doi:10.1007/s00424-020-02439-5
- Kohanski, M.A., Dwyer, D.J., Hayete, B., Lawrence, C.A., Collins, J.J., 2007. A Common Mechanism of Cellular Death Induced by Bactericidal Antibiotics. *Cell* 130, 797–810. doi:10.1016/j.cell.2007.06.049
- Kolb, H., 1987. Mouse models of insulin dependent diabetes: low-dose streptozotocin-induced diabetes and nonobese diabetic (NOD) mice. *Diabetes Metab. Rev.* 3, 751–778. doi:10.1002/dmr.5610030308
- Kuno, T., Hirayama-Kurogi, M., Ito, S., Ohtsuki, S., 2018. Reduction in hepatic secondary bile acids caused by short-term antibiotic-induced dysbiosis decreases mouse serum glucose and triglyceride levels. *Sci. Rep.* 1–15. doi:10.1038/s41598-018-19545-1
- Kuribayashi, H., Miyata, M., Yamakawa, H., Yoshinari, K., Yamazoe, Y., 2012. Enterobacteria-mediated deconjugation of taurocholic acid enhances ileal farnesoid X receptor signaling. *Eur.J. of Pharmacol.* 697, 132–138. doi:10.1016/j.ejphar.2012.09.048
- Lam, P.L., Wong, R.S.M., Lam, K.H., Hung, L.K., Wong, M.M., Yung, L.H., Ho, Y.W., Wong, W.Y., Hau, D.K.P., Gambari, R., Chui, C.H., 2020. The role of reactive oxygen species in the biological activity of antimicrobial agents: An updated mini review. *Chem. Biol. Interact.* 320, 109023. doi:10.1016/j.cbi.2020.109023
- Langmead, B., Salzberg, S.L., 2012. Fast gapped-read alignment with Bowtie 2. *Nat. Methods* 9, 357–359. doi:10.1038/nmeth.1923
- Layeghifard, M., Hwang, D.M., Guttman, D.S., 2017. Disentangling Interactions in the Microbiome: A Network Perspective. *Trends Microbiol.* 25, 217–228. doi:10.1016/j.tim.2016.11.008
- Lee H.L., Si H.Y., Jung M.O.H., Myung G.L., 2010. Pharmacokinetics of drugs in rats with diabetes mellitus induced by alloxan or streptozocin: comparison with those in patients with type I diabetes mellitus. *J. Pharm. Pharmacol.* 62: 1–23. doi:10.1211/jpp.62.01.0001
- Lei, Z., Huhman, D.V., Sumner, L.W., 2011. Mass Spectrometry Strategies in Metabolomics. *J. Biol. Chem.* 286, 25435–25422. doi:10.1074/jbc.R111.238691
- Ley, R.E., 2014. Harnessing Microbiota to Kill a Pathogen: The sweet tooth of *Clostridium difficile*. *Nat. Med.* 20, 248–249. doi:10.1038/nm.3494
- Li, H., Durbin, R., 2010. Fast and accurate long-read alignment with Burrows–Wheeler transform. *Bioinformatics* 26, 589–595. doi:10.1093/bioinformatics/btp698
- Li, T., Francl, J.M., Boehme, S., Ochoa, A., Zhang, Y., Klaassen, C.D., Erickson, S.K., Chiang, J.Y.L., 2012. Glucose and Insulin Induction of Bile Acid Synthesis: Mechanisms and

- Implication in Diabetes and Obesity*. *J. Biol. Chem.* 287, 1861–1873. doi:10.1074/jbc.M111.305789
- Liao, Y., Smyth, G.K., Shi, W., 2014. featureCounts: an efficient general purpose program for assigning sequence reads to genomic features. *Bioinformatics*, 30, 923–930. doi:10.1093/bioinformatics/btt656
- Liu, S., Qin, P., Wang, J., 2019. High-Fat Diet Alters the Intestinal Microbiota in Streptozotocin-Induced Type 2 Diabetic Mice. *Microorganisms* 7, 1–12. doi:10.3390/microorganisms7060176
- Lobritz, M.A., Belenky, P., Porter, C.B.M., Gutierrez, A., Yang, J.H., Schwarz, E.G., Dwyer, D.J., Khalil, A.S., Collins, J.J., 2015. Antibiotic efficacy is linked to bacterial cellular respiration. *Proc. Natl. Acad. Sci. USA.* 112, 8173–8180. doi:10.1073/pnas.1509743112
- Love, M.I., Huber, W., Anders, S., 2014. Moderated estimation of fold change and dispersion for RNA-seq data with DESeq2. *Genome Biol.* 15, 31–21. doi:10.1186/s13059-014-0550-8
- Lu, J., Breitwieser, F.P., Thielen, P., Salzberg, S.L., 2017. Bracken: estimating species abundance in metagenomics data. *PeerJ Comput. Sci.* 3, 1–17. doi:10.7717/peerj-cs.104
- Luan, H., Wang, X., Cai, Z., 2019. Mass spectrometry-based metabolomics: Targeting the crosstalk between gut microbiota and brain in neurodegenerative disorders. *Mass Spectrom. Rev.* 38, 22–33. doi:10.1002/mas.21553
- Lundgren, P., Thaiss, C.A., 2020. The microbiome-adipose tissue axis in systemic metabolism. *Am. J. Physiol. Gastrointest. Liver Physiol.* 318, G717–G724. doi:10.1152/ajpgi.00304.2019
- Lynch, J.B., Sonnenburg, J.L., 2012. Prioritization of a plant polysaccharide over a mucus carbohydrate is enforced by a *Bacteroides* hybrid two-component system. *Mol. Microbiol.* 85, 478–491. doi:10.1111/j.1365-2958.2012.08123.x
- Ma, Q., Li, Y., Wang, J., Li, P., Duan, Y., Dai, H., An, Y., Cheng, L., Wang, T., Wang, C., Wang, T., Zhao, B., 2020. Investigation of gut microbiome changes in type 1 diabetic mellitus rats based on high-throughput sequencing. *Biomed. Pharmacother.* 124, 109873. doi:10.1016/j.biopha.2020.109873
- Makki, K., Deehan, E.C., Walter, J., Bäckhed, F., 2018. The Impact of Dietary Fiber on Gut Microbiota in Host Health and Disease. *Cell Host Microbe* 23, 705–715. doi:10.1016/j.chom.2018.05.012
- Mardo, K., Visnapuu, T., Vija, H., Aasamets, A., Viigand, K., Alamäe, T., 2017. A Highly Active Endo-Levanase BT1760 of a Dominant Mammalian Gut Commensal *Bacteroides theta* Cleaves Not Only Various Bacterial Levans, but Also Levan of Timothy Grass. *PLoS ONE* 12, e0169989–25. doi:10.1371/journal.pone.0169989
- Martens, E.C., Chiang, H.C., Gordon, J.I., 2008. Mucosal glycan foraging enhances fitness and transmission of a saccharolytic human gut bacterial symbiont. *Cell Host Microbe* 4, 447–457. doi:10.1016/j.chom.2008.09.007
- Martínez, I., Perdicaro, D.J., Brown, A.W., Hammons, S., Carden, T.J., Carr, T.P., Eskridge, K.M., Walter, J., 2013. Diet-Induced Alterations of Host Cholesterol Metabolism Are Likely To Affect the Gut Microbiota Composition in Hamsters. *Appl. Environ. Microbiol.* 79, 516–524. doi:10.1128/AEM.03046-12
- McCoy, J.G., Levin, E.J., Zhou, M., 2015. Structural insight into the PTS sugar transporter EIIC. *Biochim. Biophys. Acta.* 1850, 577–585. doi:10.1016/j.bbagen.2014.03.013
- McIver, L.J., Abu-Ali, G., Franzosa, E.A., Schwager, R., Morgan, X.C., Waldron, L., Segata, N., Huttenhower, C., 2018. bioBakery: a meta’omic analysis environment. *J. Bioinform.* 34, 1235–1237. doi:10.1093/bioinformatics/btx754

- McLaren, M.R., Willis, A.D., Callahan, B.J., 2019. Consistent and correctable bias in metagenomic sequencing experiments. *eLife* 8, e46923. doi:10.7554.eLife.46923
- McMurdie, P.J., Holmes, S., 2013. phyloseq: An R Package for Reproducible Interactive Analysis and Graphics of Microbiome Census Data. *PLoS ONE* 8, e61217–11. doi:10.1371/journal.pone.0061217
- Meadows, J.A., Wargo, M.J., 2015. Carnitine in bacterial physiology and metabolism. *Microbiology* 161, 1161–1174. doi:10.1099/mic.0.000080
- Mewis, K., Lenfant, N., Lombard, V., Henrissat, B., 2016. Dividing the Large Glycoside Hydrolase Family 43 into Subfamilies: a Motivation for Detailed Enzyme Characterization. *Appl. Environ. Microbiol.* 82, 1686–1692. doi:10.1128/AEM.03453-15
- Meylan, S., Porter, C.B.M., Yang, J.H., Belenky, P., Gutierrez, A., Lobritz, M.A., Park, J., Kim, S.H., Moskowicz, S.M., Collins, J.J., 2017. Carbon Sources Tune Antibiotic Susceptibility in *Pseudomonas aeruginosa* via Tricarboxylic Acid Cycle Control. *Cell Chem. Biol.* 24, 195–206. doi:10.1016/j.chembiol.2016.12.015
- Miller, K.A., Phillips, R.S., Mrazek, J., Hoover, T.R., 2013. Salmonella Utilizes D-Glucosaminase via a Mannose Family Phosphotransferase System Permease and Associated Enzymes. *J. Bacteriol.* 195, 4057–4066. doi:10.1128/JB.00290-13
- Mimee, M., Tucker, A.C., Voigt, C.A., Lu, T.K., 2015. Programming a Human Commensal Bacterium, *Bacteroides theta*, to Sense and Respond to Stimuli in the Murine Gut Microbiota. *Cell Syst.* 1, 62–71. doi:10.1016/j.cels.2015.06.001
- Moore, B.S., Hertweck, C., Hopke, J.N., Izumikawa, M., Kalaitzis, J.A., Nilsen, G., O'Hare, T., Piel, J., Shipley, P.R., Xiang, L., Austin, M.B., Noel, J.P., 2002. Plant-like Biosynthetic Pathways in Bacteria: From Benzoic Acid to Chalcone *J. Nat. Prod.* 65, 1956–1962. doi:10.1021/np020230m
- Motyl, K., McCabe, L.R., 2009. Streptozotocin, Type I Diabetes Severity and Bone. *Biol. Proced. Online* 11, 296–315. doi:10.1007/s12575-009-9000-5
- Nawrocki, K.L., Wetzell, D., Jones, J.B., Woods, E.C., McBride, S.M., 2018. Ethanolamine is a Valuable Nutrient Source that Impacts *Clostridium difficile* Pathogenesis. *Environ. Microbiol.* 20, 1419–1435. doi:10.1111/1462-2920.14048
- Neis, E., Dejong, C., Rensen, S., 2015. The Role of Microbial Amino Acid Metabolism in Host Metabolism. *Nutrients* 7, 2930–2946. doi:10.3390/nu7042930
- Newman, M.A., Petri, R.M., Gröll, D., Zebeli, Q., Metzler-Zebeli, B.U., 2018. Transglycosylated Starch Modulates the Gut Microbiome and Expression of Genes Related to Lipid Synthesis in Liver and Adipose Tissue of Pigs. *Front. Microbiol.* 9, 5245–17. doi:10.3389/fmicb.2018.00224
- Ng, K.M., Aranda-Díaz, A., Tropini, C., Frankel, M.R., Van Treuren, W., O'Loughlin, C.T., Merrill, B.D., Yu, F.B., Pruss, K.M., Oliveira, R.A., Higginbottom, S.K., Neff, N.F., Fischbach, M.A., Xavier, K.B., Sonnenburg, J.L., Huang, K.C., 2019. Recovery of the Gut Microbiota after Antibiotics Depends on Host Diet, Community Context, and Environmental Reservoirs. *Cell Host Microbe* 26, 650–665.e4. doi:10.1016/j.chom.2019.10.011
- Noecker, C., Eng, A., Srinivasan, S., Theriot, C.M., Young, V.B., Jansson, J.K., Fredricks, D.V., Borenstein, E., 2016. Metabolic Model-Based Integration of Microbiome Taxonomic and Metabolomic Profiles Elucidates Mechanistic Links between Ecological and Metabolic Variation. *mSystems*, 1(1): e00013-15. doi:10.1128/mSystems.00013-15
- Nothias, L.-F., Petras, D., Schmid, R., Dührkop, K., Rainer, J., Sarvepalli, A., Protsyuk, I., Ernst, M., Tsugawa, H., Fleischauer, M., Aicheler, F., Aksenov, A.A., Alka, O., Allard, P.-M.,

- Barsch, A., Cachet, X., Caraballo-Rodriguez, A.M., Da Silva, R.R., Dang, T., Garg, N., Gauglitz, J.M., Gurevich, A., Isaac, G., Jarmusch, A.K., Kameník, Z., Kang, K.B., Kessler, N., Koester, I., Korf, A., Le Gouellec, A., Ludwig, M., Martin, C.H., McCall, L.-I., McSayles, J., Meyer, S.W., Mohimani, H., Morsy, M., Moyne, O., Neumann, S., Neuweger, H., Nguyen, N.H., Nothias-Esposito, M., Paolini, J., Phelan, V.V., Pluskal, T., Quinn, R.A., Rogers, S., Shrestha, B., Tripathi, A., van der Hoof, J.J.J., Vargas, F., Weldon, K.C., Witting, M., Yang, H., Zhang, Z., Zubeil, F., Kohlbacher, O., Böcker, S., Alexandrov, T., Bandeira, N., Wang, M., Dorrestein, P.C., 2020. Feature-based molecular networking in the GNPS analysis environment. *Nat. Methods* 17, 905-908. doi:10.1038/s41592-020-0933-6
- Oliphant, K., Allen-Vercoe, E., 2019. Macronutrient metabolism by the human gut microbiome: major fermentation by-products and their impact on host health. *Microbiome* 7, 1–15. doi:10.1186/s40168-019-0704-8
- Ormsby, M.J., Logan, M., le A Johnson, S.Å., McIntosh, A., Fallata, G., Papadopoulou, R., Papachristou, E., Hold, G.L., Hansen, R., Ijaz, U.Z., Russell, R.K., Gerasimidis, K., Wall, D.M., 2019. Inflammation associated ethanolamine facilitates infection by Crohn's disease-linked adherent-invasive *Escherichia coli*. *EBioMedicine* 43, 325–332. doi:10.1016/j.ebiom.2019.03.071
- Overbeek, R., Olson, R., Pusch, G.D., Olsen, G.J., Davis, J.J., Disz, T., Edwards, R.A., Gerdes, S., Parrello, B., Shukla, M., Vonstein, V., Wattam, A.R., Xia, F., Stevens, R., 2014. The SEED and the Rapid Annotation of microbial genomes using Subsystems Technology (RAST). *Nucleic Acids Res.* 42, D206–D214. doi:10.1093/nar/gkt1226
- Patterson, E., Stanton, C., Cryan, J.F., Fitzgerald, G.F., Ross, R.P., Dinan, T.G., Fitzgerald, P., Marques, T.M., Cotter, P.D., O'Sullivan, O., 2015. Streptozotocin-induced type-1-diabetes disease onset in Sprague–Dawley rats is associated with an altered intestinal microbiota composition and decreased diversity. *Microbiology* 161, 182–193. doi:10.1099/mic.0.082610-0
- Pluskal, T., Castillo, S., Villar-Briones, A., Orešič, M., 2010. MZmine 2: Modular framework for processing, visualizing, and analyzing mass spectrometry-based molecular profile data. *BMC Bioinformatics* 11, 1–11. doi:10.1186/1471-2105-11-395
- Poretzky, R., Rodriguez-R, L.M., Luo, C., Tsementzi, D., Konstantinidis, K.T., 2014. Strengths and Limitations of 16S rRNA Gene Amplicon Sequencing in Revealing Temporal Microbial Community Dynamics. *PLoS ONE* 9, e93827–12. doi:10.1371/journal.pone.0093827
- Pruesse, E., Quast, C., Knittel, K., Fuchs, B.M., Ludwig, W., Peplies, J., Glockner, F.O., 2007. SILVA: a comprehensive online resource for quality checked and aligned ribosomal RNA sequence data compatible with ARB. *Nucleic Acids Research* 35, 7188–7196. doi:10.1093/nar/gkm864
- Qin, J., Li, Y., Cai, Z., Li, S., Zhu, J., Zhang, F., Liang, S., Zhang, W., Guan, Y., Shen, D., Peng, Y., Zhang, D., Jie, Z., Wu, W., Qin, Y., Xue, W., Li, J., Han, L., Lu, D., Wu, P., Dai, Y., Sun, X., Li, Z., Tang, A., Zhong, S., Li, X., Chen, W., Xu, R., Wang, M., Feng, Q., Gong, M., Yu, J., Zhang, Y., Zhang, M., Hansen, T., Sanchez, G., Raes, J., Falony, G., Okuda, S., Almeida, M., LeChatelier, E., Renault, P., Pons, N., Batto, J.-M., Zhang, Z., Chen, H., Yang, R., Zheng, W., Li, S., Yang, H., Wang, J., Ehrlich, S.D., Nielsen, R., Pedersen, O., Kristiansen, K., Wang, J., 2012. A metagenome-wide association study of gut microbiota in type 2 diabetes. *Nature* 490, 55–60. doi:10.1038/nature11450
- Quinn, R.A., Melnik, A.V., Vrbanc, A., Fu, T., Patras, K.A., Christy, M.P., Bodai, Z., Belda-Ferre, P., Tripathi, A., Chung, L.K., Downes, M., Welch, R.D., Quinn, M., Humphrey, G.,

- Panitchpakdi, M., Weldon, K.C., Aksenov, A., Silva, R., Avila-Pacheco, J., Clish, C., Bae, S., Mallick, H., Franzosa, E.A., Lloyd-Price, J., Bussell, R., Thron, T., Nelson, A.T., Wang, M., Leszczynski, E., Vargas, F., Gauglitz, J.M., Meehan, M.J., Gentry, E., Arthur, T.D., Komor, A.C., Poulsen, O., Boland, B.S., Chang, J.T., Sandborn, W.J., Lim, M., Garg, N., Lumeng, J.C., Xavier, R.J., Kazmierczak, B.I., Jain, R., Egan, M., Rhee, K.E., Ferguson, D., Raffatellu, M., Vlamakis, H., Haddad, G.G., Siegel, D., Huttenhower, C., Mazmanian, S.K., Evans, R.M., Nizet, V., Knight, R., Dorrestein, P.C., 2020. Global chemical effects of the microbiome include new bile-acid conjugations. *Nature* 579, 123–129. doi:10.1038/s41586-020-2047-9
- Ranjan, R., Rani, A., Metwally, A., McGee, H.S., Perkins, D.L., 2016. Analysis of the microbiome: Advantages of whole genome shotgun versus 16S amplicon sequencing. *Biochem. Biophys. Res. Commun.* 469, 967–977. doi:10.1016/j.bbrc.2015.12.083
- Rayner, C.K., Horowitz, M., 2006. Gastrointestinal motility and glycemic control in diabetes: the chicken and the egg revisited? *Journal of Clinical Investigation* 116, 299–302. doi:10.1172/JCI27758
- Reese, A.T., Carmody, R.N., 2019. Thinking Outside the Cereal Box: Noncarbohydrate Routes for Dietary Manipulation of the Gut Microbiota. *Appl. Environ. Microbiol.* 85, 1–17. doi:10.1128/AEM.02246-18
- Rey, F.E., Faith, J.J., Bain, J., Muehlbauer, M.J., Stevens, R.D., Newgard, C.B., Gordon, J.I., 2010. Dissecting the *in vivo* metabolic potential of two human gut acetogens. *J. Biol. Chem.* 285, 22082–22090. doi:10.1074/jbc.M110.117713
- Rhen, M., 2019. *Salmonella* and Reactive Oxygen Species: A Love-Hate Relationship. *J. Innate Immunity* 11, 216–226. doi:10.1159/000496370
- Ridlon, J.M., Kang, D.J., Hylemon, P.B., Bajaj, J.S., 2014. Bile acids and the gut microbiome. *Curr. Opin. Gastroenter.* 30, 332–338. doi:10.1097/MOG.0000000000000057
- Rivera-Chávez, F., Zhang, L.F., Faber, F., Lopez, C.A., Byndloss, M.X., Olsan, E.E., Xu, G., Velazquez, E.M., Lebrilla, C.B., Winter, S.E., Bäuml, A.J., 2016. Depletion of Butyrate-Producing Clostridia from the Gut Microbiota Drives an Aerobic Luminal Expansion of *Salmonella*. *Cell Host Microbe* 19, 443–454. doi:10.1016/j.chom.2016.03.004
- Rowley, C.A., Anderson, C.J., Kendall, M.M., 2018. Ethanolamine Influences Human Commensal *Escherichia coli* Growth, Gene Expression, and Competition with Enterohemorrhagic *E. coli* O157:H7. *mBio* 9, e01429–18. doi:10.1128/mBio.01429-18
- Sabatino, A., Regolisti, G., Cosola, C., Gesualdo, L., Fiaccadori, E., 2017. Intestinal Microbiota in Type 2 Diabetes and Chronic Kidney Disease. *Curr. Diab. Rep.* 1–9. doi:10.1007/s11892-017-0841-z
- Saeedi, P., Petersohn, I., Salpea, P., Malanda, B., Karuranga, S., Unwin, N., Colagiuri, S., Guariguata, L., Motala, A.A., Ogurtsova, K., Shaw, J.E., Bright, D., Williams, R., 2019. Global and regional diabetes prevalence estimates for 2019 and projections for 2030 and 2045: Results from the International Diabetes Federation Diabetes Atlas, 9th edition. *Diabetes Res. Clin. Pract.* 157, 107843–27. doi:10.1016/j.diabres.2019.107843
- Sato, H., Zhang, L.S., Martinez, K., Chang, E.B., Yang, Q., Wang, F., Howles, P.N., Hokari, R., Miura, S., Tso, P., 2016. Antibiotics Suppress Activation of Intestinal Mucosal Mast Cells and Reduce Dietary Lipid Absorption in Sprague-Dawley Rats. *Gastroenterology* 151, 923–932. doi:10.1053/j.gastro.2016.07.009
- Schoeler, M., Caesar, R., 2019. Dietary lipids, gut microbiota and lipid metabolism. *Rev. Endocr. Metab. Disord.* 20, 461–472. doi:10.1007/s11154-019-09512-0

- Schrimpe-Rutledge, A.C., Codreanu, S.G., Sherrod, S.D., McLean, J.A., 2016. Untargeted Metabolomics Strategies—Challenges and Emerging Directions. *J. Am. Soc. Mass Spectrom.* 27, 1897–1905. doi:10.1007/s13361-016-1469-y
- Segata, N., Izard, J., Waldron, L., Gevers, D., Miropolsky, L., Garrett, W.S., Huttenhower, C., 2011. Metagenomic biomarker discovery and explanation. *Genome Biol.* 12, R60. doi:10.1186/gb-2011-12-6-r60
- Segata, N., Waldron, L., Ballarini, A., Narasimhan, V., Jousson, O., Huttenhower, C., 2012. Metagenomic microbial community profiling using unique clade-specific marker genes. *Nat. Methods*, 8, 811-814.
- Shin, A., Preidis, G.A., Shulman, R., Kashyap, P.C., 2019. The Gut Microbiome in Adult and Pediatric Functional Gastrointestinal Disorders. *Clin. Gastroenterol. Hepatol.* 17, 256–274. doi:10.1016/j.cgh.2018.08.054
- Sliwkowski, M.X., Stadtman, T.C., 1988. Selenoprotein A of the clostridial glycine reductase complex: Purification and amino acid sequence of the selenocysteine-containing peptide. *Proc. Natl. Acad. Sci. USA.* 85, 368–371.
- Smits, S.A., Leach, J., Sonnenburg, E.D., Gonzalez, C.G., Lichtman, J.S., Reid, G., Knight, R., Manjurano, A., Changalucha, J., Elias, J.E., Dominguez-Bello, M.G., Sonnenburg, J.L., 2017. Seasonal cycling in the gut microbiome of the Hadza hunter-gatherers of Tanzania. *Science* 357, 802–806. doi:10.1126/science.aan4834
- Sonnenburg, J.L., Xu, J., Leip, D.D., Chen, C.-H., Westover, B.P., Weatherford, J., Buhler, J.D., Gordon, J.I., 2005. Glycan foraging in vivo by an intestine-adapted bacterial symbiont. *Science* 307, 1952–1955. doi:10.1126/science.1109051
- Srikumar, S., Fuchs, T.M., 2011. Ethanolamine Utilization Contributes to Proliferation of *Salmonella enterica* Serovar Typhimurium in Food and in Nematodes. *Appl. Environ. Microbiol.* 77, 1–10. doi:10.1128/AEM.01403-10
- Staley, C., Weingarden, A.R., Khoruts, A., Sadowsky, M.J., 2017. Interaction of gut microbiota with bile acid metabolism and its influence on disease states. *Appl. Microbiol. Biotechnol.* 101, 47–64. doi:10.1007/s00253-016-8006-6
- Steinert, R.E., Lee, Y.-K., Sybesma, W., 2020. Vitamins for the Gut Microbiome. *Trends Mol. Med.* 26, 137–140. doi:10.1016/j.molmed.2019.11.005
- Stokes, J.M., Lopatkin, A.J., Lobritz, M.A., Collins, J.J., 2019. Bacterial Metabolism and Antibiotic Efficacy. *Cell Metab.* 30, 251–259. doi:10.1016/j.cmet.2019.06.009
- Tanes, C., Bittinger, K., Gao, Y., Friedman, E.S., Nessel, L., Paladhi, U.R., Chau, L., Panfen, E., Fischbach, M.A., Braun, J., Xavier, R.J., Clish, C.B., Li, H., Bushman, F.D., Lewis, J.D., Wu, G.D., 2021. Role of dietary fiber in the recovery of the human gut microbiome and its metabolome. *Cell Host Microbe* 1–20. doi:10.1016/j.chom.2020.12.012
- Tang, M., Etokidem, E., Lai, K., 2016. The Leloir Pathway of Galactose Metabolism – A Novel Therapeutic Target for Hepatocellular Carcinoma. *Anticancer Res.* 36, 6265–6272. doi:10.21873/anticancer.11221
- Taylor, S.J., Winter, S.E., 2020. Salmonella finds a way: Metabolic versatility of *Salmonella enterica* serovar Typhimurium in diverse host environments. *PLoS Pathog* 16. doi:10.1371/journal.ppat.1008540
- Terrapon, N., Lombard, V., Gilbert, H.J., Henrissat, B., 2015. Automatic prediction of polysaccharide utilization loci in Bacteroidetes species. *Bioinformatics* 31, 647–655. doi:10.1093/bioinformatics/btu716

- Thaiss, C.A., Levy, M., Grosheva, I., Zheng, D., Soffer, E., Blacher, E., Braverman, S., Tengeler, A.C., Barak, O., Elazar, M., Ben-Zeev, R., Lehavi-Regev, D., Katz, M.N., Pevsner-Fischer, M., Gertler, A., Halpern, Z., Harmelin, A., Amar, S., Serradas, P., Grosfeld, A., Shapiro, H., Geiger, B., Elinav, E., 2018. Hyperglycemia drives intestinal barrier dysfunction and risk for enteric infection. *Science* 359, 1376–1383. doi:10.1126/science.aar3318
- The Human Microbiome Project Consortium, 2012. A framework for human microbiome research. *Nature* 486, 215–221. doi:10.1038/nature11209
- Theriot, C.M., Bowman, A.A., Young, V.B., 2016. Antibiotic-Induced Alterations of the Gut Microbiota Alter Secondary Bile Acid Production and Allow for *Clostridium difficile* Spore Germination and Outgrowth in the Large Intestine. *mSphere* 1, e00045–15–16. doi:10.1128/mSphere.00045-15
- Theriot, C.M., Young, V.B., 2015. Interactions Between the Gastrointestinal Microbiome and *Clostridium difficile*. *Annu. Rev. Microbiol.* 69, 445–461. doi:10.1146/annurev-micro-091014-104115
- Thiennimitr, P., Winter, S.E., Winter, M.G., Xavier, M.N., Tolstikov, V., Huseby, D.L., Sterzenbach, T., Tsohis, R.M., Roth, J.R., Bäuml, A.J., 2011. Intestinal inflammation allows *Salmonella* to use ethanolamine to compete with the microbiota. *Proc. Natl. Acad. Sci. USA* 108, 1–6. doi:10.1073/pnas.1107857108
- Thomas, V.C., Kinkead, L.C., Janssen, A., Schaeffer, C.R., Woods, K.M., Lindgren, J.K., Peaster, J.M., Chaudhari, S.S., Sadykov, M., Jones, J., Mohamadi AbdelGhani, S.M., Zimmerman, M.C., Bayles, K.W., Somerville, G.A., Fey, P.D., 2013. A Dysfunctional Tricarboxylic Acid Cycle Enhances Fitness of *Staphylococcus* β -Lactam Stress. *mBio* 4, e00437–13. doi:10.1128/mBio.00437-13
- Thompson, L.R., Sanders, J.G., McDonald, D., Amir, A., Ladau, J., Locey, K.J., Prill, R.J., Tripathi, A., Gibbons, S.M., Ackermann, G., Navas-Molina, J.A., Janssen, S., Kopylova, E., Vázquez-Baeza, Y., González, A., Morton, J.T., Mirarab, S., Zech Xu, Z., Jiang, L., Haroon, M.F., Kanbar, J., Zhu, Q., Jin Song, S., Kosciulek, T., Bokulich, N.A., Lefler, J., Brislawn, C.J., Humphrey, G., Owens, S.M., Hampton-Marcell, J., Berg-Lyons, D., McKenzie, V., Fierer, N., Fuhrman, J.A., Clausen, A., Stevens, R.L., Shade, A., Pollard, K.S., Goodwin, K.D., Jansson, J.K., Gilbert, J.A., Knight, R., The Earth Microbiome Project Consortium, 2017. A communal catalogue reveals Earth’s multiscale microbial diversity. *Nature* 551, 457–463. doi:10.1038/nature24621
- Tian, L., Wang, X.-W., Wu, A.-K., Fan, Y., Friedman, J., Dahlin, A., Waldor, M.K., Weinstock, G.M., Weiss, S.T., Liu, Y.-Y., 2020. Deciphering functional redundancy in the human microbiome. *Nat. Commun.* 1–11. doi:10.1038/s41467-020-19940-1
- Townsend, G.E., II, Han, W., Schwalm, N.D., III, Hong, X., Bencivenga-Barry, N.A., Goodman, A.L., Groisman, E.A., 2020. A Master Regulator of *Bacteroides theta* Gut Colonization Controls Carbohydrate Utilization and an Alternative Protein Synthesis Factor. *mBio* 11, 34–15. doi:10.1128/mBio.03221-19
- Tzin, V., Galili, G., 2010. The Biosynthetic Pathways for Shikimate and Aromatic Amino Acids in *Arabidopsis thaliana*, *The Arabidopsis Book*. doi:10.1199/tab.0132
- Ugarte, M., Brown, M., Hollywood, K.A., Cooper, G.J., Bishop, P.N., Dunn, W.B., 2012. Metabolomic analysis of rat serum in streptozotocin-induced diabetes and after treatment with oral triethylenetetramine (TETA). *Genome Med.* 4, 35. doi:10.1186/gm334

- Ussar, S., Haering, M.-F., Fujisaka, S., Lutter, D., Lee, K.Y., Li, N., Gerber, G.K., Bry, L., Kahn, C.R., 2017. Regulation of Glucose Uptake and Enteroendocrine Function by the Intestinal Epithelial Insulin Receptor. *Diabetes* 66, 886–896. doi:10.2337/db15-1349
- Vacca, M., Celano, G., Calabrese, F.M., Portincasa, P., Gobbetti, M., De Angelis, M., 2020. The Controversial Role of Human Gut Lachnospiraceae. *Microorganisms* 8, 573–25. doi:10.3390/microorganisms8040573
- Vollmer, M., Esders, S., Farquharson, F.M., Neugart, S., Duncan, S.H., Schreiner, M., Louis, P., Maul, R., Rohn, S., 2018. Mutual Interaction of Phenolic Compounds and Microbiota: Metabolism of Complex Phenolic Apigenin- C- and Kaempferol- O-Derivatives by Human Fecal Samples. *J. Agric. Food Chem.* 66, 485–497. doi:10.1021/acs.jafc.7b04842
- Vrieze, A., Out, C., Fuentes, S., Jonker, L., Reuling, I., Kootte, R.S., van Nood, E., Holleman, F., Knaapen, M., Romijn, J.A., Soeters, M.R., Blaak, E.E., Dallinga-Thie, G.M., Reijnders, D., Ackermans, M.T., Serlie, M.J., Knop, F.K., Holst, J.J., van der Ley, C., Kema, I.P., Zoetendal, E.G., De Vos, W.M., Hoekstra, J.B.L., Stroes, E.S., Groen, A.K., Nieuwdorp, M., 2014. Impact of oral vancomycin on gut microbiota, bile acid metabolism, and insulin sensitivity. *J. Hepatol.* 60, 824–831. doi:10.1016/j.jhep.2013.11.034
- Wang, C.-Y., Liao, J.K., 2012. A Mouse Model of Diet-Induced Obesity and Insulin Resistance, in: Allen, I.C. (Ed.), *Mouse Models of Innate Immunity, Methods Mol. Biol.* 821, 421–433. doi:10.1007/978-1-61779-430-8_27
- Wang, M., Carver, J.J., Phelan, V.V., Sanchez, L.M., Garg, N., Peng, Y., Nguyen, D.D., Watrous, J., Kaponov, C.A., Luzzatto-Knaan, T., Porto, C., Bouslimani, A., Melnik, A.V., Meehan, M.J., Liu, W.-T., Crüsemann, M., Boudreau, P.D., Esquenazi, E., Sandoval-Calderón, M., Kersten, R.D., Pace, L.A., Quinn, R.A., Duncan, K.R., Hsu, C.-C., Floros, D.J., Gavilan, R.G., Kleigrewe, K., Northen, T., Dutton, R.J., Parrot, D., Carlson, E.E., Aigle, B., Michelsen, C.F., Jelsbak, L., Sohlenkamp, C., Pevzner, P., Edlund, A., McLean, J., Piel, J., Murphy, B.T., Gerwick, L., Liaw, C.-C., Yang, Y.-L., Humpf, H.-U., Maansson, M., Keyzers, R.A., Sims, A.C., Johnson, A.R., Sidebottom, A.M., Sedio, B.E., Klitgaard, A., Larson, C.B., Boya P, C.A., Torres-Mendoza, D., Gonzalez, D.J., Silva, D.B., Marques, L.M., Demarque, D.P., Pociute, E., O'Neill, E.C., Briand, E., Helfrich, E.J.N., Granatosky, E.A., Glukhov, E., Ryffel, F., Houson, H., Mohimani, H., Kharbush, J.J., Zeng, Y., Vorholt, J.A., Kurita, K.L., Charusanti, P., McPhail, K.L., Nielsen, K.F., Vuong, L., Elfeki, M., Traxler, M.F., Engene, N., Koyama, N., Vining, O.B., Baric, R., Silva, R.R., Mascuch, S.J., Tomasi, S., Jenkins, S., Macherla, V., Hoffman, T., Agarwal, V., Williams, P.G., Dai, J., Neupane, R., Gurr, J., Rodríguez, A.M.C., Lamsa, A., Zhang, C., Dorrestein, K., Duggan, B.M., Almaliti, J., Allard, P.-M., Phapale, P., Nothias, L.-F., Alexandrov, T., Litaudon, M., Wolfender, J.-L., Kyle, J.E., Metz, T.O., Peryea, T., Nguyen, D.-T., VanLeer, D., Shinn, P., Jadhav, A., Müller, R., Waters, K.M., Shi, W., Liu, X., Zhang, L., Knight, R., Jensen, P.R., Palsson, B.O., Pogliano, K., Linnington, R.G., Gutiérrez, M., Lopes, N.P., Gerwick, W.H., Moore, B.S., Dorrestein, P.C., Bandeira, N., 2016. Sharing and community curation of mass spectrometry data with Global Natural Products Social Molecular Networking. *Nat. Biotechnol.* 34, 828–837. doi:10.1038/nbt.3597
- Wang, M., Firman, J., Liu, L., Yam, K., 2019. Review Article A Review on Flavonoid Apigenin: Dietary Intake, ADME, Antimicrobial Effects, and Interactions with Human Gut Microbiota. *BioMed Res. Int.* 2019, 1–18. doi:10.1155/2019/7010467

- Wang, Q., Qiong, Garrity, G.M., Tiedje, J.M., Cole, J.R., 2007. Naïve bayesian classifier for rapid assignment of rRNA sequences into the new bacterial taxonomy. *Appl. Environ. Microbiol.* 73, 5261–5267. doi:10.1128/AEM.00062-07
- Wang T.J., Larson M.G., Vasani R.S., Cheng S., Rhee E.P., McCabe E., Lewis G.D., Fox C.S., Jacques P.F., Fernandez C., O'Donnell C.J., Carr S.A., Mootha V.K., Florez J.C., Souza A., Melander O., Clish C.B., Gerszten R.E., 2011. Metabolite profiles and the risk of developing diabetes. *Nat. Med.* 17(4), 448-53. doi: 10.1038/nm.2307
- Wang, X., Xia, K., Yang, X., Tang, C., 2019. Growth strategy of microbes on mixed carbon sources. *Nat. Commun.* 10, 1–7. doi:10.1038/s41467-019-09261-3
- Westfall, S., Lomis, N., Singh, S.P., Dai, S.Y., Prakash, S., 2015. The Gut Microflora and its Metabolites Regulate the Molecular Crosstalk between Diabetes and Neurodegeneration. *J. Diabetes Metab.* 06, 1–17. doi:10.4172/2155-6156.1000577
- Westreich, S.T., Treiber, M.L., Mills, D.A., Korf, I., Lemay, D.G., 2018. SAMSA2: a standalone metatranscriptome analysis pipeline. *BMC Bioinform.* 19, 1–11. doi:10.1186/s12859-018-2189-z
- Winter, S.E., Thiennimitr, P., Winter, M.G., Butler, B.P., Huseby, D.L., Crawford, R.W., Russell, J.M., Bevins, C.L., Adams, L.G., Tsolis, R.M., Roth, J.R., Bäuml, A.J., 2010. Gut inflammation provides a respiratory electron acceptor for Salmonella. *Nature* 467, 426–429. doi:10.1038/nature09415
- Witten, I.H., Bell, T.C., 1991. The Zero-Frequency Problem: Estimating the Probabilities of Novel Events in Adaptive Text Compression. *IEEE Trans. Inf. Theor.* 137, 1–10. doi:10.1109/18.87000
- Wohlgemuth, S., Keller, S., Kertscher, R., Stadion, M., Haller, D., Kisling, S., Jahreis, G., Blaut, M., Loh, G., 2011. Intestinal steroid profiles and microbiota composition in colitic mice. *Gut Microbes* 2, 159–166. doi:10.4161/gmic.2.3.16104
- Wood, D.E., Lu, J., Ben Langmead, 2019. Improved metagenomic analysis with Kraken 2. *Genome Biol.* 20, 1–13. doi:10.1186/s13059-019-1891-0
- Wu, J., Yan, L.-J., 2015. Streptozotocin-induced type 1 diabetes in rodents as a model for studying mitochondrial mechanisms of diabetic β cell glucotoxicity. *Diabetes Metab. Syndr. Obes.* 2, 181-8. doi:10.2147/DMSO.S82272
- Xiao, L., Sonne, S.B., Feng, Q., Chen, N., Xia, Z., Li, X., Fang, Z., Zhang, D., Fjære, E., Midtbø, L.K., Derrien, M., Hugenholtz, F., Tang, L., Li, J., Zhang, J., Liu, C., Hao, Q., Vogel, U.B., Mortensen, A., Kleerebezem, M., Licht, T.R., Yang, H., Wang, J., Li, Y., Arumugam, M., Wang, J., Madsen, L., Kristiansen, K., 2017. High-fat feeding rather than obesity drives taxonomical and functional changes in the gut microbiota in mice. *Microbiome* 5, 1–12. doi:10.1186/s40168-017-0258-6
- Yan, H., Yu, B., Degroote, J., Spranghers, T., Noten, N., Majdeddin, M., Poucke, M., Peelman, L., Vrieze, J., Boon, N., Gielen, I., De Smet, S., Chen, D., Michiels, J., 2020. Antibiotic affects the gut microbiota composition and expression of genes related to lipid metabolism and myofiber types in skeletal muscle of piglets. *BMC Vet. Res.* 16, 1–12. doi:10.1186/s12917-020-02592-0
- Yang, M., Liu, Y., Xie, H., Wen, Z., Zhang, Y., Wu, C., Huang, L., Wu, J., Xie, C., Wang, T., Peng, W., Liu, S., Chen, L., Liu, X., 2019. Gut Microbiota Composition and Structure of the Ob/Ob and Db/Db Mice. *Int. J. Endocrinol.* 2019, 1–9. doi:10.1155/2019/1394097

- Yin, R., Xue, Y., Hu, J., Hu, X., Shen, Q., 2020. The effects of diet and streptozotocin on metabolism and gut microbiota in a type 2 diabetes mellitus mouse model. *Food Agric. Immunol.* 31, 723–739. doi:10.1080/09540105.2020.1761302
- Yoon, M.Y., Yoon, S.S., 2018. Disruption of the Gut Ecosystem by Antibiotics. *Yonsei Med. J.* 59, 4–12. doi:10.3349/ymj.2018.59.1.4
- Yoshii, K., Hosomi, K., Sawane, K., Kunisawa, J., 2019. Metabolism of Dietary and Microbial Vitamin B Family in the Regulation of Host Immunity. *Front. Nutr.* 6, 562–12. doi:10.3389/fnut.2019.00048
- Zeng, M.Y., Inohara, N., Nunez, G., 2017. Mechanisms of inflammation-driven bacterial dysbiosis in the gut. *Mucosal Immunol.* 10, 18–26. doi:10.1038/mi.2016.75
- Zhang, H., Li, Y., Wang, C., Wang, X., 2018. Understanding the high l-valine production in *Corynebacterium glutamicum* VWB-1 using transcriptomics and proteomics. *Sci. Rep.* 8, 1–18. doi:10.1038/s41598-018-21926-5
- Zhang, J., Kobert, K., Flouri, T., Stamatakis, A., 2014. PEAR: a fast and accurate Illumina Paired-End reAd mergeR. *Bioinformatics* 30, 614–620. doi:10.1093/bioinformatics/btt593
- Zhang, M., Lv, X.-Y., Xu, Z.-G., Chen, L., 2008. The Characterization of High-Fat Diet and Multiple Low-Dose Streptozotocin Induced Type 2 Diabetes Rat Model. *Exp. Diabetes Res.* 2008, 1–9. doi:10.1155/2008/704045
- Zhang, T., Li, Q., Cheng, L., Buch, H., Zhang, F., 2019. Akkermansia muciniphila is a promising probiotic. *Microb. Biotechnol.* 12, 1109–1125. doi:10.1111/1751-7915.13410
- Zheng, X., Huang, F., Zhao, A., Lei, S., Zhang, Y., Xie, G., Chen, T., Qu, C., Rajani, C., Dong, B., Li, D., Jia, W., 2017. Bile acid is a significant host factor shaping the gut microbiome of diet-induced obese mice. *BMC Biology* 15, 1–15. doi:10.1186/s12915-017-0462-7

Chapter 4: Discussion and Future Directions

Local Metabolic Environment as a Determinant of *in vivo* Antibiotic Susceptibility

The meteoric expansion of the microbiome field since in the 2010s has cemented our understanding of the intrinsic role that resident microbes play in the proper health and development of mammals (Bäckhed et al., 2012; Consortium, 2012; Stiemsma and Michels, 2018). With this comes a collective recognition that off-target antibiotic susceptibility within the microbiome is a particularly troublesome side effect that has serious impacts on host well-being (Blaser, 2011; Dethlefsen and Relman, 2011; Ferrer et al., 2017). Thus, a pressing area of research is the characterization of antibiotic susceptibility determinants within the microbiome, as understanding these mechanisms may inform the development of microbiome-protective therapeutic strategies. Recently, Cabral et al. demonstrated that the metabolic state of resident microbes is a key factor contributing to bactericidal antibiotic susceptibility within the microbiome (Cabral et al., 2019). Specifically, the preferential utilization of simple carbohydrate substrates over polysaccharide fermentation can impact antibiotic tolerance phenotypes in select members of the microbiome (Cabral et al., 2019). This dissertation expands upon this foundational study by addressing how real-world sources of macronutrient variation in the gut (via changes in host dietary intake and perturbation of host metabolic function) modify *in vivo* drug susceptibility. Chapter 2 demonstrates that high-sugar/high-fat Western diets potentiate antibiotic activity by impacting gut carbohydrate metabolism (Cabral et al., 2020). Chapter 3 shows that chemotherapeutic induction of hyperglycemia is sufficient to impact microbiome metabolic function in a manner that exacerbates antibiotic-induced dysbiosis. While this work makes significant progress in detailing how diet and host function can shape microbial metabolism in the microbiome, it has generated a body of subsequent research questions. This discussion will address some of these remaining research topics and present relevant preliminary data.

Specificity of Antibiotic Selection to Macronutrient and Metabolism-based Susceptibility:

Dietary Composition

The studies presented in this dissertation focus on the bactericidal drugs ciprofloxacin (Chapter 2) and amoxicillin (Chapter 3) which are two of the most frequently prescribed fluoroquinolone and β -lactam antibiotics in the United States, respectively (Durkin et al., 2018). While both drugs elicit significant microbial dysbiosis, previous work demonstrates that the functional response of the microbiome is somewhat drug-dependent, likely due to species-level differences in susceptibility and inherent differences in drug mechanism of action (Cabral et al., 2019). Thus, an immediate question raised from this dissertation is whether diet and host-related increases in antibiotic-induced dysbiosis are conserved across drug classes or are specific to the selected antibiotics. While the most straightforward means to test this would be to repeat these studies with a broader range of antimicrobial agents, the time, personnel, and cost required to do so would quickly become prohibitive, and there is existing complimentary literature to suggest the study observations may be conserved.

With respect dietary modification, the first of many supporting lines of evidence comes from Cabral et al. (Cabral et al., 2019). After identifying a carbohydrate substrate-dependent amoxicillin tolerance phenotype in *Bacteroides thetaiotaomicron*, Cabral et al. revealed that dietary glucose supplementation potentiates amoxicillin susceptibility *in vivo* (Cabral et al., 2019). Thus, increased monosaccharide abundance can enhance amoxicillin-based dysbiosis, which is akin to the high-sugar diet-based increase in ciprofloxacin susceptibility observed in Chapter 2 (Cabral et al., 2020). Furthermore, consumption of Western-style diets has been shown to worsen both antibiotic-induced dysbiosis and dysbiosis-related complications in multiple studies that have

significant variation in choice of bactericidal drug class, candidate antibiotics within each class, route of administration, and treatment duration (An et al., 2021; Cabral et al., 2020; Hyoju et al., 2019; Lee et al., 2020; Y. Liu et al., 2021). Across these works, Western diet intake is associated with increased expansion of Proteobacteria and pathobionts after administration of cephalosporin-type β -lactams, lincosamides, aminoglycosides, and mixed-class cocktails (Hyoju et al., 2019; Lee et al., 2020; Mefferd et al., 2020). Colonization resistance and infection outcomes also appear to be widely impacted, as Western diet consumption increases total pathogen burden in multiple infections models, represses pathogen clearance, and accelerates the incidence of lethality after antibiotic administration (An et al., 2021; Hyoju et al., 2019; Y. Liu et al., 2021; Mefferd et al., 2020). Characterization of host tissues following streptomycin treatment suggests that Western diets may contribute to worsened dysbiosis by additionally impairing intestinal epithelium metabolism, which can increase inflammation and create a pathobiont-permissive environment in the gut (Lee et al., 2020). However, this hypothesis remains to be confirmed in other antibiotic treatments. Together with the findings presented in Chapter 2, these works suggest that Western diet consumption functions as a microbiome damaging force during bactericidal antibiotic treatment, regardless of drug class. A key consistency across these studies is that Western diets are deficient in dietary fibers and thus likely impact fiber metabolism within the microbiome. In fact, complementary research has shown that the addition of dietary fibers to mouse chow is sufficient to prevent both loss in microbiome diversity and enhance colonization resistance against *Clostridioides difficile* after antibiotic challenge (Mefferd et al., 2020; Schnizlein et al., 2020). Strikingly, this protection occurred in both a β -lactam and a mixed drug class cocktail model, suggesting that the protective capacity of dietary fibers is conserved across multiple bactericidal drug classes including β -lactams (penicillins and cephalosporins), aminoglycosides (kanamycin

and gentamicin), nitroimidazoles, polymyxins, and glycopeptides (Schnizlein et al., 2020). Overall, the data consistently highlight that dietary composition plays a critical role in determining the severity of antibiotic-induced dysbiosis across bactericidal antibiotic classes, although more work is required to fully characterize species-level susceptibility mechanisms.

Specificity of Antibiotic Selection to Macronutrient and Metabolism-based Susceptibility: Host Metabolic Function

Chapter 3 demonstrates that streptozotocin (STZ)-induced hyperglycemia is associated with transcriptional and metabolic restructuring of the gut microbiome that ultimately exacerbates amoxicillin-induced dysbiosis. Unlike the growing consensus of the Western diet's role in antibiotic toxicity, the literature surrounding the impact of STZ and antibiotic therapy on the microbiome is somewhat scant. Fortunately, to examine the role that antibiotic selection plays on STZ's capacity to worsen dysbiosis, we can rely on previously collected data. When conducting the research described in Chapter 3, we originally included a ciprofloxacin-treated group for both hyperglycemic and normoglycemic mice at the 24-hour time point described. As such, we generated 16S ribosomal RNA (rRNA) sequencing and untargeted metabolomics data from STZ-treated and control mice during ciprofloxacin exposure. These data were ultimately excluded from Chapter 3 due to spatial constraints and the robustness of the amoxicillin data, thus these findings will be discussed here. However, the discussion of these data will primarily focus on the differences between *ciprofloxacin-treated* hyperglycemic and normoglycemic mice, as the vehicle-treated control comparison has been discussed at length in Chapter 3.

Following a two-week habituation period, 7-week-old male C57BL/6J mice were given a single intraperitoneal injection of either STZ or a sham vehicle. After 48 hours, animals were

assessed for hyperglycemia and subsequently randomized. The next day, ciprofloxacin (12.5 mg/kg) or a vehicle control was administered *ad libitum* via the drinking water for 24 hours before animals were sacrificed and their cecal contents were collected for taxonomic profiling and untargeted metabolomics as described in Chapter 3 (Figure 1A). Using 16S rRNA sequencing, we observed that STZ-induced hyperglycemia was associated with a divergence in β -diversity both before and after ciprofloxacin (Figure 1B). Interestingly, hyperglycemia had no impact on the post-antibiotic expansion of Firmicutes (Figure 1C, Figure 1D). Although hyperglycemia appeared to exaggerate the loss of Bacteroidetes (Figure 1C), the difference in abundance was not statistically significant (Figure 1E).

To profile host-dependent differences in taxonomic composition after ciprofloxacin treatment, we performed differential abundance testing on genus-level amplicon sequence variants (ASV) (Love et al., 2014). Surprisingly, the abundance of very few taxa were host-dependent in response to ciprofloxacin. Hyperglycemic mice had a less severe reduction in true *Clostridia* and *Parasutterella* (Figure 2C: positive interaction) and did not experience the increase in *Duncaniella* exhibited by controls (Figure 2A: negative interaction) (Cruz-Morales et al., 2019; Lawson and Rainey, 2016). Interestingly, *Parasutterella* has been recently implicated in the regulation of both the colonic bile acid and cholesterol pools (Ju et al., 2019). It is possible that STZ-related depletion of the cecal bile pool as described in Chapter 3 may create a semi-protective environment for *Parasutterella* via nutrient limitation. Meanwhile, *Duncaniella* has been shown to possess an extensive carbohydrate focused gene repertoire, and the relative lack of carbohydrate breakdown in STZ-treated communities may be involved in its static abundance (Chung et al., 2020; Lagkouvardos et al., 2019). In both cases, however, this is purely speculative, as it is impossible to confirm the cause of these taxonomic shifts without functional profiling of the microbiome

through transcriptomics or proteomics. Regardless, these data lie in direct contrast with the findings presented in Chapter 3, where hyperglycemia-related microbiome function significantly impacted taxonomic restructuring after amoxicillin. Currently, we lack sufficient data to assert whether this disparity is due to (1) an inability to profile species-level taxonomic shifts because of the reduced resolution of 16S rRNA sequencing compared to metagenomics or (2) if the taxonomic restructuring phenotype is a specific response to β -lactam stress (Clooney et al., 2016; Poretsky et al., 2014; Ranjan et al., 2016). Analyzing ciprofloxacin-treated hyperglycemic and normoglycemic microbiomes using metagenomics should ultimately resolve this uncertainty.

To further profile the differences between STZ-treated and control communities after ciprofloxacin exposure, we again profiled genera-level differential ASV abundances. We found that STZ and ciprofloxacin co-treatment increased the abundance of *Neglecta* and significantly decreased the *Kineothrix*, *Eisenbergiella*, and *Acutalibacter* genera (Figure 2B). Because paired metagenomic and metatranscriptomic sequencing were not performed, it is impossible to make definitive claims about microbiome function in these samples. However, computational tools like PICRUSt can be implemented to predict metagenome content from 16S data, allowing for functional inference (Douglas et al., 2020; Y.-X. Liu et al., 2021). Using PICRUSt2, we predicted differences in MetaCyc pathway-related gene content that were uniquely affiliated with hyperglycemic or normoglycemic mice after ciprofloxacin (Figure 2C). Strikingly, despite their similar taxonomic compositions, the predicted functional metagenomic capacity of the STZ and ciprofloxacin cotreated microbiota was distinct from that of normoglycemic controls. Overall, hyperglycemic communities had a greater variety of associated MetaCyc pathways with notable enrichment in nucleotide metabolism, monosaccharide capture, menaquinone generation, aerobic respiration, and TCA cycle activity (Figure 2C). The increased capacity for monosaccharide

import and primary respiration is congruent with the amoxicillin-specific findings in Chapter 3, where elevated environmental sugar levels prompted increased phosphotransferase import and glycolysis within the hyperglycemic microbiota. Interestingly, in Chapter 2 we observed that both normal and Western diet-fed mice downregulated TCA cycle activity in response to ciprofloxacin, and Cabral et al. demonstrated community-wide reductions in nucleotide, nucleoside, and TCA function after ciprofloxacin treatment (Cabral et al., 2020; 2019). Thus, modifications in TCA activity appear to be a conserved microbiome response to this antibiotic, and differences in respiratory capacity between STZ-treated and control mice may be indicative of divergence in microbiome function, although this hypothesis cannot be confirmed without functional screening of the microbiome.

Next, we profiled the cecal metabolome in hyperglycemic and normoglycemic mice during ciprofloxacin treatment using both quadrupole flow injection electrospray time-of-flight mass spectrometry (Q-TOF-MS; Figure 3) and liquid chromatography tandem mass spectrometry (LC-MS/MS; Figure 4). First, we performed Principal Coordinates Analysis on metabolite abundance, and found that, just like with amoxicillin, the cecal metabolome is divergent in a host-dependent manner after ciprofloxacin treatment (Figure 3A). We then performed differential abundance testing to examine which Q-TOF-MS metabolites and KEGG pathways were altered after ciprofloxacin exposure, and which had altered abundances during antibiotic treatment in a host-dependent manner (Figure 3B-3D). After ciprofloxacin administration, hyperglycemic communities were enriched for metabolites involved in purine metabolism, peptidoglycan synthesis, and dietary-fiber components like isoflavonoids and phenylpropanoids (Figure 3B). Simultaneously, metabolites involved in nitrogen metabolism, carbon fixation, energy carrier generation, catabolism, pyruvate processing, and TCA activity were all depleted in STZ-treated

communities relative to normoglycemic controls (Figure 3B). It is likely that the reduction in central carbon metabolites (pyruvate, TCA, energy carrier generation, etc.) reflects diminished transcription of the affiliated pathways and represents a ciprofloxacin-specific response akin to what was identified in Chapter 2, although transcriptional analysis is required to confirm this (Cabral et al., 2020; 2019). The spike in purine and peptidoglycan metabolites may additionally indicate increased ciprofloxacin activity in STZ-treated animals, as ciprofloxacin causes lethal stalling of DNA replication that can induce bioaccumulation of nucleotides, nucleosides, and cell wall synthesis components (de Lastours and Fantin, 2015; Dorries et al., 2014; Falla and Chopra, 1998).

Supporting evidence for host-dependent microbiome function during ciprofloxacin treatment can be seen in the differentially abundant metabolites that are subjected to host interaction (Figure 3C, Figure 3D). As with amoxicillin, STZ-treated communities exhibited an overall increase in multiple sugar and sugar alcohols, including hexonic acids, ribitol, and pentose during ciprofloxacin treatment (Figure 3C). This suggests that STZ-induced hyperglycemia results in increased cecal monosaccharide concentrations regardless of antibiotic drug class used. Multiple features involved central carbon metabolism showed host-specific regulation in response to ciprofloxacin, including carnitine electron acceptors, nicotinate, pyruvate oxime, isocitrate, and malate (Bernal et al., 2007; Meadows and Wargo, 2015) (Figure 3C). Furthermore, metabolites involved in nucleotide generation (conjugated and unconjugated uracil, inosine, deoxyuridine), cholesterol metabolism, tryptophan metabolism (indole-3-acetate), heme processing (dueteroporphyrin IX), amino acid generation (3-dehydroshikimate, 6-methylnicotinamide, ketovaline, etc.), and lipid processing are all differentially regulated between STZ-treated and normoglycemic mice during ciprofloxacin exposure (Figure 3C, Figure 3D) (Böttcher et al., 2014;

Roager and Licht, 2018; Sachar et al., 2016). While some LC-MS/MS based metabolite changes such as decreased bile acids and enrichment of 3-hydroxy-4-methoxycinnamic acid were conserved ciprofloxacin responses (Figure 4A, Figure 4B), the abundance of carnitine species were significantly elevated in STZ-treated samples compared to controls further supporting divergence in electron transport between hosts (Figure 4C). Together these data suggest that STZ-induced hyperglycemia is sufficient to significantly impact the cecal metabolome after ciprofloxacin, as it does during amoxicillin treatment. In Chapter 3, significant divergence in the cecal metabolome during antibiotic exposure was correlated with host-specific changes in microbiome function, and we anticipate that this trend holds true for ciprofloxacin treatment. Again, transcriptional assessment of the microbiota during drug challenge will be required to confirm this hypothesis and rule out any metabolite changes related to host secretions or activity of the intestinal epithelium.

Finally, we implemented the MIMOSA computational algorithm to try and identify PICRUSt2-predicted metagenomes that could explain the variation in metabolome composition between hyperglycemic and normoglycemic communities (Figure 5) (Noecker et al., 2016). In both hosts, *Parasutterella*, *Turicibacter*, and *Bacteroides* were the largest contributors to metabolome variation (Figure 5A, Figure 5B). Interestingly, the clostridial Firmicutes genus *Oscillibacter* had a significant contribution to fumarate levels in hyperglycemic communities, suggesting this taxon may help shape the metabolic function of the microbiome during ciprofloxacin treatment (Figure 5B). When comparing the antibiotic-treated metabolomes against one another, MIMOSA was able to identify 6 taxa that were positively correlated with a subset of metabolites, including the enriched *Neglecta* genus (Figure 5C). However, these data are reliant on *in silico* modeling and thus are insufficient to mechanistically describe how these candidate taxa contribute to metabolite variation. Use of species-level annotations derived from

metagenomics should improve the model generated by MIMOSA and increase the accuracy of metabolome taxon stratification (Noecker et al., 2016).

Although this preliminary examination of hyperglycemia's impact on ciprofloxacin susceptibility does not include microbiome function, these data stand in agreement with the model presented in Chapter 3. Specifically, STZ-induced hyperglycemia is correlated with significant restructuring of the cecal metabolome and modification of microbiome functional capacity after antibiotic treatment in both β -lactam and fluoroquinolone treatment regimens. A major caveat, however, is that the untargeted metabolomics protocol used here and in Chapter 3 cannot distinguish between host-derived and microbially-derived compounds, thus alternative strategies will need to be implemented to confirm if a metabolite shift is bacterial in origin (Gertsman and Barshop, 2018). One strategy, that we chose to implement in Chapter 3, is the inclusion of parallel metatranscriptomics which can provide orthogonal confirmation for some pathways. Recently, *in silico* algorithms like MIMOSA and MelonnPan have been developed to pair metagenomic and metabolomic data, by comparing metabolite abundances with total gene content (Mallick et al., 2019; Noecker et al., 2016). Ideally, one could additionally perform RNA sequencing of the host epithelium and compare both microbiome and host transcriptional activity against the metabolome. However, some metabolites feed into shared reaction between host and microbiome and thus may not be able to be explicitly characterized as “host-derived” or “microbially-derived” using current computation tools (Gertsman and Barshop, 2018). Ultimately detangling host-microbiome interactions during antibiotic perturbation will require holistic examinations that implement multiple analytical strategies to overcome the inherent complexity of the gut ecosystem.

Structural and Compositional Variation of Macronutrients Impacts Microbiome Function

In Chapter 2, we demonstrated that feeding mice a Western diet worsens antibiotic-induced dysbiosis and perturbs carbohydrate metabolism in the gut (Cabral et al., 2020). An immediate question based off these data is whether the observed impacts on microbiome function were because of (1) a synergistic effect of elevated fats, sugars, and fiber starvation, or (2) the result of altering a single macronutrient component. An initial, albeit correlative, way to address this is to compare the diet formulation used in Chapter 2 against those in the other studies using Western diets, like those discussed earlier in this Chapter. Comparing formulation can facilitate the identification of shared and divergent ingredients which can be subsequently kept or eliminated from a working model of diet-induced antibiotic susceptibility. However, the moniker “Western diet” is a bit of a blanket term that describes any diet formulation that elevates fat and carbohydrate content relative to protein and fiber (Hintze et al., 2018). Even amongst open-source commercial vendors, Western diets can vary in fat and carbohydrate formulation which has obvious implications on the comparison of research findings. In our work and the studies discussed earlier, the selected diets were from different vendors, but all used a mixture of corn starch and maltodextrin as the carbohydrate source, and a lard and soybean oil mixture as the fat source, albeit at slightly different concentrations (approximately 10 percent fat and 40 percent carbohydrates in Chapter 2 versus 40 percent fat and 40 percent carbohydrates in the compared works) (An et al., 2021; Cabral et al., 2020; Hyoju et al., 2019; Lee et al., 2020). Our work and that of Lee et al. used formulations that included low levels (less than 5%) of cellulose fibers, while An et al. used a cellulose and inulin mixture, and Hyoju et al. used a fiber-free formulation (An et al., 2021; Cabral et al., 2020; Hyoju et al., 2019; Lee et al., 2020). Given the vast difference in fat content between these studies, it is likely that carbohydrate elevation and fiber reduction are more important than fat in determining microbiome dysbiosis while consuming a Western diet (Morrison et al., 2020;

Satokari, 2020). Assuming this hypothesis is correct, the next logical questions are (1) how does the abundance of these two macronutrients impact host digestion and thus (2) microbiome metabolism, (3) is this unique to corn starch and maltodextrin, and (4) what are ways we can experimentally confirm this?

Host digestion and compound bioavailability should be one of the first considerations when evaluating the impact of dietary composition on microbiome function. The transport of monosaccharides in the small intestine is unique to the target substrate and subjected to differential regulatory loops (Merino et al., 2020). For example, small intestinal uptake of fructose is passively mediated while glucose uptake is an active process (Merino et al., 2020). Additionally, while both sugars are processed in the liver, only glucose has insulin-dependent hepatic processing (Merino et al., 2020). Recently, it was demonstrated that the bulk of host-related fructose and glucose metabolism occurs within the small intestine (Jang et al., 2018), suggesting that the intestinal demand for these compounds will be critical in determining the rate of metabolite overflow into the colon. Another key determinant of metabolite absorption rate is intestinal transit time, which itself is dependent on diet-dependent viscosity of chyme (Grundy et al., 2016; Müller et al., 2018). The obvious implication here is that the commercial formulation of Western diets may rely on different monosaccharide sources, and thus may elicit disparate changes to microbiome function due to differences in host sugar uptake. Furthermore, the heterogeneity of sugar intake in humans may help explain differences in results gleaned from rodent-based Western diet studies and those in patient populations (Hintze et al., 2018). Experimentally, host sugar uptake rates can be confirmed by monitoring the expression of these transporters or using isotopically labeled sugars that can be tracked as they are coupled to a transporter. An interesting avenue of future research would be to examine the activity of sugar transporters on different Western diet formulations and

then subsequently profile metabolite overflow to the colon and how that impacts microbial metabolism. These data would help create a more nuanced understanding of how host sugar regulates the behavior of the colonic microbiota which could in turn be leveraged to mitigate antibiotic-induced dysbiosis. Perhaps a sucrose formulated diet will worsen dysbiosis more severely than a fructose formulated diet. Additional research should also consider that cardiometabolic function is an additional host-related control mechanism for sugar transport. It is likely that metabolically perturbed hosts will have disparate responses to Western diet supplementation than normal hosts, which has significant implications on therapeutic development.

Variations in monosaccharide composition may also impact microbial function through differential regulation of carbon catabolite repression (CCR). CCR is a highly conserved metabolic regulatory mechanism by which bacteria can preferentially repress the utilization of secondary carbon sources when preferred substrates are available (Görke and Stülke, 2008; Warner and Lolkema, 2003). Ingested monosaccharides can suppress microbiome polysaccharide utilization via CCR in some species (Chen et al., 2018; Di Rienzi and Britton, 2020). Traditionally, only a minor fraction (less than 5 percent) of ingested sugars reaches the large intestine, thus the overall repression of fiber fermentation is likely low (Koepsell, 2020). To systemically profile how excess sugar intake dysregulates fiber fermentation, and thus drug susceptibility, animal models can be implemented. However, it is key that dietary alterations are limited to one sugar additive at a time, as this should prevent confounding metabolic phenotypes from occurring. Cabral et al. actually implemented this strategy when profiling glucose's impact on amoxicillin-based dysbiosis (Cabral et al., 2019). Sugar-related changes in microbiome fermentative capacity can be examined by combining transcriptional quantification of carbohydrate-active enzymes (CAZymes) and targeted

metabolomics to quantify short-chain fatty acid abundance. Transcriptomic and proteomics can additionally quantify the activity of catabolite repression systems, as CCR homologs have been identified in a wide array of bacteria (Görke and Stülke, 2008). While this approach will not capture all syntrophic microbial interactions, small scale cross-feeding can be described for species of interest by performing the experiments in a consortium-colonized gnotobiotic animal. A systematic approach like this could ultimately generate a catalogue sugar-specific microbiome responses. These data would have far-reaching therapeutic potential, particularly within the field of personalized nutrition. Next steps would then leverage this catalog to examine antibiotic susceptibility as it relates to sugar-induced microbiome phenotypes.

If excessive sugar intake can potentiate antibiotic toxicity in the gut, can excessive dietary fiber intake be protective? Examination of high-fiber intake in human cohorts demonstrates that vegans and vegetarians have higher microbiome diversity and positive metabolic phenotypes compared to omnivores (Angelis et al., 2020; Bolte et al., 2021; Franco-de-Moraes et al., 2017). This has made fiber supplementation an attractive therapeutic strategy to mitigate dysbiosis, although attempts to generate a catch-all prebiotic have had mixed results in humans (Shah et al., 2020). In mice, dietary fiber supplementation has been shown to be protective. Specifically, Schnizlein et al. showed that supplementing mouse chow with just 5 percent xanthan gum was sufficient to reduce antibiotic-induced dysbiosis and protect against post-treatment infection (Schnizlein et al., 2020). An important caveat to consider when discussing a fiber-based therapeutic is that dietary fiber is a blanket term for a chemically diverse set of compounds that are not uniformly metabolized by the microbiome. The microbiota's capacity for fermentation and the rate of these reactions will ultimately be determined by fiber structure and microbiome composition. For example, branched and rigidly structured polysaccharides are less accessible and

have delayed *in vivo* fermentation (Rumpagaporn et al., 2015; Warren et al., 2018; Z. Zhou et al., 2013). Concurrently, the microbiome exhibits extensive fiber-related niche adaptation, where some taxa are generalists with many polysaccharide utilization systems, and others are specialists that use a select subset of fibers (Cantu-Jungles and Hamaker, 2020; Coker et al., 2021; Payling et al., 2020). Preliminary work on fiber-based therapeutics in humans have shown high inter-individual variation in microbiome responses to fibers like fructooligosaccharides, cellulose, and inulin (Cantu-Jungles and Hamaker, 2020). Interestingly, these polysaccharides are favored by generalist fiber degraders, while compounds like type-IV resistant starches and insoluble β -glucans elicit more consistent responses from specialist degraders (Cantu-Jungles and Hamaker, 2020; Deehan et al., 2020). This variation in fermentation phenotypes means that the development of individually tailored fiber prebiotics should be prioritized over a catch-all therapeutic.

Extensive research will be required to generate these precision medicines. Like with sugars, a key first step will be the generation of an expansive library describing fiber-specific microbiome responses before and after antibiotic administration. Currently, some *in silico* algorithms like DRAM and SACCHARIS can be used to discover novel CAZymes and resolve ambiguous CAZyme annotations from metagenomic and metatranscriptomic data, which will aid in fiber-related functional profiling (Jones et al., 2018; Klassen et al., 2021; Shaffer et al., 2020). To track species-specific metabolism during fiber supplementation, isotopic labeling strategies like bioorthogonal non-canonical amino acid tagging or bioorthogonal click chemistry can allow for real-time tracking of microbiome-glycan interactions when paired with fluorescence *in situ* hybridization (Kalesh and Denny, 2019; Klassen et al., 2021; Kolb et al., 2001; Y. Wang et al., 2020). Fully characterizing the diversity of polysaccharide-based microbiome metabolism may facilitate the creation of tailored fiber therapeutics. Hypothetically, an individual's baseline

microbiome function may be assessed, and this data could dictate an appropriate fiber cocktail formulation to elicit desired functional responses. For example, fiber therapeutics could be tailored to diet intake and delivered prophylactically before antibiotic administration to prevent dysbiosis, although this type of individualized medicine is probably years away from development.

Detangling the Complex Phenotypes of Metabolic Diseases and their Impact on Microbiome Function

The findings presented in Chapter 3 were reliant on the single-dose STZ model, which causes irreversible hyperglycemia via targeted ablation of pancreatic β -cells (Deeds et al., 2011; Goyal et al., 2016). This model causes glucose dysregulation by preventing insulin synthesis and has the advantage of triggering dysglycemia without microbiome-impactful dietary modifications, as discussed in Chapter 3. While our work described significant changes in microbiome function a few days after injection, these changes were ultimately associative. Thus, we can immediately ask if alterations in microbiome function were (1) a direct consequence of insulin deficiency or (2) due to secondary changes from dysglycemia.

It is possible that the metabolic restructuring observed in the STZ-treated microbiome is related to insulin's role in protein metabolism. Insulin is a potent regulator of protein digestion and can trigger a shift from anabolic to catabolic amino acid metabolism in the host (Weber et al., 1981; Brooks et al., 1986). Specifically, insulin simultaneously increased the ileal uptake of amino acids and regulates muscular amino acid demand (Weber et al., 1981; Hasselgren et al., 1987; Groen et al., 2016). To that end, type-I diabetes mellitus (DM) patients, who are insulin deficient, experience marked muscular atrophy, increased skeletal muscle protein degradation, and hyperaminoacidemia from said breakdown (Møller and Nair, 2008; Aquilani, 2004; Herbert and

Nair, 2010; Sala and Zorzano, 2015). Increases in amino acid fermentation have been detected in the gut microbiome of type-I and type-II DM patients, suggesting elevated colonic amino acid levels (Macías-Acosta et al., 2021; Winther et al., 2021). Thus, insulin disruption may prevent host amino acid uptake, which would increase the total load available to the colonic microbiota. In turn, this readily available carbon source could increase the metabolic rate of local microbes, which results in increased antibiotic susceptibility based off our findings. The amino acid elevation hypothesis could be quickly confirmed by performing a direct quantification of amino acid loads from cecal/fecal material using a Bradford assay or proteomic approach.

A straightforward means to test the importance of insulin to perturbed microbiome metabolism would be to repeat the experiments described in Chapters 3 and 4 with the inclusion of a rescue group receiving exogenous insulin. Preliminary studies have demonstrated that in addition to improving cardiometabolic and intestinal phenotypes, insulin therapy can shift microbiome composition by reducing *Bacteroides* abundance (Pircalabioru et al., 2021; Tate et al., 2017; H. Wang et al., 2020). For amoxicillin, reducing *Bacteroides* may be beneficial by preventing the total outgrowth of this taxa after antibiotic administration. Thus, insulin delivery may be sufficient to reverse hyperglycemia-related shifts in microbial metabolism and alter antibiotic activity within the gut. There is wide diversity in commercially available insulins that vary in their absorption rate and circulation time. For example, naturally derived insulins are metabolized on the scale of hours, while certain synthetic insulins remain in circulation for days (Warshauer et al., 2020). A possible therapeutic strategy could be the prophylactic delivery of long-circulating synthetic insulin to shift microbiome metabolism before and during antibiotic treatment, however significant mechanistic frameworks need to be developed before this type of therapeutic strategy is viable.

A key framework missing from Chapter 3 is the temporal dynamics of hyperglycemia-related microbiome shifts. The microbiome responds to dietary and xenobiotic introduction within hours, thus the findings in Chapter 3 likely present a hyperglycemia steady state rather than transitory shifts in microbiome function. A quick fix would be to longitudinally characterize microbiome function using our multi-omic approach immediately after STZ administration. Incorporating RNA sequencing of host tissues would be a great addition in future works and could help resolve some ambiguity in host versus microbe-derived phenotypes. Future studies would also benefit from the implementation of spatially informed metabolomics using approaches like metaFISH (a combination of fluorescence *in situ* hybridization and MALDI-TOF mass spectrometry) to examine the diversity of metabolic shifts within the microbiome at species-scale during dysglycemic development (Geier et al., 2020).

While temporally characterizing host-microbe interactions during chemotherapeutic hyperglycemia is intellectually interesting, it unfortunately may not inform the development of viable therapeutics, as metabolic syndromes are phenotypically diverse and more complex in humans than in research animals (Bezirtzoglou et al., 2021). For example, pancreatogenic diabetes mellitus (DM) has unique etiology to type-I and type-II DM, which also have divergent pathologies and immune phenotypes (Siljander et al., 2019; Talukdar et al., 2021; Thaiss et al., 2018; H. Zhou et al., 2020). While insulin is the first line therapy for type-I DM, metformin is the choice antidiabetic for type-II DM, meaning that the considerations for microbiome-protective approaches during antibiotic administration will vary between these patient populations. Microbiome composition and function have been heavily implicated in the pathology of type-II DM and the efficacy of metformin, meaning that the severity of antibiotic-induced dysbiosis may be heavily individualized (Bezirtzoglou et al., 2021; Elbere et al., 2020). Notably, there is growing evidence

that pre-treatment microbiome compositions (especially *Bacteroides* abundance) can impact the success of metformin delivery and the severity of gastrointestinal side effects (Elbere et al., 2020; Silamiķele et al., 2021). Interestingly, metformin has been demonstrated to restore short-chain fatty acid production and shift bile acid processing within the microbiome, suggesting it has significant microbiome-modulatory properties (Pircalabioru et al., 2021; Silamiķele et al., 2021; Vila et al., 2020; Wu et al., 2017). Assuming metformin can restore fermentative metabolism in some patient microbiomes, antidiabetic therapy could be combined with antibiotic administration to fine tune the severity of dysbiosis. Alternatively, dietary modification could be combined with metformin to restore glucose regulation in dysglycemic patients before antibiotic administration in a stepwise fashion. However, a more complete mechanistic understanding of interactions between the microbiome and antidiabetic compounds will be required before personalized approaches that mitigate antibiotic dysbiosis can be implemented in patients with metabolic disease.

Conclusions

The work presented in this dissertation builds upon an existing model of antibiotic susceptibility by which the metabolic activity of gut-resident microbes dictates their capacity to survive antibiotic exposure (Cabral et al., 2019). Specifically, we use a combination of high-throughput ‘omics platforms to characterize the transcriptome and metabolome of the cecal microbiome during exposure to bactericidal antibiotics. These data highlight that host-related sources of nutrient variation, whether from changes in diet or induction of host dysglycemia, are sufficient to perturb metabolic homeostasis in the cecum and worsen antibiotic-induced dysbiosis. These data, while robust, describe early-stage examinations of how diet and host function shape

antibiotic susceptibility. Ultimately, more work is required to translate these findings into viable therapeutic targets, but hopefully these data can help inform the development of precision medicine approaches to mitigating microbiome dysbiosis.

Materials and Methods

The data described in this chapter were obtained using the same methods implemented in Chapter 3, with the exception of antibiotic dosing. Ciprofloxacin was delivered via the drinking water to C57BL/6J mice at a concentration of 12.5 mg/kg. For the remaining materials and methods details, please refer to Chapter 3: Materials and Methods

16S and metabolomics data are available upon request. Please contact Peter Belenky at peter_belenky@brown.edu for all data inquiries related to this Chapter.

Main Figures, Titles, and Legends

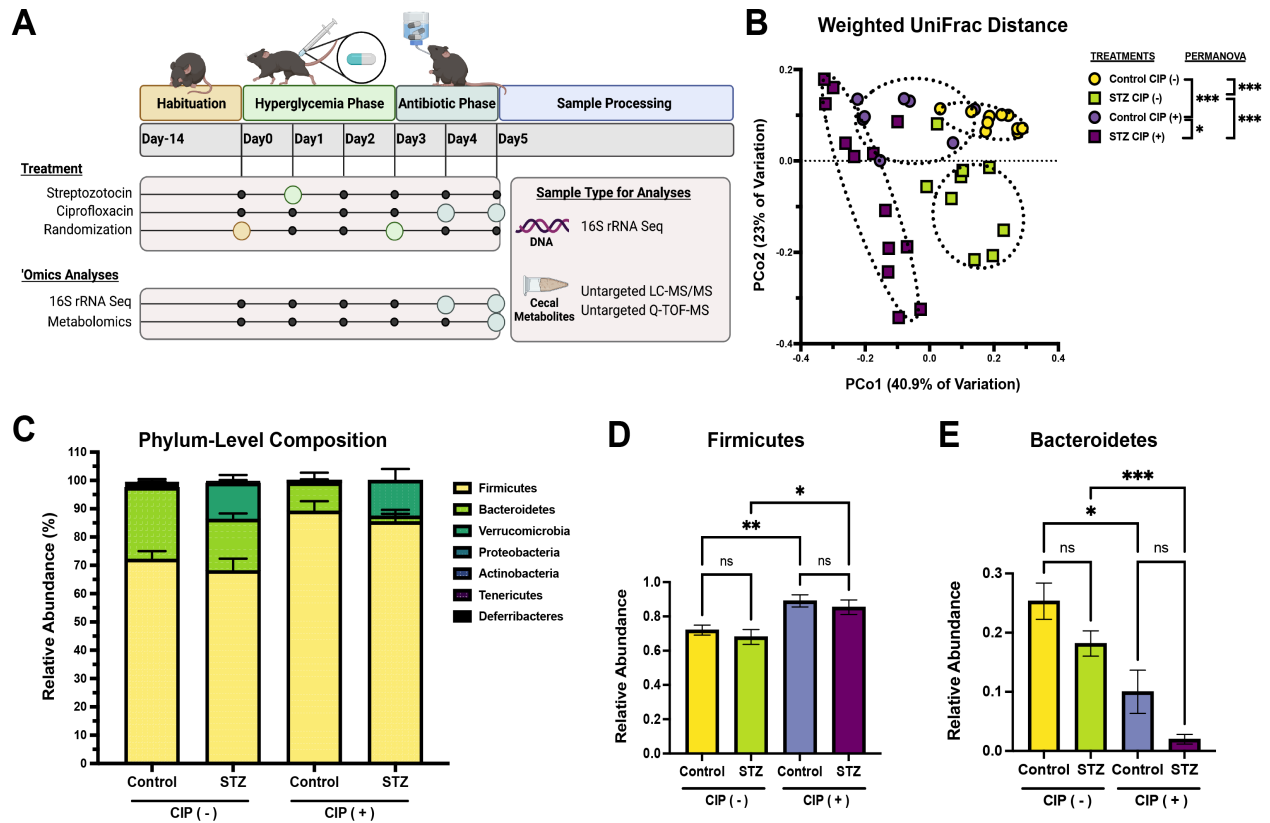


Figure 1: Impact of streptozotocin and ciprofloxacin on microbiome composition.

A. Experimental design of this study. Figure was created with BioRender.com

B. Bray-Curtis Dissimilarity between 16S rRNA amplicons from experimental groups with permutational ANOVA.

C. Relative abundance of the five-most prominent bacterial phyla. Data represent mean \pm SEM.

D. Relative abundance of Firmicutes. Data represent mean \pm SEM

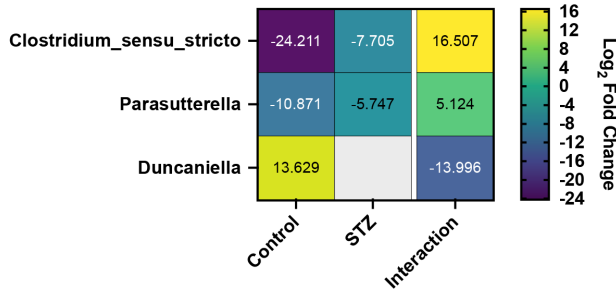
E. Relative abundance of Bacteroidetes. Data represent mean \pm SEM

N = 8 to 14 per group;

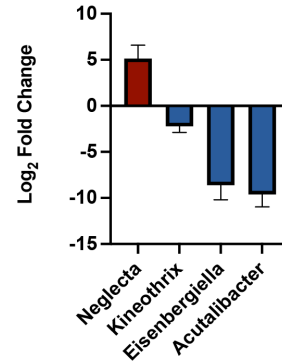
For D & E: Welch's ANOVA and Dunnet T3 test for multiple hypothesis correction

(* $p < 0.05$, ** $p < 0.01$, *** $p < 0.001$)

A Change in Genera after Ciprofloxacin



B Change in Genera after Ciprofloxacin



C Predicted MetaCyc Pathway Abundance after Ciprofloxacin

Higher in Control (Blue)
Higher in STZ (Purple)

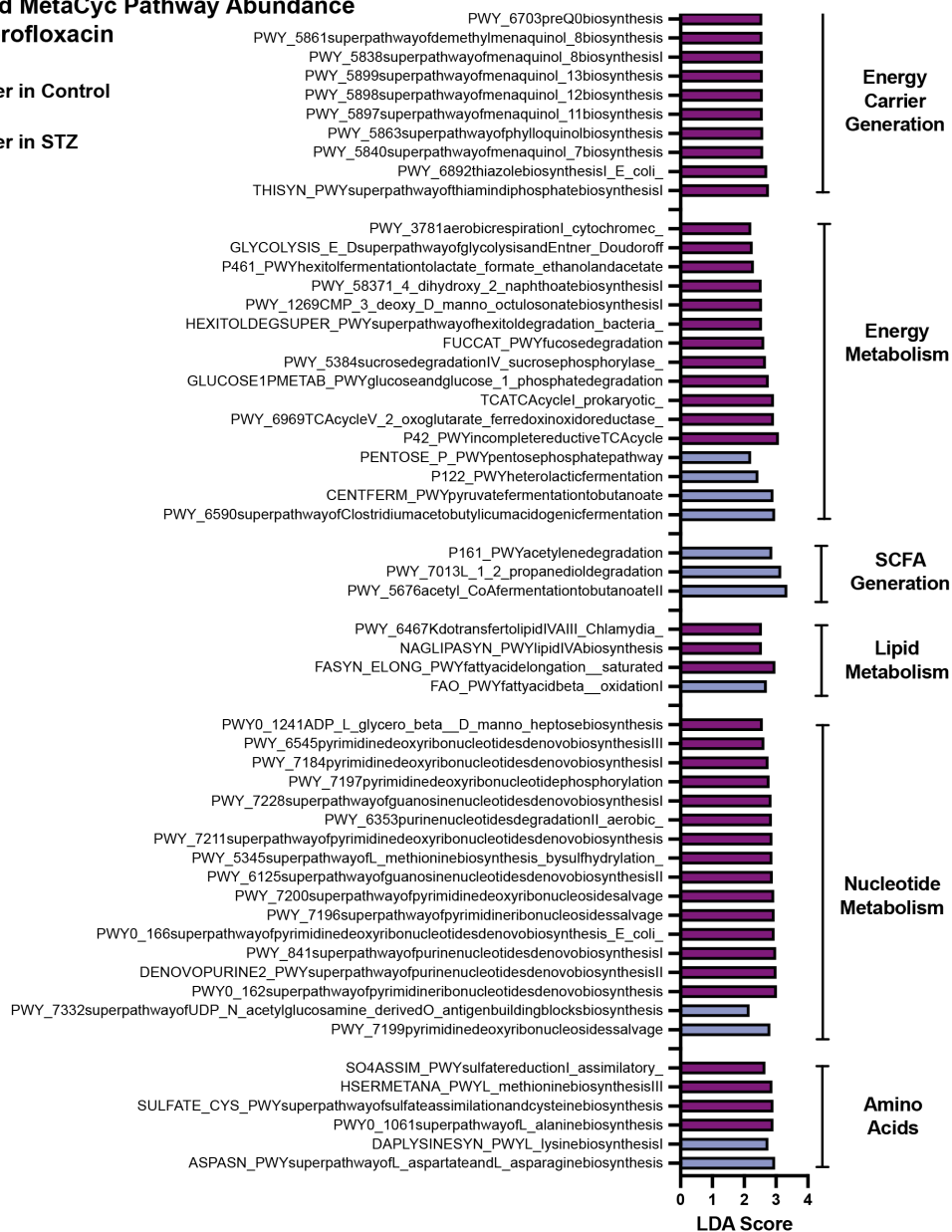


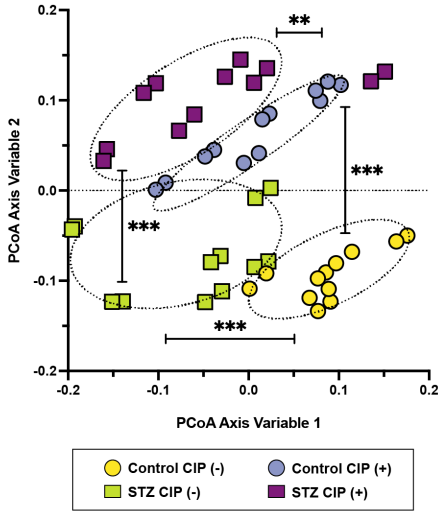
Figure 2: Host hyperglycemia differentially impacts genus-level composition and metagenomic potential after ciprofloxacin.

- A. Differentially abundant genus-level 16S rRNA read. Data represent \log_2 fold of change of ciprofloxacin-treated samples versus vehicle controls \pm SEM.
- B. Differentially abundant genus-level 16S rRNA reads. Data represent \log_2 fold of change \pm SEM of normoglycemic ciprofloxacin-treated samples versus STZ and ciprofloxacin co-treated samples.
- C. Linear discriminant analysis of PICRUS2-predicted metagenome content. Data represent normoglycemic ciprofloxacin-treated samples versus STZ and ciprofloxacin co-treated samples.

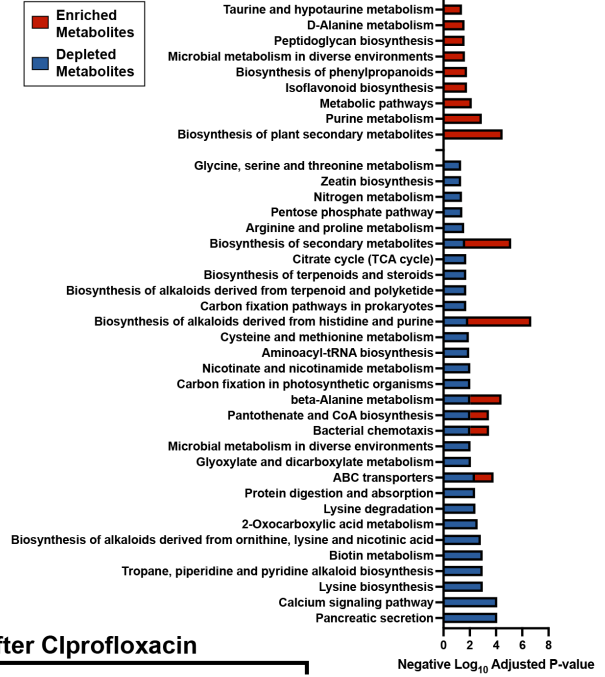
N = 8 to 14 per group.

Differentially abundant = Benjamini Hochberg adjusted $p < 0.05$.

A O-TOF-MS Bray-Curtis Dissimilarity

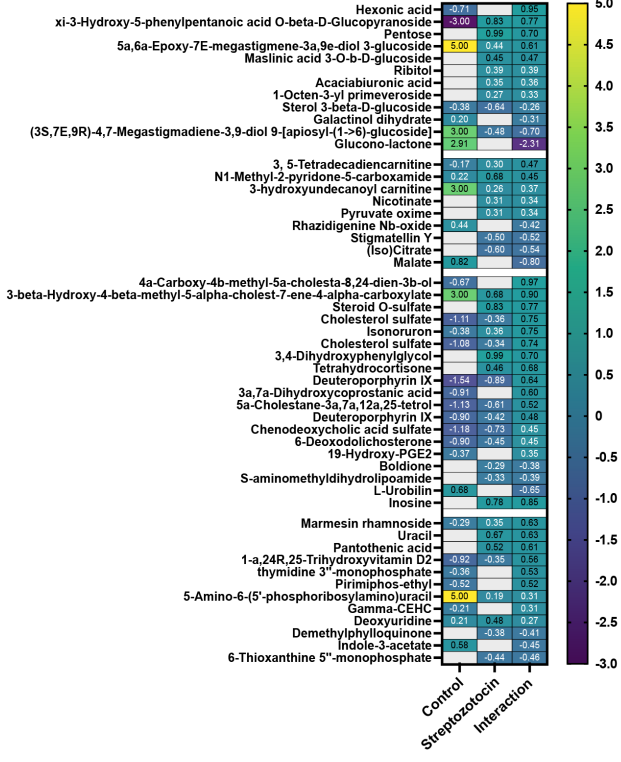


B Q-TOF-MS Pathway Enrichment



Q-TOF-MS Abundance Change After Ciprofloxacin

C Carbohydrate, Energy & Nucleotide Metabolism



D Amino Acid & Lipid Metabolism

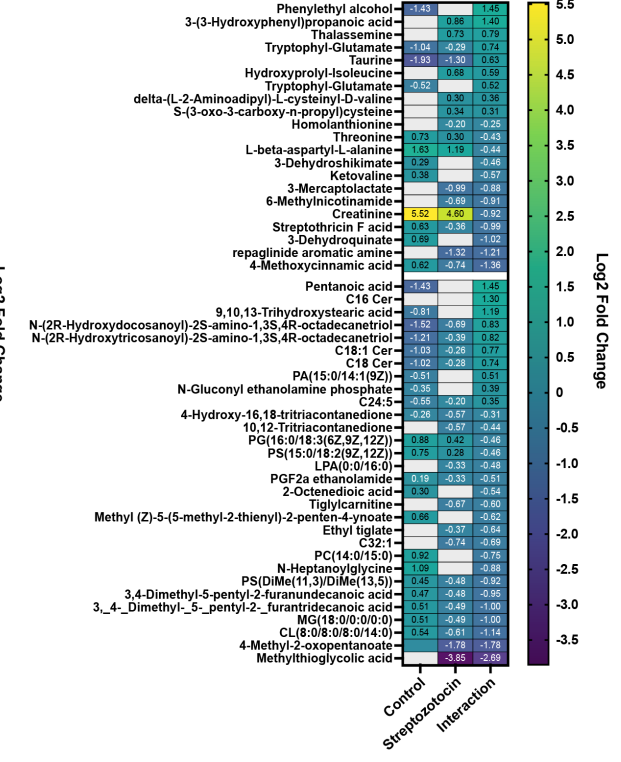


Figure 3: Hyperglycemia is associated with Q-TOF-MS metabolome divergence during ciprofloxacin treatment.

- A. Bray-Curtis Dissimilarity of Q-TOF-MS metabolite extracts from experimental groups with permutational ANOVA.
- B. KEGG pathway enrichment of differentially abundant Q-TOF-MS metabolites in STZ and ciprofloxacin treated mice versus normoglycemic ciprofloxacin-treated mice.
- C. Differentially abundant Q-TOF-MS metabolite features involved in carbohydrate, energy, and nucleotide metabolism. Data represent control and STZ-treated mice after ciprofloxacin treatment with interaction values versus vehicle-treated controls.
- D. Differentially abundant Q-TOF-MS metabolite features involved in amino acid and lipid metabolism. Data represent control and STZ-treated mice after ciprofloxacin treatment with interaction values versus vehicle-treated controls.

N = 12 per group.

Differentially abundant = Benjamini Hochberg adjusted $p < 0.05$.

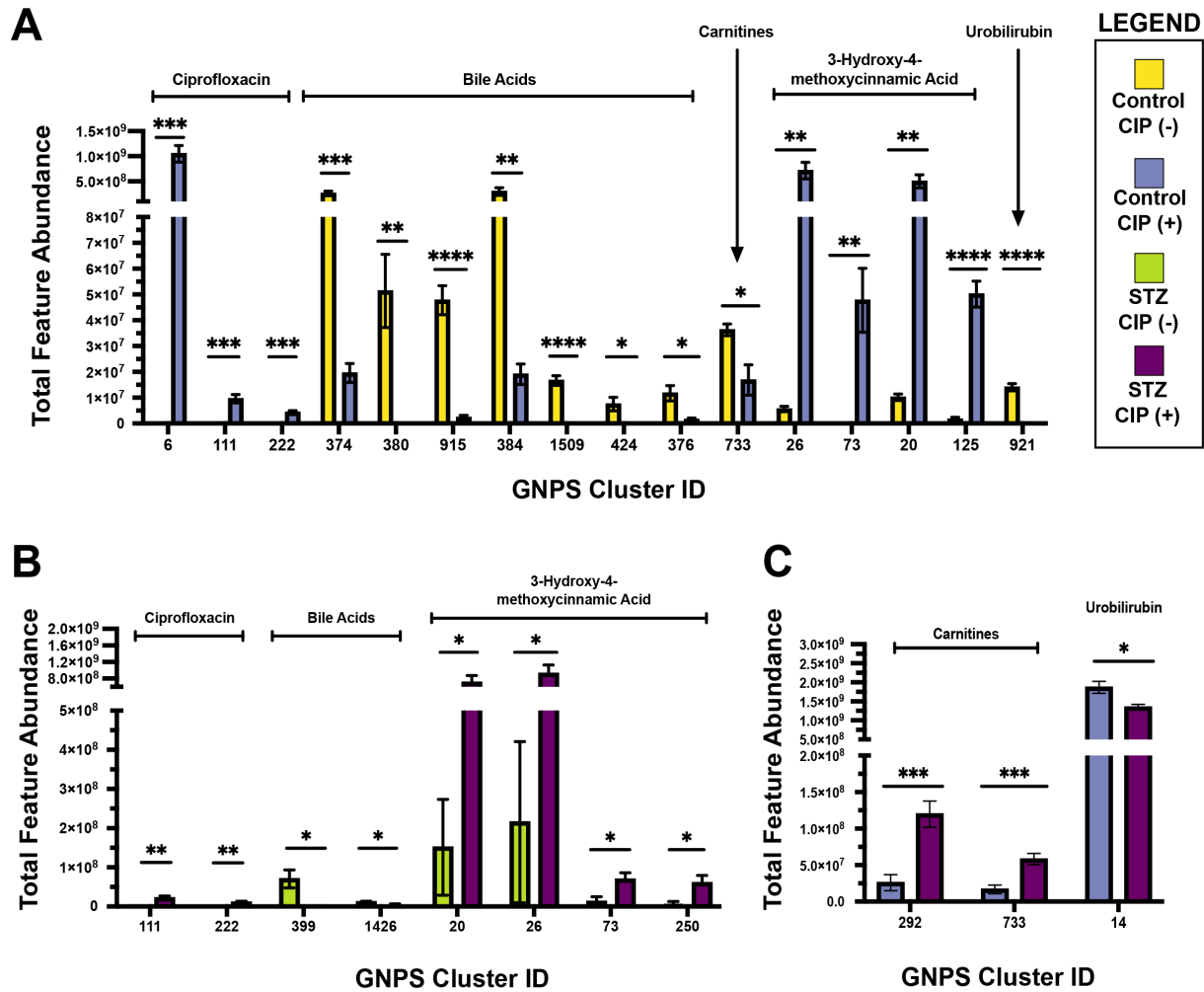


Figure 4 Hyperglycemia is associated with LC-MS/MS metabolome divergence during ciprofloxacin treatment. Differentially abundant GNPS-annotated clusters between that contain known metabolites within the cluster. Clusters were selected from the top-50 most relevant features via Random Forest Testing. Comparison is between

- Normoglycemic ciprofloxacin-treated mice versus vehicle controls
- Hyperglycemic ciprofloxacin-treated mice versus vehicle controls
- Hyperglycemic ciprofloxacin-treated mice versus normoglycemic ciprofloxacin-treated controls.

N = 12 per group.

(* p < 0.05, ** p < 0.01, *** p < 0.001; Welch's Unpaired T-test)

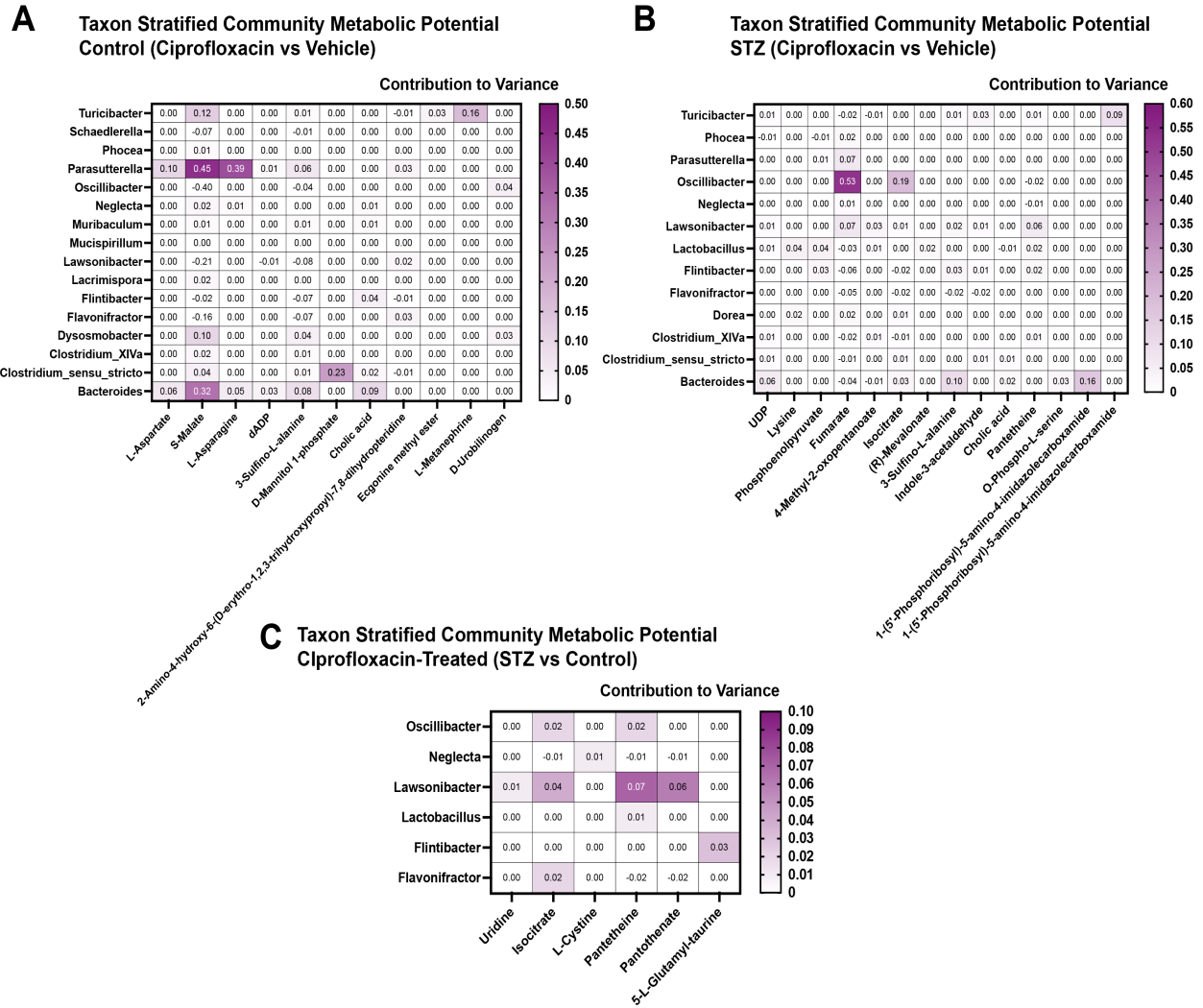


Figure 5: Taxon-stratified community metabolic potential during STZ and ciprofloxacin treatment. Community metabolic potential was calculated using the MIMOSA (version 2.0) algorithm by comparing Q-TOF-MS metabolite abundances and PICRUSt2-predicted metagenomic content. Data represent:

- A. Normoglycemic ciprofloxacin-treated mice versus vehicle controls
- B. Hyperglycemic ciprofloxacin-treated mice versus vehicle controls
- C. Hyperglycemic ciprofloxacin-treated mice versus normoglycemic ciprofloxacin-treated controls.

N = 8 to 14 per group

References

- An, J., Zhao, X., Wang, Y., Noriega, J., Gewirtz, A.T., Zou, J., 2021. Western-style diet impedes colonization and clearance of *Citrobacter rodentium*. *PLoS Pathog* 17, e1009497–22. doi:10.1371/journal.ppat.1009497
- Angelis, M., Ferrocino, I., Calabrese, F.M., Filippis, F., Cavallo, N., Siragusa, S., Rampelli, S., Cagno, R., Rantsiou, K., Vannini, L., Pellegrini, N., Lazzi, C., Turrone, S., Lorusso, N., Ventura, M., Chieppa, M., Neviani, E., Brigidi, P., Toole, P.W.O.X., Ercolini, D., Gobetti, M., Cocolin, L., 2020. Diet influences the functions of the human intestinal microbiome. *Sci Rep* 10, 1–15. doi:10.1038/s41598-020-61192-y
- Aquilani, R., 2004. Amino acid administration in patients with diabetes mellitus: supplementation or metabolic therapy? *Am. J. Cardiol.* 93 (8A), 21A-22A. doi: 10.1016/j.amjcard.2003.11.005
- Bäckhed, F., Fraser, C.M., Ringel, Y., Sanders, M.E., Sartor, R.B., Sherman, P.M., Versalovic, J., Young, V., Finlay, B.B., 2012. Defining a Healthy Human Gut Microbiome: Current Concepts, Future Directions, and Clinical Applications. *Cell Host Microbe* 12, 611–622. doi:10.1016/j.chom.2012.10.012
- Bernal, V., Sevilla, Á., Cánovas, M., Iborra, J.L., 2007. Production of L-carnitine by secondary metabolism of bacteria. *Microb. Cell. Fact.* 6, 31–17. doi:10.1186/1475-2859-6-31
- Bezirtzoglou, E., Stavropoulou, E., Kantartzi, K., Tsigalou, C., Voidarou, C., Mitropoulou, G., Prapa, I., Santarmaki, V., Kompoura, V., Yanni, A.E., Antoniadou, M., Varzakas, T., Kourkoutas, Y., 2021. Maintaining Digestive Health in Diabetes: The Role of the Gut Microbiome and the Challenge of Functional Foods. *Microorganisms* 9, 1–24. doi:10.3390/microorganisms9030516
- Blaser, M., 2011. Antibiotic overuse: Stop the killing of beneficial bacteria. *Nature* 476, 393–394. doi:10.1038/476393a
- Bolte, L.A., Vila, A.V., Imhann, F., Collij, V., Gacesa, R., Peters, V., Wijmenga, C., Kurilshikov, A., Campmans-Kujipers, M.J.E., Fu, K., Dijkstra, G., Zhernakova, A., Weersma, R.K., 2021. Long-term dietary patterns are associated with pro- inflammatory and anti-inflammatory features of the gut microbiome. *Gut* 70, 1287–1298. doi:10.1136/gutjnl-2020-322670
- Böttcher, C., Chapman, A., Fellermeier, F., Choudhary, M., Scheel, D., Glawischnig, E., 2014. The Biosynthetic Pathway of Indole-3-Carbaldehyde and Indole-3-Carboxylic Acid Derivatives in *Arabidopsis*. *Plant Physiol.* 165, 841–853. doi:10.1104/pp.114.235630
- Brooks, D.C., Bessey, P.Q., Black, P.R., Aoki, T.T., Wilmore, D.W., 1986. Insulin stimulates branched chain amino acid uptake and diminishes nitrogen flux from skeletal muscle in injured patients. *J. Surg. Res.* 40 (4), 395-405. Doi:10.1016/0022-4804(86)90205-2
- Cabral, D.J., Penumutchu, S., Reinhart, E.M., Zhang, C., Korry, B.J., Wurster, J.I., Nilson, R., Guang, A., Sano, W.H., Rowan-Nash, A.D., Li, H., Belenky, P., 2019. Microbial Metabolism Modulates Antibiotic Susceptibility within the Murine Gut Microbiome. *Cell Metab.* 30, 800–823.e7. doi:10.1016/j.cmet.2019.08.020
- Cabral, D.J., Wurster, J.I., Korry, B.J., Penumutchu, S., Belenky, P., 2020. Consumption of a Western-Style Diet Modulates the Response of the Murine Gut Microbiome to Ciprofloxacin. *mSystems* 5, 51–19. doi:10.1128/mSystems.00317-20
- Cantu-Jungles, T.M., Hamaker, B.R., 2020. New View on Dietary Fiber Selection for Predictable Shifts in Gut Microbiota. *Appl. Environ. Sci.* 11, e02179–19. doi:10.1128/mBio.02179-19
- Chen, C., Lu, Y., Wang, L., Yu, H., Tian, H., 2018. CcpA-Dependent Carbon Catabolite Repression Regulates Fructooligosaccharides Metabolism in *Lactobacillus plantarum*. *Front. Microbiol.* 9, 1–12. doi:10.3389/fmicb.2018.01114

- Chung, Y.W., Gwak, H.-J., Moon, S., Rho, M., Ryu, J.-H., 2020. Functional dynamics of bacterial species in the mouse gut microbiome revealed by metagenomic and metatranscriptomic analyses. *PLoS ONE* 15, e0227886–19. doi:10.1371/journal.pone.0227886
- Clooney, A.G., Fouhy, F., Sleator, R.D., O’ Driscoll, A., Stanton, C., Cotter, P.D., Claesson, M.J., 2016. Comparing Apples and Oranges?: Next Generation Sequencing and Its Impact on Microbiome Analysis. *PLoS ONE* 11, e0148028–16. doi:10.1371/journal.pone.0148028
- Coker, J.K., Moyne, O., Rodionov, D.A., Zengler, K., 2021. Carbohydrates great and small, from dietary fiber to sialic acids: How glycans influence the gut microbiome and affect human health. *Gut Microbes* 13, 1–19. doi:10.1080/19490976.2020.1869502
- Cruz-Morales, P., Orellana, C.A., Moutafis, G., Moonen, G., Rincon, G., Nielsen, L.K., Marcellin, E., 2019. Revisiting the Evolution and Taxonomy of Clostridia, a Phylogenomic Update. *Genome Biol. Evol.* 11, 2035–2044. doi:10.1093/gbe/evz096
- de Lastours, V., Fantin, B., 2015. Impact of fluoroquinolones on human microbiota. Focus on the emergence of antibiotic resistance. *Future Microbiol.* 10, 1241–1255. doi:10.2217/fmb.15.40
- Deeds, M.C., Anderson, J.M., Armstrong, A.S., Gastineau, D.A., Hiddinga, H.J., Jahangir, A., Eberhardt, N.L., Kudva, Y.C., 2011. Single dose streptozotocin-induced diabetes: considerations for study design in islet transplantation models. *Lab Anim.* 45, 131–140. doi:10.1258/la.2010.010090
- Deehan, E.C., Yang, C., Perez-Muñoz, M.E., Nguyen, N.K., Cheng, C.C., Triador, L., Zhang, Z., Bakal, J.A., Walter, J., 2020. Precision Microbiome Modulation with Discrete Dietary Fiber Structures Directs Short-Chain Fatty Acid Production. *Cell Host Microbe* 27, 389–404.e6. doi:10.1016/j.chom.2020.01.006
- Dethlefsen, L., Relman, D.A., 2011. Incomplete recovery and individualized responses of the human distal gut microbiota to repeated antibiotic perturbation. *Proc. Natl. Acad. Sci. USA.* 108, 4551–4561. doi:10.1073/pnas.1000087107
- Di Rienzi, S.C., Britton, R.A., 2020. Adaptation of the Gut Microbiota to Modern Dietary Sugars and Sweeteners. *Adv. Nutr.* 11, 616–629. doi:10.1093/advances/nmz118
- Dorries, K., Schlueter, R., Lalk, M., 2014. Impact of Antibiotics with Various Target Sites on the Metabolome of *Staphylococcus aureus*. *Antimicrob. Agents Chemother.* 58, 7151–7163. doi:10.1128/AAC.03104-14
- Douglas, G.M., Maffei, V.J., Zaneveld, J.R., Yurgel, S.N., Brown, J.R., Taylor, C.M., Huttenhower, C., Langille, M.G., 2020. PICRUSt2 for prediction of metagenome function. *Nat. Biotechnol.* 38, 1–4. doi:10.1038/s41587-020-0550-z
- Durkin, M.J., Jafarzadeh, S.R., Hseuh, K., Sallah, Y.H., Munshi, K.D., Henderson, R.R., Fraser, V.J., 2018. Outpatient Antibiotic Prescription Trends in the United States: A National Cohort Study. *Infect. Contr. Hosp. Epidemiol.* 39, 584–589. doi:10.1017/ice.2018.26
- Elbere, I., Silamiķelis, I., Dindune, I.I., Kainina, I., Ustinova, M., Zaharenko, L., Silamiķele, L., Rovite, V., Gudra, D., Konrade, I., Sokolovska, J., Pirags, V., Kloviņš, J., 2020. Baseline gut microbiome composition predicts metformin therapy short-term efficacy in newly diagnosed type 2 diabetes patients. *PLoS ONE* 15, 1–19. doi:10.1371/journal.pone.0241338
- Falla, T.J., Chopra, I., 1998. Joint tolerance to β -lactam and fluoroquinolone antibiotics in *Escherichia coli* results from overexpression of *hipA*. *Antimicrob. Agents Chemother.* 42, 3282–3284.
- Ferrer, M., Méndez-García, C., Rojo, D., Barbas, C., Moya, A., 2017. Antibiotic use and microbiome function. *Biochem. Pharmacol.* 134, 114–126. doi:10.1016/j.bcp.2016.09.007

- Franco-de-Moraes, A.C., Almeida-Pititto, B., Fernandes, G., Gomes, E.P., Pereira, A., Ferreira, S.R.G., 2017. Worse inflammatory profile in omnivores than in vegetarians associates with the gut microbiota composition. *Diab. Metab. Syndr.* 9, 1–8. doi:10.1186/s13098-017-0261-x
- Geier, B., Sogin, E.M., Michellod, D., Janda, M., Kompauer, M., Spengler, B., Dubilier, N., Liebeke, M., 2020. Spatial metabolomics of in situ host–microbe interactions at the micrometre scale. *Nat. Microbiol.* 5, 498–510. doi:10.1038/s41564-019-0664-6
- Gertsman, I., Barshop, B.A., 2018. Promises and pitfalls of untargeted metabolomics. *J. Inherit. Metab. Dis.* 41, 355–366. doi:10.1007/s10545-017-0130-7
- Goyal, S.N., Reddy, N.M., Patil, K.R., Nakhate, K.T., Ojha, S., Patil, C.R., Agrawal, Y.O., 2016. Challenges and issues with streptozotocin-induced diabetes - A clinically relevant animal model to understand the diabetes pathogenesis and evaluate therapeutics. *Chem. Biol. Interact.* 244, 49–63. doi:10.1016/j.cbi.2015.11.032
- Görke, B., Stülke, J., 2008. Carbon catabolite repression in bacteria: many ways to make the most out of nutrients. *Nat. Rev. Micro.* 6, 613–624. doi:10.1038/nrmicro1932
- Groen, B.B.L., Hortsman, A.M.H., Hamer, H.M., de Haan, M., van Kranenburg, J., Bierau, J., Poeze, M., Wodzig, W.K.W.H., Rasmussen, B.B., van Loon, L.J.C., 2016. Increasing Insulin Availability Does Not Augment Postprandial Muscle Protein Synthesis Rates in Healthy Young and Older Men. *J. Clin. Endocrinol. Metab.* 101, 3978-3988. doi:10.1210/jc.2016-1436
- Grundy, M.M.-L., Edwards, C.H., Mackie, A.R., Gidley, M.J., Butterworth, P.J., Ellis, P.R., 2016. Re-evaluation of mechanisms of dietary fibre and implications for macronutrient bioaccessibility, digestion, and postprandial metabolism. *Br. J. Nutr.* 116 (5), 816-833. doi:10.1017/S0007114516002610
- Hasselgren, P.O., Warner, B.W., James, J.H., Takehara, H., Fischer., 1987. Effect of insulin on amino acid uptake and protein turnover in skeletal muscle from septic rats. Evidence for insulin resistance and protein breakdown. *Arch. Surg.* 122 (2), 228-233. doi:10.101001/archsurg.1987.01400140110015
- Herbert, S.L., Nair, K.S., 2010. Protein Metabolism in Type 1 Diabetes. *Clin. Nutr.* 29, 13. doi:10.1016/j.clnu.2009.09.001
- Hintze, K.J., Benninghoff, A.D., Cho, C.E., Ward, R.E., 2018. Modeling the Western Diet for Preclinical Investigations. *Adv. Nutr.* 9, 263–271. doi:10.1093/advances/nmy002
- Hyoju, S.K., Zaborin, A., Keskey, R., Sharma, A., Arnold, W., van den Berg, F., Kim, S.M., Gottel, N., Bethel, C., Charnot-Katsikas, A., Jianxin, P., Adriaansens, C., Papazian, E., Gilbert, J.A., Zaborina, O., Alverdy, J.C., 2019. Mice Fed an Obesogenic Western Diet, Administered Antibiotics, and Subjected to a Sterile Surgical Procedure Develop Lethal Septicemia with Multidrug-Resistant Pathobionts. *mBio* 10, e00903–19. doi:10.1128/mBio.00903-19
- Jang, C., Hui, S., Lu, W., Cowan, A.J., Morscher, R.J., Lee, G., Liu, W., Tesz, G.J., Birnbaum, M.J., Rabinowitz, J.D., 2018. The small intestine coverts dietary fructose into glucose and organic acids. *Cell Metab.* 27, 351-361. doi:10.1016/j.cmet.2017.12.016
- Jones, D.R., Thomas, D., Alger, N., Ghavidel, A., Inglis, G.D., Abbott, D.W., 2018. SACCHARIS: an automated pipeline to streamline discovery of carbohydrate active enzyme activities within polyspecific families and de novo sequence datasets. *Biotechnol. Biofuels* 11, 1–15. doi:10.1186/s13068-018-1027-x
- Ju, T., Kong, J.Y., Stothard, P., Willing, B.P., 2019. Defining the role of *Parasutterella*, a previously uncharacterized member of the core gut microbiota. *ISME J.* 13, 1520–1534. doi:10.1038/s41396-019-0364-5

- Kalesh, K., Denny, P.W., 2019. A BONCAT-iTRAQ method enables temporally resolved quantitative profiling of newly synthesised proteins in *Leishmania mexicana* parasites during starvation. *PLoS Negl. Trop. Dis.* 13, e0007651. doi:10.1371/journal.pntd.0007651
- Klassen, L., Xing, X., Tingley, J.P., Low, K.E., King, M.L., Reintjes, G., Abbott, D.W., 2021. Approaches to Investigate Selective Dietary Polysaccharide Utilization by Human Gut Microbiota at a Functional Level. *Front. Microbiol.* 12, 1–11. doi:10.3389/fmicb.2021.632684
- Koepsell, H., 2020. Glucose transporters in the small intestine in health and disease. *Pflugers Arch.* 472, 1–42. doi:10.1007/s00424-020-02439-5
- Kolb, H.C., Finn, M.G., Sharpless, K.B., 2001. Click Chemistry: Diverse Chemical Function from a Few Good Reactions. *Angew. Chem. Int. Ed.* 40, 2004–2021. doi:10.1002/1521-3773(20010601)40:11<2004::aid-anie2004>3.3.co;2-x
- Lagkouvardos, I., Lesker, T.R., Hitch, T.C.A., Gálvez, E.J.C., Smit, N., Neuhaus, K., Wang, J., Baines, J.F., Abt, B., Stecher, B., Overmann, J., Strowig, T., Clavel, T., 2019. Sequence and cultivation study of Muribaculaceae reveals novel species, host preference, and functional potential of this yet undescribed family. *Microbiome* 7, 1–15. doi:10.1186/s40168-019-0637-2
- Lawson, P.A., Rainey, F.A., 2016. Proposal to restrict the genus *Clostridium* Prazmowski to *Clostridium butyricum* and related species. *Int. J. Syst. Evol. Microbiol.* 66, 1009–1016. doi:10.1099/ijsem.0.000824
- Lee, J.-Y., Cevallos, S.A., Byndloss, M.X., Tiffany, C.R., Olsan, E.E., Butler, B.P., Young, B.M., Rogers, A.W.L., Nguyen, H., Kim, K., Choi, S.-W., Bae, E., Lee, J.H., Min, U.-G., Lee, D.-C., Bäuml, A.J., 2020. High-Fat Diet and Antibiotics Cooperatively Impair Mitochondrial Bioenergetics to Trigger Dysbiosis that Exacerbates Pre-inflammatory Bowel Disease. *Cell Host Microbe* 28, 1–19. doi:10.1016/j.chom.2020.06.001
- Liu, Y., Yang, K., Jia, Y., Shi, J., Tong, Z., Fang, D., Yang, B., Su, C., Li, R., Xiao, X., Wang, Z., 2021. Gut microbiome alterations in high-fat-diet-fed mice are associated with antibiotic tolerance. *Nat. Microbiol.* 6, 874–884. doi:10.1038/s41564-021-00912-0
- Liu, Y.-X., Qin, Y., Chen, T., Lu, M., Qian, X., Guo, X., Bai, Y., 2021. A practical guide to amplicon and metagenomic analysis of microbiome data. *Protein Cell* 12, 315–330. doi:10.1007/s13238-020-00724-8
- Love, M.I., Huber, W., Anders, S., 2014. Moderated estimation of fold change and dispersion for RNA-seq data with DESeq2. *Genome Biol.* 15, 31–21. doi:10.1186/s13059-014-0550-8
- Mallick, H., Franzosa, E.A., McIver, L.J., Banerjee, S., Sirota-Madi, A., Kostic, A.D., Clish, C.B., Vlamakis, H., Xavier, R.J., Huttenhower, C., 2019. Predictive metabolomic profiling of microbial communities using amplicon or metagenomic sequences. *Nat. Commun.* 10, 1–11. doi:10.1038/s41467-019-10927-1
- Macías-Acosta, M.P., Valerdi-Costreras, L., Bustos-Angel, E.D., García-Reyes, R.A., Alvarez-Zavala, M., González-Ávila., 2021. Involvement of the fecal amino acid profile in a clinical and anthropometric study of Mexican patients with insulin resistance and type 2 diabetes mellitus. *Amino Acids*. doi: 10.1007/s00726-021-03107-3
- Meadows, J.A., Wargo, M.J., 2015. Carnitine in bacterial physiology and metabolism. *Microbiology* 161, 1161–1174. doi:10.1099/mic.0.000080
- Mefferd, C.C., Bhute, S.S., Phan, J.R., Villarama, J.V., Do, D.M., Alarcia, S., Abel-Santos, E., Hedlund, B.P., 2020. A High-Fat/High-Protein, Atkins-Type Diet Exacerbates *Clostridioides* (*Clostridium*) *difficile* Infection in Mice, whereas a High-Carbohydrate Diet Protects. *mSystems* 5, e00765–19. doi:10.1128/mSystems.00765-19

- Merino, B., Fernández-Díaz, C.M., Cózar-Castellano, I., Perdomo, G., 2020. Intestinal Fructose and Glucose Metabolism in Health and Disease. *Nutrients* 12, 94. doi:10.3390/nu12010094
- Møller, N., Nair, K.S., 2008. Diabetes and Protein Metabolism. *Diabetes* 57, 3-4. doi:10.2337/db07-1581
- Morrison, K.E., Jašarević, E., Howard, C.D., Bale, T.L., 2020. It's the fiber, not the fat: significant effects of dietary challenge on the gut microbiome. *Microbiome* 8, 1–11. doi:10.1186/s40168-020-0791-6
- Müller, M., Canfora, E.E., Blaak, E.E., 2018. Gastrointestinal Transit Time, Glucose Homeostasis and Metabolic Health: Modulation of Dietary Fibers. *Nutrients* 10 (3), 275. doi:10.3390/nu10030275
- Noecker, C., Eng, A., Srinivasan, S., Theriot, C.M., Young, V.B., Jansson, J.K., Fredricks, D.N., Borestein, E., 2016. Metabolic Model-Based Integration of Microbiome Taxonomic and Metabolomic Profiles Elucidates Mechanistic Links between Ecological and Metabolic Variation. *mSystems* 1, e00013–15. doi:10.1128/mSystems.00013-15
- Payling, L., Fraser, K., Loveday, S.M., Sims, I., Roy, N., McNabb, W., 2020. The effects of carbohydrate structure on the composition and functionality of the human gut microbiota. *Trends Food Sci. Technol.* 97, 233–248. doi:10.1016/j.tifs.2020.01.009
- Pircalabioru, G.G., Corcionivoschi, N., Gundogdu, O., Chifiriuc, M.-G., Marutescu, L.G., Ispas, B., Savu, O., 2021. Dysbiosis in the Development of Type I Diabetes and Associated Complications: From Mechanisms to Targeted Gut Microbes Manipulation Therapies. *Int. J. Mol. Sci.* 22, 1–17. doi:10.3390/ijms22052763
- Poretzky, R., Rodriguez-R, L.M., Luo, C., Tsementzi, D., Konstantinidis, K.T., 2014. Strengths and Limitations of 16S rRNA Gene Amplicon Sequencing in Revealing Temporal Microbial Community Dynamics. *PLoS ONE* 9, e93827–12. doi:10.1371/journal.pone.0093827
- Ranjan, R., Rani, A., Metwally, A., McGee, H.S., Perkins, D.L., 2016. Analysis of the microbiome: Advantages of whole genome shotgun versus 16S amplicon sequencing. *Biochem. Biophys. Res. Commun.* 469, 967–977. doi:10.1016/j.bbrc.2015.12.083
- Roager, H.M., Licht, T.R., 2018. Microbial tryptophan catabolites in health and disease. *Nat. Commun.* 9, 1–10. doi:10.1038/s41467-018-05470-4
- Rumpagaporn, P., Reuhs, B.L., Kaur, A., Patterson, J.A., Keshavarzian, A., Hamaker, B.R., 2015. Structural features of soluble cereal arabinoxylan fibers associated with a slow rate of in vitro fermentation by human fecal microbiota. *Carbohydr. Polym.* 130, 191–197. doi:10.1016/j.carbpol.2015.04.041
- Sachar, M., Anderson, K.E., Ma, X., 2016. Protoporphyrin IX: the Good, the Bad, and the Ugly. *J. Pharmacol. Exper. Ther.* 356, 267–275. doi:10.1124/jpet.115.228130
- Sala, D., Zorzano, A., 2015. Differential control of muscle mass in type 1 and type 2 diabetes mellitus. *Cell Mol. Life Sci.* 72 (20), 3802–3817. doi:10.1007/s00018-015-1954-7
- Satokari, R., 2020. High Intake of Sugar and the Balance between Pro- and Anti-Inflammatory Gut Bacteria. *Nutrients* 12, 1–4. doi:10.3390/nu12051348
- Schnizlein, M.K., Vendrov, K.C., Edwards, S.J., Martens, E.C., Young, V.B., 2020. Dietary Xanthan Gum Alters Antibiotic Efficacy against the Murine Gut Microbiota and Attenuates *Clostridioides difficile* Colonization. *mSphere* 5, e00708–19. doi:10.1128/mSphere.00708-19
- Shaffer, M., Borton, M.A., McGivern, B.B., Zayed, A.A., La Rosa, S.L., Solden, L.M., Liu, P., Narrowe, A.B., Rodríguez-Ramos, J., Bolduc, B., Gazitúa, M.C., Daly, R.A., Smith, G.J., Vik, D.R., Pope, P.B., Sullivan, M.B., Roux, S., Wrighton, K.C., 2020. DRAM for distilling

- microbial metabolism to automate the curation of microbiome function. *Nucleic Acids Res.* 48, 8883–8900. doi:10.1093/nar/gkaa621
- Shah, B.R., Bin Li, Sabbah, Al, H., Xu, W., Mráz, J., 2020. Effects of prebiotic dietary fibers and probiotics on human health: With special focus on recent advancement in their encapsulated formulations. *Trends Food Sci. Technol.* 102, 178–192. doi:10.1016/j.tifs.2020.06.010
- Silamiķele, L., Silamiķelis, I., Ustinova, M., Kalniņa, Z., Elbere, I., Petrovska, R., Kalniņa, I., Kloviņš, J., 2021. Metformin Strongly Affects Gut Microbiome Composition in High-Fat Diet-Induced Type 2 Diabetes Mouse Model of Both Sexes. *Front. Endocrinol.* 12, 1–16. doi:10.3389/fendo.2021.626359/full
- Siljander, H., Honkanen, J., Knip, M., 2019. Microbiome and type 1 diabetes. *EBioMedicine* 46, 512–521. doi:10.1016/j.ebiom.2019.06.031
- Stiemsma, L.T., Michels, K.B., 2018. The Role of the Microbiome in the Developmental Origins of Health and Disease. *Pediatrics* 141, e20172437–22. doi:10.1542/peds.2017-2437
- Talukdar, R., Sarkar, P., Jakkampudi, A., Sarkar, S., Aslam, M., Jandhyala, M., Deepika, G., Unnisa, M., Reddy, D.N., 2021. The gut microbiome in pancreatogenic diabetes differs from that of Type 1 and Type 2 diabetes. *Sci. Rep.* 11, 1–12. doi:10.1038/s41598-021-90024-w
- Tate, M., Deo, M., Cao, A.H., Hood, S.G., Huynh, K., Kiriazis, H., Du, X.-J., Julis, T.L., Figtree, G.A., Dusting, G.J., Kaye, D.M., Ritchie, R.H., 2017. Insulin replacement limits progression of diabetic cardiomyopathy in the low-dose streptozotocin-induced diabetic rat. *Diabetes Vasc. Dis. Res.* 14, 423–433. doi:10.1177/1479164117710390
- Thaiss, C.A., Levy, M., Grosheva, I., Zheng, D., Soffer, E., Blacher, E., Braverman, S., Tengeler, A.C., Barak, O., Elazar, M., Ben-Zeev, R., Lehavi-Regev, D., Katz, M.N., Pevsner-Fischer, M., Gertler, A., Halpern, Z., Harmelin, A., Amar, S., Serradas, P., Grosfeld, A., Shapiro, H., Geiger, B., Elinav, E., 2018. Hyperglycemia drives intestinal barrier dysfunction and risk for enteric infection. *Science* 359, 1376–1383. doi: 10.1126/science.aar3318
- The Human Microbiome Project Consortium, 2012. Structure, function and diversity of the healthy human microbiome. *Nature* 486, 207–214. doi:10.1038/nature11234
- Vila, A.V., Collij, V., Sanna, S., Sinha, T., Imhann, F., Bourgonje, A.R., Mujagic, Z., Jonkers, D.M.A.E., Masclee, A.A.M., Fu, J., Kurilshikov, A., Wijmenga, C., Zhernakova, A., Weersma, R.K., 2020. Impact of commonly used drugs on the composition and metabolic function of the gut microbiota. *Nat. Commun.* 362, 1–11. doi:10.1038/s41467-019-14177-z
- Wang, H., Tang, W., Zhang, P., Zhang, Z., He, J., Zhu, D., Bi, Y., 2020. Modulation of gut microbiota contributes to effects of intensive insulin therapy on intestinal morphological alteration in high-fat-diet-treated mice. *Acta Diabetol.* 57, 455–467. doi:10.1007/s00592-019-01436-0
- Wang, Y., Zhang, C., Lai, J., Zhao, Y., Lu, D., Bao, R., Feng, X., Zhang, T., Liu, Z., 2020. Noninvasive PET tracking of post-transplant gut microbiota in living mice. *Eur. J. Nucl. Med. Mol. Imaging* 47, 991–1002. doi:10.1007/s00259-019-04639-3
- Warner, J.B., Lolkema, J.S., 2003. CcpA-Dependent Carbon Catabolite Repression in Bacteria. *Microbiol. Mol. Biol. Rev.* 67, 475–490. doi:10.1128/MMBR.67.4.475-490.2003
- Warren, F.J., Fukuma, N., Mikkelsen, D., Flanagan, B.M., Williams, B.A., Lisle, A.T., Cuiv, P.O., Morrison, M., Gidley, M.J., 2018. Food Starch Structure Impacts Gut Microbiome Composition. *mSphere* 3, e00086–18. doi:10.1128/mSphere.00086-18
- Warshauer, J.T., Bluestone, J.A., Anderson, M.S., 2020. New Frontiers in the Treatment of Type 1 Diabetes. *Cell Metab.* 31, 46–61. doi:10.1016/j.cmet.2019.11.017

- Weber Jr., F.L., Veach, G.L., Friedman, D.W., 1981. Effects on insulin and glucagon on the uptake of amino acids from arterial blood by canine ileum. *Dig. Dis. Sci.* 26, 113-118. doi:10.1007/BF01312226
- Winther, S.A., Mannerla, M.M., Frimodt-Møller, M., Persson, F., Hansen, T.W., Lehto, M., Hörkkö, S., Blaut, M., Forsblom, C., Groop, p.-H., Rossing, P., 2021. Fecal biomarkers of type 1 diabetes with and without diabetic nephropathy. *Sci. Rep.* 11, 15208. doi:10.1038/s41598-021-94747-8
- Wu, H., Esteve, E., Tremaroli, V., Khan, M.T., Caesar, R., Mannerås-Holm, L., Ståhlman, M., Olsson, L.M., Serino, M., Planas-Fèlix, M., Xifra, G., Mercader, J.M., Torrents, D., Burcelin, R., Ricart, W., Perkins, R., Fernández-Real, J.M., Bäckhed, F., 2017. Metformin alters the gut microbiome of individuals with treatment-naive type 2 diabetes, contributing to the therapeutic effects of the drug. *Nat. Med.* 23, 850–858. doi:10.1038/nm.4345
- Zhou, H., Sun, L., Zhang, S., Zhao, X., Gang, X., Wang, G., 2020. Evaluating the Causal Role of Gut Microbiota in Type 1 Diabetes and Its Possible Pathogenic Mechanisms. *Front. Endocrinol.* 11, 1–13. doi:10.3389/fendo.2020.00125
- Zhou, Z., Zhang, Y., Zheng, P., Chen, X., Yang, Y., 2013. Starch structure modulates metabolic activity and gut microbiota profile. *Anaerobe* 24, 71–78. doi:10.1016/j.anaerobe.2013.09.012

Appendix I:
Antibiotic Persistence as a Metabolic Adaptation:
Stress, Metabolism, the Host, and New Directions

Originally published in *Pharmaceuticals*, 01 February 2018, Vol 11, No. 14.
DOI: 10.3390/ph11010014

Antibiotic Persistence as a Metabolic Adaptation: Stress, Metabolism, the Host, and New Directions

Damien J. Cabral^{1,+}, Jenna I. Wurster^{1,+}, Peter Belenky^{1,#}

¹ Department of Molecular Microbiology and Immunology, Brown University, Providence, RI 02906, USA

⁺ Damien J. Cabral and Jenna I. Wurster contributed equally to this work

[#] Address correspondence to Peter Belenky, peter_belenky@brown.edu

Abstract

Persistence is a phenomenon during which a small fraction of a total bacterial population survives treatment with high concentrations of antibiotics for an extended period of time. In conjunction with biofilms, antibiotic persisters represent a major cause of recalcitrant and recurring infections, resulting in significant morbidity and mortality. In this review, we discuss the clinical significance of persister cells and the central role of bacterial metabolism in their formation, specifically with respect to carbon catabolite repression, sugar metabolism, and growth regulation. Additionally, we will examine persister formation as an evolutionary strategy used to tolerate extended periods of stress and discuss some of the response mechanisms implicated in their formation. To date, the vast majority of the mechanistic research examining persistence has been conducted in artificial *in vitro* environments that are unlikely to be representative of host conditions. Throughout this review, we contextualize the existing body of literature by discussing how *in vivo* conditions may create ecological niches that facilitate the development of persistence. Lastly, we identify how the development of next generation sequencing and other “big data” tools may enable researchers to examine persistence mechanisms within the host to expand our understanding of their clinical importance.

Keywords

Persistence, Tolerance, Metabolism, Biofilms, Next-Generation Sequencing

List of Abbreviations

CCR	Carbon Catabolite Repression
FISH	Fluorescence <i>In Situ</i> Hybridization
LCMD	Laser-Capture Microdissection
MRSA	Methicillin-Resistant <i>Staphylococcus aureus</i>
NTHi	Non-Typable <i>Haemophilus influenzae</i>
OM	Otitis Media
PASH	Persistence As Stuff Happens
PMF	Proton Motive Force
ROS	Reactive Oxygen Species
SSTI	Skin and Soft Tissue Infection
TCA	Tricarboxylic Acid
Tn-seq	Transposon Sequencing

Introduction

The discovery of antibiotics and their widespread use in the 20th century represent a significant milestone in human history. Commercial antibiotics have saved innumerable lives, but their efficacy has declined at an alarming rate due to the spread of antibiotic resistance. Within a decade of the first major utilization of penicillin therapy in soldiers during World War II (Michiels et al., 2016), penicillin resistance became a significant clinical burden and signaled the beginning of an “arms race” between pathogenic bacteria and pharmaceutical development (Ventola, 2015). In addition to resistance, physicians such as Joseph Bigger were vexed by a concerning phenomenon; although penicillin was frequently and successfully used to treat *Staphylococcal* wound infections, therapies often failed to completely sterilize the infection site, ultimately resulting in severe infection relapse and mortality (Bigger, 1944). Bigger coined the term “persisters” to describe a minority subpopulation of bacterial cells that could survive antibiotic challenge in the absence of resistance (Bigger, 1944; Ventola, 2015). Here, we define persisters as a small fraction of a total bacterial population that can survive long-term treatment with high concentrations of antibiotics. However, unlike resistant bacteria, most of these cells regain sensitivity after regrowth and new treatment typically results in the same small surviving fraction. Additionally, the phenomenon of tolerance is closely related to and often confused with persistence. Tolerance also enables bacterial cells to survive exposure to lethal concentrations of antibiotics; however, unlike persisters, tolerant cells make up a larger portion of the population and they are only temporarily protected from antibiotic exposure.

Over the last 60 years, an expansive body of work has focused on characterizing the genetic determinants, molecular mechanisms, and epidemiology of antibiotic resistance. Although the breadth of research on antibiotic persistence is less robust, the past decade has seen burgeoning

interest in persistence as a cause of clinical therapeutic failure (Michiels et al., 2016). In recent years, the defining characteristics of persisters and their formation have been codified in primary literature and multiple reviews (Brauner et al., 2016; Harms et al., 2016; Lewis, 2010; 2007; Maisonneuve and Gerdes, 2014; Olive and Sasseti, 2016). In this review, we aim to link work from the distinct fields of systems biology and *in vivo* clinical microbiology. Although these fields have been operating somewhat independently, we feel they are intrinsically related and together can help to decipher the heterogeneous phenomenon of antibiotic persistence. We will discuss antibiotic persistence as it relates to bacterial metabolism, specifically focusing on how carbon catabolite repression, sugar metabolism, and growth regulation are involved in persister formation. We will contextualize these findings by discussing how *in vivo* conditions create ecological niches that facilitate persistence development. Finally, we will discuss how persister formation represents a unique evolutionary strategy to combat antibiotic stress as well as some of the response mechanisms implicated in persister formation.

As we discuss this previous research, it is important to consider that a majority of mechanistic studies on persisters have been conducted under artificial conditions *in vitro*. In reality, antibiotics act on and induce persisters in complex polymicrobial communities that are themselves profoundly impacted by the host environment. Thus, the insight generated from this work may not be fully biologically relevant or clinically applicable. However, the development of new tools based on next-generation sequencing and “big data” analysis may allow us to study persistence and persistence-related processes in the host. Throughout this review, we will identify applications where these tools can be utilized to expand our understanding.

Persistence as an Evolutionary Adaptation

The term persistence describes the ability of a bacterial subpopulation to survive antibiotic exposure due to non-heritable phenotypic variation that is distinct from the mechanisms that generate resistance (Michiels et al., 2016). Persisters represent a small fraction of the total cells, but their survival allows the population to survive times of high antibiotic exposure (Brauner et al., 2016). After stress subsides, persisters revert to an antibiotic-sensitive state, reinitiate growth, and repopulate the local environment. In fact, post-treatment sensitization towards antibiotics is a definitive characteristic of persister cells (Maisonneuve and Gerdes, 2014). This phenomenon is akin to ecological succession, where antibiotic pressure represents a bottleneck event and persisters are the first to subsequently utilize available nutrients and environmental niches. Like a wildfire that decimates a forest, antibiotic exposure wipes out 99 percent of a susceptible community while persister cells survive as a result of their transient antibiotic tolerance. As the sole survivors of antibiotic exposure, these persister cells then function as the pioneer “species” in a now-vacant ecological niche and subsequently lose their tolerant phenotype as they repopulate and grow towards a steady state community. In this manner, persistence can be viewed as an evolutionary strategy by which a population assures its survival through a few key members.

As an adaptive trait, persistence is heterogeneous and emerges via multiple mechanisms. Persistence has thus been categorized into subtypes for clarification. First, time-dependent persistence is contingent on growth rate reductions within the persister subpopulation that reduce antibiotic uptake and target availability (Balaban et al., 2004). Time-dependent persistence can be further subdivided into Type I and Type II persistence, where Type I is triggered by a reduced lag time and Type II is triggered by growth rate reduction (Balaban et al., 2004; Brauner et al., 2016). Second, dose-dependent persistence is an adaptive response in which transient overexpression of efflux pumps and stress response pathways facilitate survival during antibiotic challenge (Balaban

et al., 2004; Brauner et al., 2016; Nandakumar et al., 2014). The PASH (Persistence As Stuff Happens) model has recently gained popularity and suggests that both time- and dose-dependent persistence are the result of stochastic errors in metabolism, cell division, and stress responses and is thus analogous to spontaneous mutations observed in antibiotic resistance (Grant and Hung, 2013). PASH suggests that persistence is a form of bet-hedging or adaptive behavior in which a small subset of the population exhibits randomized phenotypic variation. The utilization of toxin-antitoxin modules serves as one example of this bet-hedging strategy. Perhaps the best characterized of these systems is the *hipAB* module in *Escherichia coli* (Rotem et al., 2010). In this case, *E. coli* enters a dormant state once the levels of the *hipA* toxin exceed a certain threshold (Rotem et al., 2010). Overexpression of *hipA* increases the tolerance of *E. coli* to bactericidal antibiotics (Keren et al., 2004). However, these toxin levels fluctuate within a population in the absence of antibiotics, suggesting that they may represent a generalized response that allows bacterial populations to survive sudden stress (Keren et al., 2004; Levin and Rozen, 2006; Rotem et al., 2010). Compared to antibiotic resistance, this randomization confers a selective advantage with a significantly diminished fitness cost and reduced need for compensatory adaptations (MacLean and Vogwill, 2014).

Vogwill et al. recently aimed to identify whether persistence and resistance represent complementary, albeit divergent, survival strategies that bacteria have co-opted to survive antibiotic and environmental stressors (Vogwill et al., 2016). After challenging various *Pseudomonas* species with ciprofloxacin and rifampin, they found that persistence and resistance generation were mechanistically unrelated but positively correlated, suggesting that they represent complementary, rather than competitive, evolutionary strategies (Vogwill et al., 2016). Persistence is a plastic trait, while resistance is genetically encoded. If antibiotic exposure is constant, there

would be no need for the evolution of plastic traits and selection would favor resistance. However, if antibiotic exposure is transient, selection should favor phenotypic plasticity due to the higher fitness costs of resistance relative to persistence. By maintaining a variant subpopulation, the bacterial population, as a whole, ensures its survival in times of transient stress (Vogwill et al., 2016).

Thanks to technological expansion in genomics during the last decade, persister research can capitalize on next-generation methods used in virulence and antibiotic resistance studies. Transposon-sequencing (Tn-seq) is an attractive, massively parallel means of identifying persister-associated gene targets *in vivo* under various selective conditions (Figure 1A) (Powell et al., 2016; Santiago, 2015; Valentino et al., 2014). Tn-seq has the potential to confirm the importance of known persister genes under specific stress conditions as well as identify novel persistence mechanisms in the host. In addition to new *in vivo* work, retrospective genomic studies can be used to identify known persister genes with varying amounts of selective pressure. Specifically, it may be beneficial to analyze clinical isolates of common pathogenic bacteria taken over the last sixty years of antimicrobial availability to ascertain evolutionary pressure and conservation of key persister genes (Figure 1B) (Vogwill et al., 2016).

Biofilms Can Promote Antibiotic Persistence in Clinical Settings.

While persister development is an adaptive strategy at an individual level, bacteria can also exhibit community structure can aid in bacterial fitness and promote persister development, particularly if community-wide adaptations to survive antibiotic challenge. Committing to a biofilm community the biofilm is slow growing in nature (Lewis, 2001). Biofilms are an amalgam of one or more bacterial species structure can aid in bacterial fitness and promote persister

development, particularly if the biofilm is that colonize and adhere to physical surfaces in a density-dependent manner. The biofilm creates slow growing in nature (Lewis, 2001). Biofilms are an amalgam of one or more bacterial species that colonize heterogeneous gradients in signaling molecules, nutrients, and environmental exposures that and adhere to physical surfaces in a density-dependent manner. The biofilm creates heterogeneous gradients in signaling molecules, nutrients, and environmental exposures that generate diverse micro-niches (Michiels et al., 2016). Biofilm formation is found ubiquitously across microbial phyla and facilitates colonization of both abiotic and biotic surfaces with relative ease (Cohen et al., 2013).

Biofilms are characteristically stress-resilient, and they are a great example of how population size and fitness are positively correlated through the Allee effect (Goswami et al., 2017). The Allee effect describes scenarios in which biological characteristics correlate the population density of a given ecosystem with the fitness of individual species or the population within that ecosystem (Goswami et al., 2017). In microbial ecology, biofilms increase the total population density irrespective of whether they are mono- or polymicrobial. As the population becomes stabilized by density, intraspecies variation and thus fitness drastically increases due to cooperative interactions and reduced genetic drift (Davey and OToole, 2000; Roches et al., 2018). The biofilm as a total population exhibits antibiotic tolerance and increased cooperative interactions within the population might generate conditions that increase persister cell formation.

Clinically, biofilms are associated with antibiotic recalcitrance, infection recurrence, and persister formation (Michiels et al., 2016). Biofilm formation has been documented in both Gram-positive and Gram-negative pathogens and is clinically significant in various infection types, ranging from skin and soft tissue infections (SSTI), implanted device infections, urinary tract infections, endocarditis, otitis media, and more (Cohen et al., 2013; Goneau et al., 2014; Grant and

Hung, 2013; Lebeaux et al., 2014; Perez et al., 2014). Approximately 50 percent of all nosocomial infections originate from implanted medical devices such as prosthetic joints, catheters, and prosthetic heart valves, all of which provide abiotic surfaces for the development of biofilms (Grant and Hung, 2013). In patients, tissue location and biofilm progression can result in varied antibiotic exposure even in the presence of clinically appropriate dosing (MacLean and Vogwill, 2014). Ultimately, this results in bacterial exposure to sub-inhibitory antibiotic concentrations, which can promote persister development (Dörr et al., 2010; Kudrin et al., 2017; MacLean and Vogwill, 2014; Shah et al., 2006).

Biofilm formation appears to confer significant fitness advantages to pathogenic bacteria. As an environment subject to ecological drivers, biofilms promote intraspecies variation that encourages persister development. Lee et al. have suggested that heterogeneity promotes antibiotic tolerance through the altruistic behavior of a few variant subpopulations within the biofilm (Lee et al., 2010). This “bacterial charity” is analogous to kin selection, where a subset of cells obtains resistance- or persistence-conferring capacity and provides protection to others. Lee found that mutations in indole production were directly correlated to charity events in polymicrobial biofilms. By challenging *E. coli* strains to increasing concentrations of fluoroquinolones, they found that a highly resistant and high indole-producing subpopulation triggered overall biofilm tolerance via indole signaling (Lee et al., 2010). Biofilms are ultimately important to the study of persister formation because they represent the endogenous ecological structures that many bacteria will adopt within a host (Jefferson, 2004).

Persister cells are implicated as a causative agent in a multitude of biofilm-related recurrent infections including urinary tract infections, where sub-inhibitory antibiotic concentrations promote persister development and multi-drug tolerance (Blango and Mulvey, 2010; Goneau et

al., 2014; Parsek and P. K. Singh, 2003). In otitis media (OM), a commonly chronic or recurrent infection, the formation of a polymicrobial biofilm is initiated by opportunistic members of the nasopharyngeal microbiota that migrate towards the inner ear and trigger infection (Perez et al., 2014). In OM, the role of cooperative intraspecies interactions has been well documented. In polymicrobial biofilms, cooperation promotes multi-drug tolerance by persister cells (Perez et al., 2014). Specifically, *Moraxella catarrhalis* provides passive β -lactam protection to *Streptococcus pneumoniae* and non-typable *Haemophilus influenzae* (NTHi), and in turn they provide tolerance towards fluoroquinolones by promoting *M. catarrhalis* persister cell formation (Perez et al., 2014). Here, as in periprosthetic joint implant infections, biofilm formation functions as a vehicle for persister cell development (Urish et al., 2016). In *Staphylococcal* infections, recurrent SSTIs have been associated with biofilms in response to prolonged antibiotic exposure, including last-line therapies such as vancomycin (Conlon et al., 2016). In catheter-related bloodstream infections, there is an effective relapse rate of approximately 20 percent, due to surviving persister populations within catheter-adhered biofilms (Lebeaux et al., 2014). Even extended antibiotic therapy at 1000-fold inhibitory concentrations is insufficient to eliminate the biofilm (Lebeaux et al., 2014). Thus, the theme of a biofilm functioning as an environment that promotes tolerant infections and persister cell development is prominent in clinical settings.

The question then becomes how can we study persister formation in host-related biofilms? As with persister gene evolution, Tn-seq is an attractive option in which a host-related biofilm infection model can be established with a high-density transposon insertion library (Figure 1A). Alternatively, persister-specific Fluorescence In-Situ Hybridization (FISH) could be used to isolate biofilms from *in vivo* contexts and identify persisters in their native environment by quantifying expression of persister elements such as toxin-antitoxin systems (Briley et al., 2014;

Nistico et al., 2009). Laser-capture microdissection (LCMD) could then be coupled with transcriptomic analysis to isolate specific, persister-containing fragments of the biofilm, assess their transcriptional activity, and decouple it from culture-specific or *in vitro*-specific variation (Figure 1C). The great strength of LCMD coupled with FISH is that it allows the transcriptional analysis of populations enriched for persisters. A similar approach could and has been taken to analyze transcriptional response of persisters in liquid culture using flow cytometry sorting (Henry and Brynildsen, 2016; Orman and Brynildsen, 2013a). While these approaches enrich for persisters, clear challenges related to intrinsically low abundance of persisters still remain. However, as single-cell sequencing technologies advance, many of these challenges can be effectively solved by enabling analysis of rare persister cells (Avraham et al., 2015; Heacock-Kang et al., 2017; Hör et al., 2018; Kang et al., 2015; Saliba et al., 2016; 2017; Wang et al., 2015). The key to each of these approaches is that they allow monitoring of persister biology in biofilms generated within the host, providing additional translational impact.

Growth, Metabolism, and ATP Production

The formation of biofilms and persister cells represent two interrelated yet phenotypically distinct strategies utilized by bacteria to tolerate antibiotic treatment. Despite their differences, however, growth rate and the underlying metabolic state are crucial determinants of the antibiotic tolerance displayed by both biofilm and persister cells. As a complex ecological environment, biofilms exhibit heterogeneity in their population structure and metabolic activity. Cells proximal to the center of the biofilm can exhibit marked dormancy relative to cells in the periphery (Walters et al., 2003). As a result, antibiotic efficacy is highest at the air interface, where metabolic activity is highest (Walters et al., 2003). Additionally, the growth rate of biofilm cells has been shown to

be a major determinant of antibiotic susceptibility in both *Pseudomonas aeruginosa* and *E. coli* (Jöers et al., 2010; Tanaka et al., 1999). Similar dynamics have also been observed in non-biofilm persister cells. Tolerance and persistence are closely associated with the rate and phase of bacterial growth (Betts et al., 2002; Gutierrez et al., 2017; Lobritz et al., 2015; Nandakumar et al., 2014; R. Singh et al., 2009). For example, slow growth rates have been shown to permit stable tolerant phenotypes in *E. coli* (Fung et al., 2010), and both *P. aeruginosa* and *S. aureus* display an increase in persister formation in mid-exponential and stationary phase while remaining unchanged in early exponential phase (Keren et al., 2004). Conversely, maintaining bacterial cultures in early exponential phase has been found to completely eliminate persisters (Keren et al., 2004; Lewis, 2010). Furthermore, *E. coli* has demonstrated an ability to modulate its lag time to match the duration of antibiotic exposure when subjected to repeated treatments (Fridman et al., 2014). Therefore, modulation of growth rate appears to be an adaptive and transient response to antibiotic exposure.

A major contributing factor to variations in growth rate is nutrient availability, with nutrient limitation having long been known to induce persistence. Glucose deprivation has been shown to increase the formation of persisters and increase biofilm tolerance to fluoroquinolone and β -lactam treatment (Amato et al., 2013; Bernier et al., 2013). Conversely, stationary phase *E. coli* cells can be sensitized to ciprofloxacin by supplementing oxygen and carbon sources (Gutierrez et al., 2017). Furthermore, *E. coli* grown in minimal media with limited glucose availability have higher expression of the efflux pump *acrB*, suggesting that sugar metabolism may have wide-ranging effects that include drug efflux (Bailey et al., 2006). It appears that amino acid deprivation is prerequisite for tolerance; however, deprivation of glucose in addition to amino acids produces

bacteria that are highly tolerant of β -lactams, fluoroquinolones, and aminoglycosides (Fung et al., 2010).

Long-term starvation of *Mycobacterium tuberculosis* reduces susceptibility to rifampicin, isoniazid, and metronidazole and induces shifts in the expression of central metabolic pathways such as amino acid biosynthesis, energy metabolism, and lipid biosynthesis (Betts et al., 2002). Most notably, starvation down-regulates the expression of many glycolysis and TCA cycle enzymes. Additionally, the NADH dehydrogenase operon and most of the ATP synthase complex, both of which contribute to the production of ATP, are dramatically downregulated (Betts et al., 2002). Conversely, starvation induced a significant upregulation of the fumarate reductase gene *frdA*, which is a component of a complex which serves as an anaerobic electron transport chain in similar bacteria (Betts et al., 2002). These changes allow *M. tuberculosis* to enter a tolerant state by decreasing growth rate while maintaining viability (Betts et al., 2002). Taken together, these findings further demonstrate that phenotypic plasticity in bacteria is critical to surviving antibiotic exposure events.

Bacteria may also reduce their metabolic flux and enter a persistent state through the utilization of the glyoxylate shunt. The glyoxylate shunt is a variant of the TCA cycle that enables net carbon assimilation by bypassing steps that generate carbon dioxide (Dunn et al., 2009; Kornberg and Krebs, 1957; Kornberg and Madsen, 1957). In *M. tuberculosis*, treatment with three distinct antibiotics (rifampicin, isoniazid, and streptomycin) is known to induce the expression of isocitrate lyase (*icl*), a component of the glyoxylate shunt that converts isocitrate to glyoxylate and succinate (Dunn et al., 2009; Nandakumar et al., 2014). Furthermore, deletion of *icl* dramatically increases the susceptibility of *M. tuberculosis* to those drugs (Nandakumar et al., 2014). While nutrient starvation decreases the expression of most metabolic genes in *M. tuberculosis*, it has little

effect on genes within the glyoxylate shunt, such as *icl* (Betts et al., 2002). Utilization of the glyoxylate shunt decreases flux through the TCA cycle and reduces NADH and ATP production (Nandakumar et al., 2014; R. Singh et al., 2009). As a result, usage of the glyoxylate shunt is thought to result in reduced levels of reactive oxygen species (ROS), which may contribute to its protective effect (Lobritz et al., 2015; Nandakumar et al., 2014; R. Singh et al., 2009). Similar effects were seen in response to aluminum toxicity in *Pseudomonas fluorescens*, suggesting that metabolic tolerance mechanisms are utilized in other types of stress responses (R. Singh et al., 2009). However, defects in the glyoxylate shunt have been shown to increase biofilm formation and tolerance of oxidative stress in *P. aeruginosa*, suggesting that this strategy is not universally employed, even amongst closely related bacteria (Ahn et al., 2016).

Another stark example of metabolic modulation and persistence development is the phosphate metabolism gene *phoU* (Li and Y. Zhang, 2007). *E. coli* mutants lacking *phoU* are unable to resume growth following β -lactam exposure and are more susceptible to numerous antibiotics and stress conditions. While wild type persisters remain unsusceptible to all antibiotics tested, *phoU* mutants that survive initial antibiotic perturbation remain susceptible to β -lactams. Furthermore, loss of *phoU* sensitizes stationary phase *E. coli* to ampicillin, which requires active growth for effective killing of wild type cells (Li and Y. Zhang, 2007). Cells lacking *phoU* upregulate genes involved in energy production; for this reason, it has been suggested that *phoU* regulates persistence by reducing the expression of metabolic genes in response to stressors such as nutrient limitation or antibiotic exposure (Li and Y. Zhang, 2007).

While persister cells, by definition, are not growing during antibiotic challenge, they can and do originate from actively dividing bacteria. Using fluorescent reporters for growth and metabolism, it was estimated that persisters constitute approximately 1 percent of stationary phase

cells within an exponentially growing *E. coli* culture (Orman and Brynildsen, 2013b). Within that same culture, only 0.01 percent of persisters originated from actively growing cells. However, because of the high prevalence of growing cells in an exponential culture, as many as 20 percent of persisters may originate from active cells (Orman and Brynildsen, 2013b). Within the growing populations, decreased reductase activity was found to be closely associated with persister formation. In fact, growing cells with low reductase activity were 40 times more likely to become persisters (Orman and Brynildsen, 2013b). Other studies have shown that bacterial cells with lower rates of protein synthesis were more likely to be persisters (Shah et al., 2006). Interestingly, the gene expression profile for these cells more closely resembled exponential- rather than stationary-phase cells. Though energy metabolism was decreased in general, these cells also had increased expression of toxin-antitoxin systems (Shah et al., 2006). Therefore, this suggests that although decreased metabolism does greatly increase the likelihood of persister formation, it is not sufficient to explain the phenotype (Orman and Brynildsen, 2013b; Shah et al., 2006).

It is clear that bacterial metabolic state is a major determinant of persister and biofilm formation *in vitro*. However, the metabolic conditions experienced *in vitro* are likely to differ dramatically from those encountered within the host. Therefore, it is likely that host metabolism plays a major role in bacterial functional potential (Yang et al., 2017). Within the microbiome, metagenomics and metatranscriptomics can be utilized to profile the prevalence and expression of well-known tolerance and persistence genes in a polymicrobial community (Figure 1A). However, such analyses will not exclusively profile persister cells due to their rarity but may identify factors that allow populations to survive antibiotic treatment and promote persistence.

Carbon Catabolite Repression Systems Coordinate Antibiotic Persistence and Tolerance

Pathogenic microbes are heterotrophic and rely on a variety of carbon sources for growth (Carvalho et al., 2011). The ability to sense and efficiently utilize a diverse pool of carbon sources, which increases nutritional fitness, is contingent upon highly coordinated metabolite sensing coupled with rapid and appropriate responses. Bacterial growth and metabolism are intricately linked to the availability of carbon sources and cellular responses to this availability. Thus, persister formation is also closely linked to carbon flux within the cell.

Perhaps one of the best described and most conserved metabolite response systems is the carbon catabolite repression (CCR) system. CCR is a global regulatory mechanism by which utilization of secondary carbon sources is dampened in the presence of preferred carbon sources such as glucose (Görke and Stülke, 2008). In Gram-negative species, CCR is activated by transcriptional repression of a pro-catabolic cyclic-AMP-CRP protein complex. In Gram-positive species, CCR is negatively regulated. Environmental glucose triggers phosphorylation of the histidine protein (HPr), which complexes with a pleiotropic transcription factor, carbon catabolite protein A (CcpA). This heterotropic complex binds to responsive DNA elements, thereby repressing catabolic gene expression (Görke and Stülke, 2008). CcpA has been demonstrated to regulate a massive proportion of glucose-responsive genes, almost 80 percent in *Bacillus subtilis*, and carbon sources have been implicated in *E. coli* persister formation, hinting at a possible connection between CCR and persisters (Bizzini et al., 2007).

Nutrient transitions, starvation, and the CCR response have been recently implicated as important triggers of antibiotic tolerance (Michiels et al., 2016; Willenborg et al., 2014). Experimental inactivation of *ccpA* has been shown to decrease tolerance in various clinically relevant species (Fridman et al., 2014). In *E. coli*, CCR knockout increases sensitivity to penicillin due to ablation of metabolic flux (Willenborg et al., 2014). In *Streptococcus gordonii*, *ccpA*

knockout ablates tolerance to multiple drug classes, both *in vitro* and in a rat endocarditis model (Bizzini et al., 2007). Complementation with a functional *ccpA* copy is experimentally sufficient to restore tolerance in both clinical and laboratory strains (Bizzini et al., 2007). *Streptococcus suis*, a zoonotic pig pathogen, and *Streptococcus pneumoniae* lose tolerance to β -lactam antibiotics when *ccpA* is mutated or deleted (Bizzini et al., 2007). In methicillin-resistant *S. aureus* (MRSA), *ccpA* deletion results in severe reductions in β -lactam and glycopeptide resistance amongst highly resistant strains despite the presence of genetically encoded resistance determinants (Bizzini et al., 2007; Sadykov et al., 2011).

Staphylococcus epidermidis growth and tolerance is enhanced *in vitro* through *ccpA*. Recently, TCA cycle activity and CCR linkage have been identified as the connecting mechanisms (Thomas et al., 2013). Interestingly, this linkage seems conserved across *Staphylococci*. In *S. aureus*, *ccpA* represses TCA cycle genes, removing inhibition of intercellular adhesion and biofilm formation, which themselves have been implicated in increased antibiotic tolerance (Thomas et al., 2013). In a clinical context, many *Staphylococcal* infections cause abscess formation, where preferred carbon sources are limited (Mansour et al., 2016). Thus, catabolism of secondary carbon sources must be highly regulated in order to adopt an antibiotic-tolerant biofilm lifestyle. As previously discussed, the formation of these tolerant biofilms has the potential to increase persister formation. Clinically, the connection between CCR, tolerance, and persistence has many implications, particularly for hosts with metabolic disorders. In hyperglycemic patients, for example, it is possible that increased glucose bioavailability triggers CCR activity, protecting pathogenic microbes from therapeutic regimens while increasing virulence and infection burden.

Sugar Metabolism and the Eradication of Persisters

Within carbon catabolism, sugar metabolism has been shown to be of particular importance in persister development. For this reason, several studies have explored the therapeutic potential of exploiting bacterial sugar metabolism to increase the efficacy of existing antibiotics against persisters (Allison et al., 2011; Barraud et al., 2013; Meylan et al., 2017). It has long been known that uptake of aminoglycoside antibiotics is driven by proton motive force (PMF) (Eswaran et al., 2004; Taber et al., 1987). PMF is known to be significantly lower in metabolically quiescent persister cells, which significantly limits the uptake and effectiveness of aminoglycosides (Allison et al., 2011; Eswaran et al., 2004; Meylan et al., 2017; Taber et al., 1987). A study by Allison et al. demonstrated that supplementation with pyruvate or metabolites that enter upper glycolysis (namely glucose, mannitol, and fructose) increased PMF and the uptake of aminoglycosides in *S. aureus* and *E. coli* (Allison et al., 2011). As a result, they found that supplementation with these metabolites increased killing of persisters by three orders of magnitude. Conversely, metabolites that enter in lower glycolysis or the pentose phosphate and Entner–Doudoroff pathways showed little potentiation. Additionally, mannitol and fructose increased the efficacy of gentamicin against biofilms *in vitro* and *in vivo* by 4 and 1.5 orders of magnitude, respectively. However, the same potentiating effect was not observed with β -lactams. Because β -lactams require active bacterial growth for efficacy, this finding demonstrates that the persister cells have not been induced into an actively growing state by the addition of the metabolites. Additionally, treatment with the protonophore carbonyl cyanide m-chlorophenyl hydrazine (CCCP), an uncoupler of oxidative phosphorylation that reduces PMF, abolished the potentiating effect seen with aminoglycoside treatment. Taken together, these findings suggest that supplementation with central carbon metabolites induces PMF and facilitates uptake of aminoglycosides, thus potentiating their efficacy against persisters (Allison et al., 2011; Orman and Brynildsen, 2013b).

Similar work has been recently published using *P. aeruginosa* (Barraud et al., 2013; Meylan et al., 2017). In this case, metabolites from the lower TCA cycle and glycolysis, namely fumarate, succinate, pyruvate, and acetate, sensitized persister and biofilm cells to the aminoglycoside tobramycin (Meylan et al., 2017). Conversely, supplementation with the upper TCA cycle metabolite glyoxylate was found to have a protective effect. As demonstrated by Allison et al., these effects appear to be largely explained by the changes within central carbon metabolism (Allison et al., 2011; Meylan et al., 2017). Supplementation with fumarate stimulated the TCA cycle and electron transport chain activity, thus generating PMF and facilitating uptake of tobramycin. Conversely, glyoxylate decreased cellular respiration while having no significant impact on PMF. Interestingly, supplementing both fumarate and glyoxylate increases PMF and aminoglycoside uptake while decreasing respiration. These cells remain tolerant to aminoglycosides, indicating that decreased cellular respiration can reduce toxicity and compensate for increased uptake (Meylan et al., 2017).

Based on these observations, it is clear that bacterial metabolism and nutrient availability, particularly of sugars and central carbon metabolites, are important determinants of antibiotic efficacy against persisters. Therefore, it is important to understand the availability of these nutrients within the host during infection and how they alter bacterial metabolism. The use of next-generation tools will undoubtedly aid in addressing multi-faceted and complex questions such as this (Figure 1A). For example, metabolomic techniques can be utilized to characterize the metabolites present within a given niche inside the host (Yang et al., 2017). Pairing this metabolomic data with transcriptomic data from bacteria isolated from the microbiome or an infection may lend insights into the interplay between host and pathogen metabolism. Doing so

may also help identify conditions within the host that are likely to foster the development of tolerance and persistence.

Cellular Permeability, Proton Motive Force, and Persistence

Carbon metabolism, particularly of sugars, has been demonstrated to have direct and indirect effects on antibiotic uptake and efflux in persistent and tolerant bacteria. Therefore, increasing efflux or decreasing membrane permeability may represent a complementary strategy to tolerate antibiotics by preventing their intracellular accumulation. For example, the uptake of aminoglycoside antibiotics has been demonstrated to be highly PMF-dependent (Eswaran et al., 2004; Taber et al., 1987). PMF is known to be significantly lower in metabolically quiescent persister cells, which significantly limits the uptake and effectiveness of this particular class of antibiotics (Allison et al., 2011; Fraimow et al., 1991; Meylan et al., 2017). As discussed previously, stimulating PMF through supplementation with TCA cycle metabolites has been shown to increase the uptake and efficacy of this class of antibiotics against persisters (Allison et al., 2011; Meylan et al., 2017). PMF also has an indirect effect on antibiotic uptake through the action of efflux proteins. In total, there are four major families of efflux proteins found in prokaryotes that utilize PMF as an energy source: major facilitator (MF), multidrug and toxic efflux (MATE), resistance-modulation-division (RND), and small multidrug resistance (SMR) (Eswaran et al., 2004; Jiafeng et al., 2015; Paulsen et al., 1996; Webber, 2003). *P. aeruginosa* has been found to overexpress various efflux pumps that provide protection against multiple classes of antibiotics during aminoglycoside exposure or biofilm growth (De Kievit et al., 2001; Hocquet et al., 2003; Soto, 2013; L. Zhang and Mah, 2008). This response appears to be dependent on dose and length of antibiotic exposure, suggesting that these are adaptive responses (Hocquet et al.,

2003). Conversely, inhibiting efflux pumps in *P. aeruginosa*, *E. coli*, and *M. tuberculosis* have been found to sensitize those bacteria to various classes of antibiotics (Colangeli et al., 2005; Lomovskaya et al., 2001). Within *P. aeruginosa* biofilms, the expression pattern of the MexAB-OprM efflux pump was found to be highest at the substratum, where oxygen and nutrient availability is lowest (De Kievit et al., 2001).

Perhaps the most compelling evidence for the role of efflux in bacterial persistence can be found in a 2016 article by Pu et al. (Pu et al., 2016). In this work, *E. coli* persister cells were observed to have reduced levels of cytoplasmic β -lactam accumulation due to enhanced expression and activity of the central efflux component TolC (Pu et al., 2016). Eliminating the *ompF* and *ompC* channels (which allow for diffusion of β -lactams) did not significantly alter persister formation rates or change the intracellular antibiotic concentration relative to non-persister cells. However, knocking out or inhibiting TolC significantly attenuated persister formation and increased intracellular levels of antibiotics (Gerdes and Semsey, 2016; Pu et al., 2016). It should be noted that these persister cells were confirmed to be metabolically dormant, suggesting that the persistence phenotype encompasses both passive (reduced metabolism) and active (efflux) responses to antibiotics.

Exploiting the permeability of persister cells without modulating bacterial metabolism may present an alternative strategy to treating infections (Toit, 2016). Early studies using daptomycin demonstrated that it was effective in a concentration-dependent manner against stationary phase and metabolically arrested MRSA (Mascio et al., 2007). Furthermore, daptomycin was found to be significantly more effective in these situations than β -lactams, which require active bacterial growth. Daptomycin increases cellular permeability by disrupting outer bacterial membranes, thus bypassing the requirement of active metabolism to be effective (Mascio et al., 2007).

Modulating cellular permeability of bacteria may also increase the efficacy and expand the spectrum of activity of existing antibiotics (Herisse et al., 2017; Morones-Ramirez et al., 2013). Supplementation with ionic silver has been shown to increase the membrane permeability of Gram-negative biofilm cells by stimulating production of hydroxyl radicals that disrupt disulfide bonds and result in misfolded membrane proteins (Morones-Ramirez et al., 2013). This disruption of membrane permeability was found to potentiate the activity of bactericidal antibiotics — ampicillin, ofloxacin, and gentamicin— while sensitizing *E. coli* to vancomycin, a Gram-positive-specific antibiotic. Furthermore, silver was able to enhance the activity of gentamicin in a mouse biofilm infection model (Morones-Ramirez et al., 2013). Silver was also observed to potentiate gentamicin in the presence of CCCP, suggesting that this effect is not PMF-dependent (Herisse et al., 2017). Taken together, these findings suggest that disrupting membrane permeability of metabolically dormant biofilm cells may be capable of expanding the spectrum of activity of current antibiotics (Herisse et al., 2017; Morones-Ramirez et al., 2013). Similar effects have also been observed when aminoglycosides are administered after a hypoionic shock; however, the exact mechanism and therapeutic potential of this strategy is currently unclear (Jiafeng et al., 2015).

To date, most of the studies linking cellular permeability to antibiotic tolerance in biofilms and persisters have been performed *in vitro*. As a result, the clinical relevance of this phenomenon is currently unclear. However, utilization of next generation sequencing and its integration with older technologies may enable researchers to shed light on the role that cellular permeability and drug uptake play during antibiotic treatment of an infection. For example, fluorescently labeled antibiotics have been used in numerous studies to measure cellular drug uptake *in vitro* (Allison et al., 2011; Meylan et al., 2017; Pu et al., 2016). It may be possible to utilize these compounds to measure drug uptake within a population of bacteria isolated from an infection model *in vivo*.

Furthermore, their use could allow researchers to sort bacteria using fluorescence-activated cell sorting (FACS) based on their level of drug uptake and perform transcriptomic analysis on the resulting populations. Additionally, the use of animal models would enable researchers to manipulate host metabolism to determine its impact on bacterial drug uptake and efflux during infection and antibiotic therapy.

Stress Responses and Persistence: The Stringent Response

Nutrient limitation, metabolic flux, drug efflux, and growth rate are not the only mechanisms by which persisters can arise. As the PASH model states, active transcriptional responses can trigger persisters, and major transcriptional responses are undoubtedly coupled with metabolic shifts. Recently, links between CCR and antibiotic tolerance have implicated the involvement of the stringent response (Gaca et al., 2013). The stringent response is a stress response pathway that activates during amino acid deprivation, fatty acid limitation, and other stressors (Geiger et al., 2014; Strugeon et al., 2016). Stringent response pathways are activated via (p)ppGpp alarmone concentrations, which modulate subsequent cellular responses such as transcription, replication, and gyrase-mediated negative DNA supercoiling (Lebeaux et al., 2014). (p)ppGpp is synthesized and maintained by members of the RelA/SpoT Homolog (RSH) enzyme superfamily (Atkinson et al., 2011; Hauryliuk et al., 2015). When cellular concentrations of (p)ppGpp are high enough, the alarmone interacts with RNA polymerase and the DskA ribosome binding protein, ultimately reducing translational fidelity due to a reduction in the pool of filled aminoacyl-tRNAs (Lebeaux et al., 2014). Because the stringent response can modulate so many processes involved in direct targets of antibiotics, it has been implicated in tolerance development

and biofilm recalcitrance, which likely share mechanistic triggers with persister development (Lebeaux et al., 2014).

Bacterial mutants lacking the stringent response, such as a *relQ-rsh* double knockout in *Enterococcus faecalis*, exhibit divergence in various metabolic operons, glycerol uptake, and glycerol metabolism (Gaca et al., 2013). These processes have been demonstrated to be under the control of CcpA in *E. faecalis*. This double knockout strain has significantly perturbed levels of *ccpA* transcription, indicating an inability to accurately sense metabolic cues and properly adapt. In *S. aureus*, double knockouts of *rel-rsh* have aberrant intracellular pools of (p)ppGpp, suggesting an inability to control the pace or directionality of carbon flux (Gaca et al., 2013). This inability to properly adapt to nutrient availability changes likely leads to nutrient starvation and limitation. This leads to dysbiosis of NAD⁺/NADH ratios, increased ROS generation, and unbalanced cellular homeostasis (Gaca et al., 2013).

Ghosh et al. found that when *Mycobacterium smegmatis* populations were challenged with nutrient depletion, stringent response pathways were activated, representing a form of adaptive switching that generates persisters (Ghosh et al., 2011). *In vitro* deletion of *relA* in *E. coli* ablates (p)ppGpp synthesis, and experimental nutrient starvation fails to elicit penicillin tolerance in this mutant (Grant and Hung, 2013). Furthermore, the stringent response appears to be critical to persistence development in *E. coli*, as deletion of several pathway components inhibits persister formation *in vitro* (Maisonneuve et al., 2013). In *P. aeruginosa*, antibiotic tolerance in nutrient-limited and biofilm contexts is mediated by active responses to starvation rather than by passive effects of growth and arrest, which closely resembles the PASH model of persistence (Nguyen et al., 2011). In Pseudomonads, the stringent response can be linked to tolerance via reduction of oxidative stress in cells. By inactivating protective mechanisms, biofilms become sensitized to

multiple antibiotic classes by several orders of magnitude. In experimental knockouts of *relA* and *spoT*, cells were unable to produce (p)ppGpp during serine starvation (Nguyen et al., 2011). When challenged with ofloxacin during starvation, wild type cells had a 2300-fold reduced killing, while knockout strains exhibited only a 34-fold reduction in antibiotic killing (Nguyen et al., 2011). Ultimately, stringent response inactivation appears to modulate antibiotic tolerance via relief of oxidant stress, and this stress response has likely conserved functionality in persister cell formation.

The stringent response has also been linked to indole-mediated antibiotic tolerance. Vega et al. found that indole production in *Salmonella enterica* increased basal tolerance and that indole signaling could be induced in both monoculture and in co-culture with *E. coli* (Vega et al., 2012). Indole production during stationary phase coupled with nutrient limitation leads to increased levels of persisters. Indole production functions as a form of intraspecies signaling to promote transcriptional activation of efflux pumps and oxidative stress protection in neighboring cells (Grant and Hung, 2013). (p)ppGpp overexpression increases antibiotic tolerance and inhibits peptidoglycan and phospholipid synthesis, indicating a link between amino acid starvation, oxidative stress, the stringent response, and antibiotic tolerance (Lebeaux et al., 2014).

As a generalized stress response with protective functionality against nutrient limitation and oxidative stress, it seems likely that stringent response activation is co-opted for an in-host lifestyle. Bacteria frequently encounter nutrient limitation within hosts and must subvert oxidative damage from the host immune system in order to colonize, establish infection, and persist (Fisher et al., 2017; Mansour et al., 2016). Additionally, bacteria must be able to withstand nutrient limitation during host-to-host transmission events. Transcriptomics could be implemented to study

the role of the stringent response in *in vivo* persister formation during an induced infection. In a clinical setting, biopsy samples could be subjected to the same transcriptional profiling.

Stress Responses and Persistence: The SOS Response

The stringent response is not the sole stressor implicated in persistence development. Under biofilm conditions, stringent response activation increases basal expression of the SOS DNA repair regulon (Strugeon et al., 2016). The SOS response is a highly conserved gene pathway that allows cells to survive genotoxic stressors, including β -lactam and fluoroquinolone antibiotics, and is well-known to be involved in persistence development in a variety of clinically relevant species (Dörr et al., 2010; Grant and Hung, 2013).

A pivotal study by Dorr et al. challenged the previous contention that persister formation was only due to stochastic dormancy (Dörr et al., 2010). Instead, they proposed that persister cells are actively able to survive antibiotic stress via an increase in efficient drug efflux and DNA lesion repair via either transient overexpression or environmental activation of the SOS pathway (Dörr et al., 2010). Experimental knockdown of *recA* and *recBC*, key players in the SOS response, caused complete ablation of persister formation after 6 hours of antibiotic exposure, suggesting that persisters experienced and were unable to mitigate antibiotic-induced DNA lesions. *E. coli* strains that constitutively express the SOS regulon had a 20-fold increase in persister formation upon ciprofloxacin challenge. When challenged with mitomycin C, these mutants demonstrated a 180-fold increased induction of persistence, suggesting a functional SOS response is necessary for antibiotic persistence (Dörr et al., 2010). Bernier et al. expanded upon this work and found that SOS induction is necessary for ofloxacin tolerance and proposed that SOS induction might lead to persistence development in biofilms (Bernier et al., 2013). Their findings support the complex

interconnectedness between metabolic flux systems, the stringent response, and SOS repair pathways in promoting persistence development.

A major trigger for persistence development is exposure to sub-inhibitory concentrations of antibiotics, which mimics *in vivo* drug accumulation after clinical administration (Michiels et al., 2016). Daily dosing of aminoglycosides selects for almost complete persister enrichment in *Klebsiella pneumoniae* and periodic daptomycin exposure leads to high persister enrichment in *S. aureus* (Mechler et al., 2015). When challenged to multi-antibiotic panels, *E. coli* persister formation was enhanced by both ciprofloxacin and gentamicin treatment while *S. aureus* persistence activity increased under ampicillin treatment. These findings suggest some interspecies variation or drug-specific variation in persistence mechanisms. Interestingly, ampicillin pretreatment increased the rate of cross-tolerance to non-related drug classes due to β -lactam activation of the SOS pathway in *S. aureus* (Goneau et al., 2014). SOS-deficient *E. coli* strains failed to produce persisters during ciprofloxacin challenge but were able to produce gentamicin persisters since gentamicin does not directly cause DNA lesions (Goneau et al., 2014). This suggests that persisters are actively synthesizing DNA and are sensitive to perturbations in DNA integrity.

Sub-inhibitory drug concentrations are of high clinical relevance. Realistically, serum antibiotic levels are only at inhibitory concentrations for a short portion of the regimen (Odenholt, 2000). As a result, bacteria spend most therapeutic time at sub-inhibitory concentrations while inside a host, and this is drastically exaggerated in biofilm antibiotic exposure. Interestingly, it is this transient concentration that elicits and selects for tolerance (Schultz et al., 2017). However, insufficient data is available regarding bacterial responses during these transient, sub-therapeutic concentrations. Significant insight can be gained by profiling physiological and transcriptional

responses of pathogens isolated from the site of infection as the effective antibiotic concentration is reduced by host metabolism.

Future Directions

The past decade has brought many advancements in the study of bacterial persistence. Despite these advances, persistent infections remain a major public health burden and work is needed to translate new discoveries to improved clinical outcomes. One potential area of research that could help bridge this gap is determining the role that host metabolism plays in bacterial persistence. To date, the vast majority of persistence research has been conducted *in vitro* under nutrient conditions that differ considerably from what is found *in vivo*. Human metabolism is a complex phenotypic trait that is dependent on a multitude of factors such as genetics, diet, and microbiome composition (Devaraj et al., 2013; Kastenmüller et al., 2015; Lam and Ravussin, 2016; Wu et al., 2015). Further complicating the role of human metabolism is the fact that the human host comprises of a multitude of micro-niches that harbor vastly different nutrient conditions. A breadth of research has demonstrated that metabolic activity is a key factor in the development of bacterial persistence. Therefore, it is likely that nutrient availability in these micro-niches may act as a determinant of bacterial metabolism and thus persister formation. If so, understanding the impact that human metabolism plays in bacterial persistence and treatment efficacy is crucial to improving patient outcomes. Furthermore, uncovering the links between host metabolism and bacterial persistence could open the door to new therapeutic strategies that improve the efficacy of treatment by modulating host metabolism. Such strategies could lay the foundation for personalized medicine by allowing medical professionals to tailor treatment based on infection site and the patient's overall metabolic state.

Another untapped area of research is the potential link between persister formation and the microbiome. Most, if not all, pre-existing persister research has been conducted *in vitro* using human pathogens. However, it is unknown if persister formation occurs within the complex polymicrobial communities that comprise the microbiome. Though persistence is typically viewed negatively in the context of recurrent clinical infections, it is possible that it may serve a beneficial role in the context of the microbiome. Antibiotic treatment is known to decrease the diversity and count of bacteria in a number of niches within these communities, which, in turn are associated with dysbiosis and other negative health outcomes (Cabral et al., 2017; Ge et al., 2017; Rodrigues et al., 2017; Sommer and Dantas, 2011; Theriot et al., 2016; Zaura et al., 2015). However, a form of persistence may enable beneficial microbes to survive perturbations such as antibiotic treatment, infection, or dietary shifts, thus allowing them to replenish a healthy microbiota. Conversely, these strategies could also explain the bloom of opportunistic pathogens following antibiotic therapy. In either case, it is crucial to understand if and how persistence mechanisms are utilized in the context of the microbiome.

Addressing these questions would have been logistically daunting in past decades due to the diversity of the microbiome and the inability to culture many of its resident microbes. However, the advance of next-generation sequencing technologies in the past decade has enabled new insights into the development of persistence. For example, experiments utilizing RNA-Seq demonstrated that persisters overexpress the TolC efflux pump, indicating a previously unknown role of drug efflux in this phenomenon (Pu et al., 2016). Additionally, Henry et al. recently developed a platform that integrated fluorescence-activated cell sorting (FACS), traditional antibiotic susceptibility assays, and next-generation sequencing to assay persister physiology (Henry and Brynildsen, 2016). The extreme rarity of persisters within polymicrobial communities

makes many *in vivo* analyses logistically difficult. The development of single-cell sequencing technologies, combined with persister enrichment protocols such as FACS and LCMD, present robust avenues for analysis *in vitro* and *in vivo* (Avraham et al., 2015; Heacock-Kang et al., 2017; Hör et al., 2018; Kang et al., 2015; Saliba et al., 2016; 2017; Wang et al., 2015). Critically, many of the methods that utilize these technologies are culture independent. Therefore, they may serve as powerful tools that will allow researchers to determine the mechanisms underlying persistence in complex microbial communities or during infection.

Acknowledgments

This review was supported by funding received from the COBRE Center for Computation Biology of Human Disease (NIH P20GM109035) and from the National Science Foundation Graduate Research Fellowship (Grant No. 1644760)

Author Contributions

J.I.W. and D.J.C. contributed equally to this work. J.I.W. and D.J.C. performed the literature review and wrote the manuscript. J.I.W. created the figure. P.B. and D.J.C. prepared the manuscript for publication. P.B. conceptualized the work. All authors reviewed and approved its final version

Declaration of Interests

The authors declare no conflict of interest. The funding sponsors had no role in the writing of the manuscript.

Main Figures, Titles, and Legends

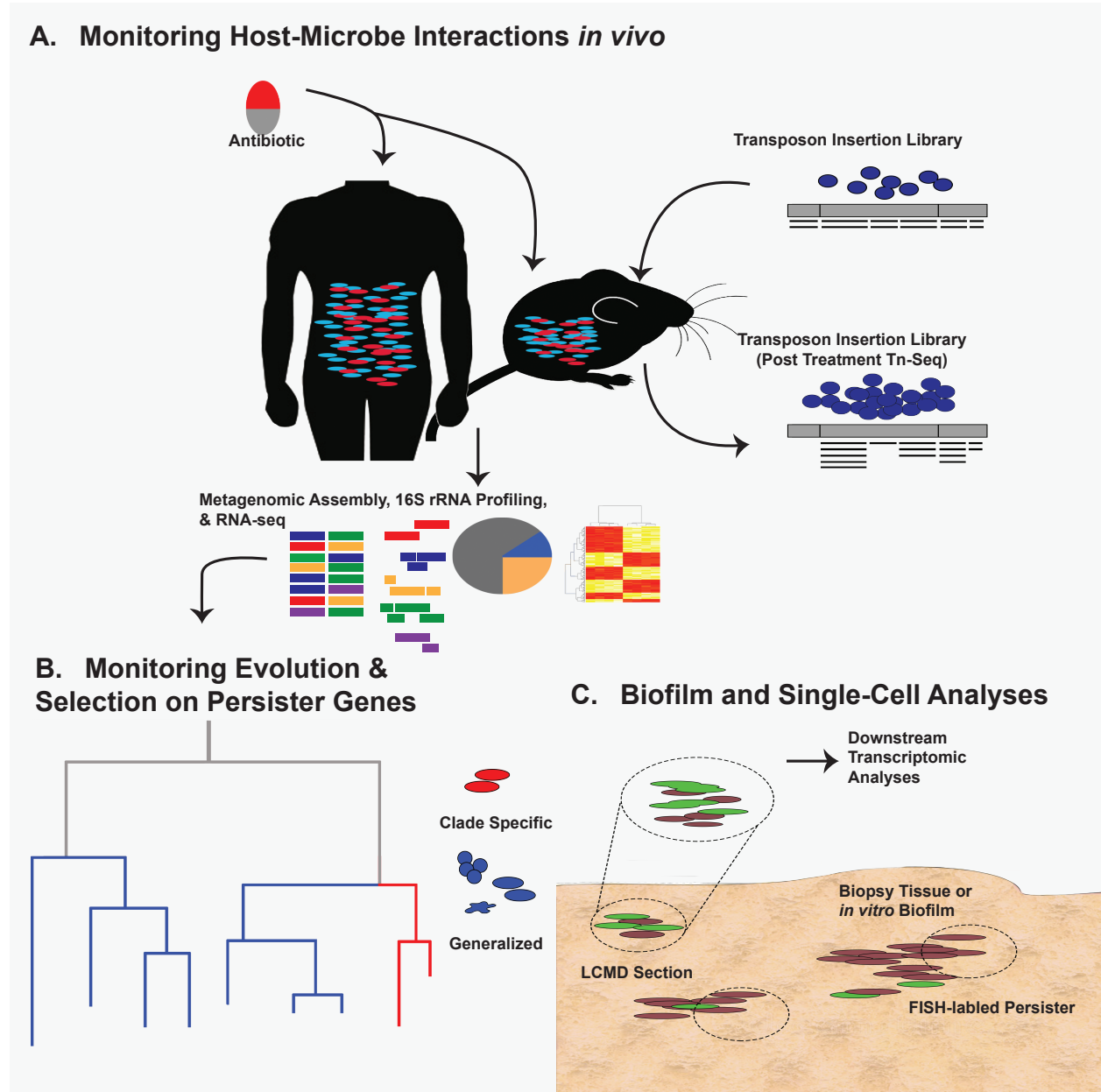


Figure 1. Utilization of next-generation technologies for studying persister cells.

- A. Both human patients and murine models provide an opportunity to study *in vivo* persister formation via 16S rRNA profiling, community metagenomics, and RNA-Seq of the intestinal flora following antibiotic exposure. Single-organisms persister formation can be studied *in vivo* through animal infection with high-density transposon insertion libraries and Tn-Seq.
- B. Metagenomic and RNA-Seq data can be used to study selective pressure on persister genes in either closely related or divergent taxa. This can be done in retrospective clinical cohort groupings or in animal model infections over the course of antibiotic therapy, identifying

how certain therapeutic regimens can select for the expression of specific (red) or ubiquitous (blue) persister elements.

- C. Persisters can be studied from either *in vitro*-generated biofilms or patient biopsy-derived biofilms. Persister-specific Fluorescence *in-situ* Hybridization (FISH) labeling can allow for visualization and study of persisters within the 3D context of the biofilm, and laser-capture microdissection (LCMD) sectioning can facilitate labeled cell extraction for downstream transcriptomic analyses.

References

- Ahn, S., Jung, J., Jang, I.-A., Madsen, E.L., Park, W., 2016. Role of Glyoxylate Shunt in Oxidative Stress Response. *J. Biol. Chem.* 291, 11928–11938. doi:10.1074/jbc.M115.708149
- Allison, K.R., Brynildsen, M.P., Collins, J.J., 2011. Metabolite-enabled eradication of bacterial persisters by aminoglycosides. *Nature* 473, 216–220. doi:10.1038/nature10069
- Amato, S.M., Orman, M.A., Brynildsen, M.P., 2013. Metabolic Control of Persister Formation in *Escherichia coli*. *Mol. Cell* 50, 475–487. doi:10.1016/j.molcel.2013.04.002
- Atkinson, G.C., Tenson, T., Hauryliuk, V., 2011. The RelA/SpoT Homolog (RSH) Superfamily: Distribution and Functional Evolution of ppGpp Synthetases and Hydrolases across the Tree of Life. *PLoS ONE* 6, 1–21. doi:10.1371/journal.pone.0023479
- Avraham, R., Haseley, N., Brown, D., Penaranda, C., Jijon, H.B., Trombetta, J.J., Satija, R., Shalek, A.K., Xavier, R.J., Regev, A., Hung, D.T., 2015. Pathogen Cell-to-Cell Variability Drives Heterogeneity in Host Immune Responses. *Cell* 162, 1309–1321. doi:10.1016/j.cell.2015.08.027
- Bailey, A.M., Webber, M.A., Piddock, L.J.V., 2006. Medium Plays a Role in Determining Expression of *acrB*, *marA*, and *soxS* in *Escherichia coli*. *Antimicrob. Agents Chemother.* 50, 1071–1074. doi:10.1128/AAC.50.3.1071-1074.2006
- Balaban, N.Q., Nathalie, Merrin, J., Chait, R., Kowalik, L., Leibler, S., 2004. Bacterial Persistence as a Phenotypic Switch. *Science* 305, 1622–1625. doi: 10.1126/science.1099390
- Barraud, N., Buson, A., Jarolimek, W., Rice, S.A., 2013. Mannitol enhances antibiotic sensitivity of persister bacteria in *Pseudomonas aeruginosa* biofilms. *PLoS ONE* 8, e84220. doi:10.1371/journal.pone.0084220
- Bernier, S.P., Lebeaux, D., DeFrancesco, A.S., Valomon, A., Soubigou, G., Coppée, J.-Y., Ghigo, J.-M., Beloin, C., 2013. Starvation, Together with the SOS Response, Mediates High Biofilm-Specific Tolerance to the Fluoroquinolone Ofloxacin. *PLoS Genet.* 9, e1003144–14. doi:10.1371/journal.pgen.1003144
- Betts, J.C., Lukey, P.T., Robb, L.C., McAdam, R.A., Duncan, K., 2002. Evaluation of a nutrient starvation model of *Mycobacterium tuberculosis* persistence by gene and protein expression profiling. *Mol. Microbiol.* 43, 717–731. doi:10.1046/j.1365-2958.2002.02779.x.
- Bigger, J.W., 1944. Treatment of Staphylococcal Infections with Penicillin by Intermittent Sterilisation. *The Lancet* 244, 497–500. doi:10.1016/S0140-6736(00)74210-3
- Bizzini, A., Entenza, J.M., Moreillon, P., 2007. Loss of penicillin tolerance by inactivating the carbon catabolite repression determinant *CcpA* in *Streptococcus gordonii*. *J. Antimicrob. Chemother.* 59, 607–615. doi:10.1093/jac/dkm021
- Blango, M.G., Mulvey, M.A., 2010. Persistence of iropathogenic *Escherichia coli* in the face of multiple antibiotics. *Antimicrob. Agents Chemother.* 54, 1855–1863. doi:10.1128/AAC.00014-10
- Brauner, A., Fridman, O., Gefen, O., Balaban, N.Q., 2016. Distinguishing between resistance, tolerance and persistence to antibiotic treatment. *Nat. Rev. Microbiol.* 14, 320–330. doi:10.1038/nrmicro.2016.34
- Briley, K.A., Camilleri, L.B., Fields, M.W., 2014. 3D-fluorescence in situ hybridization of intact, anaerobic biofilm. *Methods Mol. Biol.* 1151, 189–197. doi:10.1007/978-1-4939-0554-6_13
- Cabral, D.J., Wurster, J.I., Flokas, M.E., Alevizakos, M., Zabat, M., Korry, B.J., Rowan, A.D., Sano, W.H., Andreatos, N., Ducharme, R.B., Chan, P.A., Mylonakis, E., Fuchs, B.B., Belenky,

- P., 2017. The salivary microbiome is consistent between subjects and resistant to impacts of short-term hospitalization. *Sci. Rep.* 7, 1–13. doi:10.1038/s41598-017-11427-2
- Carvalho, S.M., Kloosterman, T.G., Kuipers, O.P., Neves, A.R., 2011. CcpA Ensures Optimal Metabolic Fitness of *Streptococcus pneumoniae*. *PLoS ONE* 6, e26707–16. doi:10.1371/journal.pone.0026707
- Cohen, N.R., Lobritz, M.A., Collins, J.J., 2013. Microbial Persistence and the road to drug resistance. *Cell Host Microbe* 13, 632–642. doi:10.1016/j.chom.2013.05.009
- Colangeli, R., Helb, D., Sridharan, S., Sun, J., Varma-Basil, M., Hazbón, M.H., Harbacheuski, R., Megjugorac, N.J., Jacobs, W.R., Holzenburg, A., Sacchettini, J.C., Alland, D., 2005. The *Mycobacterium tuberculosis* *iniA* gene is essential for activity of an efflux pump that confers drug tolerance to both isoniazid and ethambutol. *Mol. Microbiol.* 55, 1829–1840. doi:10.1111/j.1365-2958.2005.04510.x
- Conlon, B.P., Rowe, S.E., Gandt, A.B., Nuxoll, A.S., Donegan, N.P., Zalis, E.A., Clair, G., Adkins, J.N., Cheung, A.L., Lewis, K., 2016. Persister formation in *Staphylococcus aureus* is associated with ATP depletion. *Nat. Microbiol.* 1, 16051–16. doi:10.1038/nmicrobiol.2016.51
- Davey, M.E., OToole, G.A., 2000. Microbial Biofilms: from Ecology to Molecular Genetics. *Microbiol. Mol. Biol. Rev.* 64, 847–867. doi: 10.1128/MMBR.64.6.847-867.2000
- De Kievit, T.R., Parkins, M.D., Gillis, R.J., Srikumar, R., Ceri, H., Poole, K., Iglewski, B.H., Storey, D.G., 2001. Multidrug efflux pumps: expression patterns and contribution to antibiotic resistance in *Pseudomonas aeruginosa* biofilms. *Antimicrob. Agents Chemother.* 45, 1761–1770. doi:10.1128/AAC.45.6.1761-1770.2001
- Devaraj, S., Hemarajata, P., Versalovic, J., 2013. The Human Gut Microbiome and Body Metabolism: Implications for Obesity and Diabetes. *Clin. Chem.* 59, 617–628. doi:10.1373/clinchem.2012.187617
- Dörr, T., Vulic, M., Lewis, K., 2010. Ciprofloxacin causes persister formation by inducing the TisB toxin in *Escherichia coli*. *PLoS Biol.* 8, e1000317. doi:10.1371/journal.pbio.1000317
- Dunn, M.F., Ramirez-Trujillo, J.A., Hernandez-Lucas, I., 2009. Major roles of isocitrate lyase and malate synthase in bacterial and fungal pathogenesis. *Microbiology* 155, 3166–3175. doi:10.1099/mic.0.030858-0
- Eswaran, J., Koronakis, E., Higgins, M.K., Hughes, C., Koronakis, V., 2004. Three's company: component structures bring a closer view of tripartite drug efflux pumps. *Curr. Opin. Struct. Biol.* 14, 741–747. doi:10.1016/j.sbi.2004.10.003
- Fisher, R.A., Gollan, B., Helaine, S., 2017. Persistent bacterial infections and persister cells. *Nat Rev. Micro.* 15, 453–464. doi:10.1038/nrmicro.2017.42
- Fraimow, H.S., Greenman, J.B., Leviton, I.M., Dougherty, T.J., Miller, M.H., 1991. Tobramycin uptake in *Escherichia coli* is driven by either electrical potential or ATP. *J. Bacteriol.* 173, 2800–2808. doi:10.1128/jb.173.9.2800-2808.1991
- Fridman, O., Goldberg, A., Ronin, I., Shores, N., Balaban, N.Q., 2014. Optimization of lag time underlies antibiotic tolerance in evolved bacterial populations. *Nature* 513, 418–421. doi:10.1038/nature13469
- Fung, D.K.C., Chan, E.W.C., Chin, M.L., Chan, R.C.Y., 2010. Delineation of a bacterial starvation stress response network which can mediate antibiotic tolerance development. *Antimicrob. Agents Chemother.* 54, 1082–1093. doi:10.1128/AAC.01218-09
- Gaca, A.O., Kajfasz, J.K., Miller, J.H., Liu, K., Wang, J.D., Abranches, J., Lemos, J.A., 2013. Basal Levels of (p)ppGpp in *Enterococcus faecalis*: the Magic beyond the Stringent Response. *mBio* 4, e00646–13. doi:10.1128/mBio.00646-13

- Ge, X., Ding, C., Zhao, W., Xu, L., Tian, H., Gong, J., Zhu, M., Li, J., Li, N., 2017. Antibiotics-induced depletion of mice microbiota induces changes in host serotonin biosynthesis and intestinal motility. *J. Transl. Med.* 15, 1–9. doi:10.1186/s12967-016-1105-4
- Geiger, T., Kastle, B., Gratani, F.L., Goerke, C., Wolz, C., 2014. Two Small (p)ppGpp Synthases in *Staphylococcus aureus* Mediate Tolerance against Cell Envelope Stress Conditions. *J. Bacteriol.* 196, 894–902. doi:10.1128/JB.01201-13
- Gerdes, K., Semsey, S., 2016. Microbiology: Pumping persisters. *Nature* 534, 41–42. doi:10.1038/nature18442
- Ghosh, S., Sureka, K., Ghosh, B., Bose, I., Basu, J., Kundu, M., 2011. Phenotypic heterogeneity in mycobacterial stringent response. *BMC Syst. Biol.* 5, 1–13. doi:10.1186/1752-0509-5-18
- Goneau, L.W., Yeoh, N.S., MacDonald, K.W., Cadieux, P.A., Burton, J.P., Razvi, H., Reid, G., 2014. Selective Target Inactivation Rather than Global Metabolic Dormancy Causes Antibiotic Tolerance in Uropathogens. *Antimicrob. Agents Chemother.* 58, 2089–2097. doi:10.1128/AAC.02552-13
- Goswami, M., Bhattacharyya, P., Tribedi, P., 2017. Allee effect: the story behind the stabilization or extinction of microbial ecosystem. *Arch. Microbiol.* 199, 185–190. doi:10.1007/s00203-016-1323-4
- Görke, B., Stülke, J., 2008. Carbon catabolite repression in bacteria: many ways to make the most out of nutrients. *Nat. Rev. Microbiol.* 6, 613–624. doi:10.1038/nrmicro1932
- Grant, S.S., Hung, D.T., 2013. Persistent bacterial infections, antibiotic tolerance, and the oxidative stress response. *Virulence* 4, 273–283. doi:10.4161/viru.23987
- Gutierrez, A., Jain, S., Bhargava, P., Hamblin, M., Lobritz, M.A., Collins, J.J., 2017. Understanding and Sensitizing Density-Dependent Persistence to Quinolone Antibiotics. *Mol. Cell* 68, 1147–1154.e3. doi:10.1016/j.molcel.2017.11.012
- Harms, A., Maisonneuve, E., Gerdes, K., 2016. Mechanisms of bacterial persistence during stress and antibiotic exposure. *Science* 354, 1–11. doi:10.1126/science.aaf4268
- Hauryliuk, V., Atkinson, G.C., Murakami, K.S., Tenson, T., Gerdes, K., 2015. Recent functional insights into the role of (p)ppGpp in bacterial physiology. *Nat. Rev. Microbiol.* 13, 289–309. doi:10.1038/nrmicro3448
- Heacock-Kang, Y., Sun, Z., Zarzycki-Siek, J., McMillan, I.A., Norris, M.H., Bluhm, A.P., Cabanas, D., Fogen, D., Vo, H., Donachie, S.P., Borlee, B.R., Sibley, C.D., Lewenza, S., Schurr, M.J., Schweizer, H.P., Hoang, T.T., 2017. Spatial transcriptomes within the *Pseudomonas aeruginosa* biofilm architecture. *Mol. Microbiol.* 106, 976–985. doi:10.1111/mmi.13863
- Henry, T.C., Brynildsen, M.P., 2016. Development of Persister-FACSeq: a method to massively parallelize quantification of persister physiology and its heterogeneity. *Sci. Rep.* 6, 25100. doi:10.1038/srep25100
- Herrisse, M., Duverger, Y., Martin-Verstraete, I., Barras, F., Ezraty, B., 2017. Silver potentiates aminoglycoside toxicity by enhancing their uptake. *Mol. Microbiol.* 105, 115–126. doi:10.1111/mmi.13687
- Hocquet, D., Vogne, C., Garch, El, F., Vejux, A., Gotoh, N., Lee, A., Lomovskaya, O., Plésiat, P., 2003. MexXY-OprM efflux pump is necessary for a adaptive resistance of *Pseudomonas aeruginosa* to aminoglycosides. *Antimicrob. Agents Chemother.* 47, 1371–1375. doi:10.1128/AAC.47.4.1371-1375.2003
- Hör, J., Gorski, S.A., Vogel, J., 2018. Bacterial RNA Biology on a Genome Scale. *Mol. Cell* 70, 785–799. doi:10.1016/j.molcel.2017.12.023

- Jefferson, K.K., 2004. What drives bacteria to produce a biofilm? *FEMS Microbiol. Lett.* 236, 163–173. doi:10.1016/j.femsle.2004.06.005
- Jiafeng, L., Fu, X., Chang, Z., 2015. Hypoionic shock treatment enables aminoglycosides antibiotics to eradicate bacterial persisters. *Sci. Rep.* 5, 894. doi:10.1038/srep14247
- Jōers, A., Kaldalu, N., Tenson, T., 2010. The frequency of persisters in *Escherichia coli* reflects the kinetics of awakening from dormancy. *J. Bacteriol.* 192, 3379–3384. doi:10.1128/JB.00056-10
- Kang, Y., McMillan, I., Norris, M.H., Hoang, T.T., 2015. Single prokaryotic cell isolation and total transcript amplification protocol for transcriptomic analysis. *Nat. Protoc.* 10, 974–984. doi:10.1038/nprot.2015-058
- Kastenmüller, G., Raffler, J., Gieger, C., Suhre, K., 2015. Genetics of human metabolism: an update. *Hum. Mol. Genet.* 24, R93–R101. doi:10.1093/hmg/ddv263
- Keren, I., Kaldalu, N., Spoering, A., Wang, Y.P., Lewis, K., 2004. Persister cells and tolerance to antimicrobials. *FEMS Microbiol. Lett.* 230, 13–18. doi:10.1016/S0378-1097(03)00856-5
- Kornberg, H.L., Krebs, H.A., 1957. Synthesis of Cell Constituents from C2-Units by a Modified Tricarboxylic Acid Cycle. *Nature* 179, 988–991. doi: 10.1038/179988a0
- Kornberg, H.L., Madsen, N.B., 1957. Synthesis of C4-dicarboxylic acids from acetate by a “glyoxylate bypass” of the tricarboxylic acid cycle. *Biochim. Biophys. Acta* 24, 651–653.
- Kudrin, P., Varik, V., Oliveira, S.R.A., Beljantseva, J., Del Peso Santos, T., Dzhygyr, I., Rejman, D., Cava, F., Tenson, T., Hauryliuk, V., 2017. Subinhibitory Concentrations of Bacteriostatic Antibiotics Induce *relA*-Dependent and *relA*-Independent Tolerance to β -Lactams. *Antimicrob. Agents Chemother.* 61, e02173–16–17. doi:10.1128/AAC.02173-16
- Lam, Y.Y., Ravussin, E., 2016. Analysis of energy metabolism in humans: A review of methodologies. *Mol. Metab.* 5, 1057–1071. doi:10.1016/j.molmet.2016.09.005
- Lebeaux, D., Ghigo, J.-M., Beloin, C., 2014. Biofilm-Related Infections: Bridging the Gap between Clinical Management and Fundamental Aspects of Recalcitrance toward Antibiotics. *Microbiol. Mol. Biol. Rev.* 78, 510–543. doi:10.1128/MMBR.00013-14
- Lee, H.H., Molla, M.N., Cantor, C.R., Collins, J.J., 2010. Bacterial charity work leads to population-wide resistance. *Nature* 467, 82–85. doi:10.1038/nature09354
- Levin, B.R., Rozen, D.E., 2006. Non-inherited antibiotic resistance. *Nat. Rev. Microbiol.* 4, 556–562. doi:10.1038/nrmicro1445
- Lewis, K., 2010. Persister cells. *Annu. Rev. Microbiol.* 64, 357–372. doi:10.1146/annurev.micro.112408.134306
- Lewis, K., 2007. Persister cells, dormancy and infectious disease. *Nat. Rev. Microbiol.* 5, 48–56. doi:10.1038/nrmicro1557
- Lewis, K., 2001. Riddle of biofilm resistance. *Antimicrob. Agents Chemother.* 45, 999–1007. doi:10.1128/AAC.45.4.999-1007.2001
- Li, Y., Zhang, Y., 2007. PhoU is a persistence switch involved in persister formation and tolerance to multiple antibiotics and stresses in *Escherichia coli*. *Antimicrob. Agents Chemother.* 51, 2092–2099. doi:10.1128/AAC.00052-07
- Lobritz, M.A., Belenky, P., Porter, C.B.M., Gutierrez, A., Yang, J.H., Schwarz, E.G., Dwyer, D.J., Khalil, A.S., Collins, J.J., 2015. Antibiotic efficacy is linked to bacterial cellular respiration. *Proc. Natl. Acad. Sci. USA.* 112, 8173–8180. doi: 10.1073/pnas.1509743112
- Lomovskaya, O., Warren, M.S., Lee, A., Galazzo, J., Fronko, R., Lee, M., Blais, J., Cho, D., Chamberland, S., Renau, T., Leger, R., Hecker, S., Watkins, W., Hoshino, K., Ishida, H., Lee, V.J., 2001. Identification and characterization of inhibitors of multidrug resistance efflux

- pumps in *Pseudomonas aeruginosa*: novel agents for combination therapy. *Antimicrob. Agents Chemother.* 45, 105–116. doi:10.1128/AAC.45.1.105-116.2001
- MacLean, C.R., Vogwill, T., 2014. Limits to compensatory adaptation and the persistence of antibiotic resistance in pathogenic bacteria. *Evol. Med. Public Health* 2015, 4–12. doi:10.1093/emph/eou032
- Maisonneuve, E., Castro-Camargo, M., Gerdes, K., 2013. (p)ppGpp Controls Bacterial Persistence by Stochastic Induction of Toxin-Antitoxin Activity. *Cell* 154, 1140–1150. doi:10.1016/j.cell.2013.07.048
- Maisonneuve, E., Gerdes, K., 2014. Molecular Mechanisms Underlying Bacterial Persisters. *Cell* 157, 539–548. doi:10.1016/j.cell.2014.02.050
- Mansour, S.C., Pletzer, D., la Fuente-Núñez, de, C., Kim, P., Cheung, G.Y.C., Joo, H.-S., Otto, M., Hancock, R.E.W., 2016. Bacterial Abscess Formation Is Controlled by the Stringent Stress Response and Can Be Targeted Therapeutically. *EBioMedicine* 12, 219–226. doi:10.1016/j.ebiom.2016.09.015
- Mascio, C.T.M., Alder, J.D., Silverman, J.A., 2007. Bactericidal action of daptomycin against stationary-phase and nondividing *Staphylococcus aureus* cells. *Antimicrob. Agents Chemother.* 51, 4255–4260. doi:10.1128/AAC.00824-07
- Mechler, L., Herbig, A., Paprotka, K., Fraunholz, M., Nieselt, K., Bertram, R., 2015. A Novel Point Mutation promotes growth phase-dependent daptomycin tolerance in *Staphylococcus aureus*. *Antimicrob. Agents Chemother.* 59, 5366–5376. doi:10.1128/AAC.00643-15
- Meylan, S., Porter, C.B.M., Yang, J.H., Belenky, P., Gutierrez, A., Lobritz, M.A., Park, J., Kim, S.H., Moskowitz, S.M., Collins, J.J., 2017. Carbon Sources Tune Antibiotic Susceptibility in *Pseudomonas aeruginosa* via Tricarboxylic Acid Cycle Control. *Cell Chem. Biol.* 24, 195–206. doi:10.1016/j.chembiol.2016.12.015
- Michiels, J.E., Van den Bergh, B., Verstraeten, N., Michiels, J., 2016. Molecular mechanisms and clinical implications of bacterial persistence. *Drug Resist. Updat.* 29, 76–89. doi:10.1016/j.drug.2016.10.002
- Morones-Ramirez, J.R., Winkler, J.A., Spina, C.S., Collins, J.J., 2013. Silver enhances antibiotic activity against gram-negative bacteria. *Sci. Transl. Med.* 5, 190ra81–190ra81. doi:10.1126/scitranslmed.3006276
- Nandakumar, M., Nathan, C., Rhee, K.Y., 2014. Isocitrate lyase mediates broad antibiotic tolerance in *Mycobacterium tuberculosis*. *Nat. Commun.* 5, 1–10. doi:10.1038/ncomms5306
- Nguyen, D., Joshi-Datar, A., Lepine, F., Bauerle, E., Olakanmi, O., Beer, O., McKay, G., Siehnel, R., Schafhauser, J., Wang, Y., Britigan, B.E., Singh, P.K., 2011. Active Starvation Responses Mediate Antibiotic Tolerance in Biofilms and Nutrient-Limited Bacteria. *Science* 334, 982–986. doi:10.1126/science.1211037
- Nistico, L., Gieseke, A., Stoodley, P., Hall-Stoodley, L., Kerschner, J.E., Ehrlich, G.D., 2009. Fluorescence “in situ” hybridization for the detection of biofilm in the middle ear and upper respiratory tract mucosa. *Methods Mol. Biol.* 493, 191–213. doi:10.1007/978-1-59745-523-7_12
- Odenholt, I., 2000. Pharmacodynamic effects of subinhibitory antibiotic concentrations. *Int. J. Antimicrob. Agents* 17, 1–8. doi: 10.1016/s0924-8579(00)00243-0
- Olive, A.J., Sasseti, C.M., 2016. Metabolic crosstalk between host and pathogen: sensing, adapting and competing. *Nat. Rev. Microbiol.* 14, 221–234. doi:10.1038/nrmicro.2016.12

- Orman, M.A., Brynildsen, M.P., 2013a. Establishment of a method to rapidly assay bacterial persister metabolism. *Antimicrob. Agents Chemother.* 57, 4398–4409. doi:10.1128/AAC.00372-13
- Orman, M.A., Brynildsen, M.P., 2013b. Dormancy Is Not Necessary or Sufficient for Bacterial Persistence. *Antimicrob. Agents Chemother.* 57, 3230–3239. doi:10.1128/AAC.00243-13
- Parsek, M.R., Singh, P.K., 2003. Bacterial Biofilms: An Emerging Link to Disease Pathogenesis. *Annu. Rev. Microbiol.* 57, 677–701. doi:10.1146/annurev.micro.57.030502.090720
- Paulsen, I.T., Brown, M.H., Skurray, R.A., 1996. Proton-dependent multidrug efflux systems. *Microbiol. Rev.* 60, 575–608. doi: 10.1128/mr.60.4.575-608.1996
- Perez, A.C., Pang, B., King, L.B., Tan, L., Murrah, K.A., Reimche, J.L., Wren, J.T., Richardson, S.H., Ghandi, U., Swords, W.E., 2014. Residence of *Streptococcus pneumoniae* and *Moraxella catarrhalis* within polymicrobial biofilm promotes antibiotic resistance and bacterial persistence in vivo. *Pathog. Dis.* 70, 280–288. doi:10.1111/2049-632X.12129
- Powell, J.E., Leonard, S.P., Kwong, W.K., Engel, P., Moran, N.A., 2016. Genome-wide screen identifies host colonization determinants in a bacterial gut symbiont. *Proc. Natl. Acad. Sci. USA.* 113, 13887–13892. doi:10.1073/pnas.1610856113
- Pu, Y., Zhao, Z., Li, Y., Zou, J., Ma, Q., Zhao, Y., Ke, Y., Zhu, Y., Chen, H., Baker, M.A.B., Ge, H., Sun, Y., Xie, X.S., Bai, F., 2016. Enhanced Efflux Activity Facilitates Drug Tolerance in Dormant Bacterial Cells. *Mol. Cell* 62, 284–294. doi:10.1016/j.molcel.2016.03.035
- Roches, Des, S., Post, D.M., Turley, N.E., Bailey, J.K., Hendry, A.P., Kinnison, M.T., Schweitzer, J.A., Palkovacs, E.P., 2018. The ecological importance of intraspecific variation. *Nat. Ecol. Evol.* 150, 1–10. doi:10.1038/s41559-017-0402-5
- Rodrigues, R.R., Greer, R.L., Dong, X., DSouza, K.N., Gurung, M., Wu, J.Y., Morgun, A., Shulzhenko, N., 2017. Antibiotic-Induced Alterations in Gut Microbiota Are Associated with Changes in Glucose Metabolism in Healthy Mice. *Front. Microbiol.* 8, 3389–14. doi:10.3389/fmicb.2017.02306
- Rotem, E., Loinger, A., Ronin, I., Levin-Reisman, I., Gabay, C., Shores, N., Biham, O., Balaban, N.Q., 2010. Regulation of phenotypic variability by a threshold-based mechanism underlies bacterial persistence. *Proc. Natl. Acad. Sci. USA.* 107, 12541–12546. doi:10.1073/pnas.1004333107
- Sadykov, M.R., Hartmann, T., Mattes, T.A., Hiatt, M., Jann, N.J., Zhu, Y., Ledala, N., Landmann, R., Herrmann, M., Rohde, H., Bischoff, M., Somerville, G.A., 2011. CcpA coordinates central metabolism and biofilm formation in *Staphylococcus epidermidis*. *Microbiology* 157, 3458–3468. doi:10.1099/mic.0.051243-0
- Saliba, A.-E., Li, L., Westermann, A.J., Appenzeller, S., Stapels, D.A.C., Schulte, L.N., Helaine, S., Vogel, J., 2016. Single-cell RNA-seq ties macrophage polarization to growth rate of intracellular *Salmonella*. *Nat. Microbiol.* 2, 1–8. doi:10.1038/nmicrobiol.2016.206
- Saliba, A.-E., Santos, S.C., Vogel, J., 2017. New RNA-seq approaches for the study of bacterial pathogens. *Current Opinion in Microbiology* 35, 78–87. doi:10.1016/j.mib.2017.01.001
- Santiago, M., 2015. A new platform for ultra-high density *Staphylococcus aureus* transposon libraries. *BMC Genomics* 16, 1–18. doi:10.1186/s12864-015-1361-3
- Schultz, D., Palmer, A.C., Kishony, R., 2017. Regulatory Dynamics Determine Cell Fate following Abrupt Antibiotic Exposure. *Cell Syst.* 5, 509–517.e3. doi:10.1016/j.cels.2017.10.002
- Shah, D., Zhang, Z., Khodursky, A., Kaldalu, N., Kurg, K., Lewis, K., 2006. Persisters: a distinct physiological state of *E. coli*. *BMC Microbiology* 6, 53. doi:10.1186/1471-2180-6-53

- Singh, R., Lemire, J., Mailloux, R.J., Chenier, D., Hamel, R., Appanna, V.D., 2009. An ATP and Oxalate Generating Variant Tricarboxylic Acid Cycle Counters Aluminum Toxicity in *Pseudomonas fluorescens*. *PLoS ONE* 4, e7344. doi:10.1371/journal.pone.0007344
- Sommer, M.O., Dantas, G., 2011. Antibiotics and the resistant microbiome. *Curr. Opin. Microbiol.* 14, 556–563. doi:10.1016/j.mib.2011.07.005
- Soto, S.M., 2013. Role of efflux pumps in the antibiotic resistance of bacteria embedded in a biofilm. *Virulence* 4, 223–229. doi:10.4161/viru.23724
- Strugeon, E., Tilloy, V., Ploy, M.-C., Da Re, S., 2016. The Stringent Response Promotes Antibiotic Resistance Dissemination by Regulating Integron Integrase Expression in Biofilms. *mBio* 7, e00868–16–9. doi:10.1128/mBio.00868-16
- Taber, H.W., Mueller, J.P., Miller, P.F., Arrow, A.S., 1987. Bacterial uptake of aminoglycoside antibiotics. *Microbiol. Rev.* 51, 439–457. doi:10.1128/mmbr.51.4.439-457.1987
- Tanaka, G., Shigeta, M., Komatsuzawa, H., Sugai, M., Suginaka, H., Usui, T., 1999. Effect of the Growth Rate of *Pseudomonas aeruginosa* Biofilms on the Susceptibility to Antimicrobial Agents: β -Lactams and Fluoroquinolones. *Chemother.* 45, 28–36. doi:10.1159/000007162
- Theriot, C.M., Bowman, A.A., Young, V.B., 2016. Antibiotic-Induced Alterations of the Gut Microbiota Alter Secondary Bile Acid Production and Allow for *Clostridium difficile* Spore Germination and Outgrowth in the Large Intestine. *mSphere* 1, e00045–15–16. doi:10.1128/mSphere.00045-15
- Thomas, V.C., Kinkead, L.C., Janssen, A., Schaeffer, C.R., Woods, K.M., Lindgren, J.K., Peaster, J.M., Chaudhari, S.S., Sadykov, M., Jones, J., Mohamadi AbdelGhani, S.M., Zimmerman, M.C., Bayles, K.W., Somerville, G.A., Fey, P.D., 2013. A Dysfunctional Tricarboxylic Acid Cycle Enhances Fitness of *Staphylococcus epidermidis* During β -Lactam Stress. *mBio* 4, e00437–13. doi:10.1128/mBio.00437-13
- Toit, Du, A., 2016. Bacterial physiology: Persisters are under the pump. *Nat. Rev. Microbiol.* 14, 332–333. doi:10.1038/nrmicro.2016.72
- Urish, K.L., DeMuth, P.W., Kwan, B.W., Craft, D.W., Ma, D., Haider, H., Tuan, R.S., Wood, T.K., Davis, C.M., 2016. Antibiotic-tolerant *Staphylococcus aureus* Biofilm Persists on Arthroplasty Materials. *Clin. Orthop. Relat. Res.* 474, 1649–1656. doi:10.1007/s11999-016-4720-8
- Valentino, M.D., Foulston, L., Sadaka, A., Kos, V.N., Villet, R.A., Santa Maria, J., Lazinski, D.W., Camilli, A., Walker, S., Hooper, D.C., Gilmore, M.S., 2014. Genes Contributing to *Staphylococcus aureus* fitness in abscess- and infection-related ecologies. *mBio* 5, e01729–14–e01729–14. doi:10.1128/mBio.01729-14
- Vega, N.M., Allison, K.R., Khalil, A.S., Collins, J.J., 2012. Signaling-mediated bacterial persister formation. *Nat. Chem. Biol.* 8, 431–433. doi:10.1038/nchembio.915
- Ventola, C.L., 2015. The Antibiotic Resistance Crisis. *P.T.* 40, 277–283. PMID: 25859123
- Vogwill, T., Comfort, A.C., Furió, V., MacLean, R.C., 2016. Persistence and resistance as complementary bacterial adaptations to antibiotics. *J. Evol. Biol.* 29, 1223–1233. doi:10.1111/jeb.12864
- Walters, M.C., Roe, F., Bugnicourt, A., Franklin, M.J., Stewart, P.S., 2003. Contributions of antibiotic penetration, oxygen limitation, and low metabolic activity to tolerance of *Pseudomonas aeruginosa* biofilms to ciprofloxacin and tobramycin. *Antimicrob. Agents Chemother.* 47, 317–323. doi:10.1128/AAC.47.1.317-323.2003
- Wang, J., Chen, L., Chen, Z., Zhang, W., 2015. RNA-seq based transcriptomic analysis of single bacterial cells. *Integr. Biol.* 7, 1466–1476. doi:10.1039/C5IB00191A

- Webber, M.A., 2003. The importance of efflux pumps in bacterial antibiotic resistance. *J. Antimicrob. Chemother.* 51, 9–11. doi:10.1093/jac/dkg050
- Willenborg, J., Willms, D., Bertram, R., Goethe, R., Valentin-Weigand, P., 2014. Characterization of multi-drug tolerant persister cells in *Streptococcus suis*. *BMC Microbiol.* 14, 120–9. doi:10.1186/1471-2180-14-120
- Wu, H., Tremaroli, V., Bäckhed, F., 2015. Linking Microbiota to Human Diseases: A Systems Biology Perspective. *Trends Endocrinol. Metab.* 26, 758–770. doi:10.1016/j.tem.2015.09.011
- Yang, J.H., Bhargava, P., McCloskey, D., Mao, N., Palsson, B.O., Collins, J.J., 2017. Antibiotic-Induced Changes to the Host Metabolic Environment Inhibit Drug Efficacy and Alter Immune Function. *Cell Host Microbe* 22, 757–765.e3. doi: 10.1016/j.chom.2017.10.020
- Zaura, E., Brandt, B.W., Teixeira de Mattos, M.J., Buijs, M.J., Caspers, M.P.M., Rashid, M.U., Weintraub, A., Nord, C.E., Savell, A., Hu, Y., Coates, A.R., Hubank, M., Spratt, D.A., Wilson, M., Keijser, B.J.F., Crielaard, W., 2015. Same Exposure but Two Radically Different Responses to Antibiotics: Resilience of the Salivary Microbiome versus Long-Term Microbial Shifts in Feces. *mBio* 6, e01693–15. doi:10.1128/mBio.01693-15
- Zhang, L., Mah, T.-F., 2008. Involvement of a novel efflux system in biofilm-specific resistance to antibiotics. *J. Bacteriol.* 190, 4447–4452. doi:10.1128/JB.01655-07